



EST 1892

**London
South Bank
University**

**Development of an environmentally
benign and optimised biodiesel
production process**

by

Omar Aboelazayem

A thesis submitted in partial fulfilment of

the requirements for the award of

Doctor of Philosophy in Chemical, Process and Energy Engineering

Centre for Energy and Environment Research

School of Engineering

London South Bank University

February 2019

© Copyright to London South Bank University (LSBU)

Declaration

I declare that the thesis has been composed by myself with fabulous support of my supervisors. The thesis is submitted for examination in consideration of the award of a degree of Doctor of Philosophy in Chemical, Process and Energy Engineering. I would like to emphasise that it is my personal effort and that the work has not be submitted for any other degree or professional qualification. Furthermore, I took reasonable care to ensure that the work is original and to the best of my knowledge, does not breach copyright law and has not been taken from other sources except where such work has been cited and acknowledged within the text.

Dedication

I would like to dedicate this work to my grandfather, Professor Mahmoud Zahran, who passed away in September 2018. I always remember and cherish his unflinching commitment to my education and research. I have been continuously imagining the moment that I would be able to show him my PhD Thesis. I wish if it was possible to share these moments with him.

May Allah bless his soul, forgive him, make his grave a garden and grant him the highest levels of paradise. Amen.

Acknowledgements

The journey to PhD would not have been possible without the massive support of my family, supervisors, colleagues and friends.

I express my deep gratitude to my supervisors; Professor Basu Saha (London South Bank University, LSBU) and Professor Mamdouh Gadalla (The British University in Egypt, BUE). Their assistance and support from starting of my PhD until achieving the current stage of thesis submission have been invaluable. Special thanks to Professor Saha, whose confidence and outlook in my research inspired me and provided me with self-confidence. Special thanks to Professor Gadalla, whose selfless time and care were sometimes all that have kept me going. I could emphasise that it has been such an honour to work under their supervision.

I am greatly thankful to Mr Ken Unadat, Mr William Cheung and Mr Charles Coster for their immense technical support and guidance in the laboratories. Special thanks to Dr. Rim Saada, Victor Onyenkeadi, Anwar Sahbel and Dr. Ousmane Abdoulaye for their substantial guidance during my very first months of the PhD.

I am thankful for the effective and supportive research environment that I have experienced in School of Engineering from Professor David Mba, Professor Asa Barber, Dr Sandra Dudley, Ms Nicole Auguste, Mr Andrew Casey, Mr John Harper, Ms Sunita Selvarajan and Ms Ayindo Dalouba. In addition, special thanks to London Doctoral Academy (LDA) team and LSBU Research Office represented by Professor Peter Doyle, Mrs Louise Thompson (Campbell), Ms Cosimina Drago, Professor Graeme Maidment and Professor Paul Ivey who have tremendously developed my research skills and push my research towards better opportunities.

I also express my thanks to my professors and teachers; Professor Nour Elgendy (Egyptian Petroleum Research Institute), Professor Fatma Ashour (Cairo University), Professor Mohamed El-Shahir, Professor Mostafa Radwan and Professor Mostafa Soliman (BUE) for their continuing support and encouragement. I especially thank Professor Maguid Hassan (Dean of Engineering, BUE) for his enduring support and recognition.

I would like to thank the collaboration team between LSBU and BUE including Mrs Louise Thompson (Campbell), Mrs Mandy Maidment, Mrs Hoda Hosni, Mrs Ghada Ghoniem and Professor Yehia Behei-El-Din for establishing the opportunity for joining this programme.

Thanks to my PhD peers; Anwar Sahbel, Mohamed Balha, Youmna Ahmedy, Hamed Ali, Victor Onyenkeadi, Zahra Echresh, Dr. Ertan Sidiqqi, Ahmed Daoud, Bisi Olaniyan, Shahenda Mahran, Yusuf Umar, Mahiuddin Alamgir, Fereshteh Hogatisaeidi, Ahmed Borg, Masud Rana, Noha Abdelrahman, Yara Ahmed, Mohamed Nabawy, May Nagy, Ridouan Chaouki, Antigoni Paspali, Tara Ghatauray, Dr. Hassan Zabihi, Nura Makwashi and Dr. Ivy Sagbana from whom I have learnt and enjoyed my PhD journey.

I would like to express my deep gratitude to my close family members who have been continuously inspiring and believing in me. Special gratitude and appreciation for my parents who have supported me emotionally and financially. I have learned from them the real meaning of love. To my brothers, Dr. Ahmed Aboelazayem and Mr Mohamed Aboelazayem who have always been by my side when I feel down.

Many thanks to my family members; Mrs Ekbal Aboelazayem, Dr. Khaled Aboelazayem, Dr Ahmed Zahran, Dr Iman Zahran, Mrs Azza Aboelazayem, Mrs Maha Aboelazayem, Mr Mokhtar Elkholy, Dr Aliaa Atef, Dr Mostafa Elmalky, Dr. Ibtesam Shokier, Dr. Ahmed Elashwal, Eng. Mahmoud Elkholy, Mr Mohamed Elkholy, Dr. Mohamed Khaled, Dr. Abeer Khaled, Mrs Iman Elmalky, Dr. Ibrahim Elashwal, Dr. Aya Elashwal, Ms Omnia Elashwal, Mr Omar Zahran and Mr Adam Zahran.

Finally, special thanks to my lovely friends; Mady Abohashish, Mohamed Sherin, Mohamed Ibrahim, Mennatallah Labib, Ahmed Allam, Omar Mazen, Melis Durmaz, Chen Yuting, Valeria Perli, Zakarya Badawy, Marwa Mohamed, Ahmed Ramy and Marwa Khaled.

Abstract

The challenges of reducing the world's excessive dependence on fossil fuels and atmospheric accumulation of greenhouse gases have led to the development of alternative sustainable biodiesel. Recently, non-catalytic biodiesel production using supercritical technology has received a significant interest due to its numerous advantages including short reaction time, high yield of biodiesel, elimination of catalyst preparation and separation costs and its applicability for various feedstock.

This study has introduced an in-depth assessment for the valorisation of both low and high acid values waste cooking oils (WCO) into biodiesel using supercritical methanolysis. The effects of different process variables have been investigated including methanol to oil (M:O) molar ratio, temperature, pressure and time. Both transesterification and esterification reactions have been extensively studied. Different responses have been investigated for this study including overall biodiesel yield, glycerol yield and FFAs conversion. Response surface methodology (RSM) *via* Box-Behnken Design (BBD) and Central Composite Design (CCD) has been used to investigate the effect of the process variables and their interactions on the reaction responses. In addition, overall reaction kinetics for both transesterification and esterification reactions have been studied where both have been reported as pseudo-first order reactions. Thermodynamics of the reaction has been analysed to report the thermodynamic data of the reaction including Arrhenius constant and activation energy. The kinetic studies have resulted in 50.5 kJ/mol for transesterification reaction and 34.5 kJ/mol for esterification reaction.

Numerical and graphical optimisation have been employed to minimise the process conditions and to maximise the production of biodiesel where the optimal conditions of the low acidity WCO have been developed at M:O molar ratio of 37:1, reaction temperature of 253.5 °C, reaction pressure of 198.5 bar in 14.8 min reaction time for 91% biodiesel yield. However, for high acidity WCO the optimal conditions have been developed at M:O molar ratio of 25:1, reaction temperature of 265 °C and reaction pressure of 110 bar in 20 min for 98% biodiesel yield. Further, this work has developed a heat exchanger network (HEN) that has achieved the optimal process energy requirements based on Pinch method.

Table of contents

Declaration	i
Dedication	ii
Acknowledgements	iii
Abstract	v
Table of contents	vi
Nomenclature	xiii
List of figures	xvi
List of tables	xx
Publications	xxiii
1. Introduction	1
1.1. Background	1
1.2. Motivation.....	3
1.3. Research aims and objectives	4
1.4. Contributions to knowledge	4
1.5. Structure of the thesis	5
2. Literature review	7
2.1. Introduction	7
2.2. Biodiesel production methodologies.....	8
2.2.1. Conventional methods.....	8
2.2.2. Microreactors.....	9
2.2.3. High shear mixing.....	14
2.2.4. Microwave	17
2.2.5. Ultrasonic.....	21

2.2.6.	Supercritical technology.....	25
2.3.	Progress in supercritical biodiesel production	26
2.3.1.	Glycerol-accompanied biodiesel production	26
2.3.1.1.	Methanol	26
2.3.1.2.	Ethanol.....	34
2.3.1.3.	<i>n</i> -Propanol and <i>n</i> -butanol.....	38
2.3.2.	Glycerol-free biodiesel production	39
2.3.2.1.	Methyl acetate.....	40
2.3.2.2.	Dimethyl Carbonate (DMC).....	42
2.3.2.3.	Methyl <i>tert</i> -butyl ether (MTBE)	43
2.4.	Effect of different supercritical reaction variables on biodiesel production	45
2.4.1.	Effect of reaction temperature	45
2.4.2.	Effect of reaction pressure.....	49
2.4.3.	Effect of reaction time	50
2.4.4.	Effect of alcohol to oil ratio.....	53
2.5.	Progress in supercritical biodiesel process design and simulation	55
2.5.1.	Chemical components selection	55
2.5.2.	Thermodynamic model selection	56
2.5.3.	Reactants pre-treatment.....	57
2.5.4.	Reactor simulation.....	58
2.5.5.	Product separation	59
2.5.6.	Process energy integration	60
2.6.	Conclusions.....	61
3.	Biodiesel synthesis from low acidity waste cooking oil.....	62
3.1.	Introduction	62
3.2.	Materials and methods.....	62

3.2.1. Materials	62
3.2.2. Experimental setup	62
3.2.3. Experimental design	64
3.2.4. Statistical analysis	67
3.2.5. Reaction Kinetics	67
3.2.6. Physicochemical properties	68
3.2.7. Gas chromatographic analysis	69
3.3. Results and discussions	70
3.3.1. Model fitting and adequacy checking	70
3.3.2. Effect of reaction variables	74
3.3.2.1. Effect of methanol to oil molar ratio	74
3.3.2.2. Effect of reaction temperature	75
3.3.2.3. Effect of reaction pressure	77
3.3.2.4. Effect of reaction time	77
3.3.3. Optimisation of reaction variables	79
3.3.4. Validation of predicted optimum conditions	79
3.3.5. Kinetic study	80
3.3.6. Biodiesel properties	82
3.4. Conclusions	84
4. Valorisation of high acid value waste cooking oil into biodiesel	84
4.1. Introduction	84
4.2. Materials and methods	85
4.2.1. Materials	85
4.2.2. Experimental Procedures	85
4.2.2.1. Supercritical methanolysis	85
4.2.2.2. WCO and biodiesel characterisation	86

4.2.2.3. Preparation of standard solution	87
4.2.2.4. Derivatisation of WCO sample	87
4.2.2.5. Gas chromatographic analysis	88
4.2.3. Experimental Design	88
4.2.4. Statistical analysis	89
4.3. Results and discussion	91
4.3.1. Analysis of biodiesel and glycerol yields.....	91
4.3.1.1. Development of regression model	91
4.3.1.2. Model adequacy checking.....	92
4.3.1.3. Effect of process variables	99
4.3.1.3.1. Effect of individual process variables	99
4.3.1.3.2. Effect of variables interactions on the responses.....	101
4.3.1.4. Process optimisation and experimental validation	106
4.3.2. Analysis of FAME yields for individual FAMEs	107
4.3.2.1. Chromatogram analysis of derivatised WCO	107
4.3.2.2. Calibration curves for standards	108
4.3.2.3. FAME yield calculations	110
4.3.2.4. Models development and adequacy checking	110
4.3.2.5. Effect of process variables and their interactions.....	121
4.3.2.5.1. Interactive effect of methanol:oil molar ratio and reaction time	121
4.3.2.5.2. Interactive effect of reaction temperature and pressure	124
4.3.2.6. Process optimisation	126
4.4. Conclusions.....	127
5. Kinetics, optimisation and simulation of free fatty acids conversion into biodiesel.....	128
5.1. Introduction	128
5.2. Material and methods.....	129
5.2.1. Materials	129
5.2.2. Experimental procedures.....	130

5.2.2.1.	Analysis of overall FFAs conversion	130
5.2.2.2.	Chromatographic analysis of FFAs conversion	130
5.2.2.2.1.	Preparation of standard solutions	130
5.2.2.2.2.	Calibration curves for standards	131
5.2.2.2.3.	FFAs conversion calculations	132
5.2.3.	Experimental design and analysis	132
5.2.4.	Reaction kinetics	133
5.2.5.	Reactor Simulation	134
5.3.	Results and discussion	134
5.3.1.	Overall conversion of FFAs	134
5.3.1.1.	Development of regression model equation.....	134
5.3.1.2.	Model adequacy checking.....	137
5.3.1.3.	Effect of process variables and their interactions.....	142
5.3.1.3.1.	Effect of M:O molar ratio	143
5.3.1.3.2.	Effect of reaction temperature.....	145
5.3.1.3.3.	Interactive effect of M:O molar ratio and reaction temperature	146
5.3.1.3.4.	Effect of reaction pressure	147
5.3.1.3.5.	Effect of reaction time	147
5.3.1.3.6.	Interactive effect of reaction pressure and time	147
5.3.1.4.	Process optimisation	150
5.3.1.5.	Reaction kinetics.....	151
5.3.1.6.	Reactor simulation	153
5.3.2.	Chromatographic analysis of individual FFAs.....	155
5.3.2.1.	Chromatographic method development	155
5.3.2.2.	Development of regression model equation.....	159
5.3.2.3.	Model adequacy checking.....	161
5.3.2.4.	Effect of process variables and their interactions.....	163
5.3.2.4.1.	Effect of M:O molar ratio	164
5.3.2.4.2.	Effect of reaction time	165
5.3.2.4.3.	Interactive effect of M:O molar ratio and reaction time.....	165

5.3.2.4.4. Effect of reaction pressure	167
5.3.2.4.5. Effect of reaction temperature.....	168
5.3.2.4.6. Interactive effect of reaction pressure and temperature	168
5.4. Process optimisation	170
5.5. Conclusions.....	174
6. Conceptual design of an energy integrated scheme for supercritical biodiesel production	175
6.1. Introduction	175
6.2. Materials and methods.....	177
6.2.1. Chemical components	177
6.2.2. Thermodynamic model	178
6.2.3. Plant capacity, unit operations and operating conditions	178
6.3. Process design.....	179
6.3.1. Non-catalytic reactor.....	185
6.3.2. Separation of unreacted methanol.....	185
6.3.3. Glycerol separation.....	186
6.3.4. Biodiesel purification.....	187
6.4. Process integration	187
6.4.1. Mass integration	188
6.4.2. Heat integration	189
6.5. Conclusions.....	198
7. Conclusions and recommendations for future work	198
7.1. Conclusions.....	198
7.2. Challenges and recommendations.....	199
7.2.1. Oxidation stability study	199

7.2.2. Extensive integrated processes	199
7.2.3. Two-steps reactions	200
7.2.4. Glycerol-free biodiesel	200
7.2.5. Techno-economic analysis	201
7.2.6. Thermal and storage stability study	201
References.....	204

Nomenclature

2FI	Two factors interaction
ANOVA	Analysis of variance
B:O	Butanol to oil
BBD	Box-Bhneken design
CaLaO	Calcium and Lanthanum mixed oxides
CaO	Calcium oxide
CEoS	Combined equation of state
CO	Carbon monoxide
CO ₂	Carbon dioxide
CMR	Catalytic membrane reactor
CSTR	Continuous stirred tank reactor
DG	Diglycerides
DMC	Dimethyl carbonate
DOE	Design of experiments
E:O	Ethanol to oil
EOS	Equation of state
FAAE	Fatty acid alkyl-ester
FABE	Fatty acid butyl-ester
FAME	Fatty acid methyl-ester
FAPE	Fatty acid propyl-ester
FAGC	Fatty acid glycerol carbonate

FFA	Free fatty acid
FID	Flame ionisation detector
GC	Gas chromatography
GHG	Greenhouse gases
GL	Glycerol
GTBE	Glycerol <i>tert</i> -butyl ether
H ₂ SO ₄	Sulphuric acid
HEN	Heat exchanger network
KOH	Potassium hydroxide
LLE	Liquid-liquid equilibrium
M:O	Methanol to oil
MEN	Mass exchanger network
MG	Monoglycerides
MTBE	Methyl <i>tert</i> -butyl ether
NaOH	Sodium hydroxide
NO _x	Nitrogen oxides
NRTL	Non-random two liquids
OFAT	One factor at a time
P:O	Propanol to oil
PEG	Polyethylene glycol
R ²	Coefficient of correlation
R ² _{Adj}	Adjusted coefficient of determination
R ² _{Pred}	Predicted coefficient of determination

RD	Reactive distillation
RSM	Response surface methodology
SO _x	Sulphur oxides
SRK	Soave-Redlich Kwong
TAN	Total acid number
TG	Triglycerides
TPA	Terephthalic acid
TPEC	Total primary energy consumption
USR	Ultra-shear reactor
VDU	Vacuum distillation unit
VLE	Vapour-liquid equilibrium
VLLLE	Vapour-liquid-liquid equilibrium
WCO	Waste cooking oil
WHEN	Work-heat exchanger network

List of figures

Figure 1.1. World's energy consumption, adapted from (BP, 2017)	2
Figure 2.1. A schematic of T-Shaped plexiglass micromixer, adapted from (Sepahvand et al., 2014)	11
Figure 2.2. Schematic for the integrated high-shear mixing and microwave-assisted systems, adapted from (Choedkiatsakul et al., 2015b).....	15
Figure 2.3. A schematic for typical microwave-assisted experimental setup, adapted from (Lertsathapornsuk et al., 2008)	18
Figure 2.4. A schematic for a typical microwave-assisted experimental setup, adapted from (Mostafaei et al., 2015)	23
Figure 2.5. Novel spiral reaction used for supercritical ethanolysis, adapted from (Farobie et al., 2015)	36
Figure 2.6. Interactive effect between reaction temperature and M:O molar ratio (adapted from (Tan et al., 2010))	48
Figure 3.1. Schematic of the experimental setup	64
Figure 3.2. Actual experimental data <i>versus</i> predicted model.....	73
Figure 3.3. Residuals <i>versus</i> predicted response	73
Figure 3.4. Perturbation Plot	74
Figure 3.5. 3-D and contour graphs showing the effect of methanol ratio and temperature <i>versus</i> yield	76
Figure 3.6. 3-D and contour graphs showing the effect of pressure and time on yield ..	78
Figure 3.7. Rate constant calculation	81
Figure 3.8. Arrhenius plot for transesterification of WCO	82
Figure 3.9. Gas chromatogram of methyl esters in the product sample	84
Figure 4.1. A schematic of the experimental setup	86

Figure 4.2. Predicted <i>versus</i> actual values for biodiesel yield model (a) and glycerol yield model (b).....	94
Figure 4.3. Normal plot of residuals for (a) biodiesel yield model and (b) glycerol yield model	97
Figure 4.4. Plot of residuals versus predicted values of pressure variable for (a) biodiesel yield model and (b) glycerol yield model	98
Figure 4.5. Plot of residuals versus actual response for (a) biodiesel yield model and (b) glycerol yield model.....	98
Figure 4.6. Perturbation plot showing the effect of individual variables on (a) biodiesel yield and (b) glycerol yield.....	99
Figure 4.7. Interaction plot showing interactive effect of methanol ratio and temperature on biodiesel yield.....	102
Figure 4.8. 3D response surface and contour plot for M:O molar ratio and reaction temperature versus biodiesel yield	103
Figure 4.9. Interaction plot showing interactive effect of reaction pressure and time on biodiesel yield.....	104
Figure 4.10. 3D response surface and contour plot for reaction pressure and time versus biodiesel yield	105
Figure 4.11. Chromatographic results of the derivatised WCO	108
Figure 4.12. Calibration curves of FAME standard.....	109
Figure 4.13. Predicted <i>versus</i> actual values for methyl-oleate model (a), methyl-palmitate model (b) and methyl-oleate model (c)	116
Figure 4.14. Response surface of the effect of reaction time and M:O molar on the FAME yield of methyl-oleate (a), methyl-palmitate (b) and methyl-oleate (c)	123
Figure 4.15. Response surface of the effect of reaction temperature and pressure on the FAME yield of methyl-oleate (a), methyl-palmitate (b) and methyl-oleate (c)	125
Figure 5.1. Calibration curves of fatty acids standards.....	132

Figure 5.2. Predicted <i>versus</i> actual values for FFAs conversion model.....	138
Figure 5.3. Normal plot of residuals for FFA conversion model.....	140
Figure 5.4. Plot of residuals versus predicted values of temperature variable for FFA conversion model.....	141
Figure 5.5. The plot of residuals versus predicted response for FFA conversion.....	142
Figure 5.6. Response surface and contour plot for M:O molar ratio and reaction temperature versus FFA conversion.....	145
Figure 5.7. Interaction plot showing interactive effect of methanol ratio and temperature on FFA conversion.....	147
Figure 5.8. Response surface and contour plot for reaction pressure and time versus FFA conversion.....	149
Figure 5.9. Interaction plot showing interactive effect of reaction pressure and time on FFA conversion.....	150
Figure 5.10. Rate constant of esterification.....	152
Figure 5.11. Arrhenius plot for esterification of FFA.....	153
Figure 5.12. Simulated CSTR using optimum parameters obtained from the experimental study.....	155
Figure 5.13. Chromatographic results of the standard fatty acids before method modification.....	156
Figure 5.14. Chromatographic results of the standard fatty acids after method modification.....	158
Figure 5.15. Predicted versus actual values for oleic acid conversion model.....	163
Figure 5.16. Response surface and contour plot for M:O molar ratio and reaction time versus oleic acid conversion.....	166
Figure 5.17. Interaction plot showing interactive effect of methanol ratio and temperature on FFA conversion.....	167

Figure 5.18. Response surface and contour plot for reaction pressure and time versus FFA conversion	169
Figure 5.19. Interaction plot showing interactive effect of reaction pressure and time on FFA conversion	170
Figure 5.20. Surface plot showing the interactive effect of M:O molar ratio and reaction pressure on optimisation desirability	172
Figure 5.21. Surface plot showing the interactive effect of M:O molar ratio and reaction time on optimisation desirability	172
Figure 5.22. Surface plot showing the interactive effect of reaction temperature and time on optimisation desirability	173
Figure 6.1. Process flowchart for biodiesel production (numbers below streams refer to stream names	181
Figure 6.2. Source-sink mapping	189
Figure 6.3. Composite curve of the process streams	191
Figure 6.4. Heat exchanger network designed for the integrated process	192
Figure 6.5. Graphical representation of the designed HEN on T-T diagram.....	193
Figure 6.6. Auto-generated HEN for biodiesel process	194
Figure 6.7. Graphical representation of the automated proposed HEN on T-T diagram	195
Figure 6.8. Graphical representation of the literature proposed HEN on T-T diagram	196

List of tables

Table 2.1. Biodiesel production using microreactors	13
Table 2.2. Biodiesel production using high-shear mixing reactors	16
Table 2.3. Biodiesel production using microwave-assisted reactors	20
Table 2.4. Biodiesel production using ultrasonic-assisted reactors	24
Table 2.5. Recent studies using supercritical methanolysis	33
Table 2.6. Recently studied systems using supercritical ethanolysis	37
Table 2.7. Summary of the effect of reaction temperature on SC biodiesel production.	47
Table 2.8. Summary of the effect of reaction pressure on SC biodiesel production	50
Table 2.9. Summary of the effect of reaction time on SC biodiesel production	52
Table 2.10. Summary of the effect of methanol to oil ratio on SC biodiesel production	54
Table 3.1. Experimental design variables and their coded levels	65
Table 3.2. Experimental design matrix with the actual and predicted yields.....	66
Table 3.3. Properties of WCO feedstock	69
Table 3.4. Composition of the fatty acids in WCO	69
Table 3.5. Analysis of variance for response surface developed model.....	72
Table 3.6. Comparison between produced biodiesel properties and European biodiesel standard EN14214	83
Table 4.1. Physicochemical properties of WCO	87
Table 4.2. Experimental design variables and their coded levels	88
Table 4.3. Experimental design matrix with the actual and predicted yields.....	90
Table 4.4. Analysis of variance for biodiesel yield for the developed model.....	93
Table 4.5. Analysis of variance for glycerol yield for the developed model	95

Table 4.6. Optimisation constrains used to predict optimum conditions for biodiesel production	106
Table 4.7. Comparison between produced biodiesel properties and European biodiesel standard EN14214	107
Table 4.8. Composition of the fatty acids in WCO	110
Table 4.9. Experimental design matrix with the actual and predicted yields.....	115
Table 4.10. Analysis of variance for yield of methyl-oleate model.....	118
Table 4.11. Analysis of variance for yield of methyl-palmitate model	119
Table 4.12. Analysis of variance for yield of methyl-linoleate model	120
Table 4.13. Optimisation constraints used to predict optimum conditions for biodiesel production	126
Table 5.1. Experimental design matrix with the actual and predicted yields.....	136
Table 5.2. Analysis of variance for FFA conversion of the developed model	137
Table 5.3. Optimisation constraints used to predict optimum conditions for biodiesel production	151
Table 5.4. Streams data of the simulated CSTR reactor.....	154
Table 5.5. Experimental design variables and their coded levels.....	157
Table 5.6. A chromatographic data of the retention time for each fatty acid.....	158
Table 5.7. Experimental design matrix with the actual and predicted yields.....	160
Table 5.8. Analysis of variance for oleic acid conversion of the developed model	162
Table 5.9. Optimisation constraints used to predict optimum conditions for biodiesel production	171
Table 6.1. Stream table for the designed process (Part 1)	182
Table 6.2. Stream table for the designed process (Part 2)	183
Table 6.3. Summary of units operating conditions of each process	184

Table 6.4. Process hot and cold streams 190

Table 6.5. Comparative study for the HEN designs 197

Publications

Journal Publications

O. Aboelazayem, M. Gadalla, B. Saha, "Derivatisation-free characterisation and supercritical conversion of free fatty acids into biodiesel from high acid value waste cooking oil", *Renewable Energy*, vol. 143, p. 77-90, **2019**. DOI:10.1016/j.renene.2019.04.106.

O. Aboelazayem, M. Gadalla, B. Saha, "Valorisation of high acid value waste cooking oil into biodiesel using supercritical methanolysis: Experimental assessment and statistical optimisation on typical Egyptian feedstock", *Energy*, vol. 162, p. 408-420, **2018**. DOI:10.1016/j.energy.2018.07.19.

O. Aboelazayem, M. Gadalla, B. Saha, "Design and simulation of an integrated process for biodiesel production from waste cooking oil using supercritical methanolysis", *Energy*, vol. 161, p. 299-307, **2018**. DOI:10.1016/j.energy.2018.07.139.

O. Aboelazayem, M. Gadalla, B. Saha, "Biodiesel production from waste cooking oil via supercritical methanol: optimisation and kinetic reactor simulation", *Renewable Energy*, vol. 124, p. 144-154, **2018**. DOI:10.1016/j.renene.2017.06.076.

O. Aboelazayem, M. Gadalla, B. Saha, "An experimental-based energy integrated process for biodiesel production from waste cooking oil using supercritical methanol", *Chemical Engineering Transactions*, vol. 61, p. 1645-1650, **2017**. DOI:10.3303/CET1761272.

O. Aboelazayem, M. Gadalla, B. Saha, "Recent advancement in biodiesel production using supercritical technology: Progress in experimental synthesis and process simulation", *Renewable and Sustainable Energy Reviews*, submitted in September **2018**, under review.

O. Aboelazayem, M. Gadalla, B. Saha, "Esterification of free fatty acids via supercritical methanol for biodiesel production from high acid value waste cooking oil: Multi-objective optimisation, kinetic study and reactor simulation", *Biomass and Bioenergy*, submitted in November **2018**, under review.

O. Aboelazayem, M. Gadalla, B. Saha, “Biodiesel production by valorising high acid value waste cooking oil via supercritical methanol: A critical assessment of fatty acids conversion”, *Bioresource Technology*, submitted in February **2019**, under review.

Y. Umar, **O. Aboelazayem**, M. Gadalla, B. Saha, “Oxidation stability of supercritical synthesised biodiesel: A study on the effect of process parameters”, *Fuel Processing Technology*, submitted in February **2019**, under review.

O. Aboelazayem, M. Gadalla, B. Saha, “Detailed kinetic study of transesterification reactions of high acid value waste cooking oil using supercritical methanolysis”, *Scientific Reports*, to be submitted in June **2019**.

Conference Publications

O. Aboelazayem, M. Gadalla, B. Saha, “Design of an integrated process for biodiesel production using supercritical methanol: Simultaneous work and energy integration”, PRES 2019 – 22nd Conference on process Integration, Modelling and Optimisation for Energy Saving and Pollution Reduction, **2019**, Crete, Greece, October 20-23, accepted.

O. Aboelazayem, M. Gadalla, B. Saha, “Supercritical methanolysis of waste cooking oil for biodiesel synthesis: Experimental and simulation assessments”, ECOS2019 – 32nd International Conference on Efficiency, Cost, Optimisation, Simulation and Environmental Impact on Energy Systems, **2019**, Wroclaw, Poland, June 23-28, accepted.

Y. Umar, **O. Aboelazayem**, Z. Echresh, M. Gadalla, B. Saha, “Waste cooking oil valorisation into biodiesel using supercritical methanolysis: Critical assessment on the effect of water content”, EUBCE 2019 – 27th European Biomass Conference and Exhibition, **2019**, Lisbon, Portugal, May 26-31, accepted.

O. Aboelazayem, M. Gadalla, B. Saha, “Systematic multivariate optimization of biodiesel synthesis from high acid value waste cooking oil: A response surface methodology approach”, Venice2018 – 7th International Symposium on Energy from Biomass and Waste Proceedings, **2018**, Venice, Italy, October 15-18.

O. Aboelazayem, M. Gadalla, B. Saha, “Non-catalytic production of biodiesel from high acid value waste cooking oil”, 2nd International Conference on Bioresource Technology for Bioenergy, Bioproducts & Environmental Sustainability Exhibition Proceedings, **2018**, Sitges, Spain, September 16-19.

O. Aboelazayem, M. Gadalla, B. Saha, “Supercritical methanolysis of waste cooking oil for biodiesel production: Experimental assessment for evaluating the effect of free fatty acids content”, EUBCE 2018 – 26th European Biomass Conference and Exhibition Proceedings, **2018**, p. 912-916, Copenhagen, Denmark, May 14-18.

O. Aboelazayem, M. Gadalla, B. Saha, “Non-catalytic production of biodiesel using supercritical methanol: A brief review” SEEP 2018 - 11th International Conference on Sustainable Energy & Environmental Protection Proceedings, **2018**, Scotland, UK, May 8-11.

O. Aboelazayem, M. Gadalla, B. Saha, “One-step production of biodiesel from high acid value waste cooking oil using supercritical methanol”, WCCE10 - 10th World Congress of Chemical Engineering, **2017**, Barcelona, Spain, October 1-5.

O. Aboelazayem, M. Gadalla, B. Saha, “A comparative study on biodiesel production from waste cooking oils obtained from different sources using supercritical methanol”, Proceeding of the 6th World Congress on Biofuels and Bioenergy, J Bioremediat Biodegrad, 8 (5), p. 56, **2017**, London, UK, September 5-6.

O. Aboelazayem, M. Gadalla, B. Saha, “An experimental-based energy integrated process for biodiesel production from waste cooking oil using supercritical methanol”, PRES 2017 – 20th Conference on process Integration, Modelling and Optemisation for Energy Saving and Pollution Reduction, **2017**, Tianjin, China, August 21-25.

O. Aboelazayem, M. Gadalla, B. Saha, “Optimising biodiesel production from high acid value waste cooking oil using supercritical methanol,” SEEP **2017** - 10th International Conference on Sustainable Energy & Environmental Protection Proceedings, 2017, p. 57-66, DOI:10.18690/978-961-286-048-6.5, Bled, Slovenia, June 27-30.

O. Aboelazayem, O. Abdelaziz, M. Gadalla, C. Hulteberg, B. Saha, “Biodiesel production from high acid value waste cooking oil using supercritical methanol: Esterification kinetics of free fatty acids”, EUBCE 2017 – 25th European Biomass Conference and Exhibition Proceedings, **2017**, p. 1381-1387, ISBN: 978-88-89407-17-2, Stockholm, Sweden, June 12-15.

O. Aboelazayem, M. Gadalla, B. Saha, “Optimisation of biodiesel production from waste cooking oil under supercritical conditions, ” Venice2016 – 6th International Symposium on Energy from Biomass and Waste Proceedings, **2016**, Venice, Italy, November 14-17. ISBN code 978886265009

CHAPTER 1

INTRODUCTION

Outline of the chapter

This chapter gives a background to the research work, its aims and objectives, contribution to knowledge and provides an outline of the thesis. The chapter is organised as follows:

1.1. Background

1.2. Motivation

1.3. Aims and objectives

1.4. Contribution to knowledge

1.5. Outline of the thesis

1. Introduction

1.1. Background

The world's total primary energy consumption (TPEC) has recorded a steep rise within the last decades reaching 150,000,000 GW.h in 2015. About 57% growth of this value is expected by 2050 owing the rapid industrial development and urbanisation that has occurred globally. Presently, fossil fuels including petroleum and natural gas are the main sources of energy (Hajjari et al., 2017).

According to the statistical review of world's energy which is annually published by British Petroleum (BP), consumption of energy has extensively increased during the last decade as shown in Figure 1.1 (Vinet and Zhedanov, 2011). The reasons for increases in energy consumption include industrial development, population growth and inauguration of new technologies. Industrial developments in different applications require excessive energy for operations using either electricity or heating energies. Electricity consumption, which until this moment relies mostly on combustion of fossil fuels, has broadly increased. Moreover, population growth has a direct impact on energy consumption in different eras. In addition, new technologies which are invented to enhance industrial productivity, preform multitasking requirements and provide better working environment for humans have excessive impact on energy consumption. This includes special transportation means, heating/cooling equipment and electricity consumptions through electronic devices. All the above-mentioned aspects cause the depletion of fossil fuels reserves. In contrast, combustion of fossil fuels which are considered as the main source of energy contribute in environmental pollution and their emission are the main causes of global warming (Mardhiah et al., 2017).

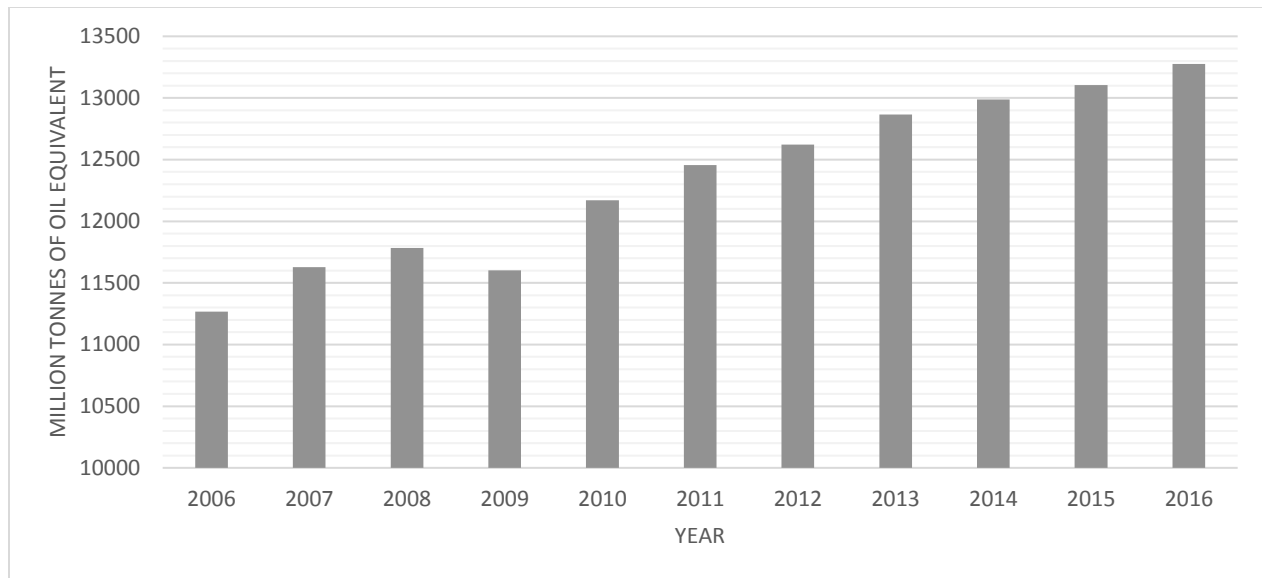


Figure 1.1. World's energy consumption, adapted from (BP, 2017)

The majority of fossil fuel consumption (58%) is recorded by the transportation sector (Hajjari et al., 2017; Kumar and Sharma, 2016; Mardhiah et al., 2017). The unstable availability of the fossil fuels has induced the tremendous increase in crude oil price from \$20/barrel to \$140/barrel in the period between 2000 and 2015, where recently the price dropped back to nearly \$60/barrel (Saluja et al., 2016). This uncertainty is a result of volatile political situation in the Middle East, where fossil fuels are mainly extracted. Additionally, energy production dependency on fossil fuels is the main reason for different environmental concerns. The combustion of fossil fuels resulted in emission of toxic gases including sulphur oxides (SO_x), nitrogen oxides (NO_x) and carbon monoxide (CO). In addition, they increase the emission of greenhouse gases (GHG), including carbon dioxide (CO₂) which have the tendency to trap enormous heat in the environment, resulting in acid rain and global warming (Aboelazayem et al., 2018).

The search on renewable, sustainable and environmentally benign sources of energy has been extensively carried out globally to reduce the dependency on fossil fuels. Biofuels have the potential to solve the environmental concerns and mitigate the climate change. Biofuels are usually synthesised from crops that absorb CO₂ through the photosynthesis process. Subsequently, they are considered as carbon neutral resources, where they

maintain the carbon cycle without additional discharge to the environment (Hasan and Rahman, 2017).

Biodiesel is a competitive alternative renewable fuel for petro-diesel. Biodiesel in particular has many advantages over fossil fuels including lower toxicity emission, higher flash point, negligible sulphur content, biodegradability and the production from renewable feedstock. It can be used as a pure fuel and can be blended with petro-diesel at any ratio. Production of biodiesel would cause an economic development mutation specially for developing countries. It will encourage employment, introduce a long term replacement for fossil fuel and reduce national dependency on energy resources imports; consequently, increase national stability and security rate (Hajjari et al., 2017).

1.2. Motivation

Presently, edible oils are the main resources for production of biodiesel. However, this global dependency on edible oil has a negative impact on food security. Using edible oils for biodiesel production has developed a global imbalance in the market demand where both food and biodiesel industries required very high production of edible oils. Consequently, the increase of food prices due to the reduction of food resources has a negative impact on the society (Mardhiah et al., 2017). Thus, the research has been shifted towards non-edible and WCOs.

The main two obstacles for biodiesel production from non-edible and WCOs are their high content of FFAs and water contents. Feedstock with either high FFAs content and/or water, require excessive pre-treatment prior to biodiesel synthesis. The pre-treatment processes include neutralisation and/or esterification reactions. The high availability of WCOs with high FFAs content from restaurants and industries has directed the research for developing an environmentally benign and sustainable biodiesel production method from high acidity feedstock.

1.3. Research aims and objectives

The aim of this work is to design an environmentally benign biodiesel production process from high acidity feedstock. To achieve this aim, the following objectives have been identified:

1. Review the previous technologies for biodiesel production from various feedstock.
2. Highlight one of the biodiesel production technologies that could be implemented for high acidity feedstock.
3. Characterise the physicochemical properties of two feedstock with different acidity.
4. Investigate the applicability of implementing supercritical methanolysis for biodiesel production from low and high acidity feedstock.
5. Apply Response Surface Methodology (RSM) technique to optimise reaction process.
6. Investigate the conversion of free fatty acids for the high acidity feedstock.
7. Study the kinetics of transesterification/esterification reactions.
8. Design and simulate a complete process for biodiesel production using supercritical methanolysis.
9. Optimise the process energy consumption using energy integration techniques.

1.4. Contributions to knowledge

This work has various contributions to knowledge in terms of experimental results, analysis, modelling, process simulation and energy integration. Firstly, this work has studied the production of biodiesel from both low and high acidity WCOs, where the optimal yield at minimum conditions has been developed for each feedstock. In addition, this work has performed several experimental modelling for biodiesel synthesis where simple regression models have been developed to represent the process responses function in process variables. Further, a derivatisation-free method of FFAs has been developed using gas chromatographic analysis. A complete process simulation for biodiesel production using the developed experimental kinetic data has been designed.

Finally, the minimum energy requirement for the process has been achieved by using an efficient heat exchanger network designed *via* graphical Pinch method.

1.5. Structure of the thesis

Brief descriptions of the chapters in the thesis are summarised as follows:

Chapter 2: Literature review

A critical review of biodiesel production methodologies has been presented to provide solid background on the previous reported methods in biodiesel research. An overview of the conventional and new methods has been discussed. The non-catalytic supercritical method has been highlighted where different alcoholic and non-alcoholic production methods have been reviewed. These have been followed by reviewing the previous process designs and simulation for biodiesel production.

Chapter 3: Supercritical biodiesel synthesis from low acidity WCO

In this chapter, detailed experimental studies have been performed on a low acidity WCO using supercritical methanol. The main aim of this chapter is to evaluate the optimal biodiesel yield at minimum reaction conditions. The effect of reaction variables on biodiesel yield has been investigated. A kinetic study of the overall transesterification reaction has been performed.

Chapter 4: Supercritical valorisation of high acid value WCO into biodiesel

The applicability and the efficiency of supercritical methanolysis to valorise high acidity WCO has been investigated in this chapter. Different analytical methods have been applied to calibrate the biodiesel yield. Experimental modelling and design techniques have been implemented. The effect of process variables and their interactions have been extensively discussed. Optimum conditions have been predicted using the developed models and have been validated experimentally.

Chapter 5: Kinetics and optimisation of FFAs conversion into biodiesel

The esterification of FFAs has been extensively studied to investigate the conversion of FFAs using different analytical techniques, including chromatographic analysis and titration. The overall FFAs conversion and the individual FFAs conversions have been reported and optimised. The effect of reaction variables and their interactions have been investigated. The kinetics of the esterification reaction has been analysed. Finally, a kinetic reactor has been designed and simulated using the developed kinetic data.

Chapter 6: Conceptual design of an integrated scheme for supercritical biodiesel production

The main aim of this thesis has been achieved in this chapter, where design and simulation of a complete process for biodiesel production has been performed. The process includes reactants conditioning, reactor design, separation of unreacted components and biodiesel purification. Additionally, mass and energy integration principles using Pinch Analysis have been applied to optimise the process energy consumption. The graphical Pinch method, that has been developed very recently, have been applied to design an efficient heat exchanger network to achieve the minimum energy requirement for the process.

Chapter 7: Conclusions and recommendations for future work

The overall conclusions for this work has been illustrated in this chapter. In addition, critical suggestions and recommendations have been made for future work.

CHAPTER 2

LITERATURE REVIEW

Outline of the chapter

This chapter gives a detailed review on the conventional and recent biodiesel production methodologies. It focuses on supercritical technologies where different production methods have been addressed. The chapter is organised as follows:

2.1. Introduction

2.2. Biodiesel production methodologies

2.3. Progress in supercritical biodiesel production

2.4. Effect of different supercritical reaction variables on biodiesel production

2.5. Progress in supercritical process design and simulation

2.6. Conclusions

2. Literature review

2.1. Introduction

Biodiesel is defined as mono-alkyl esters of long chain fatty acids derived from vegetable oils, animal fats and recently from algal lipids. Presently, biodiesel is mainly produced from edible oils e.g. sunflower, rapeseed, palm and soybean oils. However, the increasing consumption of edible crops has resulted in raising the price of edible oils as it is required for both food and biofuels industries. Hence, the research has been shifted towards non-edible and WCO to avoid the competition with food industries that affects the global food security (Mardhiah et al., 2017).

Transesterification reaction is considered the most commonly used method for biodiesel production. Simply, it is a reversible reaction where 1 mole of triglyceride reacts with 3 moles of alcohols to produce 3 mole of fatty acids alkyl esters (FAAE) and 1 mole of glycerol. Due to the biphasic heterogeneous liquid mixture between alcohol and oil, the reaction occurs at a very slow rate in the absence of catalyst. Accordingly, catalytic transesterification systems are usually applied for biodiesel production (Abidin et al., 2012; Haigh et al., 2013). Catalysts are mostly added to increase the rate of the transesterification reaction and they could be categorised to homogeneous and heterogeneous catalysts. Within each category alkaline and acidic catalysts could be implemented including sodium methoxide (CH_3ONa) and calcium oxide (CaO) for homogeneous and heterogeneous alkaline catalysts. Additionally, biological catalysts (enzymes) have been also used for transesterification reaction including lipase enzyme. Alternative methodologies have been recently reported for biodiesel production including supercritical technology, high-shear mixing, microwave and ultrasonic (Farobie and Matsumura, 2017a; Semwal et al., 2011).

This chapter aims to critically review the transesterification methodologies and addressing the recent developments in each processing method. Specifically, it provides the recent insights in supercritical transesterification/esterification process. Different supercritical transesterification schemes have been reviewed including glycerol-accompanied and glycerol-free reactions. Factors affecting the biodiesel production using supercritical

technologies have been extensively reviewed. Additionally, the recent process integration techniques for supercritical processes have been addressed.

2.2. Biodiesel production methodologies

Biodiesel production methodologies can be categorised into conventional and recently developed processes. The conventional methods of biodiesel production reflect to the catalysed systems that operates at atmospheric pressure using traditional stirring systems. These methods could be summarised in alkaline, acidic and enzymatic catalysed systems. Alternatively, recent methods have been developed for biodiesel production including microreactors, high-shear mixing, microwave assisted, ultrasound-assisted and supercritical technology. This chapter critically reviews the recent developed methodologies for biodiesel production.

2.2.1. Conventional methods

The alkaline homogeneously catalysed process, mainly CH_3ONa , has been implemented commercially for biodiesel production. The main advantage of this method is the high reaction activity, where biodiesel is produced in high quality within reasonable reaction time. Additionally, the prices of the catalysts are relatively low. However, the main drawback of this method is the high sensitivity to FFAs and water in the feedstock where high FFA content leads to saponification reaction which reduce biodiesel yield and complicate product separation. In addition, the process produces high volume of wastewater rich with catalyst washing step of the product. On the other hand, heterogeneous alkaline catalysts eliminate the wastewater and the sensitivity to FFAs in the feedstock. It also simplifies the product separation as the solid catalysts could be easily separated. However, the high cost of the catalyst preparation in addition to the high sensitivity to water content in the feedstock have limited the scaling up of the process (Abidin et al., 2013; Saha et al., 2014; Suresh et al., 2018)

Alternatively, acidic catalysed processes have lower susceptibility to FFAs content in the feedstock. The acid catalysts enhance the esterification reaction of FFAs to FFAE. However, the reaction is relatively very slow compared to other methods. Enzymatic transesterification with lipase has shown significant conversion of both triglycerides and FFAs. However, high prices of the enzymes are the main obstacles for process upscaling (Banković-Ilić et al., 2012; Leung et al., 2010; Sajjadi et al., 2016; Sotoft et al., 2010; Talebian-Kiakalaieh et al., 2013; Xu et al., 2005).

2.2.2. Microreactors

Micro-synthesis is a multidisciplinary technique which has been widely applied in engineering and science. The definition of microfluid segment is the minimum unit that could be applied in a micro-space with specific micro-properties that could improve different chemical reactions and physical operations. Various materials have been used for microreactors fabrication including ceramic, polymers, stainless steel and even glass. Eventually, microreactors offer a significant performance of mass transfer for the different reactions including multiphase and extraction reactions. In addition, it offers an excellent heat transfer resulting in substantial intensification for micro-scale processing (Yao et al., 2015).

The implementation of microreactors in biodiesel production has been introduced by Wen et al. (2009) using a zigzag micro-channel reactor. They fabricated the reactor to be used for continuous alkaline homogeneous catalysed reaction. They investigated the effect of different geometrical parameters on enhancing the reaction conversion. They reported that the efficiency of biodiesel synthesis has been enhanced by decreasing the channel size and applying more turns where smaller droplets are produced. They reported 99.5% yield of FAMEs in only 28 s reaction time at 9:1 M:O molar ratio, 56 °C, 1.2 wt% catalyst concentration. In comparison with the conventional stirring reactors, microreactors reduce the energy consumption while maintaining high yield of products.

Sun et al. (2010) implemented the technology of microreactors to reduce the time of esterification reaction for high acid value feedstock. They developed a two-steps method for faster biodiesel production through acid-catalysed process. They also investigated the effect of different reaction variables including temperature, time, methanol to acid/oil molar ratio and water/acid concentration. They reported maximum conversion of oleic acid using methyl esterification at 100 °C within 5 min. This was followed by transesterification of triglycerides where the maximum yield of FAME has been reported at 120 °C within 20 min. Additionally, they reported drop in total acid value of the acidic oil from 160 to 1.1 mg KOH/g at 100 °C, 30:1 methanol to acid molar ratio, sulphuric acid (H₂SO₄) concentration of 3 wt% at 7 min. In addition, the maximum FAME yield has reported as 99.5%. Finally, they highlighted the applicability of biodiesel production continuously from very high acid value oils using acidic catalysed pre-treated process in a relatively very short reaction time (15 min) using microreactors.

Similarly, Tanawannapong et al. (2013) reported biodiesel production from WCO with total acid value of 3.96 mg KOH/g using microtube reactor using acidic catalysed process. They investigated the effect of different process variables including M:O molar ratio (4.5:1–18:1), catalyst concentration (0.5–2 wt%), reaction temperature (55–70 °C), and reaction time (5–20 s). They optimised the process variables of biodiesel production. They reported drop in acid value through methyl esterification for 1 mg KOH/g at M:O molar ratio of 9:1, 65 °C, 1 wt% H₂SO₄ concentration within only 5 s reaction time. This has followed by transesterification of triglycerides where final yield of FAME of 91.76% has reported at M:O molar ratio of 9:1, 65 °C, 1 wt% KOH concentration within only 5 s reaction time. Hence, within less than 15 s reaction time, WCO would be converted to biodiesel with good yield of FAMEs.

Rahimi et al. (2014) studied the optimisation of biodiesel synthesis from soybean oil in a T-shaped plexiglass micromixer as shown in Figure 2.1. They used RSM *via* BBD to optimise and model the reaction. They considered five process variables through their optimisation including M:O molar ratio (6:1–12:1), temperature (55–65 °C), catalyst concentration (0.6–1.8 wt%), residence time (20–180 s) and different flow rates of reactants (1–11 ml/min). They also considered the yield of FAMEs as the process

response. They reported optimal conditions for 89% yield of FAME at 9:1 M:O molar ratio, 1.2% catalyst concentration within 180 s at 60 °C.

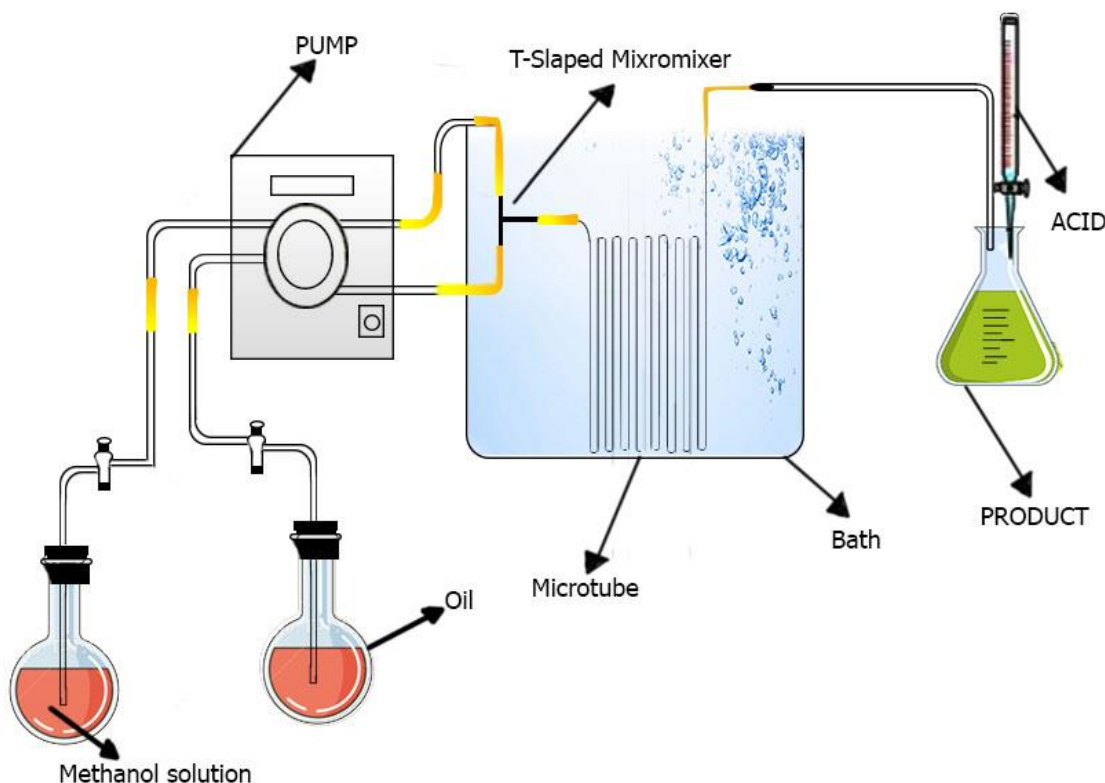


Figure 2.1. A schematic of T-Shaped plexiglass micromixer, adapted from (Sepahvand et al., 2014)

Further, Santana et al. (2016) studied the comparison between batch and microreactors for sunflower oil ethanolysis for biodiesel production using alkaline catalysed process. They have reported that the maximum biodiesel yielded from batch reactor was 94.06% in comparison to 95.8% yield of the microreactor. Jiao Liu et al. (2018) reported a novel approach for direct transesterification of fresh microalgal cells using microreactor. They proposed that using this method would allow real time microalgal fatty acids analysis without the need of drying and/or lipids extraction. They reported that using microreactors, the bottlenecks limitations of the mass transfer have been overcome. They reported that only 10 min are required for full analysis of fresh microalgal cells with polyethylene glycol (PEG) as a suspension agent.

In summary, biodiesel production using microreactors represents a significant process intensification with different advancements. The higher mass transfer rates in microreactors led to better reaction efficiency/performance and higher yield of biodiesel. The main advantages of microreactors could be summarised in the short diffusion distance and high surface area-to-volume ratio which accordingly increase the reaction rate extensively. Different factors would affect the performance of microreactors including inlet mixer type, micro-channel size and internal channel geometry (zig-zag, omega, and tesla shaped channels). However, the implementation of microreactors was very interesting since the flow was laminar. Hence, reactants mixing is considered as problematic as it requires micromixer. Another problem for application of microreactors is the scale-up of the process. The microreactors operate under very low flow rates ($\mu\text{L/h}$ to mL/h), which is considered as a great disadvantage for industrial applications (Bi et al., 2017; Budžaki et al., 2017; Tiwari et al., 2018). A summary of the recent studies using microreactor is tabulated in Table 2.1.

Table 2.1. Biodiesel production using microreactors

Oil Source	Reactor	Catalyst	Conditions	Biodiesel yield (%)	References
Soybean	Zig-zag micro-channel	KOH	M:O ratio 9:1 Temp. 56 °C KOH: 1.2 wt% Time: 28 s	99.5	(Z. Wen et al., 2009)
Cottonseed oil	Micro-structured reactor	H ₂ SO ₄ , KOH	M:O ratio 30:1,20:1 Temp. 100 °C H ₂ SO ₄ : 3 wt% KOH: 3 wt% Time: 7 min, 5 min	99.5	(Sun et al., 2010)
WCO	Microtube reactor	H ₂ SO ₄ , KOH	M:O ratio 9:1 Temp. 65 °C H ₂ SO ₄ : 1 wt% KOH: 1 wt% Time: 5 s, 6 s	91.7	(Tanawannapong et al., 2013)
Soybean	Microreactor with T-shaped plexiglass micromixer	KOH	M:O ratio 9:1 Temp. 60 °C KOH: 1.2 wt% Time: 180 s	89	(Sepahvand et al., 2014)

2.2.3. High shear mixing

The immiscibility between alcohol and vegetable oils has been considered as the main obstacle for simple transesterification reaction (Noureddini et al., 1998). It engenders the resistance of mass transfer which accordingly decrease the reaction rate. Accordingly, many researchers analysed different parameters that would increase the miscibility between alcohol and oil through increasing temperature, stirring rate and contact area. According to the fact that the biphasic heterogeneous systems depend mainly on the contact surface area between the reactants, Ma et al. (1999) examined the effect of high mixing rate on the transesterification of beef tallow. They reported that stirring rate has a significant influence on the reaction rate. However, the high energy consumption resulted from using high stirring rate would be considered as a major disadvantage.

The research has been extended for increasing the mass transfer and hence the reaction rate during the last years. Various technologies have been applied including rotating packed bed reactor and high shear rate reactor (Chen et al., 2010; Filho et al., 2010). Da Silva et al. (2011) investigated the performance of a multiple-stage ultra-shear reactor (USR) for biodiesel production from soybean oil using catalytic ethanolsis. They reported that the maximum achieved yield of 99.26 wt% at M:O molar ratio of 6:1, catalyst concentration 1.35% and only within 12 min reaction time. They reported that using USR has a significant reduction in the required reaction time in comparison with the conventional reactors. Further, Choedkiatsakul et al. (2015b) proposed a continuous integrated high-shear mixing with microwave irradiation for biodiesel synthesis. The schematic of the experimental setup is shown in Figure 2.2. They reported very high yield of biodiesel of 99.8% within only 5 min reaction time. They explained their findings to the effective mixing through diffusion in addition to the combined effect of the hybrid system. They recommended the developed hybrid system for further extensions as they reported that it has lower energy requirements than the conventional systems.

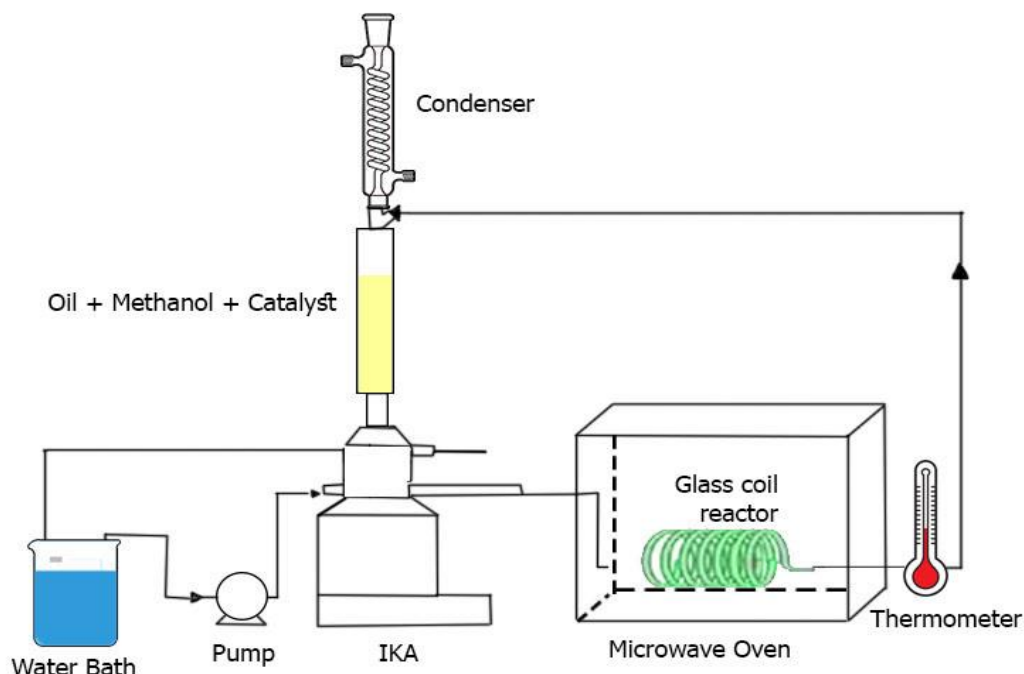


Figure 2.2. Schematic for the integrated high-shear mixing and microwave-assisted systems, adapted from (Choedkiatsakul et al., 2015b)

Recently, Sánchez-Cantú et al. (2017) proposed a novel sustainable method for biodiesel production through emulsion formation by high shear mixer. They reported that the transesterification reaction has been enhanced significantly at room temperature in just 60 s of reaction time in the presence of 1% NaOH catalyst at very high shear mixing rate of 4000 rpm. They explained their findings due to the formation of nanodroplets that act as individual mass-transfer reactors. Additionally, Sánchez-Cantú et al. (2019) optimised their previously reported method of biodiesel at atmospheric conditions. They reported 94.5% conversion within only 10 s of dispersion and increased to 97.1% within 40 s. They also performed a comparative study between the energy consumption by the novel method and the conventional method where the results indicated that the novel method consume much lower energy than the conventional one.

Hence, this approach would be as a promising alternative method for sustainable biodiesel production at atmospheric conditions. A summary of the recent studies using high-shear mixing reactors is tabulated in Table 2.2.

Table 2.2. Biodiesel production using high-shear mixing reactors

Oil Source	Reactor	Catalyst	Conditions	Biodiesel yield (%)	References
Soybean oil	USR	NaOH	M:O ratio 6:1 Temp. 56 °C NaOH: 1.35 wt% Time: 12 min	99.26	(Filho et al., 2010)
Cottonseed oil	Integrated microwave and high-shear mixing	NaOH	M:O ratio: 9:1 Temp. 65 °C Time: 5 min	99.8	(Choedkiatsakul et al., 2015b)
Soybean oil	High-shear mixer	NaOH	M:O ratio: 5:1 NaOH: 1 wt% Temp. 22 °C Time: 60 s	99.8	(Sánchez-Cantú et al., 2017)
Refined Soybean oil	High-shear mixer	NaOH	M:O ratio: 5:1 NaOH: 0.6 wt% Temp. 25 °C Time: 10 s	94.5	(Sánchez-Cantú et al., 2019)

2.2.4. Microwave

Microwave is an electromagnetic radiation within specific frequency between 0.3 and 300 GHz and wavelength between 0.01 and 1 m. It is considered as an efficient method for enhancing many chemical reactions as the energy is delivered intensively and directly to the reactants. The energy transfer (specifically heat) is considerably faster than the conventional heating methods. Accordingly, microwave-assisted reactions usually require shorter time while obtaining high yield of products (Motasemi and Ani, 2012).

Mazzocchia et al. (2004) studied the transesterification of triglycerides to FAMEs using microwave-assisted reaction with heterogeneous catalyst. They reported that the required reaction time has been decreased significantly. Azcan and Danisman (2007) studied the production of biodiesel from cottonseed oil using microwave-assisted alkaline catalysed transesterification. They compared the microwave-assisted method with the conventional method in terms of the reaction conditions. They reported that the optimum yield has been reached within 7 min at 333 K and 1.5% catalyst concentration. While using the conventional method, the reaction time requires 30 min to achieve the same yield. Hernando et al. (2007) reported similar results for the capability of microwave-assisted systems to reduce the reaction time.

Lertsathapornsuk et al. (2008) reported simultaneous neutralisation and transesterification of high acid value WCO using alkaline homogeneous catalysed ethanolysis. Figure 2.3 showed a schematic for the experimental setup. They reported 97% conversion of WCO into biodiesel at 12:1 ethanol to oil (E:O) molar ratio, 3% catalyst concentration within only 30 s reaction time. Hong et al. (2016) studied valorising WCO into biodiesel using microwave-assisted systems. They reported that WCO with high acid value should be easily converted to biodiesel with acidic catalyst using microwave reactors. They have also reported that WCOs with higher acid values require more catalyst amount, microwave power and reaction time. Priyadarshi and Paul (2018) have also reported valorisation of kitchen food waste into biodiesel using advanced microwave-assisted system. They have reported 96.89 wt% yield at 170 °C, 22 bar and 0.5 wt% catalyst concentration within only 4 min. They investigated the addition of MTBE as a co-solvent where it has showed significant improvements in FAMEs yields. Moreover, it

yielded glycerol *tert*-butyl ether (GTBE) as a value-added by-product which is used as octane enhancer for gasoline fuel.

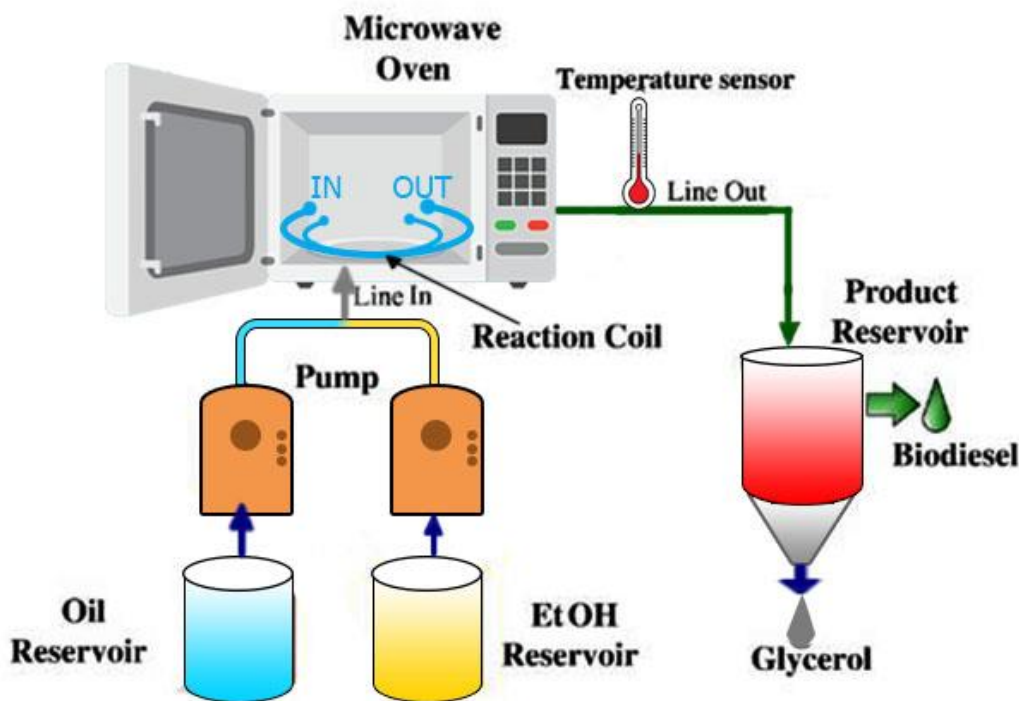


Figure 2.3. A schematic for typical microwave-assisted experimental setup, adapted from (Lertsathapornsuk et al., 2008)

Choedkiatsakul et al. (2015a) proposed a novel method for large-scale biodiesel production using continuous flow microwave reactor. They reported high ester content of 99.4% within 1.75 min at 12:1 M:O molar ratio, 400 W heating power at 70 °C. They reported energy consumption of 0.1167 kWh/L, which is considered as half of the energy consumed using the conventional method.

Ding et al. (2018) improved the efficiency of biodiesel production using acidic catalysed processes. They reported maximum yield of 99% of FAME at M:O molar ratio, ionic liquid dosage, microwave power and reaction time were 11:1, 9.17%, 168W and 6.43 h, respectively. Manco et al. (2012) studied the production of biodiesel from sunflower oil using microwave-assisted reaction. They studied the influence of adding different pebbles (boiling chips) on the reaction conditions including glass beads, ceramic pieces, carborundum. They reported that using pebbles, specifically carborundum, has significantly decreased the reaction time from 540 s (without carborundum) to 90 s (with carborundum).

In contrast, microwave assisted technology could not be implemented at industrial scale thus far. It is difficult to scale up the technology due to its short penetration of radiation into material. In addition, large sealed container has to be used for low penetration of microwave irradiation which causes a huge concern about the security. These disadvantages are the major obstacles to use this technology at industrial scale (Motasemi and Ani, 2012). A summary of the recently studied microwave-assisted reactors is given in Table 2.3.

Table 2.3. Biodiesel production using microwave-assisted reactors

Oil Source	Catalyst	Conditions	Biodiesel yield (%)	References
Cottonseed oil	KOH	M:O ratio 6:1 Temp. 60 °C KOH: 1.5 wt% Time: 7 min	91.4	(Azcan and Danisman, 2007)
WCO	NaOH	E:O ratio 12:1 Temp. 78 °C NaOH: 3 wt% Time: 30 min	97	(Lertsathapornsuk et al., 2008)
Municipal food waste	H ₂ SO ₄	Temp. 170 °C Pressure: 22 bar H ₂ SO ₄ : 0.5 wt% Time: 22 min	96.89	(Priyadarshi and Paul, 2018)
Microalgal lipids	KOH	M:O ratio 50:1 KOH: 5 wt% Time: 4 min Mixing rate: 966 rpm Water content: 80%	92	(Cui and Liang, 2014)
Refined palm oil	NaOH	M:O ratio 12:1 Temp. 70 °C Time: 1.75 min	99.4	(Choedkiatsakul et al., 2015a)
<i>Jatropha</i> oil	KOH	M:O ratio 6:1 Temp. 65 °C Time: 10 s Mixing rate: 200 rpm	90	(Lin and Chen, 2017)
Palm oil	vH ₂ SO ₄	M:O ratio 11:1 Time: 6.43 h	99	(Lin and Chen, 2017)

2.2.5. Ultrasonic

Ultrasonication is production of sound waves with high frequency that exceed the audibility limits of humans. These waves provide enough energy that required for mixing and approaching the activation energies of the several reactions. Ultrasonication process has significant chemical and physical effect on liquid-liquid heterogeneous reactions as it enhances the mass transfer through the cavitation bubbles. It enhances the production of radicals which accelerates the rate of chemical reaction during the transient collapse of bubbles. However, the physical effect could be summarised through the emulsification where micro-turbulence is generated which improves the homogeneity of the immiscible components (Ramachandran et al., 2013).

Lately, the implementation of ultrasonication in biodiesel production has gained a significant interest. Stavarache et al. (2005) introduced production of biodiesel from vegetable oils using alkaline catalysed process assisted by low frequency ultrasonic irradiations instead of mechanical stirring. They reported significant influences of ultrasonic assisted system on the process. The required time for the reaction has decreased significantly using ultrasonic assisted system in addition to lowering catalyst concentration. They observed that the ultrasonic waves with 40 kHz is considered the optimum frequency for transesterification reaction at at lower frequency and the reaction required longer time. Additionally, they reported insignificant influence of higher frequencies than 40 kHz on biodiesel production. They also proposed that using previously produced biodiesel as a solvent with intermediate polarity would increase the solubility of oil in methanol.

The ultrasonic assisted production of biodiesel has extended dramatically within the last decade. Recently, Kumar et al. (2017) developed an environmentally benign system for conversion of *Jatropha* oil into biodiesel using a continuous stirred tank reactor (CSTR) using alkaline catalyst assisted by ultrasonic irradiation. The optimum conditions for the developed system for 98.75% conversion of biodiesel within 1.09 min were reported at 5:1 M:O molar ratio, 25 °C reaction temperature, 0.75 wt% catalyst concentration and 7.5% solvent concentration. The flowrate was adjusted at 241.68 mL/min with ultrasonic amplitude of 60% and ultrasonic cycles 0.7 s. This significant rapid production of biodiesel

using the proposed system is considered as a promising method for production of biodiesel. Further, Kumar (2017) reported a single-step biodiesel production process from *Jatropha* seed by combining the extraction of oil from seeds process and the transesterification reaction of the extracted oil with alcohol using an ultrasonication assisted system. The author reported 92% of biodiesel conversion using 1:100 seed:solvent molar ratio, 1.5 wt% of catalyst within 20 min at 50% of ultrasonic amplitude and 0.3 s cycle.

Jookjantra and Wongwuttanasatian (2017) studied the optimisation of biodiesel production from refined palm oil under vacuum conditions using CaO catalyst assisted with ultrasonic waves. They investigated the influence of 6/2 pulse ultrasonic waves on biodiesel yield. They have reported 96.12% biodiesel yield at 9.69:1 M:O molar ratio, 8.77% catalyst loading, ultrasonic intensity of 4.60 W/g and 43.03 min reaction time. They reported that using pulse ultrasonication enhanced the transesterification reaction rate where higher biodiesel yield in shorter reaction time was observed in comparison with the conventional ultrasonic systems at the same intensity.

WCO is considered as a potential feedstock for biodiesel production using ultrasonic assisted systems. Aghbashlo et al. (2017) studied the optimisation of biodiesel production from WCO using piezo-ultrasonic reactor. They reported 96.63% conversion at 59.5 °C and M:O molar ratio of 6.1:1 within 10 min. Mostafaei et al. (2015) optimised biodiesel production from WCO using continuous reactor assisted by ultrasonic irradiation as shown in Figure 2.4. They considered different process variables for optimisation including irradiation distance, probe diameter, ultrasonic amplitude, vibration pulse and material flow. They reported that the optimum radiation conditions for maximum yield of biodiesel was achieved at 75 mm irradiation distance, 28 mm probe diameter, 56% amplitude, 62% vibration plus and 50 mL/min flowrate of reactants.

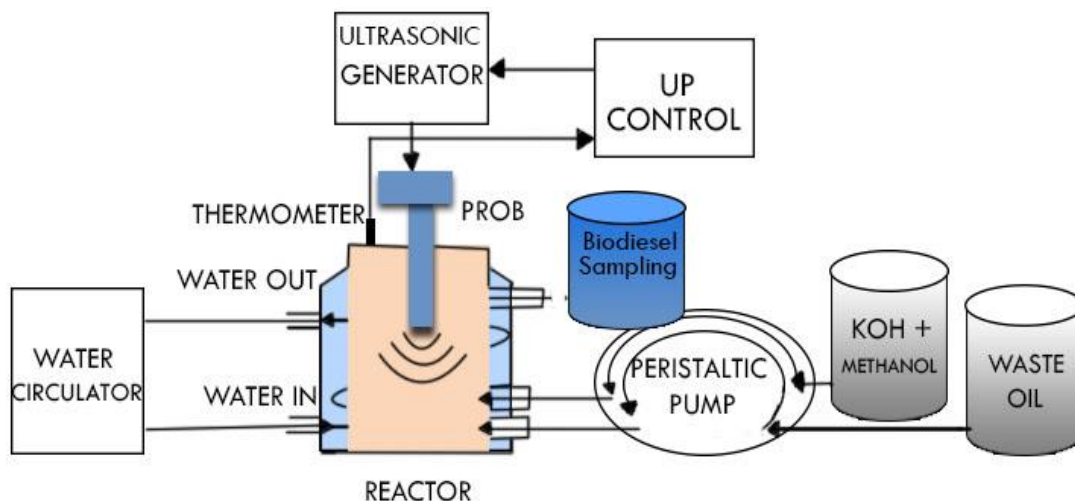


Figure 2.4. A schematic for a typical microwave-assisted experimental setup, adapted from (Mostafaei et al., 2015)

Valorisation of high acid value rubber seed oil (RSO) into biodiesel was reported using ultrasonication. Trinh et al. (2018) studied the optimisation of the pre-treatment esterification step of RSO using ultrasonic-assisted system. They reported significant conversion of FFAs with 98% conversion at 50 °C, 7.5 wt% of sulphuric acid catalyst concentration, 23:1 M:O molar ratio within 30 min. Hoseini et al. (2018) optimised biodiesel production from *Ailanthus altissima* (tree of heaven) seed oil using ultrasonication assisted process. They reported that 92.26% yield of biodiesel at 8.5:1 M:O molar ratio and 1.01 wt% catalyst loading within 4.71 min.

In summary, ultrasonic-assisted transesterification was applied for various biodiesel production techniques using different feedstocks. It is agreed in the literature that using ultrasonic-assisted systems enhances the reaction rate and increase the solubility between oil and alcohol. This is due to the fact that the created cavitation bubbles by the radiation disrupt the boundaries between liquid immiscible phases and impingement of the liquids that result in emulsification. The research on ultra-sonic assisted systems should be expanded to included larger scale reactions. A summary of the recently studied systems using ultrasonic-assisted reactors is presented in Table 2.4.

Table 2.4. Biodiesel production using ultrasonic-assisted reactors

Oil Source	Reactor	Catalyst	Conditions	Biodiesel yield (%)	References
<i>Jatropha</i> oil	CSTR	KOH	M:O ratio 5:1 Temp. 25 °C KOH: 0.75 wt% Time: 1.09 min Co-solvent: 7.5% Amplitude: 60% Ultrasonic cycle: 0.7 s	98.7	(Kumar et al., 2017)
<i>Jatropha</i> oil	CSTR	KOH	KOH: 1.5 wt% Time: 20 min Amplitude: 50% Ultrasonic cycle: 0.3 s	92	(Kumar, 2017)
Palm oil	Ultrasonic reactor	CaO	M:O ratio 9.69:1 CaO: 8.77 wt.% Time: 43.03 min	96.1	(Jookjantra and Wongwuttanasatian, 2017)
WCO	Piezo-ultrasonic reactor	KOH	M:O ratio 6.1:1 Temp. 59.5 °C Time: 10 min	96.6	(Aghbashlo et al., 2017)
RSO	Ultrasonic reactor	H ₂ SO ₄	M:O ratio 23:1 Temp. 50 °C H ₂ SO ₄ : 7.5 wt% Time: 30 min	98	(Trinh et al., 2018)
<i>Ailanthus altissima</i>	Ultrasonic reactor	KOH	M:O ratio 8.5:1 KOH: 1.01 wt% Time: 4.71 min	92.2	(Hoseini et al., 2018)
Algal Lipids	Ultrasonic reactor	KOH	M:O ratio 60:1 KOH: 1 wt% Time: 20	92	(Zhang et al., 2014)

2.2.6. Supercritical technology

Supercritical reactions occur when either any or all of the reactants are at their supercritical conditions including temperature and pressure. Conceptually, supercritical treatment is based on the change in the thermophysical properties of fluids including viscosity, polarity, specific gravity and dielectric constant. These properties are responsible for different behaviour of the fluids including conductivity, solubility and diffusivity. Supercritical technology possesses number of advantages in chemical industries as it increases the rates of both mass and heat transfer between the reactants and rapid reactions in very short time (typically at minutes' level). The properties of supercritical fluids including high solubility and low density have made them superior in most of the separation and extraction processes (Lee et al., 2014; Wen et al., 2009).

Biodiesel production process includes two main reactions; transesterification of triglycerides to FAMEs and esterification FFAs to FAMEs using alcohol. The main obstacle of this reaction is the immiscibility between oil and alcohol (usually methanol). However, when methanol is at the supercritical state, its thermophysical properties changes where it becomes soluble in the oil. Hence, transesterification/esterification reactions could easily occur without the aid of catalyst. The application of non-catalytic supercritical methanolysis of vegetable oil was introduced by Saka and Kusdiana (2001). The following section includes a comprehensive review on different supercritical techniques for biodiesel production.

Although several effective biodiesel production processes were reported and reviewed. This work has focused on the non-catalytic supercritical production of biodiesel. The following section has reviewed in details the progress of the application supercritical technology in biodiesel production.

2.3. Progress in supercritical biodiesel production

This section reviewed the recent developments in the non-catalytic production of biodiesel using supercritical technology. The processes have been divided into two categories based on the existence of glycerol in the product.

2.3.1. Glycerol-accompanied biodiesel production

Glycerol-accompanied biodiesel referred to biodiesel production through alcoholysis of triglycerides resulting in FFAE in addition to glycerol. Alcoholysis of triglycerides is considered as the standard method for biodiesel production where different alcohols were implemented through the reaction including methanol, ethanol, 1-propanol and 1-butanol. In addition, the alcoholysis reaction could be mentioned directly to the type of the alcohol used in the reaction by using different expressions including methanolysis, ethanolysis, etc.

2.3.1.1. Methanol

Methanolysis of triglycerides is the most commonly used process for biodiesel production due to the high similarity of the properties of FAMES and petroleum diesel fuel. In addition, the simple chemical structure of methanol resulted in biodiesel production with lower density and viscosity than other alcohols (Vyas et al., 2010).

Non-catalytic biodiesel production through supercritical methanolysis was introduced by Saka and Kusdiana (2001). They investigated the applicability of biodiesel production using catalyst-free methanolysis at the critical conditions of methanol i.e. temperature and pressure of 239 °C and 8.09 MPa, respectively. They reported that 40% of the rapeseed oil was converted within only 30 s to methyl esters. They stated that 95% conversion of the oil was achieved within 240 s. The same authors extended their findings by performing a kinetic study of supercritical methanolysis of rapeseed oil (Kusdiana and Saka, 2001). They reported that the reaction is first order with respect to triglycerides. Based on their experimental results they have considered reaction temperature of 350 °C and M:O molar ratio of 42:1 as the optimum conditions for supercritical methanolysis of rapeseed oil. This

research was extended dramatically and included numerous feedstocks including edible oils, non-edible oils and microalgae.

The main two obstacles for the conventional biodiesel production using homogeneous catalytic processes are of water content and FFAs in the feedstock as they enhance soap production which reduce biodiesel yield. Hence, feedstocks with either high FFAs content and/or water, require excessive pre-treatment prior to biodiesel synthesis. Warabi et al. (2004) investigated the reactivity of both triglycerides and FFAs of rapeseed oil. They reported that the reaction rate of methyl esterification of FFA using supercritical methanol is higher than transesterification of triglycerides. They explained their findings that methanol not only acts as a reactant in the reaction, but it also acts as an acidic catalyst due to the change in its dielectric constant value close to that of vegetable oil. Consequently, supercritical methanol allows the existence of homogeneous phase mixture with vegetable oil.

Additionally, Kusdiana and Saka (2004) analysed the effect of water content on biodiesel production using supercritical methanol. They reported that increasing water content in biodiesel does not have a significant effect on biodiesel yield. However, they also reported that adding water to the reactant solution has many influences on biodiesel production. The existence of water enhances the hydrolysis reaction of triglycerides and hence produce FFAs. Accordingly, three reactions were proposed during the supercritical methanolysis of rapeseed oil including hydrolysis of triglycerides to FFAs, methyl esterification of FFAs to FAMEs and methyl transesterification of triglycerides to FAMEs. They observed that higher water content in feedstock would be favourable during supercritical methanolysis. They exemplified this phenomenon due of the rate of the hydrolysis of triglycerides in higher than the transesterification of triglycerides at the supercritical conditions of methanol. They referred to the capability of water in dissolving both polar and nonpolar solutes at high temperatures.

These findings were considered as the beginning of a new era for biodiesel production from feedstocks with high FFAs including raw oils and WCOs. Feedstocks with high FFAs are not favourable for conventional catalytic processes. However the mentioned

properties would be considered as privilege when using supercritical methanol production method.

Han et al. (2005) proposed using co-solvents in supercritical methanolysis to enhance biodiesel yield. They used supercritical CO₂ to decrease the reaction conditions. They reported significant enhancement in biodiesel yield at lower reaction conditions by adding CO₂ as a co-solvent. Yin et al. (2008) extended this research by adding several co-solvents to the supercritical methanolysis reaction including hexane, CO₂ and KOH. The main purpose of adding co-solvents to the reactions is to minimise the high operational reaction conditions and to enhance the solubility of methanol in oil at milder conditions. They reported that all of the co-solvents have positive influence on biodiesel yield where adding any of the co-solvents have increased biodiesel yield in-comparison with co-solvents free reactions under the same reaction conditions. They reported optimal conditions for biodiesel production from soybean oil using supercritical methanolysis for 98% yield at 160 °C, 24:1 M:O molar ratio, 0.1 wt% of KOH within 20 min. However, Tsai et al. (2013) reported that the effect of adding carbon dioxide as a co-solvent has an insignificant effect on biodiesel yield.

High pressure phase equilibrium analysis was extensively studied between triglycerides, FAMEs and co-solvents. Hegel et al. (2008) reported several experimental phase behaviour between both mixture systems including the reactants mixture (vegetable oil and methanol) and products mixture (FAMEs, glycerol, methanol and propane). They reported that propane enhances the miscibility of methanol in oil at milder conditions. Consequently, they confirmed the applicability of co-solvents to enhance the reaction rate and increase the produced biodiesel yield.

The harsh reaction conditions of supercritical methanolysis drove the attention of several researchers for the stability of FAMEs. Thermal and oxidation stabilities were investigated during the supercritical methanolysis. Imahara et al. (2008) investigated the thermal stability of the common FAMEs derived from various feedstocks including methyl palmitate, methyl stearate, methyl oleate, methyl linoleate and methyl linolenate. The study included range of temperature between 270 °C to 350 °C. They concluded that the studied FAMEs showed good stability at 270 °C but beyond that temperature thermal

degradation of FAMEs were observed due to the isomerisation reaction of the poly-unsaturated FAMEs from *cis*-type to *trans*-type. They referred the same observations for oils with high compositions of unsaturated fatty acids including linseed and sunflower oils. They recommended to operate the supercritical methanolysis reaction up to 270 °C and strictly not to exceed 300 °C.

Xin et al. (2008) investigated the effect of the harsh reaction conditions of supercritical methanolysis on the oxidation stability of biodiesel. They examined the effect of temperature on the natural anti-oxidants (tocopherols) in the biodiesel. They reported slightly decrease in the tocopherols up to 270 °C, however, at higher temperatures a significant loss of tocopherols has been observed. Only one-third of the tocopherols remained at 360 °C. Accordingly, they recommended not to exceed 270 °C during biodiesel production using supercritical methanolysis. They reported that the exposure of biodiesel with initial high peroxide value to high temperature and pressure enhance the oxidation stability. Recently, Saluja et al. (2016) reviewed the stability of biodiesel by considering all of the stability variables including thermal, storage and oxidation stability. They highlighted the factors that affects biodiesel stability and the methods enhancing the stability of biodiesel.

Numerous studies were reported for biodiesel production through supercritical methanolysis using various feedstocks. Both edible and non-edible feedstocks were utilised for biodiesel synthesis using supercritical methanolysis in addition to microalgae.

For edible oils, rapeseed oil was firstly used by Saka and Kusdiana (2001) to investigate the possibility of supercritical methanolysis for biodiesel production. Varma et al. (2010) studied biodiesel production from sesame oil using supercritical methanol. They used high-pressure batch reactor for biodiesel synthesis. They reported increasingly effect of M:O molar ratio on the conversion of sesame oil into biodiesel up to 40:1 molar ratio. They also reported an increasing effect of temperature on the conversion up to 275 °C.

Non-edible oils were reported for biodiesel production using supercritical methanolysis. Salar-García et al. (2016) analysed biodiesel production from *Jatropha* oil using supercritical methanolysis. They reported that maximum yield of FAMEs of 99.5 mol% has been achieved at 325 °C within 90 min. They reported thermal decomposition of

biodiesel at 350 °C. Varma et al. (2010) studied biodiesel production from mustard oil using supercritical methanol.

Samniang et al. (2014) reported a comparative analysis between *Jatropha* and *Krating* oils for biodiesel production via supercritical methanolysis. They observed that the biodiesel production is extremely dependence on the feedstock properties and composition including FFAs content and FAME of unsaturated fatty acids. *Krating* oil has higher FFAs and unsaturated fatty acids than *Jatropha* oil, and hence higher FAMEs yield was resulted from *Krating* oil at milder reaction conditions than *Jatropha* oil. The optimal conditions for maximum biodiesel yield from *Krating* oil was 90.4% at 260 °C, 16 MPa and 10 min while the maximum yield of biodiesel from *Jatropha* oil was 84.6% at 320 °C and 15 MPa. García-Martínez et al. (2017) studied the optimisation of biodiesel synthesis from tobacco (*Nicotiana tabacum*) seed oil using supercritical methanolysis. They used RSM to analyse the optimum process variables combination for maximum biodiesel yield. They have achieved 92.8 mol% biodiesel yield at 300 °C and 90 min.

Castor oil attracted a huge attention as a potential feedstock for biodiesel production for several reasons, including its easily cultivation under different climatic and soil conditions, lower cost and high yield of oil from castor seed (Aboelazayem et al., 2018). Several researches were reported for castor oil conversion into biodiesel using supercritical methanolysis. Torrentes-Espinoza et al. (2017) studied the production of biodiesel from castor oil using a 10 L batch reactor via supercritical methanol. They reported that the highest conversion of castor oil into biodiesel has been achieved at 50:1 M:O molar ratio and 265.8 °C within 5 min. They developed a regression model to predict the conversion of castor oil into FAMEs within specific range of process variables. Román-Figueroa et al. (2016) reported high yield of biodiesel from supercritical methanolysis of castor oil.

Waste oils were considered as potential feedstock for biodiesel production. Specifically, using supercritical methanolysis solved most of the problems associated with valorising waste oils into biodiesel including FFAs and water content without any pre-treatment requirements. Shin et al. (2012) used supercritical methanolysis for utilising waste lard into biodiesel. They reported that without the need of any pre-treatment processes, 89.91% yield of biodiesel has been achieved at 45:1 M:O molar ratio, 335 °C, 20 MPa

within 15 min. Similarly, Demirbas (2009) compared between alkaline-catalysed methanolysis and supercritical methanolysis for biodiesel production from WCO. They reported higher biodiesel yield using supercritical methanolysis. Furthermore, several researchers reported biodiesel production from WCO using supercritical methanolysis (Ghoreishi and Moein, 2013; Patil et al., 2010; Sawangkeaw et al., 2010).

Kiss et al. (2016) reported a comparative analysis of single-step and two-steps supercritical methanolysis reactions. They considered waste oils as feedstock for their experiments. They observed that two-steps reaction (methyl esterification) produces higher biodiesel yield in milder reaction time where 91% yield at 350 °C were observed for single step transesterification compared to 95% yield at 270 °C for methyl esterification. They observed milder reaction pressure for methyl esterification of 8 MPa compared to 12 MPa for single transesterification reaction. Similarly, Tsai et al. (2013) also confirmed the positive effect of the presence of FFA in the feedstock for enhancing biodiesel yield.

Selecting WCO reduces the cost of the feedstock and eliminates any considerations of the competition with food industry (Gui et al., 2008). Tsai et al. (2013) observed that WCO recorded better results than the refined cooking oil using supercritical methanol transesterification. They reported that using WCO at 300 °C and 100 bar in 4 min the biodiesel yield was 65%. However, using refined sunflower oil required 40 min to achieve the same yield. They explained that the presence of FFA at higher concentration in WCO feedstock enhances FAME production using supercritical methanol since both esterification and transesterification reaction take place in parallel during the reaction time. Ghoreishi and Moein, (2013) concluded that the optimum conditions for biodiesel production within the supercritical methanol process at 271°C, 231 bar, 20.4 min and 33.8:1 M:O molar ratio resulting in 95.7% yield.

An economic feasibility and profitability study has been reported comparing both homogenous alkaline and supercritical methanol production plants. Each process was designed to produce 4000 tonnes of biodiesel annually. The process economics was analysed using Aspen In-Plant Cost Estimator. The study concluded that base catalysed process showed lower total capital investment. However, supercritical methanol process

was more economically preferable providing higher net present value, lower manufacturing cost and higher discounted cash flow rate of return (Lee et al., 2011).

Production of biodiesel using microalgae as a feedstock has rapidly increased through the last decades. Many reasons boosted the research on algal based biodiesel including higher biomass productivity, higher lipid accumulation and the rapid growth rate of microalgae. In addition, microalgae had the ability to grow at different environments including degraded lands, open ponds and photo-bioreactors. Finally, they had very considerable environmental benefits including bioremediation of wastewater and mitigation of greenhouse gases i.e. carbon dioxide. However, breaking of the robust cell wall of microalgae, that prevents realising the intracellular lipids of the medium, is considered as an energy-intensive process (Zhu et al., 2014).

Jazzar et al. (2015) investigated the applicability of direct supercritical methanolysis for breaking cell walls and converting the extracted lipids to biodiesel. Their study included wet and dry unwashed marine microalgae (*Nannochloropsis gaditana*). They reported successful extraction and conversion of lipids to biodiesel using single step reaction. They reported optimal conditions for biodiesel yield 0.48 g/g of lipids at 265 °C and methanol to dry algae ratio of 10:1 within 50 min reaction time. The implementation of supercritical methanolysis has been reported for soybean flakes (Xu et al., 2016). A single step reaction for extraction and transesterification of soybean full-fat lipids was successfully achieved. The maximum biodiesel reported from soybean flakes was 86% at 350 °C, 20 MPa at M:O molar ratio of 42:1 within 3 h. Zhou et al. (2017) reported extraction and conversion of lipids using supercritical methanolysis. They studied a continuous production using two kinds of microalgae including *Chrysochyta* and *Chlorella sp.* Extraction of lipids performed using supercritical CO₂ where the lipids were then fed to the reactor with supercritical methanol and CO₂ with the aid of *n*-hexane as a co-solvent. They achieved 56.31% and 63.78% of biodiesel yield for *Chrysochyta* and *Chlorella sp.*, respectively, at 340 °C, 19 MPa and M:O molar ratio of 84:1. A summary of the recently reported studied systems using supercritical methanolysis is given in Table 2.5.

Table 2.5. Recent studies using supercritical methanolysis

Oil Source	Catalyst	Optimum Conditions	Biodiesel yield (%)	References
<i>Jatropha</i> oil	N/A	Temp. 320 °C Pressure: 15 MPa Time: 20 min	84.6	(Samniang et al., 2014)
<i>Krating</i> oil	N/A	Temp: 260 °C Pressure: 16 MPa Time: 10 min	90.4	(Samniang et al., 2014)
<i>Nicotiana tabacum</i> oil	N/A	Temp: 300 °C Time: 90 min M:O ratio 50:1	92.8	(García-Martínez et al., 2017)
Castor oil	N/A	Temp. 265.8 °C Time: 5 min M:O ratio 45:1	96	(Torrentes-Espinoza et al., 2017)
Waste lard	N/A	Temp. 335 °C Pressure: 20 MPa Time: 15 min Dry algae ratio 10:1	89.9	(Shin et al., 2012)
Algal lipids	N/A	Temp. 265 °C Pressure: 11 MPa Time: 50 min M:O ratio 42:1	48	(Jazzar et al., 2015)
Soybean flakes	N/A	Temp. 350 °C Pressure: 20 MPa Time: 3 h M:O ratio 84:1	86	(Xu et al., 2016)
<i>Chrysophyta</i> Algal lipids	N/A	Temp. 340 °C Pressure: 19 MPa M:O ratio 84:1	56.3	(Zhou et al., 2017)
<i>Chlorella sp.</i> Algal lipids	N/A	Temp. 340 °C Pressure: 19 MPa	63.8	(Zhou et al., 2017)

2.3.1.2. Ethanol

Following the findings of the applicability of biodiesel production using non-catalytic single-step reaction *via* supercritical methanol, ethanol was investigated as a potential alcohol for supercritical transesterification. Biodiesel production using supercritical ethanolysis was proposed and examined by Warabi et al. (2004). They investigated several alcohols for supercritical alcoholysis of rapeseed oil including ethanol, 1-propanol, 1-butanol or 1-octanol. They reported longer reaction time for complete conversion required for production of fatty acids ethyl esters (FAEE) in comparison with FAME. They reported higher rate of ethyl esterification of FFA than ethyl transesterification of triglycerides.

Gui et al. (2009) proposed to produce 100% bio-based biodiesel, as they referred to the usage of petroleum based methanol through supercritical methanolysis. However, using bio-ethanol derived from agricultural fermentation process would enhance the sustainability of biodiesel production as it would be purely based on bio-products. They investigated the effect of different reaction parameter on biodiesel yield from palm oil including reaction time, temperature and E:O molar ratio. They reported optimal conditions for 79.2% yield of biodiesel at E:O molar ratio of 33:1 and 349 °C within 30 min reaction time. These findings were followed by a comparative analysis study between supercritical methanolysis and ethanolysis by Tan et al. (2010). They analysed the optimal conditions for supercritical methanolysis and ethanolysis using RSM and compared the optimal conditions and responses between the two methods. They observed lower yield for supercritical ethanolysis than supercritical methanolysis at the same conditions.

Continuous supercritical ethanolysis was reported by Santana et al. (2012) where production of biodiesel was investigated using a continuous fixed bed reactor *via* ion-exchange resin catalyst and CO₂ as a co-solvent. They reported 80% yield of biodiesel only within 4 min reaction at 200 °C, 200 bar and 25:1 E:O molar ratio. They implemented supercritical methanolysis on the same conditions resulting in 90% yield.

The effect of adding catalyst to the supercritical ethanolysis was investigated by Rodríguez-Guerrero et al. (2013) using NaOH. They reported that using only 0.1 wt% of NaOH has significant influence on biodiesel yield. Using Pareto-chart analysis, they reported that temperature has the most significant effect on biodiesel yield followed by reaction time. They achieved maximum biodiesel yield achieved is 98.9% using catalytic process while using non-catalytic method the maximum yield not exceeded 56.2%.

Optimisation of reaction variables is very important to reduce the process consumption of energy resulted from the high reaction conditions of supercritical alcoholysis. Muppaneni et al. (2013) studied the optimisation of biodiesel production from palm oil with the aid of hexane as a co-solvent *via* RSM. They considered four reaction variables for optimisation including E:O molar ratio, temperature, reaction time and co-solvent ratio. They developed a mathematical model representing the biodiesel yield function in the mentioned variables. They reported the optimal conditions for biodiesel production at 35:1 E:O molar ratio, 300 °C and 0.4% v/v co-solvent ratio within 20 min for 90% biodiesel yield. Rade et al. (2015a) optimised biodiesel production from degummed soybean oil using supercritical ethanolysis in a continuous reactor. They considered optimising reaction time, temperature and E:O molar ratio using design of experiments (DOE). Their results showed highly significant effect of all three reaction variables on biodiesel yield. They reported significant negative influence of E:O molar ratio on biodiesel yield. Their reported optimal yield was 62.5% at 320 °C and 15:1 E:O molar ratio within 50 min of reaction. They explained their low yield to the presence of pigments, antioxidants and phospholipids in the feedstock.

Recently, multivariate analysis of supercritical ethanolysis of soybean oil was developed (de Paula Amaral do Valle et al., 2016). In an attempt to cost reduction and simplicity of the process, they used hydrated ethanol with 92.8% w/w for the reaction without preliminary dehydration. They optimised four reaction variables including reaction time, temperature, ethanol/oil molar ratio and the ratio between the reagent volume and reactor volume. They reported optimal conditions for 97.3% yield at 320 °C, 50 min, E:O molar ratio of 49:1, reagent to reactor volume ratio of 60%.

Farobie et al. (2015) designed a novel spiral reactor for biodiesel production using supercritical ethanolsis as shown in Figure 2.5. They examined the effect of E:O molar ratio, temperature and time, at fixed pressure of 20 MPa, on biodiesel yield. They reported 93.7% yield of biodiesel at 350 °C, 1:40 E:O molar ratio in 30 min reaction time. The main advantage of their proposed reactor is the applicability of built-in heat recovery of the reaction products unlike most of the conventional reactors. Coniglio et al. (2014) reviewed most of the supercritical ethanolsis pathways including kinetics, feedstocks and effect of reaction variables. A summary of the recently reported systems using supercritical methanolsis is shown in Table 2.6.

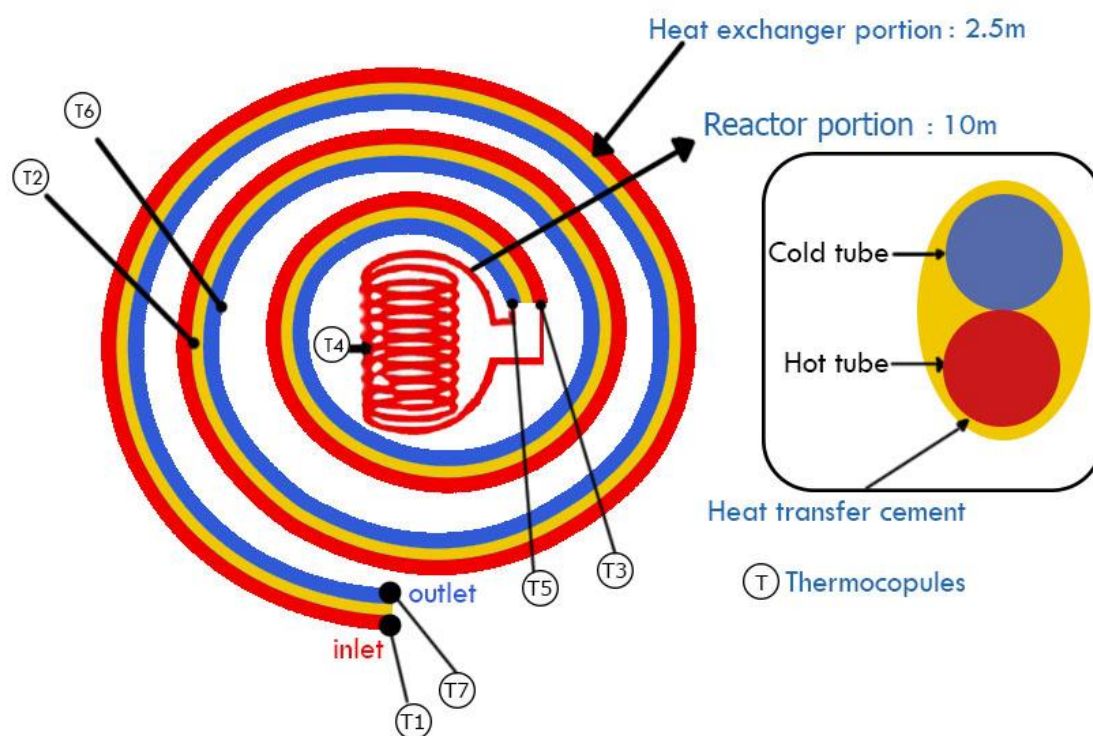


Figure 2.5. Novel spiral reaction used for supercritical ethanolsis, adapted from (Farobie et al., 2015)

Table 2.6. Recently studied systems using supercritical ethanolysis

Oil Source	Catalyst	Optimum Conditions	Biodiesel yield (%)	References
Palm oil	N/A	E:O ratio 33:1 Temp. 349 °C Time: 30 min	79.2	(Gui et al., 2009)
Sunflower oil	N/A	E:O ratio 25:1 Temp. 200 °C Pressure: 20 MPa	80	(Santana et al., 2012)
Palm oil	N/A	E:O ratio 55:1 Temp. 300 °C Time: 20 min	90	(Ponnusamy et al., 2012)
Degummed soybean oil	N/A	E:O ratio 15:1 Temp. 320 °C Time: 50 min	62.5	(Rade et al., 2015a)
Soybean oil	N/A	E:O ratio 49:1 Temp. 320 °C Time: 50 min	97.3	(de Paula Amaral do Valle et al., 2016)
Canola oil	N/A	E:O ratio 40:1 Temp. 350 °C Time: 30 min	93.7	(Farobie et al., 2015)

2.3.1.3. *n*-Propanol and *n*-butanol

Referring to the experimental findings by Man et al. (2014) that low-carbons alcohols are corrosive, hygroscopic and have low heating values, higher-carbon alcohols including propanol and butanol should be considered as alternatives alcohols for biodiesel production. In addition to the petrochemical production, *n*-propanol and *n*-butanol production were reported through fermentation processes of glucose *via* keto-acid pathway without the formation of CO₂ (unlike ethanol) (Man et al., 2014). Warabi et al. (2004) introduced biodiesel production through various alcohols including 1-propanol and 1-butanol. They reported lower methyl esters yield *via* supercritical 1-propanol and 1-butanol in comparison to methanolysis and ethanolysis.

Farobie et al. (2016) extended the research of biodiesel production using supercritical 1-propanol. They investigated the effect of different reaction variables on fatty acid propyl esters (FAPE) yield including reaction temperature and time at constant propanol to oil (P:O) molar ratio of 40:1 and constant pressure of 20 MPa. They reported that biodiesel yield increases with an increase in temperature and time. Additionally, they studied the detailed kinetics and thermodynamics of the reaction. They reported activation energy of conversion of triglyceride to diglyceride, diglyceride to monoglyceride, and monoglyceride to glycerol as 111.39, 78.99, 60.96 kJ mol⁻¹, respectively. Finally, they reported maximum yield of biodiesel of 93.8 mol% at 350 °C within 30 min.

Sun et al. (2014) optimised biodiesel production from camelina sativa oil using supercritical 1-butanol. They systematically investigated the effect of butanol to oil (B:O) molar ratio, temperature and time on the yield of fatty acids butyl esters (FABE). They reported maximum production of biodiesel of 87.6% at 305 °C and 40:1 B:O molar ratio within 80 min reaction time. They reported excellent cold properties of the produced FABEs and high heating value (39.97 MJ/kg). Accordingly, they recommended FABE as ideal transportation fuel. However, the viscosity of the produced FABEs was between 4.95 and 5.21 cSt which is in agreement with the standard ASTM D6751-08 but exceeding the standard European specification EN14214. Farobie et al. (2017) extended the research on supercritical production of FABE using continuous reactor. They studied the effect of wider temperature time range on FABE yield at constant B:O molar ratio of 1:40

and pressure of 20 MPa. Their results showed that the maximum FBE yield of 94.73 mol% has been achieved at 400 °C within 14 min reaction time. They studied the detailed kinetics of the transesterification reaction. They reported that supercritical butanol showed the lowest reactivity among the other lower-carbon alcohols in term of activation energy and reaction rates.

It is worthwhile to remark that there is a gap in the literature regarding the stability of either FAPes or FBEs. The optimal conditions for maximum production of both FAPes and FBEs have been reported at temperatures higher than 300 °C. This should be considered as for further research including thermal, oxidation and storage stability.

2.3.2. Glycerol-free biodiesel production

The world-wide biodiesel production has increased during the last decades and developed through various techniques. Subsequently, a huge production of crude glycerol (side-product) was reported recently which is beyond the market needs. Accordingly, a steep drop of the glycerol price was reported through the last years. In addition, the contamination of methanol in glycerol make the crude produced glycerol unsuitable for consumers. Hence, vacuum distillation of the produced glycerol is required to achieve the pharmaceutical grade glycerol. The high availability of the crude glycerol resulted from transesterification reaction made this treatment uneconomical (Ang et al., 2014).

As a consequence, valorising of crude glycerol to value added chemicals was considered. Numerous chemicals were reported based on crude glycerol as a raw material (Garlapati et al., 2016; Luo et al., 2016; Magdoui et al., 2017; Ren and Ye, 2015; Vlysidis et al., 2011). Other researchers reported capturing of CO₂ and reacting it with glycerol for production of value-added glycerol carbonate. Hence, it would help in minimising greenhouse gases and valorising glycerol to valuable chemical (Esteban and Vorholt, 2018; Liu and He, 2018; Wan et al., 2018).

Recently, glycerol-free biodiesel production processes were reported where alcohols are replaced with other chemicals during the transesterification reaction. Hence, glycerol production is substituted with other value-added chemicals based on the reactants.

Several alternatives for alcohols were reported including methyl acetate, dimethyl carbonate (DMC) and methyl *tert*-butyl ether (MTBE) (Farobie and Matsumura, 2015; Goembira and Saka, 2015; Ilham and Saka, 2010)

2.3.2.1. Methyl acetate

Saka and Isayama (2009) proposed substitution of alcohols with methyl acetate through supercritical production process. They reported that production of triacetin has higher value than glycerol. They confirmed the applicability for non-catalytic production of FAME using supercritical methyl acetate. They analysed different properties of the produced biodiesel including kinematic viscosity, pour point and plugging point. Additionally, they reported that blending FAME with the triacetin (bi-product) has a significant effect on improving the pour point and oxidation stability of biodiesel. Hence, biodiesel fuel blend yield would increase up to 105%. However, they reported that the blend should not exceed 20% as the kinematic viscosity of the mixture exceeded the standard specifications for biodiesel.

Goembira and Saka (2013) studied the optimisation of biodiesel production via supercritical methyl acetate. They considered reaction temperature, pressure, time and molar ratio of methyl acetate to oil through the optimisation process. They reported that up to 300 °C FAMEs have not been observed where the conversion starts with a very low rate at 320 °C. The highest yield of FAMEs obtained using supercritical methyl acetate is 96.7 wt% and 8.8 wt% of triacetin (combined blend fuel yield of 105.5 wt%) at 350 °C and 20 MPa within 45 min. Niza et al. (2013) investigated the thermal stability study for the FAME and triacetin obtained from supercritical methyl acetate transesterification. They reported that methyl-oleate decomposition recorder significant occurrence at higher temperatures than 390 °C. However, poly-unsaturated methyl esters including methyl linoleate and linolenate showed very high degradation at 390 °C where less than 50% were recovered from them. Similarly, triacetin has shown high degradation rate beyond 360 °C. They have recommended to operate the reaction at temperatures below 360 °C where still it is applicable to obtain high yield of FAME but at longer time.

Goembira and Saka (2014) extended their initial findings and investigated the effect of additives in lowering the supercritical methyl acetate conditions and overcoming the low

transesterification reaction rate. Additionally, the purpose of the additives is to avoid exceeding the reaction limits for thermal degradation. Different additives were evaluated including oleic acid, acetic acid, methanol and water. They reported significant improvement of the supercritical methyl acetate transesterification by adding water and/or acetic acid. They explained the process improvement by adding acetic acid, which acts for decomposition of triglycerides to FFAs and triacetin. Hence, higher FAME were obtained due to the higher reactivity of methyl acetate to FFAs than triglycerides. Additionally, adding water led to hydrolysis of triglycerides to FFAs and glycerol and hence increasing FAMEs. They reported that acetic acid and water mixture (aqueous solution) would have highly significant enhancement of FAMEs production. The highest yield of FAMEs of 96.8 wt% and 12.9 wt% of triacetin (combined blended fuel yield of 109.7 wt%) was achieved at milder conditions of 300 °C, 20 MPa and 42:1 molar ratio of methyl acetate to oil within 45 min reaction time after adding 10% of aqueous solution of acetic acid (concentration of 26 wt%).

The same authors implemented their findings on high acidity crude non-edible oil (*Pongamia pinnata*) (Goembira and Saka, 2015). They reported that the high acidity of the feedstock has no effect on high biodiesel producibility. Using their previously recommended optimal conditions and adding 10% of aqueous solution of acetic acid (concentration of 26 wt%), they reported 96.6 wt% of FAME and 11.5 wt% triacetin yields (combined blended fuel yield of 108.1 wt%). They examined the properties of the produced fuel where it was observed that it complies with the standard specifications.

Recently, Farobie and Matsumura, (2017b) studied continuous production of biodiesel using supercritical methyl acetate. They reported significant production of biodiesel at 380 °C and 20 MPa within 10 min. They studied the detailed kinetics of the reaction where they have reported unstable intermediate components. As a result, they reported that the reactivity of supercritical methyl acetate is very low and hence, required high temperatures. They compared the reactivity of supercritical methyl acetate, methanol, ethanol and MTBE under otherwise identical conditions. They reported that methyl acetate has the lowest reactivity followed by MTBE, ethanol and finally methanol.

2.3.2.2. Dimethyl Carbonate (DMC)

DMC is considered as an environmentally benign compound with versatile chemical properties. It is a non-toxic and biodegradable material that were considered as a green reagent for several applications. Many greener routes of DMC synthesis were reported as alternative methods for the conventional synthesis that include utilisation of phosgene which is considered as a toxic material. Recently, greener synthesis of DMC was reported by reacting CO₂ and methanol with the aid of different nanocomposite catalysts (Saada et al., 2018, 2014). Thus, utilisation of DMC for biodiesel production would develop a sustainable process where it assists reduction of greenhouse gases and producing green fuels with higher added value by-products rather than glycerol.

Ilham and Saka, (2009) introduced production of biodiesel using supercritical DMC. They reported that the reaction includes two-steps where firstly, triglyceride reacts with DMC to produce 2 moles FAME and fatty acid glycerol carbonate (FAGC). This is followed by reaction between FAGC again with DMC to produce 1 mol of FAME molecule and glycerol decarbonate. The other pathway of FFAs reaction with DMC produces FAMEs and glyoxal. They reported 94 wt% of FAME within 12 min at 350 °C and 12 MPa. They also mentioned that the by-product produced from the reaction including glycerol carbonate and citramalic acid are much higher is value than the conventional glycerol. They reported similar reactivity of DMC and methanol with triglycerides which proposing an alternative potential path for glycerol-free biodiesel synthesis.

The same authors extended their findings and proposed a novel two-steps production of biodiesel from *Jatropha curcas* oil by hydrolysis of oil in water followed by supercritical esterification of FFAs using DMC (Ilham and Saka, 2010). Their proposed method has achieved high yield of FAMEs at excellent agreement with biodiesel with biodiesel standards. The have reported 97 wt% of FAMEs by subcritical hydrolysis of triglycerides at 270 °C and 27 MPa for 25 min followed by supercritical esterification using DMC at 300 °C and 9 MPa for 15 min. They reported that this method is ideally for feedstock with high FFAs where complete hydrolysis of triglycerides would occur. Additionally, Ilham and Saka (2012) studied the optimisation of biodiesel production using supercritical DMC.

They have studied important reaction parameters for the optimisation process including reaction temperature, pressure, time, molar ratio of DMC to oil. They considered other dependant variables for selecting the optimal conditions including degree of denaturation, thermal decomposition, oxidation stability and fuel properties. They reported the optimal conditions for 97 wt% biodiesel yield at 300 °C and higher pressure 20 MPa pressure within 30 min reaction time.

2.3.2.3. Methyl *tert*-butyl ether (MTBE)

MTBE is a chemical compound that is synthesised by a chemical reaction between methanol and isobutylene. MTBE has been extensively used as an octane enhancer for gasoline engines. It was considered as one of the most powerful oxygenates and hence, it has been used widely for as a gasoline additive for improving the engine performance (Awad et al., 2018; Levchuk et al., 2014). MTBE was used broadly through the last decades. In 1998, only the USA produced more than 8.8 million tonnes of MTBE. In 2015, China consumed 7.3 million tonnes of MTBE in gasoline. However, the contamination of MTBE in soils and groundwater resulted in more than 250,000 contaminated sites only in USA. The contamination of MTBE was also detected at many European countries (Ma et al., 2017). Subsequently, MTBE was banned from being used as an additive in many countries including USA. Many researches were implemented to study the water treatment contaminated with MTBE using different technologies (Kiadehi et al., 2017; Wu, 2011; Xie et al., 2016; Zadaka-Amir et al., 2012).

Farobie et al. (2014) proposed the implementation of MTBE as a potential reactant for biodiesel production. Due to strong movement of banning MTBE from being used as octane enhancer, the authors proposed implementing MTBE in the transesterification reaction. Theoretically, the reaction of triglycerides with MTBE would result in FAMES and glycerol *tert*-butyl ether (GTBE) (1,2,3-tri-*tert*-butoxy-propane). They reported that GTBE would be an efficient replacement to MTBE as a green octane enhancer. In essence, the process would utilise a readily available compound for biodiesel production in addition to production of a valuable octane enhancer. The authors reported maximum production of biodiesel 94 wt% at MTBE to oil ratio of 40:1 at 400 °C in 12 min reaction time. A first

order reaction kinetic data was successfully fitted to the experimental results. The detailed transesterification kinetic results were reported.

Farobie and Matsumura (2015) developed a comparative study between biodiesel production using supercritical methanol ethanol and MTBE. They investigated the effect of temperature and residence time on biodiesel yields. They reported that optimal biodiesel yield was reached at 350 °C and 20 MPa within 10, 30 and 30 min for supercritical methanol, ethanol, and MTBE, respectively.

Lamba et al. (2017) investigated biodiesel production from neem and mahua oil using both supercritical methanol and MTBE. The effect of reaction temperature, pressure, time and molar ratio of both reactants with oils were highlighted. They reported thermal degradation due to pyrolysis of FAMEs at high temperatures. They also reported that methanol is more reactive than MTBE in supercritical transesterification. For supercritical methanol, they reported 83% and 99% conversions in 15 min and 10 min at 698 K for neem and mahua oil, respectively. However, for supercritical MTBE, they reported 46% and 59% conversions in 15 min at 723 K for neem and mahua oil, respectively. They studied the kinetics of the reaction resulting in pseudo first order reaction.

2.4. Effect of different supercritical reaction variables on biodiesel production

This section reviews the recent observation of the effect of different supercritical reaction variables on biodiesel production. A comprehensive discussion has been reported for the effect of each variable. Most of the researchers have investigated the linear effect of each variable based on one-factor-at-a-time (OFAT) methodology. Lately, the interactive effects of different reaction variables on the reaction responses have been reported in the literature. This section highlights the recently reported influences of different variables from a variety of feedstocks.

2.4.1. Effect of reaction temperature

Reaction temperature is an important parameter affecting supercritical reaction. The minimum operating temperature should be higher than the critical point of the implemented alcohol in the reaction i.e. 239 °C for methanol. Different studies reported the effect of reaction temperature on biodiesel production. Most of the published studies reported that reaction temperature significantly increases the reaction rate where biodiesel yield increases 2-3 times when the temperature increases from 200 and 350 °C. In addition, the increasing effect of temperature between 200 and 280 °C increases the conversion up to 7 times (Sawangkeaw et al., 2010).

Zhou et al. (2017) reported the influence of reaction temperature on *in-situ* supercritical extraction and transesterification of algal lipids. They studied the effect of four different temperatures e.g. 250, 300, 340 and 360 °C. They observed that FAME yield was increased up to 340 °C reaching 54.5%. Similarly, Jazzar et al. (2015) reported increasing effect of reaction temperature on *in-situ* supercritical extraction and transesterification of algal lipids. They reported that beyond 265 °C, the yield of FAMEs starts to decrease.

Salar-García et al. (2016) reported increasing effect of reaction temperature for biodiesel production from *Jatropha* oil. They studied the effect of temperature for both triglycerides conversion and FAME yield. They observed higher conversion and yield at 350 °C. However, they reported that the product showed higher continuous stability at 325 °C.

Similarly, Qiao et al. (2017) reported increasingly effect of temperature on FAME yield from soybean oil. Using castor oil as a feedstock, it was reported that FAME yield increased by increasing temperature up to 300 °C where thermal degradation was observed at longer reaction time (Román-Figueroa et al., 2016). Using canola oil, Farobie et al. (2017) investigated the effect of reaction temperature on butyl transesterification. The yield of butyl esters was increased by increasing the temperature between 270 to 400 °C. They studied the effect of temperature on the intermediate products including diglycerides and monoglycerides in addition to glycerol yield. Teo et al. (2015) reported 93% FAME yield from *Jatropha* oil at mild reaction temperature just above the critical point of methanol. They used mixture of calcium and lanthanum mixed oxides (CaLaO) as a catalyst to lower the supercritical conditions. Table 2.7 summarise the effect of reaction temperature on FAME yield from different feedstocks.

Table 2.7. Summary of the effect of reaction temperature on SC biodiesel production

Oil Sources	Catalyst	Co-solvent	Effect of temperature	Studied range (°C)	Optimum temperature (°C)	Biodiesel yield (%)	References
Algal lipids	N/A	n-hexane	positive	250-360	340	58	(Zhou et al., 2017)
Algal lipids	N/A	N/A	positive	245-290	255-256	48	(Jazzar et al., 2015)
<i>Jatropha</i> oil	N/A	N/A	positive	250-350	325	99.5	(Salar-García et al., 2016)
Soybean oil	N/A	N/A	positive	250-350	350	88	(Qiao et al., 2017)
Castor oil	N/A	N/A	positive	250-350	300	96.5	(Román-Figueroa et al., 2016)
Canola oil	N/A	N/A	positive	270-400	400	94.73	(Farobie et al., 2017)
<i>Jatropha</i> oil	CaLaO	N/A	positive	200-280	240	93	(Teo et al., 2015)
Soybean flakes	N/A	N/A	positive	0-300	180	86	(Xu et al., 2016)

Tan et al. (2010) optimised the biodiesel production from palm oil using RSM. They reported the interactive effect between reaction temperature and M:O molar ratio as shown in Figure 2.6. They reported that at low value of M:O molar ratio, the effect of reaction temperature is directly proportional with the yield of FAMEs. However, due to the significant interaction between the two variables, at high M:O molar ratio, the effect of temperature on biodiesel yield increases up to a certain temperature and then the yield decrease. Additionally, they reported the interactive effect between E:O molar ratio and temperature. This showed highly interactive effect where at molar ratio of ethanol, the reaction temperature has positive influence on biodiesel yield. However, at higher ratio of ethanol increasing the temperature has negative influence on biodiesel yield. Similarly, Ang et al. (2015) reported a significant interactive effect of reaction temperature and time on biodiesel yield. They reported different effect of reaction time on biodiesel yield and different levels of reaction temperature. The interactive effect displays the full effect of specific variables at different levels of other variables.

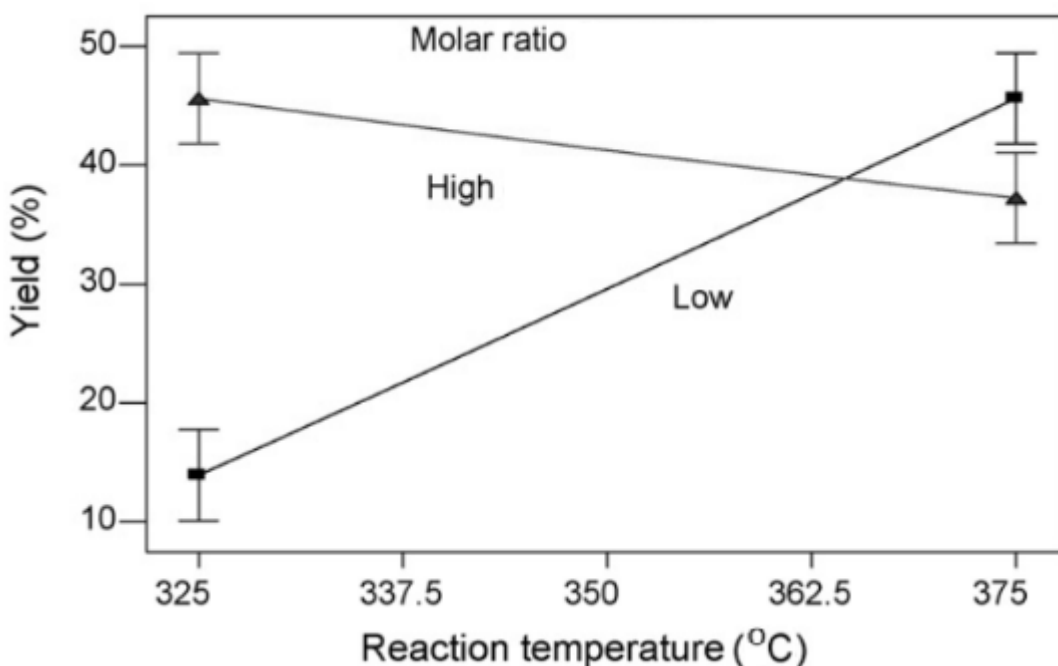


Figure 2.6. Interactive effect between reaction temperature and M:O molar ratio
(adapted from (Tan et al., 2010))

For WCO, Ghoreishi and Moein (2013) reported a significant interactive effect for reaction temperature with M:O molar ratio. They reported increasing effect of biodiesel yield by increasing the temperature at low molar ratio. However, at high molar ratio, the effect of temperature is positive up to 270 °C whereas beyond that temperature the biodiesel yield decreases.

2.4.2. Effect of reaction pressure

Previously, the pressure was not considered as an independent variable affecting the reaction where its value was monitored and reported by increasing temperature (Sawangkeaw et al., 2010). However, the recent studies considered pressure as a controllable parameter where the effect of pressure was studied at different levels.

Qiao et al. (2017) investigated the effect of reaction pressure on FAME yield. They reported increasingly effect of reaction pressure on biodiesel yield. They referred their findings in respect to the solubility between oil and methanol. They reported that at higher pressure, the solubility parameters difference between oil and methanol decrease specially beyond the critical pressure. Similarly, Xu et al. (2016) also reported an increasing effect of pressure on FAME yield from soybean flakes lipids. They studied a range of temperature between 14 and 22 MPa where they observed optimal pressure of 20 MPa for 86% yield of FAMEs.

The interactive effect of reaction pressure with reaction time with the response was infrequently reported in the literature. Ghoreishi and Moein (2013) reported a significant effect between reaction temperature and pressure on biodiesel yield. Table 2.8 summarise the effect of reaction pressure on FAME yield from different feedstock.

Table 2.8. Summary of the effect of reaction pressure on SC biodiesel production

Oil Sources	Catalyst	Co-solvent	Effect of pressure	Studied range (MPa)	Optimum pressure (MPa)	Biodiesel yield (%)	References
Soybean oil	N/A	N/A	positive	10-22	22	88	(Qiao et al., 2017)
Soybean flakes	N/A	N/A	positive	14-22	20	86	(Xu et al., 2016)

2.4.3. Effect of reaction time

Transesterification reaction time using supercritical technology is significantly lower than the conventional reaction methods. In addition, it is one of the main advantages of applying supercritical technology for biodiesel production. Generally, the optimum time for batch reactor operation is between 4 and 30 min based on the reaction conditions (Sawangkeaw et al., 2010). Saka and Kusdiana (2001) have reported high yield production of biodiesel from rapeseed oil in 4 min.

Zhou et al. (2017) reported the influence of reaction time on *in-situ* supercritical extraction and transesterification of algal lipids. They reported that the FAME yield increased up to 2 h and then decreased at longer reaction durations. They explained their findings as after 2 h, the rate of the extracted lipids decreased where FAME yield decreases accordingly. Similar results been reported for biodiesel production of biodiesel from wet microalgae (Jazzar et al., 2015). However, they investigated the effect of reaction time up to 50 min where they observed the highest yield of FAME at 50 min. On the other hand, Xu et al. (2016) investigated the effect of time on *in-situ* supercritical extraction and transesterification of soybean flakes where they concluded positive effect up to 3 h.

Salar-García et al. (2016) reported increasing effect of reaction time for biodiesel production from *Jatropha* oil. They studied the effect of time of both triglycerides conversion and FAME yield. They reported a huge conversion of triglycerides within

15 min followed by slightly increase in the conversion rate within longer time. However, reaction time has highly significant effect on FAME where the yield increases at longer reaction time. This referred to the intermediate components that were not completely converted yet to FAME. Similarly, biodiesel yield derived from castor oil increase at longer reaction times with optimum duration of 90 min (Román-Figueroa et al., 2016). Qiao et al. (2017) also reported an increasing effect of reaction time on biodiesel yield from soybean oil using Dixon rings packed reactor. They reported steep rise in yield within the first 30 min with insignificant increase at longer reaction time. However, other researchers reported 94.73% biodiesel (butyl esters) yield from canola oil only in 14 min using a continuous reactor. Using CaLaO catalyst, Teo et al. (2015) produced high yield of biodiesel from *Jatropha* oil in only 10 min reaction time. Table 2.9 summarise the effect of reaction time on FAME yield from different feedstock.

Table 2.9. Summary of the effect of reaction time on SC biodiesel production

Oil Sources	Catalyst	Co-solvent	Effect of time	Studied range (min)	Optimum time (min)	Biodiesel yield (%)	References
Algal lipids	N/A	n-hexane	positive	0-300	120	58	(Zhou et al., 2017)
Algal lipids	N/A	N/A	positive	0-50	50	48	(Jazzar et al., 2015)
<i>Jatropha</i> oil	N/A	N/A	positive	0-90	90	99.5	(Salar-García et al., 2016)
Soybean oil	N/A	N/A	positive	0-180	40	88	(Qiao et al., 2017)
Castor oil	N/A	N/A	positive	0-90	90	96.5	(Román-Figueroa et al., 2016)
Canola oil	N/A	N/A	positive	0-30	14	94.73	(Farobie et al., 2017)
<i>Jatropha</i> oil	CaLaO	N/A	positive	5-25	10	93	(Teo et al., 2015)
Soybean flakes	N/A	N/A	positive	0-300	180	86	(Xu et al., 2016)

García-Martínez et al. (2017) optimised biodiesel production from tobacco seed oil. They reported a significant interaction between reaction time and temperature. The effect of reaction time at lower temperature has positive influence on biodiesel yield. However, at higher temperatures, increasing the temperature has decreasing the biodiesel yield. They addressed the thermal degradation of products as a reasonable cause for the yield drop at longer high temperatures reactions. Similarly, Ang et al. (2015) reported significant effect of both combination of reaction time-M:O molar ratio and reaction time-temperature on biodiesel yield.

2.4.4. Effect of alcohol to oil ratio

The stoichiometric ratio of alcohol (mainly methanol) to oil molar ratio is 3:1, while the actual operating ratio usually varies from 3:1 up to 50:1. A large excess of methanol is usually required for high reaction rate as the high ratio of methanol increases the contact area with oil and decrease the transition temperature difference between of vapour-liquid-liquid (VLL) to vapour-liquid (VL) equilibria. It was reported that the mixture is partially miscible at 350 °C and 24:1 M:O molar ratio. However, at higher molar ratios e.g, 40:1 and 65:1, the mixture is completely miscible at even lower temperatures of 180 °C and 157 °C, respectively (Sawangkeaw et al., 2010). Alternatively, Qiao et al. (2017) investigated the effect of M:O molar ratio where they observed increasingly effect of molar ratio on biodiesel yield up to 42:1. They explained the decreasing effect of biodiesel yield at higher molar ratios of methanol as the huge excess of methanol dilute the reaction system and hence decrease the reaction rate. Teo et al. (2015) used CaLaO catalyst to decrease the required M:O molar ratio. They studied the effect of M:O molar ratio between the range of 14:1 and 36:1, where they observed increasing effect of FAME yield while increasing the molar ratio up to 28:1.

In-situ extraction and transesterification of algal lipids consumes excess of methanol due to the poor contact between oil and methanol from using excessive CO₂ for extraction (Jazzar et al., 2015). Zhou et al. (2017) reported the influence of M:O molar ratio on in situ supercritical extraction and transesterification of algal lipids. They reported that the FAME yield increased while increasing the ratio between 21:1 and 84:1 where higher ratios resulted in decreasing FAME yield. Xu et al. (2016) reported 41:1 M:O molar ratio

for in situ extraction and transesterification of soybean flakes lipids. The effect of reaction temperatures on FAME yield from different feedstocks are summarised in Table 2.10.

Tan et al. (2010) reported highly interactive effect of M:O molar ratio and reaction time. They observed different increasing effect of reaction time on biodiesel yield at different M:O molar ratio whereas at the higher molar ratio, the effect of temperature on biodiesel yield is more significant than at lower molar ratio.

Table 2.10. Summary of the effect of methanol to oil ratio on SC biodiesel production

Oil Sources	Catalyst	Co-solvent	Effect of methanol ratio	Studied range	Optimum ratio	Biodiesel yield (%)	References
Algal lipids	N/A	n-hexane	positive	21:1-126:1	84:1	56.31	(Zhou et al., 2017)
Soybean oil	N/A	N/A	positive	28:1-50:1	42:1	88	(Qiao et al., 2017)
<i>Jatropha</i> oil	CaLaO	N/A	positive	14:1-36:1	21:1	93	(Teo et al., 2015)
Soybean flakes	N/A	N/A	positive	12:1-50:1	42:1	86	(Xu et al., 2016)

2.5. Progress in supercritical biodiesel process design and simulation

Process design and simulation is considered as an initial step to assess the commercial feasibility of a process. A complete simulation for the proposed process is initially designed using a software by implementing the real plant data. Even with some expected difference between the real plant data and the simulated results, several available simulation software programs provide reliable results with acceptable relative errors from the real data. This is due to the advanced calculation methods based on accurate thermodynamic packages in addition to the numerous available components in the software libraries (Zhang et al., 2003).

The process design procedures involve systematic steps that start by defining of the chemical components required for the process. This is followed by selecting a suitable thermodynamic fluid package that suits the available reactions in the process. Further, the procedures continued by defining the chemical reactions of the process and providing the available data for the reaction (kinetic data), selecting the necessary units for the process i.e. reactor, mixer, distillation column, heat exchanger. Finally, the process is finalised by setting up the conditions of each process stream and operational unit i.e. temperature, pressure, flowrate, etc.

For biodiesel production, the process depends on the implemented methodology where using homogeneous catalysed process is different to either heterogeneous or non-catalytic processes. Generally, the production process is composed of different steps including pre-treatment of the oil, transesterification and/or esterification reaction, alcohol recovery and biodiesel purification.

2.5.1. Chemical components selection

The selection of chemical components of the process including all the reactants, products, catalysts and by-products is considered the initial step for the process design. The components vary based on the production methods. Frequently, methanolysis of both triglycerides and FFAs is regarded as the main implemented process. Accordingly, alcohols (available in the software library) are considered the first component in the

process (recently, some processes include glycerol-free biodiesel production where alcohols do not exist in the process). Secondly, the oil chemical component is mainly based on the composition of the oil. Typically, the oil consists of triglycerides and FFAs.

The chemical component that does not exist in the software library should be defined manually. The components definition occurred by providing the physical and chemical properties of the chemical component including density, critical conditions, boiling points, chemical structure, molecular weight, etc. Santana et al. (2010) designed and simulated biodiesel production from castor oil. The major component that represents castor oil is triricinolein which do not exist in the HYSYS software library. Subsequently, they introduced both triricinolein and ethyl ricinoleate by defining specific properties including acentric factor, critical temperature, critical pressure and molecular weight. Other components necessary for the process should be selected including catalysts, washing fluid, cooling fluid and extricating chemicals. These components depend on the selected biodiesel production methodology.

2.5.2. Thermodynamic model selection

Numerous thermodynamic models were developed to represent actual behaviour of the fluids during both chemical reactions and physical interactions. The thermodynamic models include both equation of states (EoS) and other special activity models for specific components reactions. The remarkable characteristic of biodiesel transesterification and/or esterification reaction boosted the research for suitable thermodynamic model to represent the phase equilibrium of the stated reactions.

The UNIFAC thermodynamic model was applied to model water, acid and short chain esters liquid-liquid equilibrium (LLE) ternary system. It was used widely in biodiesel process simulations with considerable results. Alternatively, non-random two liquid (NRTL) method was developed representing the correlation between ternary mixture of water, short chain esters and methanol/propanol on LLE system. It correlated the vapour-liquid equilibrium (VLE) system for mixtures of ethanol and methyl esters. Accordingly, NRTL was considered as the default thermodynamic model representing

transesterification/esterification reactions. Additionally, some other cubic models were developed representing CO₂ and short chain esters mixtures. Moreover, The Group Contribution with Association Equation of State (GCA-EoS) was extended to include fatty acid alkyl esters. It also used to predict the phase equilibria at high pressures and with other supercritical fluids (Cotabarren et al., 2014).

For supercritical transesterification/esterification fluids, it is not recommended to use NRTL activity model for the process simulation except through the reaction. At higher temperatures and/or high pressures VLE polar mixtures, it is preferable to use one of the combined equation of states (CEoS) resulted from the combination of GCA-EoS with Gibbs extended models including Peng Robinson and Soave-Redlich Kwong (SRK) (Bender et al., 2013). Recently, some researchers reported using NRTL only at the biodiesel reactor while shifting directly to Peng-Robinson EoS for other processing units e.g. heating, cooling and separating units (Lee et al., 2011).

2.5.3. Reactants pre-treatment

The pre-treatment of the reactants is considered as the first step for biodiesel synthesis. The pre-treatment processes involve several steps which are selected based on the feedstock and the implemented method. Pre-treatment could be defined as sustaining the reactants at the required conditions for the reaction i.e. temperature, pressure, acid value and residuals. West et al. (2008) designed and simulated four different processes for biodiesel production e.g. alkaline homogeneous catalysed, acidic homogeneous catalysed, alkaline heterogeneous catalysed and supercritical non-catalysed processes. They have used WCO with 5 wt% of FFA as a feedstock. Using the conventional homogeneous catalysed process, esterification of FFAs in the feedstock is considered as an essential requirement. The conversion of FFAs was simulated by esterification reaction using methanol. Hence, the pre-treatment processes include heating, cooling, separating and reaction units. However, the pre-treatment process is simpler for both heterogeneous catalysed and supercritical processes where only the pre-treatment includes mixing and maintain the reactants at the required temperature and pressure.

2.5.4. Reactor simulation

In process simulation, the simplest method to represent any chemical reaction is by using a conversion shortcut reactor. It is a tool that is used to simulate any chemical reaction based on the defined conversion without any considerations for the kinetics of the reaction. Several studies have been reported by simulating the transesterification and/or esterification reaction using conversion shortcut reactor (Budiman Abdurakhman et al., 2018; Lee et al., 2011; West et al., 2008).

Supercritical production of biodiesel requires a large excess of alcohol in order to shift the reaction towards the products. This has highlighted the problem of excessive consumption of energy required for alcohol recycling. According to Le Chatelier's principle, the reversible reaction could be shifted towards the product by either increasing the concentration of the reactants or decreasing the concentrations of the products. As a result, alternative methods have been implemented to decrease the concentration of products including reactive distillation (RD) method. RD operates both reaction and separation of the products simultaneously in a single unit operation. Hence, the chemical equilibrium is shifted toward the product without the need to adding huge excess of reactants (Boon-anuwat et al., 2015).

Boon-anuwat et al. (2015) designed and simulated two processes for biodiesel production using RD unit with both homogeneous alkaline and heterogeneous acidic catalysed systems. They also compared the designed processes' efficiency with the conventional reactor/distillation processes. They reported that using RD processes have a significant influence on reducing the required methanol, increasing biodiesel yield and eliminating the product separation at lower energy requirements in comparison to the conventional reactor/distillation processes. Recently, Petchsoongsakul et al. (2017) designed and simulated a novel hybridised esterification/transesterification reaction simultaneously in a single RD unit. They used two different heterogeneous catalysts for the process. They loaded Amberlyst-15 catalyst from the top stage of the column for FFAs esterification in addition to CaO/Al₂O₃ catalyst loading from the bottom stage for transesterification of triglycerides. They reported that using the proposed RD significantly reduced the amount

of required methanol, number of process equipment and energy consumption in comparison with the two reactive distillation systems.

Budiman Abdurakhman et al. (2018) designed and simulated biodiesel production process from WCO using catalytic membrane reactor (CMR). They compared their process with the conventional alkaline homogeneous catalysed process. They reported that catalysed membrane reactor has overcome the high acidity of the feedstock and enhanced the process intensification. They also reported that it is economically preferable than the conventional process.

Martinovic et al. (2018) performed a simulation-based techno-economic analysis for biodiesel production. The analysis was constructed to compare between biodiesel production from WCO using single step supercritical transesterification and two-steps reactions including hydrolysis of triglycerides and subsequent supercritical methyl esterification. They reported that both methods represent viable processes for biodiesel production from low quality feedstock. They reported that the two-steps reactions method has required milder process conditions where biodiesel is produced at lower cost in comparison with single-step reaction method. However, they reported that the two-steps reactions method required higher energy requirement per unit of biodiesel output. They recommended the implementation of comprehensive heat integration through the process.

2.5.5. Product separation

For the conventional glycerol-accompanied reaction, the transesterification reaction product mainly composed of alkyl esters (biodiesel), glycerol, unreacted alcohol and unreacted triglycerides. Several processes were applied to the product stream in order to have biodiesel in the pure form.

Firstly, the excess of alcohol (mostly methanol) is separated. Most of the published researches have used a distillation column to separate the excess alcohol (Budiman Abdurakhman et al., 2018; Lee et al., 2011; Sajid et al., 2016; West et al., 2008). For supercritical reactions, the enthalpy of the product stream is used to separate most of the

excess methanol through simple flash drum prior to distillation to minimise the energy required for separation (Lee et al., 2011). Glycerol separation from the product stream is an essential that could be performed using different methods, e.g. gravity settling, distillation and washing. Gravity settling using a decanter was reported in most of the literature for glycerol separation. The residuals of triglycerides in the biodiesel is also separated using vacuum distillation unit (VDU) (Granjo et al., 2017; Lee et al., 2011; Marulanda, 2012; Sajid et al., 2016; West et al., 2008).

2.5.6. Process energy integration

Supercritical transesterification and/or esterification require high operational conditions including temperature and pressure. The utilisation of the produced heat from the reaction is a vital step to minimise the cost of biodiesel. On the reactor scale, supercritical production of biodiesel is extensively higher in cost and energy consumption. However, these high energies could be utilised on the process scale by heat integration methods.

Several researchers reported different integration strategies for biodiesel production. Lee et al. (2011) designed and simulated a biodiesel production using supercritical methanol. They introduced two heat exchangers within the process to minimise the process cooling and heating energy requirements.

Fu et al. (2015) designed and simulated an integrated process for biodiesel production from WCO using acidic catalysed process. They developed a new approach for self-heat recuperation through their process. They compared their approach with the conventional process where it has resulted in energy savings of 83.5%, 88.4% and 58.8% for methanol recovery, biodiesel purification and glycerol purification stages, respectively. They reported that their approach has reduced the overall energy consumption by 71%. Other researchers proposed process integration approaches to optimise energy consumption through minimising waste heat through exergy analysis, integrated biorefinery and Pinch technology (Granjo et al., 2017; Gutiérrez et al., 2009; Martin et al., 2016; Song et al., 2015).

Gutiérrez Ortiz and de Santa-Ana, (2017) designed and simulated an energy self-sufficient process for biodiesel production using supercritical methanolysis. They used WCO as a feedstock and propane as a cosolvent. Their reaction take place at 280 °C, 128 bar in 9.7 min. Their techno-economic study resulted in biodiesel cost of 0.479 EUR/kg.

The research on process simulation and integration of supercritical production of biodiesel was increased dramatically in recent years. This is due to the process applicability and profitability in the laboratory scale where it is necessary to apply it on the pilot scale as an initial step for industrial scale. Most of the economic assessments ensure that the supercritical process is preferable and economically viable and profitable.

2.6. Conclusions

Biodiesel production using supercritical technologies has numerous advantages over conventional catalysed processes including higher reaction rates, higher biodiesel yield, shorter reaction time and applicability of a variety of feedstock. However, the harsh reaction conditions i.e. high temperature and pressure, require specific reactor materials that can stand these conditions in addition to the health and safety concerns are considered as the main obstacles for scaling-up of the process. Apart from several reported techniques in the literature for biodiesel production technologies, this work has focused on the valorisation of WCO into biodiesel using supercritical methanolysis.

CHAPTER 3

BIODIESEL SYNTHESIS FROM LOW ACIDITY WASTE COOKING OIL

Outline of the chapter

This chapter illustrates the conversion of low acidity WCO into biodiesel. Experimental design, modelling and optimisation are considered. A kinetic study for the transesterification reaction is reported. The chapter is organised as follows:

3.1. Introduction

3.2. Materials and methods

3.3. Results and discussion

3.4. Conclusions

3. Biodiesel synthesis from low acidity waste cooking oil

3.1. Introduction

In this chapter, RSM using BBD has been used to optimise production of biodiesel from the WCO using CO₂ gas as a co-solvent. The independent variables in the modelling process are M:O molar ratio, temperature, pressure and time. Biodiesel yield has been considered as the dependent response variable. ANOVA has been used to analyse the significance of the statistically developed regression model which represents the dependant variable function of all the independent variables. Physiochemical properties of the produced biodiesel have been analysed and compared to the biodiesel standard EN 14214. Kinetics of the overall transesterification reaction has been studied concluding the relevant kinetic and thermodynamics reaction constants. Finally, a kinetic reactor for the transesterification reaction has been simulated using HYSYS simulation programme based on the experimentally kinetic data.

3.2. Materials and methods

3.2.1. Materials

WCO was supplied by Uptown Biodiesel Ltd., UK. Methanol 99% (MeOH) was purchased from Fisher Scientific, UK. The standard methyl esters used for preparing calibration curves and the heptadecanoic acid methyl ester used as an internal standard were purchased from Merck, UK. The liquid CO₂ cylinder (99.9%) equipped with a dip tube was purchased from BOC Ltd., UK.

3.2.2. Experimental setup

WCO was filtered to remove the suspended particles from the cooking process. The supercritical reaction of biodiesel production was carried out in a 100-mL high pressure reactor made of stainless steel (model 49590, Parr Instrument Company, USA) which was fitted with a thermocouple (type J), heating mantle, controller (model 4848) and a mechanical stirrer. Figure 3.1 shows a schematic for the experimental setup. The oil and methanol with a specific molar ratio were added to the reactor then heated with

continuously stirring at constant rate of 300 rpm to the targeted temperature. Then, supercritical fluid pump (model SFT-10, Analytix Ltd., U.K) was used to compress CO₂ to the targeted pressure from the cylinder to the reactor. The reaction heating process started before pressurising since the vaporised methanol build-up pressure inside the reactor where the remaining pressure was obtained using pressurised CO₂ gas. The time required to reach the reaction conditions was about 15 min. The reaction time was considered once the reactor reached the targeted temperature and pressure. After the reaction time, the reactor was quenched using an ice bath to stop the reaction. The reactor was then depressurised and the reaction product separated using a centrifuge (1500 rpm, 3 min per cycle) to biodiesel and glycerol. The biodiesel was then heated to 80 °C for 30 min to recover the unreacted methanol using distillation. Finally, the pure biodiesel properties were analysed and compared with the European biodiesel standard (EN14214). The yield of the produced biodiesel was calculated by using Equation 3.1 (Gerpen, 2005).

$$BD \text{ yield (\%)} = \frac{\text{Total weight of methyl esters}}{\text{Total weight of waste oil used}} \times 100 \quad (3.1)$$

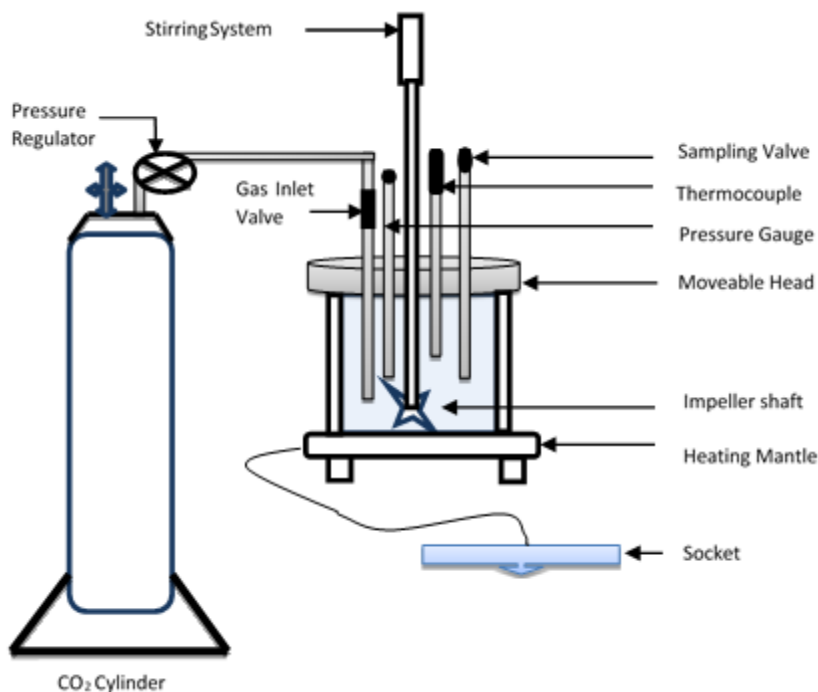


Figure 3.1. Schematic of the experimental setup

3.2.3. Experimental design

RSM is a multivariate method which is capable of developing a model representing the reaction dependant response function in the experimental studied independent variables (Qin et al., 2015). RSM was used to develop the optimum conditions for biodiesel production by studying the relationship of each variable and the response yield. The experimental runs were operated based on 4 independent variables including M:O molar ratio, temperature, pressure and time, which were labelled as A, B, C and D, respectively. Three levels for each variable were coded as -1, 0, 1 as shown in Table 3.1. BBD is one of the RSM techniques that was used to study the main effect of process variables on the response. It also studies the effect of the variables interactions on the response (Khajeh, 2009).

Biodiesel yield was selected as the response for this study. In order to minimise the effect of unexplained inconsistency in the responses, the experiments were completed in a randomised order (Jaliliannosrati et al., 2013). Twenty-nine runs were performed in a

randomised way and their response was calculated from the experimental results using Equation 3.1 as shown in Table 3.2 (Actual BD Yield).

Table 3.1. Experimental design variables and their coded levels

Factor	Code	Levels		
		-1	0	+1
M:O (molar ratio)	A	20	31	42
Temperature (°C)	B	240	260	280
Pressure (bar)	C	180	220	260
Time (min)	D	12	22	32

Table 3.2. Experimental design matrix with the actual and predicted yields

Run	M:O molar ratio (A)	Temperature (°C) (B)	Pressure (bar) (C)	Time (min) (D)	Actual BD Yield %	Predicted BD Yield %
1	31	260	220	22	96	94.2
2	20	260	220	32	85	84.2
3	31	280	220	12	91	90.0
4	20	280	220	22	85	85.3
5	42	260	260	22	92	91.9
6	31	260	220	22	93	94.2
7	31	260	260	12	88	88.2
8	42	240	220	22	87	87.2
9	31	240	260	22	85	84.5
10	42	260	220	32	92	91.3
11	31	260	220	22	94	94.2
12	20	260	220	12	82	82.2
13	20	260	180	22	81	80.9
14	31	280	220	32	90	90.1
15	42	260	220	12	91	91.3
16	31	240	220	32	84	84.7
17	31	280	260	22	91	90.8
18	20	240	220	22	79	79.1
19	42	280	220	22	93	93.5
20	31	260	260	32	89	89.2
21	20	260	260	22	84	84.2
22	31	260	220	22	94	94.2
23	31	260	180	12	85	85.3
24	31	240	220	12	83	82.7
25	31	240	180	22	82	81.7
26	31	260	180	32	86	86.3
27	31	260	220	22	94	94.2
28	31	280	180	22	88	88.1
29	42	260	180	22	90	89.5

Where, BD means Biodiesel.

3.2.4. Statistical analysis

The general quadratic equation was used to define the model as shown in Equation 3.2.

$$Y = b_0 + \sum_{i=1}^n b_i X_i + \sum_{i=1}^n b_{ii} X_i^2 + \sum_{i=1}^{n-1} \sum_{j=2}^n b_{ij} X_i X_j + \varepsilon \quad (3.2)$$

Where Y is the dependent response, b_0 is the model coefficient constant, b_i , b_{ii} , b_{ij} , are coefficients for intercept of linear, quadratic, interactive terms respectively, while X_i , X_j are independent variables ($i \neq j$). The model adequacy was checked by coefficient of correlation (R^2), adjusted coefficient of determination (R^2_{adj}) and the predicted coefficient of determination (R^2_{pred}). Investigation of the statistical significance was analysed using ANOVA by calculating the Fisher's F-test at 95% confidence level.

Numerical optimisation of the reaction conditions was concluded based on certain variables restrictions. The restrictions of the optimisation process were set for minimising temperature, pressure and time while targeting to maximising biodiesel yield response.

Design of experiments, regression analysis, graphical analysis and numerical optimisation was performed using Design Expert 10 software (Stat-Ease Inc., Minneapolis, MN, USA). Statistical significance of the results was presented by p-value, where the result is considered to be significant when p-value is < 0.05 . Predicted yields in the last column of Table 3.2, were concluded from the developed model in which is discussed in the results section.

3.2.5. Reaction Kinetics

Supercritical transesterification reaction kinetics is complex since the reaction mechanism involves transferring TG to diglycerides (DG) then to monoglycerides (MG) and finally to glycerol (GL). Esterification reaction of FFA to FAME was not been considered during the calculation since the FFA concentration is insignificant in the feedstock (TAN= 0.8 mg KOH/ g oil). For simplifying the transesterification reaction complex behaviour, the following assumptions were applied in the reaction kinetics modelling with respect to the formation of FAME (Ong et al., 2013).

- The overall supercritical transesterification reaction is irreversible.
- The change in concentration of methanol is ignored throughout the reaction since the amount of M:O molar ratio in supercritical reaction is adequately high relative to the stoichiometric amount of methanol consumed by TG.
- Glycerol-methanol side reaction is ignored.

A simplified scheme for the reaction kinetic study was performed for the overall transesterification reaction as reported previously (Ghoreishi and Moein, 2013). The kinetic and thermodynamic data of the overall reaction, including reaction rate constant (k), activation energy and frequency factor, were calculated according to Equations 3.3 to 3.6.

$$-r_{TG} = -d[TG]/dt = k [TG] \quad (3.3)$$

$$[TG] = [TG]_o (1-X) \quad (3.4)$$

$$X = 1 - \frac{[TG]}{[TG]_o} = 1 - \frac{[TG]_o - [FAME]/3}{[TG]_o} = \frac{[FAME]}{3[TG]_o} \quad (3.5)$$

$$k = A e^{\frac{-E}{RT}} \quad (3.6)$$

Where X, A and E are the conversion of TG, Arrhenius constant and activation energy, respectively.

3.2.6. Physicochemical properties

WCO feedstock properties were calibrated as shown in Table 3.3. The produced purified biodiesel from supercritical transesterification reaction using the optimum condition was analysed for evaluating its physical and chemical properties. The results were compared with the European standard of biodiesel, EN14214. The analysed properties were replicated twice and the final results were obtained as an average of the two results. The standard density was measured based on ASTM D4052 method, while the kinematic viscosity was measured according to ASTM D445 method. Total acid number (TAN) of the produced biodiesel was calibrated according to ASTM D974 method.

Table 3.3. Properties of WCO feedstock

Test	Calibration Method	Result
Kinematic viscosity at 40 °C	ASTM D-445	54.2 cSt
Density at 15 °C	ASTM D-4052	0.88 g/cm ³
TAN	ASTM D-974	0.8 mg KOH/g oil

3.2.7. Gas chromatographic analysis

Fatty acids composition of the WCO was analysed by converting them to methyl esters according to BS EN ISO 12966-2:2011 as shown in Table 3.4. The WCO and the produced samples were analysed for methyl esters content using gas GC (Thermo-Scientific, Trace 1310) equipped with a capillary column (TR-BD 30 m × 0.25 mm × 0.25 µm) and FID. Both injector and detector temperatures were adjusted at 250 °C. Helium was used as the carrier gas. The temperature programme began from 60°C and held for 2 min. Then it ramped with 10 °C/min to 200 °C and directly ramped with 1 °C/min to 210 °C. Finally, the temperature was increased to 240 °C with a ramp rate of 20 °C/min and remained for 7 min.

Table 3.4. Composition of the fatty acids in WCO

Fatty Acid	wt (%)
Palmitic	7.07
Oleic	62.63
Linoleic	23.26
Arachidonic	7.04

3.3. Results and discussions

3.3.1. Model fitting and adequacy checking

The predicted model has been examined for adequacy to report any errors associated with the normality assumptions. After performing the 29 experiments as shown in Table 3.2, and evaluating biodiesel yield (reaction response) for each run, the response analysis using BBD has been applied. Design Expert software generated a regression equation representing an empirical relationship between the response variable and the reaction parameters. The generic quadratic equation shown in Equation 3.7, which represents Equation 3.2, has been used to obtain a polynomial regression model by fitting the experimental results.

$$Y = \beta_0 + \beta_1 X_1 + \beta_2 X_2 + \beta_3 X_3 + \beta_4 X_4 + \beta_{12} X_1X_2 + \beta_{13} X_1X_3 + \beta_{14} X_1X_4 + \beta_{23} X_2X_3 + \beta_{24} X_2X_4 + \beta_{34} X_3X_4 + \beta_{11} X_1^2 + \beta_{22} X_2^2 + \beta_{33} X_3^2 + \beta_{44} X_4^2 \quad (3.7)$$

According to the data obtained from experimental results, a polynomial equation, as showed in Equation 3.8, has been developed where Y is the dependant variable (biodiesel yield); A, B, C and D are the independent variables (M:O molar ratio, temperature, pressure and time respectively). Predicted model has been validated at M:O molar ratio (20:1-42:1), temperature (240-280 °C), pressure (180-260 bar) and time (12-32 min).

$$Y = 94.2 + 4.08 A + 3.17 B + 1.42 C + 0.50 D - 0.25 AC - 0.50 AD - 0.50 BD - 3.77 A^2 - 4.14 B^2 - 3.77 C^2 - 3.14 D^2 \quad (3.8)$$

ANOVA has been applied to examine the significance of the model parameters at 95% confidence level. The significance of each parameter has been determined by F-test and p-value. The higher the value of F-test and the smaller the p-value, the more significance of the corresponding parameter (El-Gendy et al., 2014).

ANOVA has been used to validate the RSM model coefficient using F-test and p-value, these values have resulted as 65.40 and <0.0001 , respectively as shown in Table 3.5 which prove that the developed quadratic model is statistically significant with 95% confidence level. Lack-of-fit analysis is one of the adequacy checking techniques which measures the failure of the regression model to represent the experimental data points (Qin et al., 2015).

Lack-of-fit analysis of the model has been observed as to be 0.942 (not significant), which illustrate that the model has been representing most of the experimental data successfully. The determination coefficient values, R^2 and R^2_{adj} , which measure the reliability of the model fitting, have been calculated to be 0.9849 and 0.9699, respectively. These values indicate that only 0.0151 of the total variation has not been well clarified by the developed model, which ensure the model fitting to the experimental data.

The model performance has been observed using different techniques. A plot of the predicted *versus* experimental result of the biodiesel yield (Figure 3.2) showed high correlation and reasonable agreement. The good estimate for the response values from the model is clearly concluded from the similarity between the predicted and actual experimental results as shown in Figure 3.2. In addition, a plot of residual distribution *versus* predicted response has been presented to check the fitting performance of the model as shown in Figure 3.3. Residual value is defined as the difference between predicted and experimental values of the response variable. The plot confirms that the quadratic model adequately represents the experimental data as the distribution is not following a specified trend with respect to the predicted values of the response variable.

Moreover, the perturbation plot represents the effect of each variable on the reaction response as shown in Figure 3.4. The curvature of the variables from the centre point indicates the significance of each variable which confirms the statistical results obtained from ANOVA as shown in Table 3.5. Sharp curvature of the independent variables, e.g. M:O molar ratio (A), temperature (B) and pressure (C) indicates their highly significant effect as concluded from the ANOVA results. It also represents the effect of each variable, where for M:O molar ratio the plot indicates that it has progressively increasing effect on biodiesel yield until reaching the central point where it slightly decreases after this point.

Table 3.5. Analysis of variance for response surface developed model

	Sum of square	df	Mean Square	F Value	p-value	Significance
Model	580.9	14	41.4	65.4	<0.0001	HS
A-M:O	200.1	1	200.1	315.3	<0.0001	HS
B-Temperature	120.3	1	120.3	189.6	<0.0001	HS
C-Pressure	24.1	1	24.1	37.95	<0.0001	HS
D-Time	3	1	3	4.72	0.04	S
AB	0	1	0	0	1	NS
AC	0.25	1	0.25	0.39	0.54	NS
AD	1	1	1	1.57	0.23	NS
BC	0	1	0	0	1	NS
BD	1	1	1	1.57	0.23	NS
CD	0	1	0	0	1	NS
A ²	92.0	1	92	145	<0.0001	HS
B ²	111.2	1	111.2	175.3	<0.0001	HS
C ²	92	1	92	145	<0.0001	HS
D ²	64	1	64	100.8	<0.0001	HS
Residual	8.8	14	0.63			
Lack of Fit	4.08	10	0.41	0.34	0.92	NS

Where HS: Highly Significant, S: Significant and NS: Not Significant

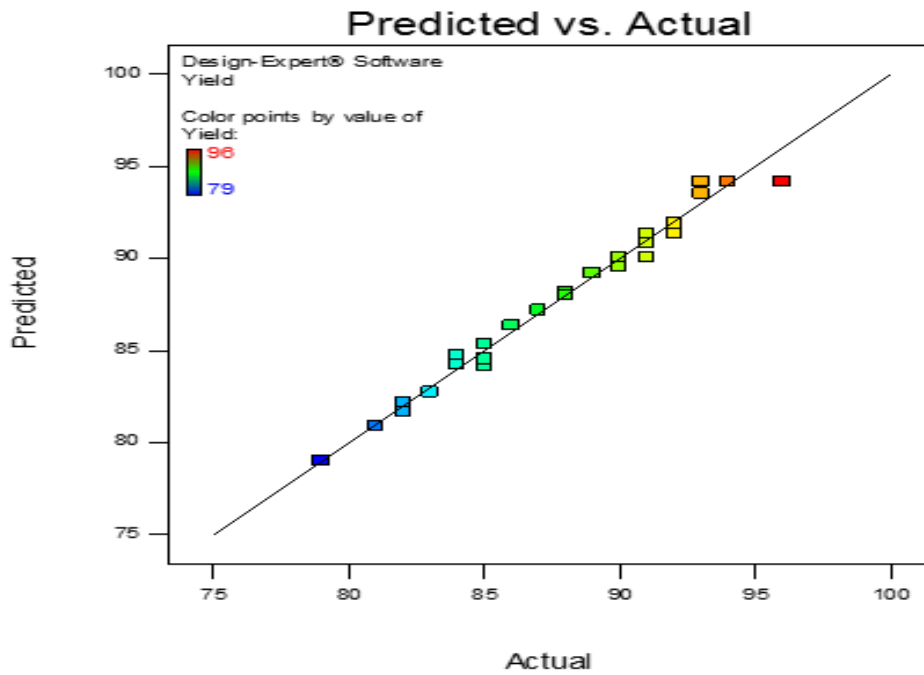


Figure 3.2. Actual experimental data versus predicted model

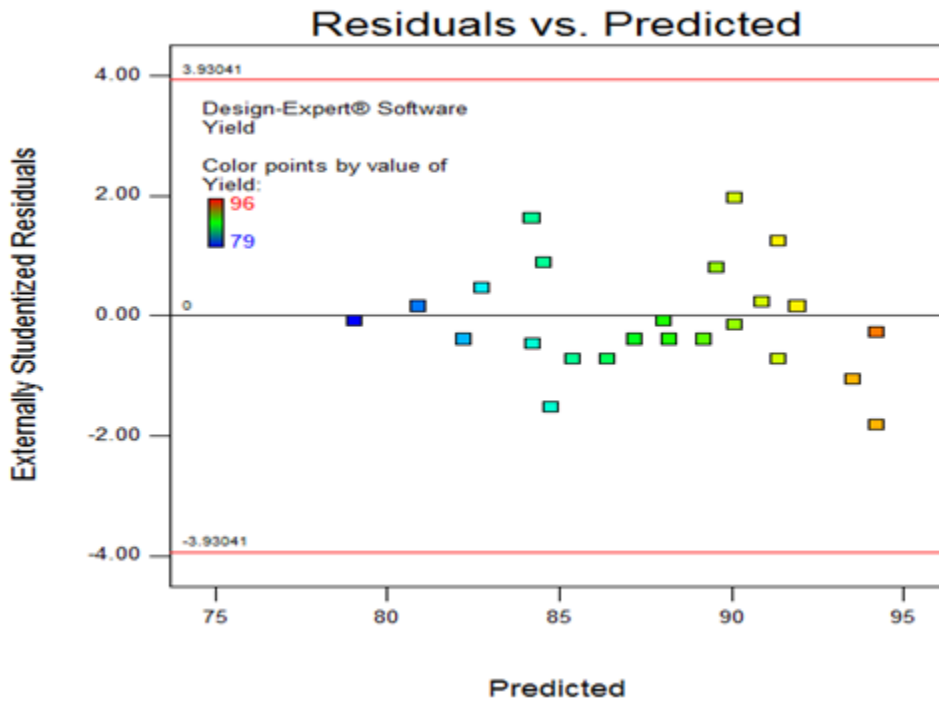


Figure 3.3. Residuals versus predicted response

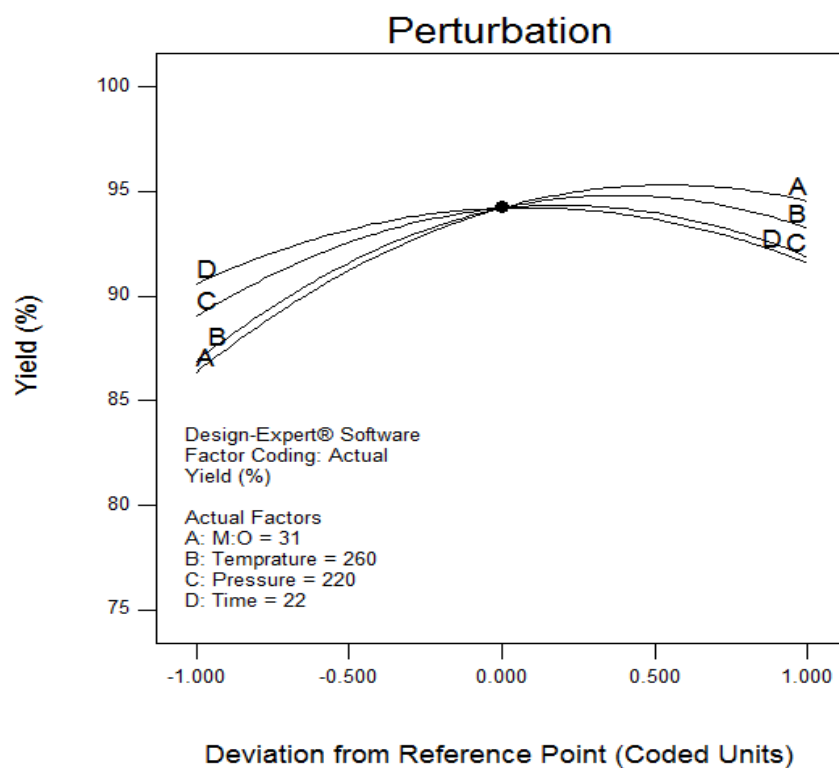


Figure 3.4. Perturbation Plot

3.3.2. Effect of reaction variables

The 3D-surface and contour plots of the biodiesel yield *versus* interaction of two independent variables are shown in Figure 3.5 Figure 3.6. In each plot, the two remaining independent variables were kept constant in their centre points.

3.3.2.1. Effect of methanol to oil molar ratio

Experimental runs have been carried out at M:O molar ratio between 20:1 and 42:1 in order to study the effect of their variation on the yield of biodiesel. Based on the ANOVA results presented in Table 3.5, M:O molar ratio parameter shows highly significant effect on the process response. At constant temperature (260 °C) the yield of biodiesel is 95.5% at a M:O molar ratio of 37:1, however it decreases to 92% at a M:O molar ratio of 42:1. It is shown in Figure 3.5, that an increase in M:O molar ratio from 20:1 to 37:1, increases the biodiesel yield. However, biodiesel yield decreases slightly at higher M:O molar ratio

values (more than 37:1). Ghoreishi and Moein (2013) reported similar phenomena at high M:O molar ratio. They reported that at M:O molar ratio higher than 34:1, the biodiesel yield starts to decrease slightly. High excess of methanol lowers the critical temperature of the reaction as methanol has lower critical condition compared to the reaction mixture components. Lowering the critical temperature of the product enhance FAME decompositions and hence reducing biodiesel yield. Moreover, FAME decomposition can enhance glycerol-methanol side reaction (Hegel et al., 2008).

3.3.2.2. Effect of reaction temperature

ANOVA results presented in Table 3.5 have shown highly significant effect of reaction temperature on the process response. It is clearly shown in Figure 3.5 that a directly proportional relation exists between temperature and biodiesel yield within the temperature range between 240 and 270 °C. However, biodiesel yield decrease slightly at higher temperature values (more than 270 °C) due to the decomposition of the produced FAME. The same observation has been reported by Ghoreishi and Moein (2013). They have observed that at a higher reaction temperature than 271 °C, biodiesel yield starts to decrease.

Design-Expert® Software

Factor Coding: Actual

Yield (%)

● Design points above predicted value

○ Design points below predicted value

79 96

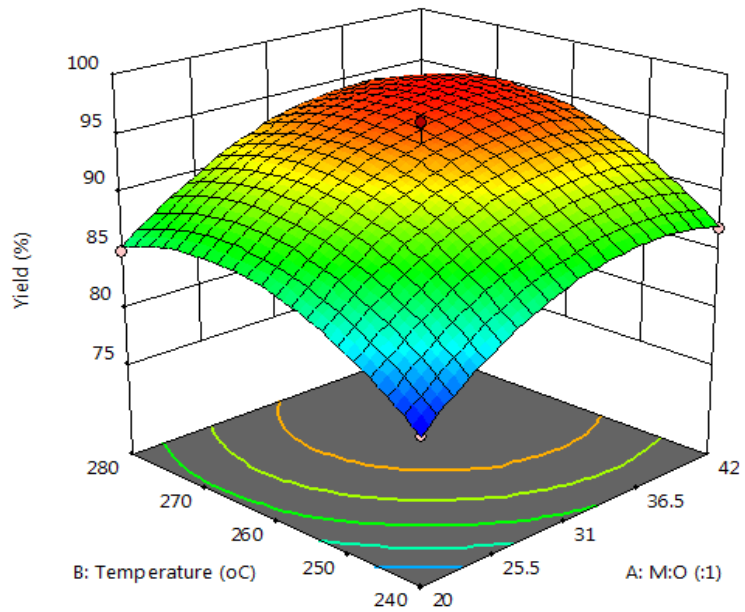
X1 = A: M:O

X2 = B: Temperature

Actual Factors

C: Pressure = 220

D: Time = 22



Design-Expert® Software

Factor Coding: Actual

Yield (%)

● Design Points

79 96

X1 = A: M:O

X2 = B: Temperature

Actual Factors

C: Pressure = 220

D: Time = 22

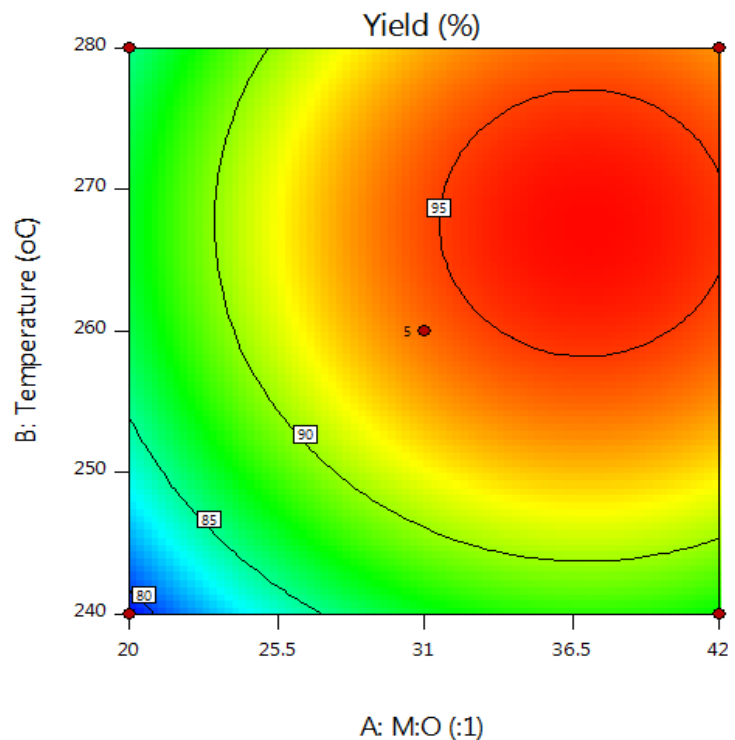


Figure 3.5. 3-D and contour graphs showing the effect of methanol ratio and temperature *versus* yield

3.3.2.3. Effect of reaction pressure

The co-solvent, CO₂ gas, has been used to pressurise the reaction. Using CO₂ as a co-solvent for the reaction enhances the solubility of methanol in oil (Han et al., 2005). As shown in Figure 3.6, reaction pressure is directly proportional with the biodiesel yield in the range of 180 to 230 bar. It has been observed that beyond 230 bar the biodiesel yield starts to decrease slightly. Kurniawan et al. (2012) reported that the pressure effect on the supercritical transesterification using compressed nitrogen gas for *Jatropha* oil is directly proportional until 220 bar and beyond that value the pressure has no effect on the biodiesel yield. Accordingly, supercritical methanolysis pressure should not exceed 230 bar.

3.3.2.4. Effect of reaction time

In this study, reaction time has been calculated once the mixture reaches the specified reaction conditions for a consistent comparison between the experiments without considering the reactions that might occur during the start-up. Reaction time has showed a directly proportional relationship to the biodiesel yield within the range of 12 to 24 min as shown in Figure 3.6. Biodiesel yield in the reaction that occurs in longer period than 24 min has been observed to decrease. This phenomenon has been reported by He et al. (2007). They have explained the decrease in the yield of biodiesel is due to the degradation of unsaturated FAME, especially under higher temperature.

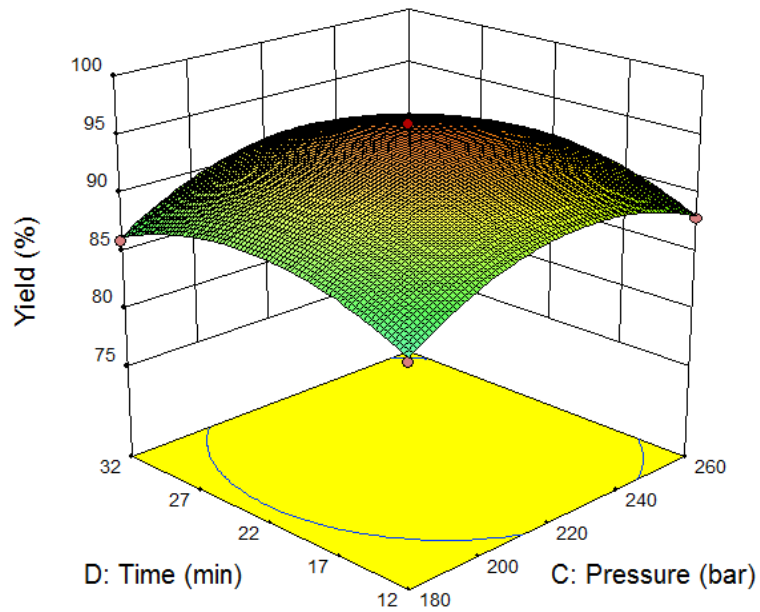
Design-Expert® Software
 Factor Coding: Actual
 Yield (%)

- ◆ Design points above predicted value
- ◆ Design points below predicted value



X1 = C: Pressure
 X2 = D: Time

Actual Factors
 A: M:O = 31
 B: Temperature = 260



Design-Expert® Software
 Factor Coding: Actual
 Yield (%)

- ◆ Design Points



X1 = C: Pressure
 X2 = D: Time

Actual Factors
 A: M:O = 31
 B: Temperature = 260

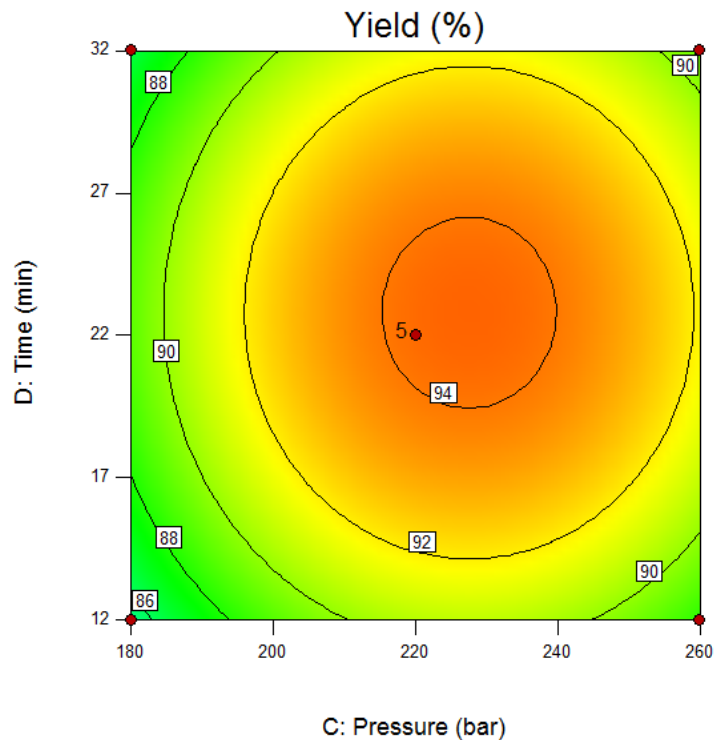


Figure 3.6. 3-D and contour graphs showing the effect of pressure and time on yield

3.3.3. Optimisation of reaction variables

Optimisation process of the supercritical methanol transesterification reaction has been carried out to define the optimum values for the independent variables affecting the dependant response variable. Design Expert software has been used to develop the numerical optimisation step by combining the desirability of each independent variable into single value and then search for optimum values for the response goals. Accordingly, in order to conclude the optimum conditions of the independent variables, a set of targets must be defined on the software to guide the optimisation process (El-Gendy et al., 2015).

Targets of the independent variables have been set based on environmental and economic considerations. For the highly energy consuming variables including temperature (B), pressure (C) and time (D) they have been set to be minimised with highly importance. While M:O molar ratio (A), has been targeted to be between the range of minimum and maximum levels without restrictions since the excess of methanol could be recovered and reused in a new transesterification reaction. Finally, the dependent response variable which is the biodiesel yield has been set to be maximised to achieve the highest yield within the independent variables targets restrictions.

The numerical optimisation technique concluded that the maximum yield that can be reached with minimum reaction temperature, pressure and time is 91% at a M:O molar ratio of 37:1, reaction temperature of 253.5°C, reaction pressure of 198.5 bar in 14.8 min.

3.3.4. Validation of predicted optimum conditions

In order to validate the optimal response values of the predicted quadratic equation, experiments have been performed at optimum condition i.e., M:O molar ratio of 37:1, reaction temperature 253 °C, reaction pressure of 199 bar and reaction time of 15 min. The experimental results showed similar response value to the predicted optimal response of 91.5% with relative error of 0.54%. The similarity between the experimental response results and the predicted optimal response confirms and verifies the accuracy and adequacy of the optimisation technique occurred by the predicted quadratic model.

3.3.5. Kinetic study

The validated quadratic model developed by RSM has been considered for predicting the experimental results required for reaction kinetics calculations. The fact which confirmed that the molecular weight of TG is three times that of FAME, as shown in Equation 3.9, has been considered for conversion calculations without analysing the final concentration of TG (Ghoreishi and Moein, 2013). Temperature range between 240 °C and 280 °C and reaction time from 12 to 20 min have been used to obtain the required kinetic data. To simplify the kinetic analysis, the kinetic data has been studied only for the overall transesterification reaction and the change in methanol concentration throughout the reaction has been ignored. Thus, the reaction order has been considered to be pseudo first order, where the rate of the reaction is a function of TG only as shown in Equations 3.3 to 3.6.

$$X = \frac{[FAME]}{3[TG]_0} = \frac{m_{FAME}/M_{FAME}}{3m_{TG_0}/M_{TG}} = \frac{m_{FAME}/3M_{FAME}}{m_{TG_0}/M_{TG}} \approx \frac{m_{FAME}}{m_{TG_0}} = Y \quad (3.9)$$

Where X and Y represent the conversion and yield of biodiesel, respectively.

A graphical plot between $|\ln(1-Y)|$ versus time within time range from 720 to 1200 s while keeping the other variables constant at the optimum conditions concluded a straight line with $R^2 = 0.983$, which illustrates that our basis of pseudo first order reaction is correct. This conclusion has been previously reported by Ong et al. (2013). They have stated that generally supercritical transesterification reactions can be considered as pseudo-first order reactions. From the straight line, reaction rate constant (k) at the optimum conditions has been concluded from the slope, which is 0.0006 s^{-1} .

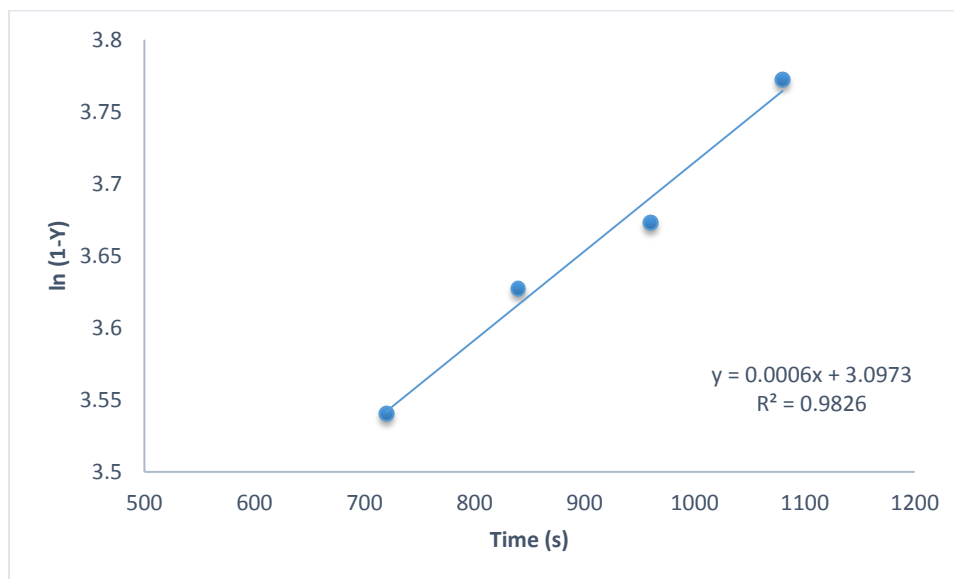


Figure 3.7. Rate constant calculation

In order to determine full analysis for the kinetic data, the reaction thermodynamic parameters have been considered in the study. Activation energy and Arrhenius constant have been calculated using Arrhenius equation. Consequently, a graphical plot between $\ln k$ and $(1/T)$ has been obtained to fit a straight line with $R^2=0.99$ resulting of activation energy and Arrhenius constant of 50.5 kJ/mol and 4.06 s⁻¹, respectively for the overall transesterification reaction. Ang et al. (2015) reported that transesterification reaction from *cerbera odollam* oil resulted in activation energy of 40 kJ/mol in the temperature range from 320 to 400 °C. They have studied the detailed transesterification reaction steps. They have concluded that the reaction of TG to DG is the rate-limiting step and that the reaction is endothermic. They have also concluded lower activation energies for different reaction steps. In this study, the activation energy was higher as it represents the energy required for the overall reaction which is responsible to convert TG to GL and FAME.

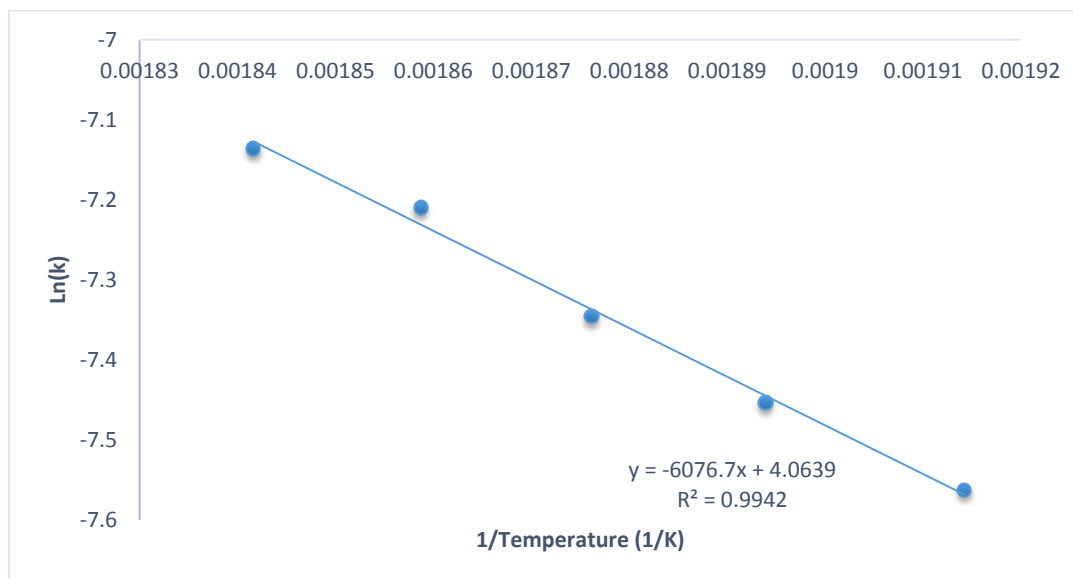


Figure 3.8. Arrhenius plot for transesterification of WCO

Ciftci and Temelli, (2013) reported that enzymatic transesterification reaction of corn oil using supercritical CO_2 concluded pseudo second-order reaction with activation energy and Arrhenius constant of 72.9 kJ/mol and 1.77×10^{11} L/mol.min. Their studied reaction conditions were within temperature range between 40 to 60 °C and under high pressure within 100 to 300 bar. Ghoreishi and Moein (2013) concluded that the activation energy for WCO was 31.71 kJ/mol and Arrhenius constant of 3.37 s^{-1} within temperature range from 240 and 280 °C. They have concluded lower activation energy since they have used WCO with FFA content of 5.65% (w/w) compared to 1.59% (w/w) for the WCO used in this study. These results confirm the conclusion by Tsai et al. (2013) that FFA content enhance biodiesel production from WCO under supercritical methanol conditions.

3.3.6. Biodiesel properties

The purified biodiesel produced at the optimum conditions (M:O molar ratio of 37:1, reaction temperature of 253 °C, reaction pressure of 199 bar and reaction time of 15 min) has been analysed to ensure that its properties are in agreement within the European Biodiesel Standard, EN14214.

Standard density of the produced biodiesel has been concluded to be 887 kg/m³, which is in agreement within the range of the European standard as shown in Table 3.6. Viscosity is the most important physical property of the biodiesel since it affects the atomisation of fuel being injected into the combustion engine chamber (Sajjadi et al., 2016). Table 3.6 shows the produced biodiesel properties and the European biodiesel standard acceptable range. Most of the physiochemical properties of the produced biodiesel are within the European standard, which ensures the quality of the produced biodiesel. A typical chromatogram of methyl esters in the optimum biodiesel sample is shown in Figure 3.9.

Table 3.6. Comparison between produced biodiesel properties and European biodiesel standard EN14214

Test	Unit	Produced biodiesel	Biodiesel (EN14214)
Density at 15°C	kg/m ³	887	860 - 900
Kinematic viscosity at 40°C	cSt	4.63	3.5 - 5
TAN	mg KOH/ g oil	0.09	< 0.5
Pour point	°C	-6	N/A
Flash point	°C	161	> 101
Cetane number		59	> 51

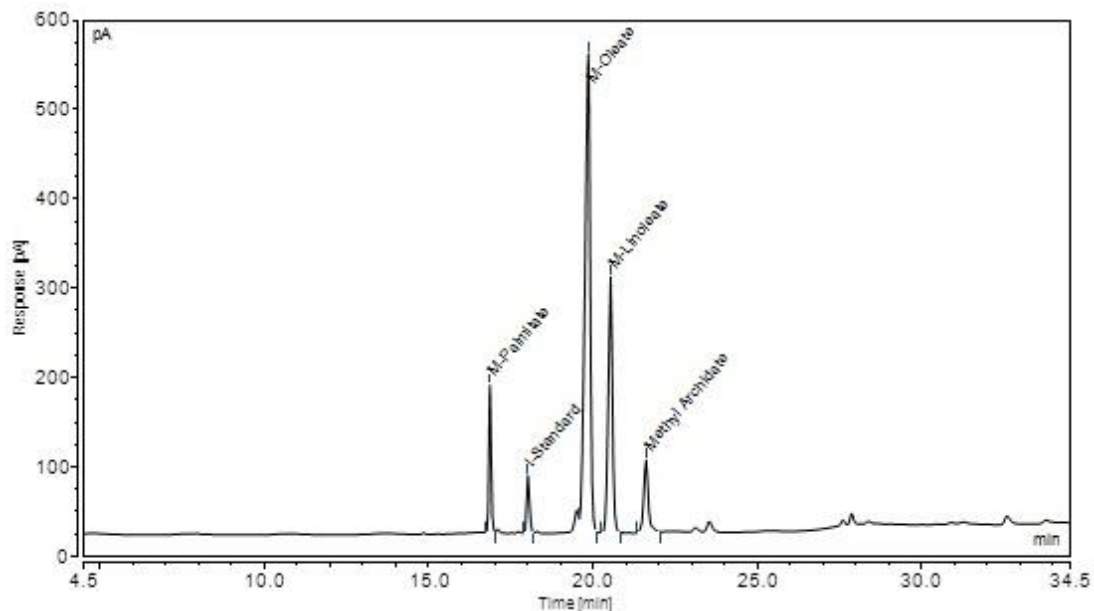


Figure 3.9. Gas chromatogram of methyl esters in the product sample

3.4. Conclusions

The production of biodiesel from low acidity WCO using supercritical methanol has been studied. Reaction variables and operating conditions of the reaction have been analysed. A quadratic polynomial model has been developed demonstrating the biodiesel yield function in four independent variables. It has been developed that the optimum biodiesel yield is 91% at M:O molar ratio of 37:1, reaction temperature of 253.5 °C, reaction pressure of 198.5 bar in 14.8 min reaction time. The optimisation results have been validated experimentally resulting in biodiesel yield of 91.5%, which shows the adequacy of the predicted optimum conditions with 0.54% relative error from the experimental results. This illustrates the accuracy of the developed model in predicting the optimal conditions. A kinetic study of the overall reaction concluded that the reaction is pseudo-first order with reaction rate constant of 0.0006 s^{-1} at the optimum conditions. The thermodynamic data including activation energy and Arrhenius constant have been calculated as 4.05 s^{-1} and 50.5 kJ/mol , respectively.

CHAPTER 4

VALORISATION OF HIGH ACID VALUE WASTE COOKING OIL INTO BIODIESEL

Outline of the chapter

This chapter discusses the valorisation of high acidity WCO into biodiesel. Experimental design, modelling and optimisation are considered. The effect of linear and interactive process variables on responses is extensively explained. Two different analysis have been applied for the responses including overall biodiesel yield and individual yield FAME of FAMEs. The chapter is organised as follows:

4.1. Introduction

4.2. Materials and methods

4.3. Results and discussion

4.3.1. Analysis of biodiesel and glycerol yields

4.3.2. Analysis of FAME yields of individual FAMEs

4.4. Conclusions

4. Valorisation of high acid value waste cooking oil into biodiesel

4.1. Introduction

The main aim of this study is to investigate the feasibility of supercritical methanolysis for biodiesel synthesis from very low quality WCO with high acid value. As high acidity WCO requires pre-treatment esterification step prior to transesterification reaction, the applicability of supercritical methanolysis to simultaneous transesterification of triglycerides and esterification of FFAs of very low quality WCO to FAME has been investigated. This work highlights and discusses the unusual results of the effect of different reaction parameters and their interactions on biodiesel and glycerol yields. In addition, the conversion of both triglycerides and FFAs have been considered. The standard methylation process has been applied for the feedstock and considered as the ideal conversion of both triglycerides and FFAs with the highest possible yield. Hence, all the experimental runs have been compared with the yield of the standard methylation process. FAME yield has been considered as the process response. Further, quadratic models have been developed representing response variables function in reaction parameters. RSM using CCD has been used for design of experiments, modelling and optimisation. Four independent process variables have been considered in this study, i.e. M:O molar ratio, temperature, pressure and time. ANOVA has been used to assess the adequacy of the predicted models and the effect of each process variable and their interactions on reaction responses. Optimisation of reaction variables has been carried out to maximise the production of biodiesel. Finally, the predicted optimum conditions have been validated experimentally.

4.2. Materials and methods

4.2.1. Materials

WCO was collected from random local restaurants and food industries in Egypt. Methanol (>99.5%), sodium chloride, sodium hydroxide, *iso*-octane, *n*-hexane and sulphuric acid were purchased from Fisher Scientific, UK. The standard pure methyl esters used for preparing calibration curves including FAME certified mixture solution (C14-C20), methyl-oleate, methyl-linoleate, methyl-palmitate, methyl-myristate and methyl-heptadecanoate (internal standard) were purchased from Merck, UK. The liquid CO₂ cylinder (99.9%) equipped with a dip tube was purchased from BOC Ltd., UK.

4.2.2. Experimental Procedures

4.2.2.1. Supercritical methanolysis

WCO was heated to 30 °C using a hot plate for liquefaction and then filtered to remove any residuals from cooking processes. The filtered WCO was used directly to the reactor without any pre-treatment steps. The reaction was carried out in a 100 mL high pressure reactor made of stainless steel (model 4590, Parr Instrument Company, USA) which is fitted with a thermocouple (type J), heating mantle, controller (model 4848) and a mechanical stirrer. A schematic of the experimental setup is shown in Figure 4.1. WCO was weighed and mixed with methanol (based on specific molar ratio). Then, the mixture was fed to the reactor and heated to the target temperature with continuous stirring at a constant rate of 300 rpm. After reaching the target temperature, vaporised methanol had already built up pressure inside the reactor which was still below the targeted pressure. A supercritical fluid pump (model SFT-10, Analytix Ltd., U.K) was used to compress CO₂ from a cylinder to the reactor in order to achieve the targeted pressure. The time required for reaching the desired temperature and pressure was approximately 15 min in all experiments. Reaction residence time counts once reaching the desired reaction conditions. After the specified residence time, the reactor was quenched using an ice bath to stop the reaction and then the reactor was depressurised. Unreacted methanol was recovered using simple distillation at 80 °C for 30 min. The reaction products were

separated using a centrifuge (1500 rpm, 3 min per cycle) to biodiesel and glycerol. Finally, biodiesel and glycerol contents were measured for yield calculations. Yield has been calculated using Equation 4.1 (Ghoreishi and Moein, 2013).

$$\text{Yield (\%)} = \frac{\text{Total weight of biodiesel}}{\text{Total weight of waste cooking oil used}} \times 100 \quad (4.1)$$

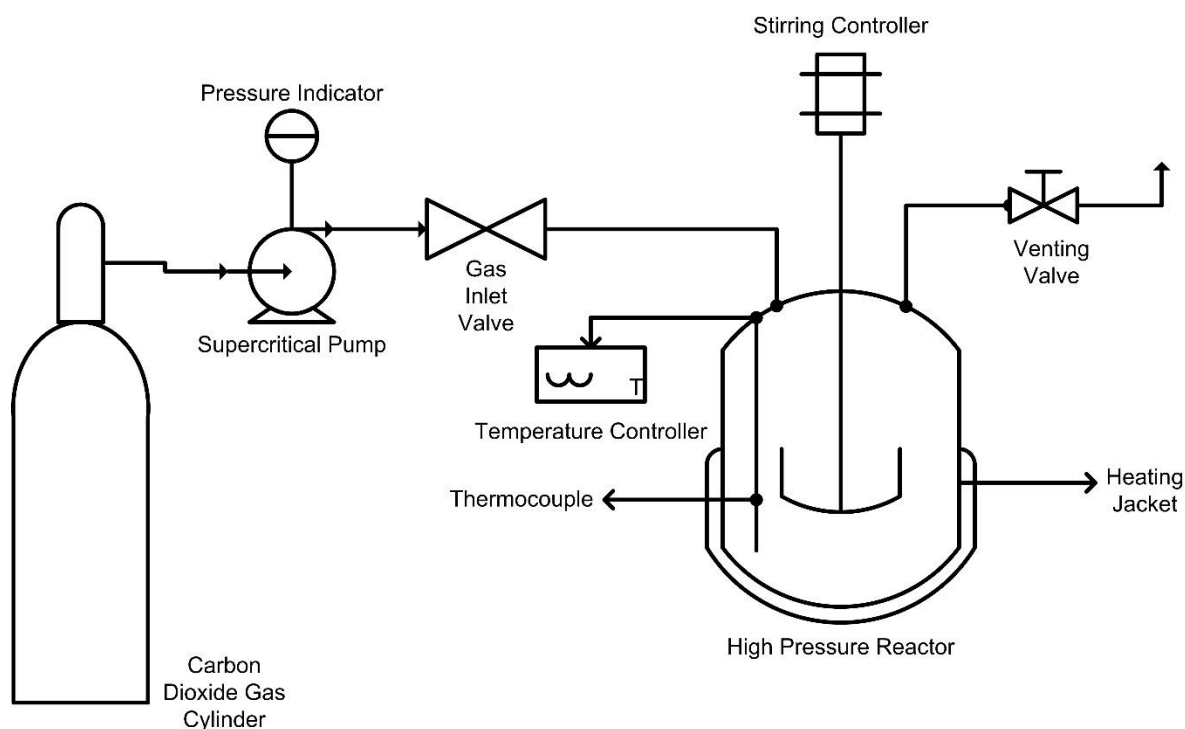


Figure 4.1. A schematic of the experimental setup

4.2.2.2. WCO and biodiesel characterisation

Standard procedures were followed to characterise properties of WCO and the produced biodiesel including ASTM D-974, ASTM D-445 and ASTM D-4052 for measuring TAN, kinematic viscosity and density, respectively. The determined properties of biodiesel were compared with the European biodiesel standard (EN14214). The analysed properties have been replicated twice and the final results have been obtained as an average of the

two results. Table 4.1 illustrates the main physicochemical properties of WCO used for the experimental analysis.

Table 4.1. Physicochemical properties of WCO

Property	Calibration Method	Results
Kinematic viscosity	ASTM D-455	60.5 cSt
Density	ATM D-4052	0.93 g/cm ³
TAN	ASTM D-947	18 mg KOH/ g oil

4.2.2.3. Preparation of standard solution

Four pure standards of FAMEs, i.e. methyl-oleate, methyl-palmitate, methyl-linoleate and methyl-myristate, were dissolved in *n*-hexane. Five different concentrations were prepared for each standard including 2, 4, 6, 8 and 10 g/L. For quantification purposes, five sets of each FAME standard accompanied by constant concentration (3 g/L) of internal standard, i.e. methyl-heptadecanoate were prepared in 2 mL vials for chromatographic analysis. In addition, a standard mixture solution has been used to verify the retention time of each FAME through an adjusted chromatographic program.

4.2.2.4. Derivatisation of WCO sample

The derivatisation process was performed according to BS EN ISO 12966-2:2011. In summary, 50 mg of WCO was added to a 10 mL volumetric one-marked flask. Then, a known concentration (0.2 mol/L) of sodium methoxide was added and the mixture was heated to boiling point as which the solution became clear. This was followed by addition of 2 drops of phenolphthalein indicator. Then, a known concentration of sulphuric acid in methanol (0.2 mol/L) was added sufficiently until the solution became colourless at which an excess of 0.2 mL of sulphuric acid solution was added. The solution was boiled for 5 min, then 4 mL and 1 mL of sodium chloride solution and *iso*-octane solution were added, respectively. Finally, the solution was well mixed and left for settling until the upper layer representing the FAME is clear. The produced FAME from derivatisation was considered

as the complete conversion of both triglycerides and FFAs where the conversion of other experimental samples was referred to the conversion of the derivatised sample.

4.2.2.5. Gas chromatographic analysis

The reference derivatised sample and the produced experimental samples were analysed for methyl esters content using GC (Thermo- Scientific, Trace 1310) equipped with a capillary column (TR-BD 30 m × 0.25 mm × 0.25 µm) and FID. Both injector and detector temperatures were adjusted at 250 °C. Helium was used as the carrier gas. The temperature programme began from 60 °C and held for 2 min. Then it ramped with 10 °C/min to 200 °C and directly ramped with 1 °C/min to 210 °C. Finally, the temperature was increased to 240 °C with a ramp rate of 20 °C/min and remained for 7 min.

4.2.3. Experimental Design

RSM was applied for the design of experiments (DOE) in order to optimise reaction parameters for higher biodiesel yield. The effect of four independent variables and their interactions on reaction responses (biodiesel and glycerol yields) were investigated using RSM based on four factors and five levels of CCD. The CCD method of RSM is the most popular optimisation tool for reaction conditions. It includes full or fractional designs with centre points that are integrated with a group of axial points, which allow better predictions of the curvature in the resulting model. In this study, the range of the selected independent variables has been studied within five levels, which have been coded as -2, -1, 0, 1, 2, as shown in Table 4.2.

Table 4.2. Experimental design variables and their coded levels

Factor	Code	Levels				
		-2	-1	0	+1	+2
M:O (molar ratio)	A	20	25	30	35	40
Temperature (°C)	B	240	250	260	270	280
Pressure (bar)	C	85	110	135	160	185
Time (min)	D	7	12	17	22	27

According to the CCD design, a 4 factors 5 levels CCD design was implemented and in total 30 experiments were carried out in this study as shown in Table 4.3. The total number of experiments was calculated based on Equation 4.2.

$$\text{Total number of experiments} = 2^n + 2n + m \quad (4.2)$$

where n is the number of independent variables and m is number of replicated centre points. This study includes 4 independent variables and hence, enough information should be provided to assist the prediction of second-order polynomial models for biodiesel and glycerol yields as responses. Thus, 16 factorial points and 8 axial points developed 30 experiments that were performed randomly including 6 replicates at the centre point for precise experimental error predictions. The experimental runs were performed in a randomised order to minimise the effect of unexplained inconsistency in the responses (Jaliliannosrati et al., 2013). The analysed reaction variables were M:O molar ratio (A), temperature (B, °C), pressure (C, bar) and time (D, min) while reaction responses were biodiesel yield (Y_1 , wt%) and glycerol yield (Y_2 , wt%).

4.2.4. Statistical analysis

Regression analysis was performed using general quadratic polynomial equation to define the model as previously reported in Section 3.2.4 in Equation 3.2. Model accuracy was checked by coefficient of correlation (R^2), adjusted coefficient of determination (R^2_{adj}) and the predicted coefficient of determination (R^2_{pred}). Investigation of the statistical significance has been analysed using ANOVA by calculating the Fisher's F-test at 95% confidence level. Design Expert 10 software (Stat-Ease Inc., Minneapolis, MN, USA) was used to design the experiments, regression analysis, graphical analysis and numerical optimisation.

Table 4.3. Experimental design matrix with the actual and predicted yields

Run	M:O ratio (A)	Temperature (°C) (B)	Pressure (bar) (C)	Time (min) (D)	Actual BD Yield %	Predicted BD Yield %	Actual GL Yield %	Predicted GL Yield %
1	30	260	135	17	89.2	88.6	10.8	11.5
2	35	250	160	22	92.1	92.6	7.90	7.82
3	35	250	110	22	94.0	93.9	7.10	6.21
4	35	270	160	22	83.0	83.5	17.7	16.6
5	35	270	110	12	89.7	90.0	10.5	9.37
6	35	250	160	12	96.9	96.4	3.2	3.45
7	25	270	160	22	94.5	94.2	4.37	5.36
8	30	260	135	17	88.4	88.6	11.6	11.5
9	25	250	110	22	94.1	94.5	5.96	5.31
10	25	250	160	22	94.2	93.9	5.70	6.01
11	30	260	85	17	99.0	98.8	0.52	1.32
12	25	270	110	12	94.4	93.8	4.50	5.34
13	25	250	160	12	91.4	91.6	8.40	7.97
14	30	260	135	17	88.6	88.6	11.6	11.5
15	35	250	110	12	94.0	94.2	5.82	5.57
16	30	240	135	17	92.0	91.9	8.15	8.83
17	30	260	185	17	96.2	96.2	4.30	3.55
18	35	270	160	12	88.5	88.0	9.50	10.8
19	30	260	135	17	88.4	88.6	11.5	11.5
20	30	260	135	27	95.0	94.4	4.36	4.98
21	30	260	135	7	92.6	93.1	5.50	4.95
22	25	270	160	12	92.4	92.5	5.90	5.97
23	20	260	135	17	90.5	90.5	9.32	9.09
24	25	250	110	12	89.2	88.7	10.7	10.9
25	30	280	135	17	87.9	87.8	12.6	11.9
26	30	260	135	17	88.6	88.6	11.6	11.50
27	40	260	135	17	85.4	85.2	14.6	14.9
28	25	270	110	22	98.4	98.9	2.08	1.01
29	30	260	135	17	88.6	88.6	11.8	11.5
30	35	270	110	22	89.2	88.9	10.2	11.3

4.3. Results and discussion

This section is divided into two parts including the analysis of overall biodiesel and glycerol yields and the chromatographic analysis of FAME yield of each FAME.

4.3.1. Analysis of biodiesel and glycerol yields

4.3.1.1. Development of regression model

Design Expert software has fitted four models for each response including; linear, two factors interactions (2FI), quadratic and cubic polynomials. Among the fitted models of each response, one model has been selected based on different statistical tests including; lack of fit analysis, R^2_{adj} , R^2_{pred} and associated aliased coefficients. The software suggested the quadratic model for both biodiesel and glycerol yield responses. Equations 4.3 and 4.4 represent the developed quadratic models with empirical relationships between responses and reaction variables within specific levels in terms of coded factors shown in Table 4.2.

$$Y_1 = 88.64 - 1.31 A - B - 0.65 C + 0.32 D - 2.34 AB - 0.17 AC - 1.54 AD - 1.04 BC - 0.17 BD - 0.86 CD - 0.18 A^2 + 0.32 B^2 + 2.23 C^2 + 1.28 D^2 \quad (4.3)$$

$$Y_2 = 11.51 + 1.46 A + 0.79 B + 0.56 C + 0.01 D + 2.36 AB + 0.22 AC + 1.58 AD + 0.91 BC + 0.34 BD + 0.93 CD + 0.13 A^2 - 0.27 B^2 - 2.27 C^2 - 1.64 D^2 \quad (4.4)$$

where Y_1 and Y_2 represent biodiesel and glycerol yields, respectively. While, A, B, C and D represent the process variables including M:O molar ratio, temperature, pressure and time, respectively.

The regression equations illustrate the effect of the reaction variables on each the response. The positive sign of each term indicates synergetic effect while the negative sign indicated antagonistic effect (El-Gendy et al., 2015). The linear coefficient represents the effect of the reaction variable on the response while the coefficient of variables interaction represents the interactive effect of the process variables. Finally, the quadratic coefficient represents the effect of variable excess on the response. As shown in Equation

4.3, M:O molar ratio, temperature and pressure have negative effect on biodiesel yield with negative sign coefficients where the increase of these variables have decreasingly effect of biodiesel yield. However, in Equation 4.4 all the linear coefficients have positive signs, which indicate that while increasing any of the process variables, e.g. M:O molar ratio, temperature, pressure and time, glycerol yield increases. It can be seen in Equations 4.3 and 4.4 that variation of M:O molar ratio (A) has the highest effect of both biodiesel and glycerol yields, where it has the largest coefficient among other variables.

4.3.1.2. Model adequacy checking

The adequacies of the predicted models have been investigated to report any error associated with the normality assumptions. Various analyses have been applied to check the adequacy of the predicted model. The R^2 evaluates the accuracy of the predicted model whereas value of R^2 gets closer to unity indicates the high similarity between predicted values of the model and the actual experimental value. The values of R^2 , R^2_{adj} , R^2_{pred} have been evaluated for biodiesel yield predicted model as 0.9913, 0.9831 and 0.9543, respectively. In addition, they have been assessed for glycerol's yield model as 0.99, 0.981 and 0.941, respectively. These results indicate that 99.13% and 99% of the total variation is qualified to the experimental variables for both biodiesel and glycerol yields, respectively. Adequacy precision value is a measure of the range for the predicted response value in comparison with its relative error (signal to noise ratio) where a value greater than 4 is desirable. The value of adequacy precision has been evaluated as 44.77 and 22.79 for models representing biodiesel and glycerol yields, respectively. These results verify that the predicted models could be used to navigate the design space.

Statistical data obtained through variance analysis have been used to determine the significance of the predicted models. Moreover, the significance effect of reaction parameters and their interactions were determined. The parameter values from ANOVA are tabulated in Tables 4.4 and 4.5.

Table 4.4. Analysis of variance for biodiesel yield for the developed model

Source	Sum of Squares	df	Mean Square	F-value	P-value	Significance
Model	406.8	14	29.0	121.5	<0.0001	HS
A-MeOH:Oil	40.8	1	40.8	171.1	<0.0001	HS
B-Temperature	24.1	1	24.1	100.9	<0.0001	HS
C-Pressure	10.1	1	10.0	42.0	<0.0001	HS
D-Time	2.51	1	2.51	10.5	0.005	S
AB	87.7	1	87.7	366.9	<0.0001	HS
AC	0.46	1	0.46	1.94	0.21	NS
AD	37.9	1	37.9	158.5	<0.0001	HS
BC	17.3	1	17.3	72.6	<0.0001	HS
BD	0.47	1	0.47	2.01	0.17	NS
CD	11.9	1	11.9	49.9	<0.0001	HS
A ²	0.91	1	0.91	3.84	0.07	NS
B ²	2.75	1	2.75	11.5	0.01	S
C ²	136.3	1	136.3	570.1	<0.0001	HS
D ²	44.9	1	44.9	187.7	<0.0001	HS
Residual	3.8	15	0.23			
Lack of Fit	3.14	10	0.31	3.54	0.08	NS
Pure Error	0.44	5	0.08			
Cor Total	410.3	29				

where HS: highly significant, S: significant and NS: not significant

According to Tables 4.4 and 4.5, the significance of each model has been evaluated based on both p-value and F-test at 95% confidence level. The smaller the p-value than 0.05, the more significance of the corresponding parameter. It has been observed that both models are highly significant with p-values of <0.0001 . These have ensured the significance of the model in representing the experimental results. Lack-of-fit analysis is one of the ANOVA techniques which measure the failure of the regression model in representing the experimental data points. The non-significant value for lack of fit test indicates a high fitting model. Lack-of-fit values for both biodiesel and glycerol yields models, respectively. The non-significance of the test illustrated that the models have represented most of the experimental data successfully. Moreover, Figure 4.2 (a and b) illustrated a graphical representation for experimental actual values *versus* predicted values using the developed models for both biodiesel and glycerol yields, respectively. The similarity between actual and predicted values has ensured the accuracy of the model in predicting the response variable.

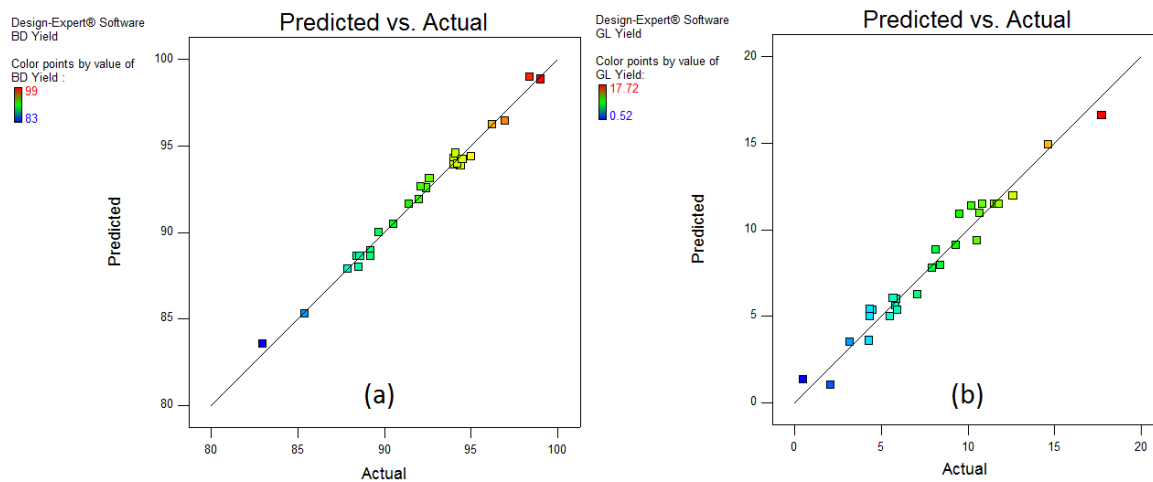


Figure 4.2. Predicted *versus* actual values for biodiesel yield model (a) and glycerol yield model (b)

Table 4.5. Analysis of variance for glycerol yield for the developed model

Source	Sum of Squares	df	Mean Square	F-Value	P-value	Significance
Model	432.8	14	30.9	33.5	<0.0001	HS
A-MeOH:Oil	51.1	1	51.1	55.3	<0.0001	HS
B-Temperature	14.8	1	14.8	16.0	0.001	HS
C-Pressure	7.4	1	7.4	8.1	0.01	S
D-Time	0.002	1	0.01	0.002	0.9	NS
AB	89.2	1	89.2	96.7	<0.0001	HS
AC	0.8	1	0.8	0.8	0.3	NS
AD	40	1	40	43.3	<0.0001	HS
BC	13.2	1	13.2	14.3	0.001	HS
BD	1.8	1	1.8	1.9	0.1	NS
CD	13.8	1	13.8	15	0.001	HS
A ²	0.45	1	0.4	0.4	0.4	NS
B ²	2.1	1	2.1	2.2	0.1	NS
C ²	140.8	1	140.8	152.6	<0.0001	HS
D ²	73.3	1	73.3	79.5	<0.0001	HS
Residual	13.8	15	0.9			
Lack of Fit	13.2	10	1.3	2.8	0.2	NS
Pure Error	0.6	5	0.1			
Cor Total	446.7	29				

Table 4.4 shows that all studied factors have significant individual effect on biodiesel yield where reaction time variable has showed the least significance effect than other variables with p-value of 0.005. The analysis also showed that there is a significant effect on biodiesel yield for variables interaction of M:O molar ratio - temperature (AB), M:O molar ratio - time (AD), temperature - pressure (BC) and pressure – time (CD). Moreover, it has been observed that both pressure and time showed significant quadratic effect on biodiesel yield.

According to Table 4.5, temperature, pressure and time showed significant individual effects on glycerol yield while reaction time showed insignificant effect on glycerol yield. Only temperature and pressure showed significant quadratic effect on glycerol yield. Although, analysis showed that there is a significant effect on glycerol yield between variables interactions of M:O molar ratio - temperature (AB), M:O molar ratio - time (AD), temperature - pressure (BC) and pressure – time (CD).

In an attempt to simplify the developed models, the insignificant variables have been excluded. According to ANOVA results presented in Tables 4.4 and 4.5, for the predicted models (Equations 4.5 and 4.6), the insignificant parameters, with p-values higher than 0.05 have been highlighted. It is shown in Table 4.4 that there is insignificant interactive effect on the response for both parameters AC and BD. In addition, the excess of M:O molar ratio (A) has statistical insignificant effect on biodiesel yield. On the other hand, reaction time (D) has insignificant effect on glycerol yield as shown in Table 4.5, however, it cannot be excluded to maintain the model hierarchal structure (Hinkelmann, 2012). Additionally, the interactions between AC and BD along with the excess of two variables including M:O molar ratio and temperature showed statistically insignificant effect on glycerol yield. Consequently, simplified reduced models have been developed for both biodiesel and glycerol yields by excluding the mentioned insignificant parameters as shown in Equations 4.5 and 4.6.

$$Y_1 = 88.43 - 1.31 A - B - 0.65 C + 0.32 D - 2.34 AB - 1.54 AD - 1.04 BC - 0.86 CD + 0.34 B^2 + 2.26 C^2 + 1.31 D^2 \quad (4.5)$$

$$Y_2 = 11.36 + 1.46 A + 0.79 B + 0.56 C + 0.01 D + 2.36 AB + 1.58 AD + 0.91 BC + 0.93 CD - 2.25 C^2 - 1.62 D^2 \quad (4.6)$$

It is necessary to check ANOVA assumptions, as they have been used to validate the predicted models. ANOVA assumptions summarised in; normality of residuals, homoscedasticity (equal variance) of residuals and random errors (Hinkelmann, 2012). Normality of residuals has been investigated using normal plot where they approximately form straight line as shown in Figure 4.3. This test ensures the validity of the first assumption where residuals are normally distributed for both biodiesel and glycerol models. Secondly, the homoscedasticity has been investigated where pressure variable (C) has been chosen as a variable sample representing the variance equality at different levels. The homoscedasticity has been examined using residuals *versus* predicted values plot. The equal range of residuals at each level concluding the homoscedasticity of the variable results as shown in Figure 4.4. Finally, the randomisation of errors has been investigated using the plot of residuals *versus* actual responses values. As shown in Figure 4.5, residuals were distributed randomly where they do not follow any specific trend. These randomised distributions validate the third assumption of ANOVA.

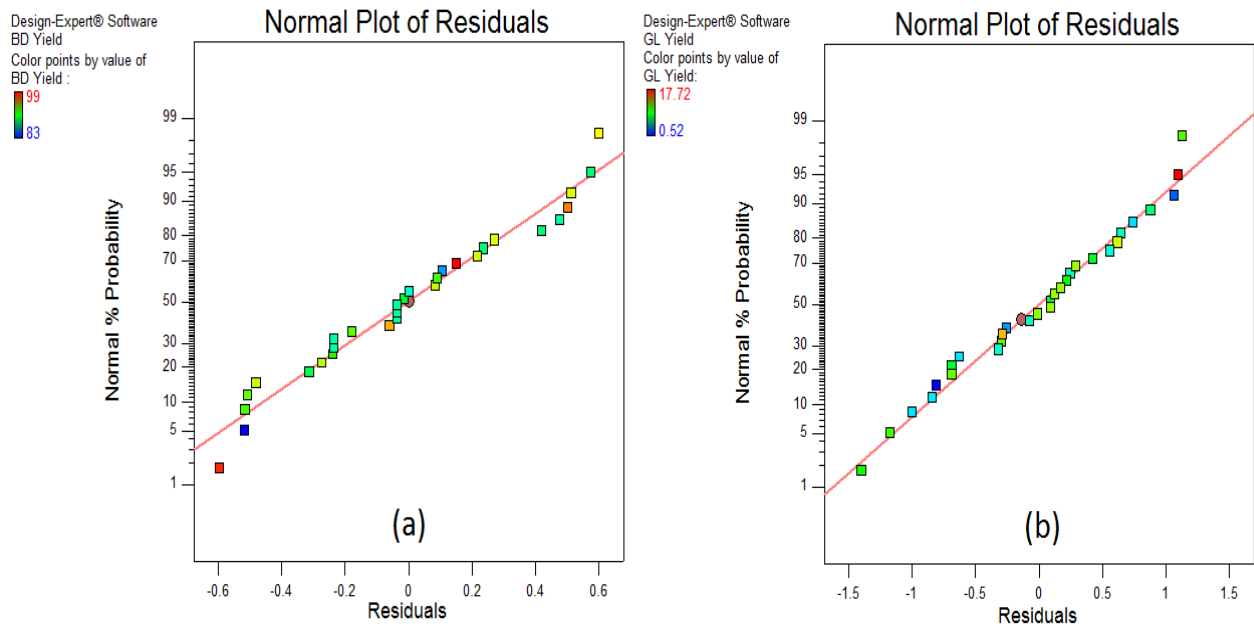


Figure 4.3. Normal plot of residuals for (a) biodiesel yield model and (b) glycerol yield model

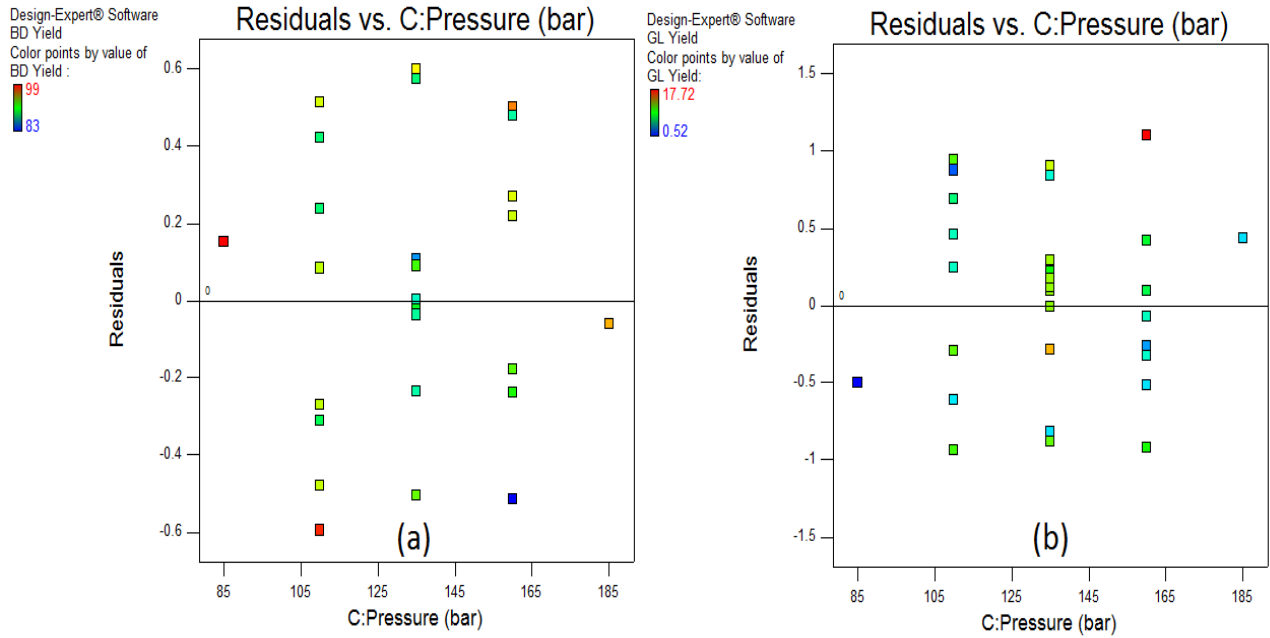


Figure 4.4. Plot of residuals versus predicted values of pressure variable for (a) biodiesel yield model and (b) glycerol yield model

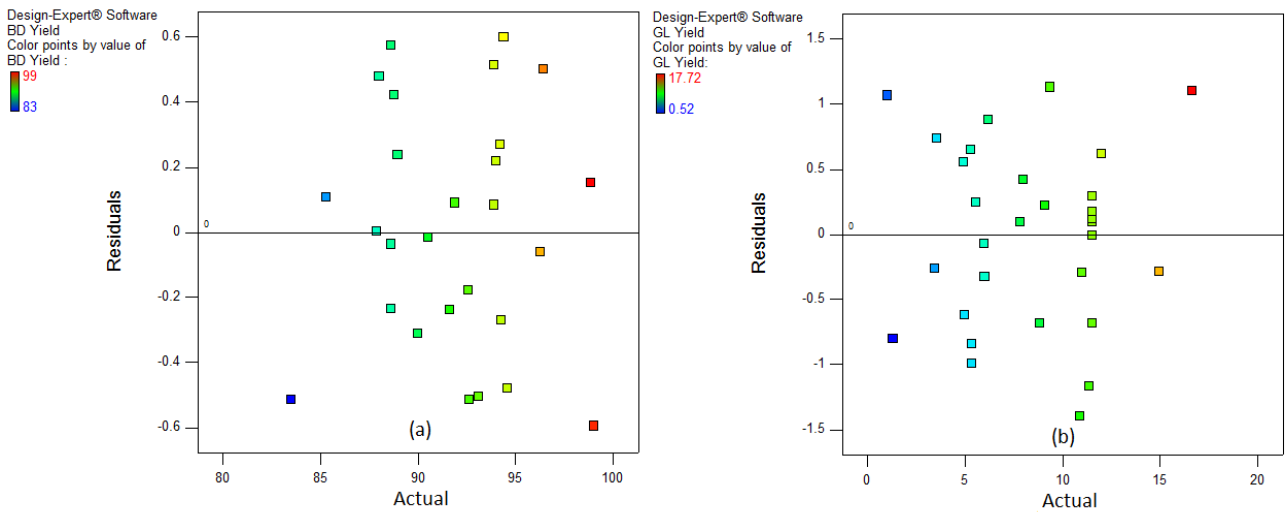


Figure 4.5. Plot of residuals versus actual response for (a) biodiesel yield model and (b) glycerol yield model

4.3.1.3. Effect of process variables

4.3.1.3.1. Effect of individual process variables

A perturbation plot was used to compare the influence of reaction variables at particular point in space. In this study, centre point of all variables has been selected as a constant point of comparison between variables. The influence of individual reaction variables on biodiesel and glycerol yields have been presented in Figure 4.6.

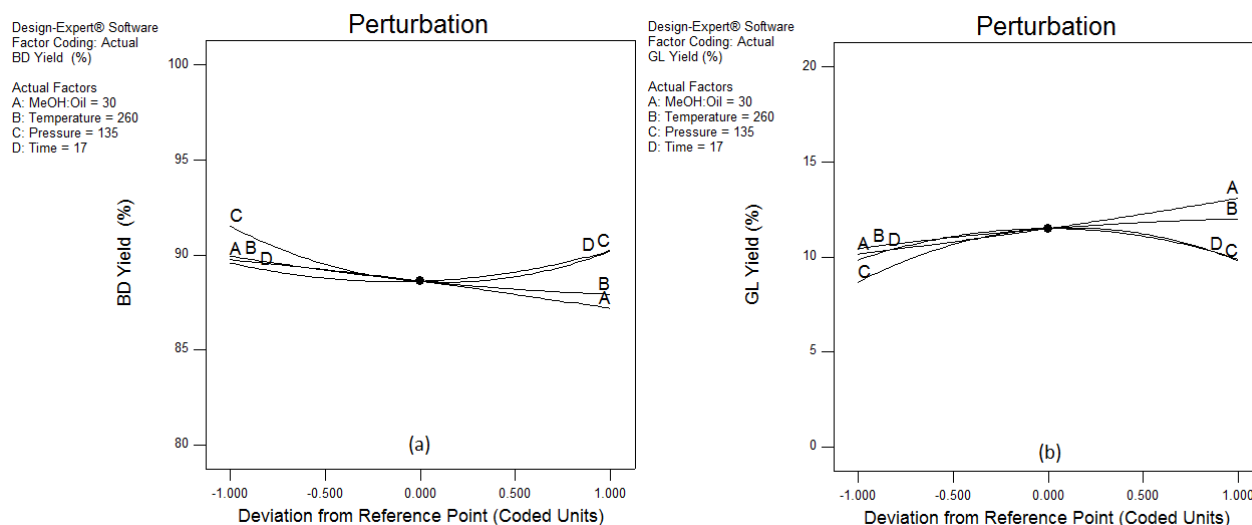


Figure 4.6. Perturbation plot showing the effect of individual variables on (a) biodiesel yield and (b) glycerol yield

One of the drawbacks of using supercritical methanol technique for biodiesel production is the usage of large excess of methanol, where it is very important to investigate its effect on the biodiesel yield for optimisation considerations. It is clearly shown in Figure 4.6a that M:O molar ratio (A) has a negative effect on biodiesel yield, where increasing M:O molar ratio decreases biodiesel yield. These findings are in agreement with previous study by Rade et al. (2015b) on high acidity soybean oil, where they reported a negative influence of alcohol to oil molar ratio on biodiesel yield. Varma et al. (2010) reported that increasing M:O molar ratio for supercritical synthesis of biodiesel does not have significant effect on biodiesel yield. They have explained these results as the formation of homogenous reaction phase only requires lower molar ratios. Accordingly, increasing methanol to oil ratio does not have a significant effect on the homogeneity of the solution. However, these results contradict previous studies for biodiesel production from WCO

using supercritical methanol (Ghoreishi and Moein, 2013). On the other hand, M:O molar ratio has positive effect on glycerol yield as shown in Figure 4.6b. This is an expected result as it has been reported previously that M:O ratio enhance transesterification reaction of which glycerol is produced (Ghoreishi and Moein, 2013).

Reaction temperature is an important parameter for supercritical production of biodiesel. It has been reported that at reaction temperature higher than 280°C, thermal degradation of FAME occurs (Imahara et al., 2008). Since the critical temperature of methanol is 240 °C, the studied temperatures ranges have been chosen between 240 °C and 280 °C. In the present study, reaction temperature has negative effect on biodiesel yield as shown in Figure 4.6a. This result contradicts previous studies where it has been reported positive impact of increasing temperature on biodiesel yield (García-Martínez et al., 2017; Román-Figueroa et al., 2016). The effect of temperature varies at different levels of M:O molar ratio. Hence, this is comprehensively discussed in section 3.3.2.1. However, glycerol yield has been positively affected by increasing reaction temperature as shown in Figure 4.6b.

Reaction pressure is one of the most important factors for supercritical transesterification reactions. It has a very high impact on the properties of the solution including density and hydrogen bond intensity (He et al., 2007). It has been reported that the effect of reaction pressure on biodiesel yield is not highly significant. In the present study, reaction pressure showed significant effect on biodiesel yield. However, the variation in biodiesel yield reported 6% while varying pressure from 85-185 bar. Moreover, slightly negative impact is shown at Equation 4.3 with very small coefficient. These results are in agreement with Tsai et al. (2013) who have reported about 7% variation in biodiesel yield when varying pressure from 10-25 MPa. Hence, they have considered constant pressure for their optimisation procedures. Nevertheless, reaction pressure showed insignificant effect on glycerol yield as shown in Table 4.5. Increasing reaction pressure from 110 to 140 bar, resulted in 4% increase in glycerol yield. However, higher values of pressure decreased glycerol yield.

In this study, reaction time has been reported to have very limited effect on biodiesel yield. Biodiesel variation has been reported to be 3% by varying time from 12 to 22 min. On the other hand, reaction time has been found to be insignificant on glycerol yield.

4.3.1.3.2. Effect of variables interactions on the responses

The interaction effect of each pair of variables has been observed from both interaction plots and ANOVA results. Moreover, 3D-surface and contour plots for biodiesel and glycerol yields *versus* interaction of two independent variables have been used to illustrate the effect of interaction. In each plot the two remaining independent variables have been kept constant at their centre points. For simplicity, this analysis only includes biodiesel yield response.

As reported in ANOVA results shown in Table 4.4, the interactive effect of M:O molar ratio and temperature has been observed as a significant variable. Figure 4.7 illustrates an interaction plot between M:O molar ratio and temperature where antagonistic interaction is clearly observed which confirms ANOVA results. Figure 4.8 represents a response surface and contour plots for M:O molar ratio and temperature interactive effect on biodiesel yield. It can be seen from Figure 4.8 that at low temperature the effect of M:O molar ratio is approximately neglected, however at higher temperatures, M:O molar ratio has negative effect on biodiesel yield. Additionally, at low M:O molar ratio, increasing reaction temperature shows positive influence on biodiesel yield. However, at high levels of M:O molar ratio, biodiesel yield decreases with an increase in temperature. These results showed the importance of studying the variables interactive effect. Román-Figueroa et al. (2016) have studied the individual yields of different FAMEs from high acidity raw castor oil using supercritical methanol. They have reported decreasing effect of methyl oleate and methyl palmitate (which are the main components of the WCO used in the present study) yields while increasing temperature starting from 250 °C at a constant M:O molar ratio of 1:40. They explained this phenomenon to the increasing rate of thermal degradation of both FAMEs and FFAs. Interaction effect of M:O molar ratio and temperature for high acidity feedstock was not reported widely.

Design-Expert® Software
Factor Coding: Actual
BD yield (%)
● Design Points
--- 95% CI Bands

X1 = A: M:O molar ratio
X2 = B: Temperature

Actual Factors
C: Pressure = 110
D: Time = 22

B- 250
B+ 270

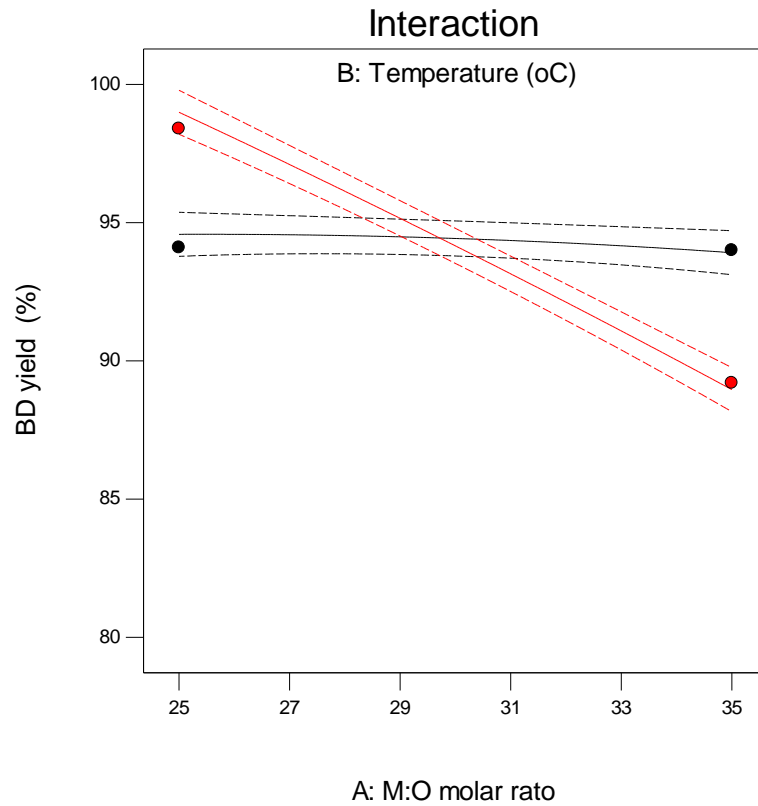


Figure 4.7. Interaction plot showing interactive effect of methanol ratio and temperature on biodiesel yield

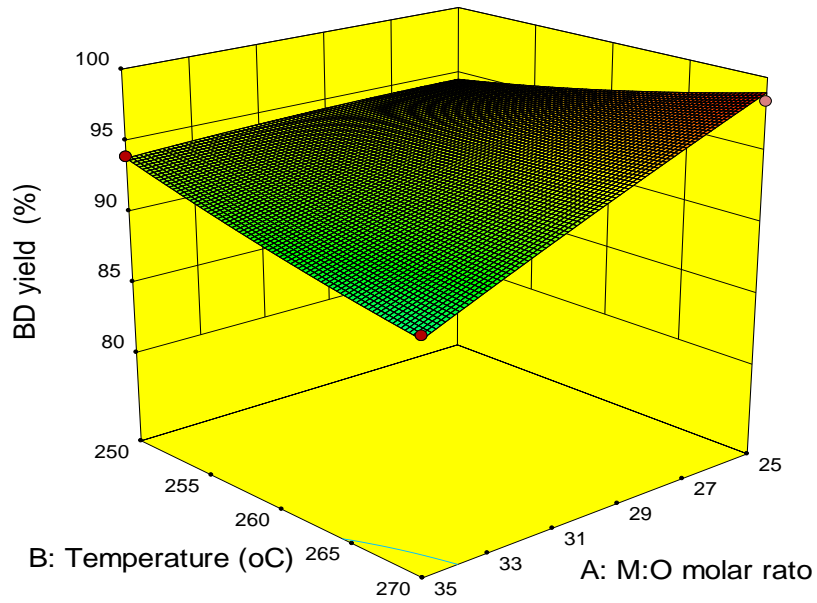
Design-Expert® Software
 Factor Coding: Actual
 BD yield (%)

● Design points above predicted value
 ● Design points below predicted value



X1 = A: M:O molar ratio
 X2 = B: Temperature

Actual Factors
 C: Pressure = 110
 D: Time = 22



Design-Expert® Software
 Factor Coding: Actual
 BD yield (%)

● Design Points



X1 = A: M:O molar ratio
 X2 = B: Temperature

Actual Factors
 C: Pressure = 110
 D: Time = 22

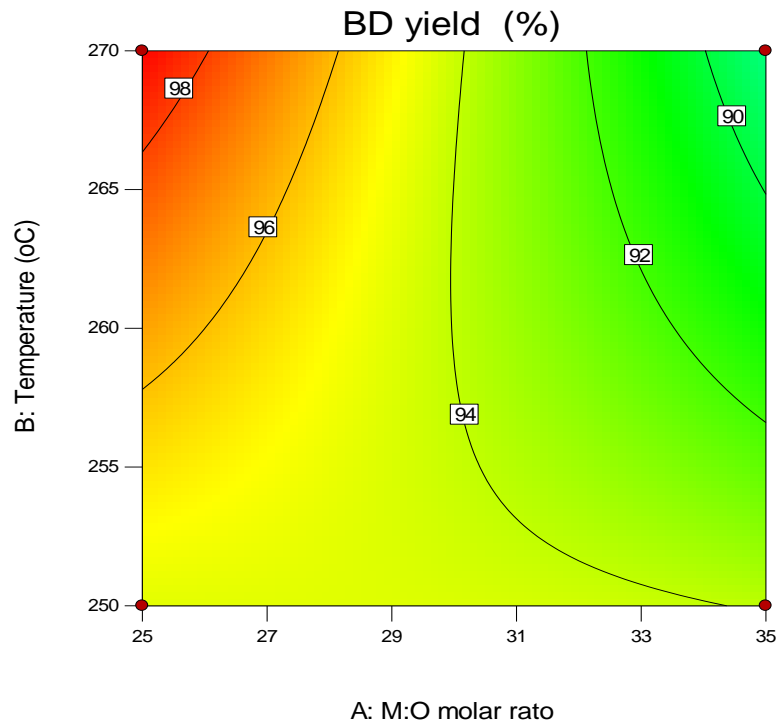


Figure 4.8. 3D response surface and contour plot for M:O molar ratio and reaction temperature versus biodiesel yield

CO₂ gas has been used to pressurise the reaction to the desired pressure using a high-pressure pump. In addition, CO₂ acts as a co-solvent, where it enhances the solubility of methanol in oil (Han et al., 2005). The exponential interactive effect of reaction pressure and time on biodiesel yield is shown in Figure 4.9, which confirms the significant effect of their interaction as reported in ANOVA in Table 4.4. As shown in Figure 4.10, reaction pressure showed negligible effect on biodiesel yield at shorter reaction times. However, slightly negative effect of reaction pressure observed at longer reaction times. It has been reported by Ong et al. (2013) that the increasing effect of pressure is not crucial as it exceeds the critical pressure of methanol. They explained that both transesterification and esterification have the same number of moles of reactants and products. Hence, the change in pressure would not affect the chemical equilibrium of reaction according to Le Chatelier's principle. While the negative effect of increasing pressure might be resulted from FAME degradation as addition of CO₂ decrease the critical point of the system and hence requires milder temperature (Han et al., 2005).

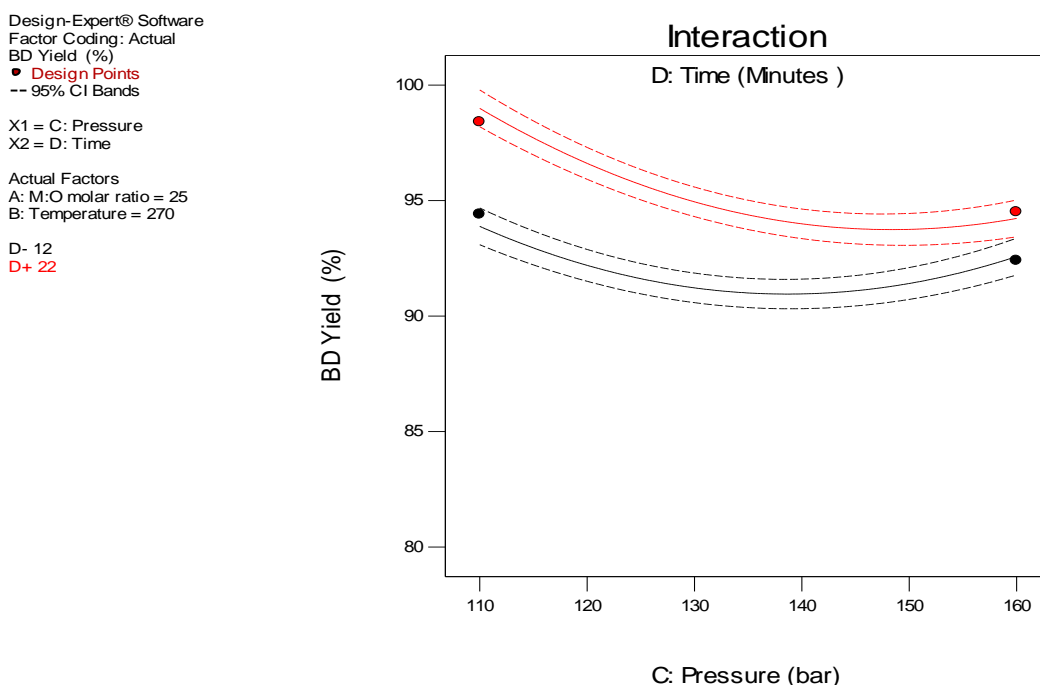


Figure 4.9. Interaction plot showing interactive effect of reaction pressure and time on biodiesel yield

Design-Expert® Software

Factor Coding: Actual

BD yield (%)

● Design points above predicted value

○ Design points below predicted value



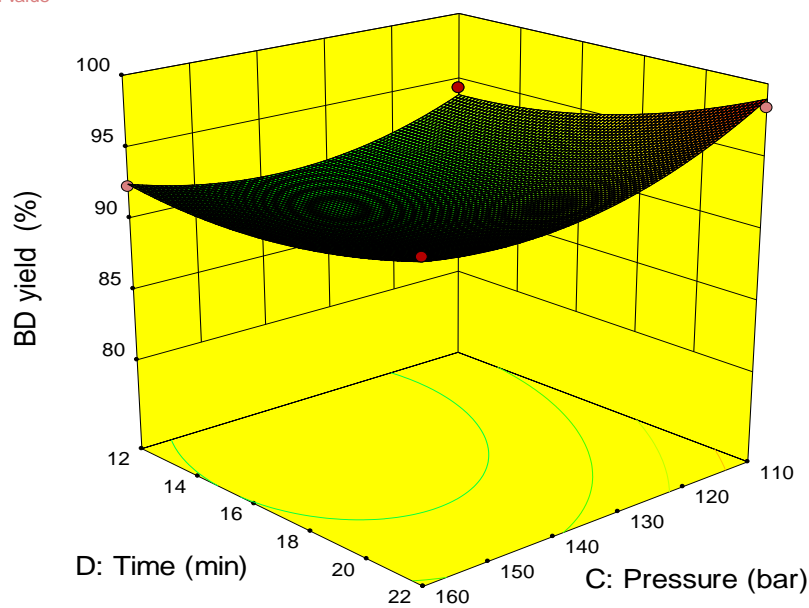
X1 = C: Pressure

X2 = D: Time

Actual Factors

A: M:O molar ratio = 25

B: Temperature = 270



Design-Expert® Software

Factor Coding: Actual

BD yield (%)

● Design Points



X1 = C: Pressure

X2 = D: Time

Actual Factors

A: M:O molar ratio = 25

B: Temperature = 270

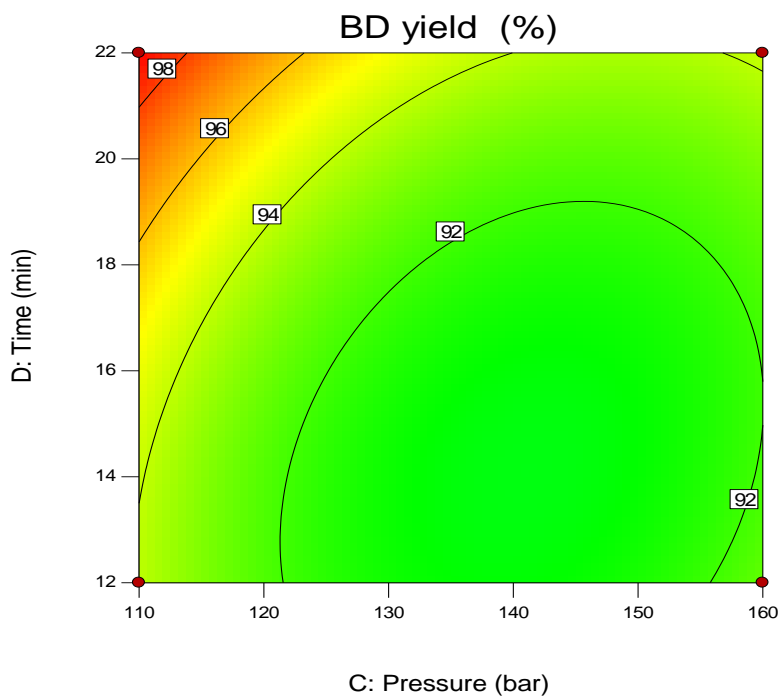


Figure 4.10. 3D response surface and contour plot for reaction pressure and time versus biodiesel yield

4.3.1.4. Process optimisation and experimental validation

The application of RSM to optimise the reaction variables affecting biodiesel production have been reported in previous studies (García-Martínez et al., 2017; Lee et al., 2015; Muthukumaran et al., 2017a; Silitonga et al., 2016). In order to optimise both reaction responses (i.e. biodiesel and glycerol yields), numerical feature using Design Expert 10 software has been implemented to evaluate the best combination of conditions for achieving the desired target. Biodiesel yield response has been set to a maximum target while minimum target of glycerol has been adjusted. The independent variables have been set to a minimum level as shown in Table 4.6. Subsequently, 40 solutions for optimum conditions have been generated by the software where the solution with highest desirability has been selected. The resulting optimum conditions achieved 98% and 2.05% for biodiesel and glycerol yield, respectively at 25:1 M:O molar ratio, 265 °C, 110 bar pressure in 20 min reaction time. In order to validate the predicted optimum conditions, three experiments have been conducted at these conditions, where the average result has been considered as the experimental outcome. The experimental validation has resulted biodiesel yield of 98.8%, which shows the adequacy of the predicted optimum conditions within 0.83% relative error from the experimental results.

Table 4.6. Optimisation constrains used to predict optimum conditions for biodiesel production

Factor	Code	Goal	Limits	
			Lower	Upper
M:O (molar ratio)	A	Minimise	25	35
Temperature (°C)	B	Minimise	250	270
Pressure (bar)	C	Minimise	110	160
Time (min)	D	Minimise	12	22
Biodiesel yield	Y ₁	Maximise	95	99
Glycerol yield	Y ₂	Minimise	0.52	17.72

The purified biodiesel produced at the optimum condition has been analysed and compared with the European Biodiesel Standard, EN14214. All the main measured physicochemical properties are within the range of the European standard as shown in Table 4.7.

Table 4.7. Comparison between produced biodiesel properties and European biodiesel standard EN14214

Test	Unit	Produced biodiesel	Biodiesel (EN14214)
Density at 15°C	kg/m ³	884	860 - 900
Kinematic viscosity at 40°C	cSt	4.6	3.5 - 5
TAN	mg KOH/ g oil	0.3	< 0.5

4.3.2. Analysis of FAME yields for individual FAMEs

4.3.2.1. Chromatogram analysis of derivatised WCO

The standard FAME mixed sample was injected to a GC to identify and verify the retention time of each FAME. Consequently, the derivatised WCO sample was injected to the GC to identify the composition of the WCO. Figure 4.11 illustrates the chromatogram of derivatised sample, where the main components have been well identified and separated. Solvents peaks of both (*n*-hexane and methanol) were excluded for better clarity. As shown in Figure 4.11, four main components were identified including methyl-oleate (C18:1), methyl-linoleate (C18:2), methyl-palmitate (C16:0) and methyl-myristate (C14:0). This indicates that four mentioned components represent the main fatty acids composition of WCO, namely oleic acid, linoleic acid, palmitic acid and myristic acid.

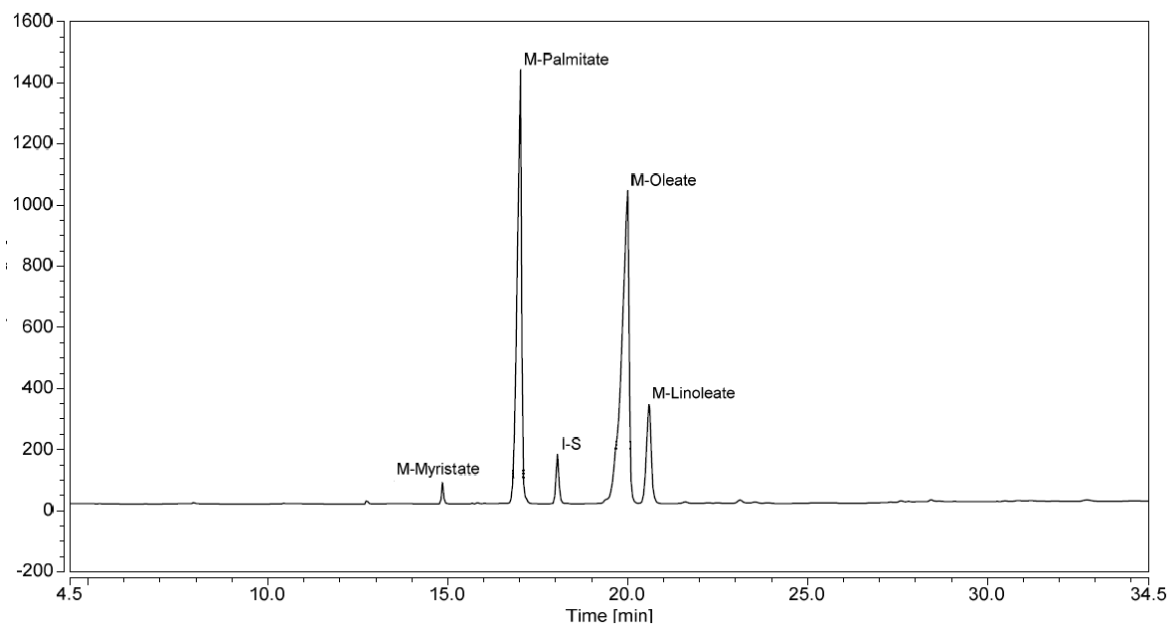


Figure 4.11. Chromatographic results of the derivatised WCO

4.3.2.2. Calibration curves for standards

For quantification process of the concentration of each component in WCO, internal standard method was adopted. Response factor of each component was determined to calculate its concentration. Only the main components identified through the chromatogram results of the derivatised sample were considered. Five different concentrations of the standard samples with fixed concentration of internal standard were prepared. Triplicate injection of each sample was performed to ensure the reliability and consistency of the response factor. Response factor of each component was calculated using a mathematical division of different area ratios (AR_i) and concentration ratios (CR_i) of the component as shown in Equation 4.7. Area ratio is defined as the ratio between the analyte area (A_i) and internal standard area (A_{is}) as shown in Equation 4.8. In addition, concentration ratio is defined as the ratio between concentration of the analyte (C_i) and the internal standard concentration (C_{is}) as shown in Equation 4.9 (Abidin et al., 2013). Accordingly, a plot between different area ratios and concentration ratios (calibration curve) was used to calculate the average response factor of each component. For

simplicity, the three main compositions of the oil including linoleic acid, palmitic acid and oleic acid were considered for calibration curves and conversion studies.

$$RF_i = \frac{\text{Area ratio of } i^{\text{th}} \text{ component, } AR_i}{\text{Concentration ratio of } i^{\text{th}} \text{ component, } CR_i} \quad (4.7)$$

$$Ar_i = \frac{\text{Area of } i^{\text{th}} \text{ component, } A_i}{\text{Area of the internal standard, } A_{IS}} \quad (4.8)$$

$$Cr_i = \frac{\text{Concentration of } i^{\text{th}} \text{ component, } C_i}{\text{Concentration of the internal standard, } C_{IS}} \quad (4.9)$$

Figure 4.12 illustrates the calibration curves for FAME standard component where the slope of each plot represents the response factor of each component. Hence, response factors of oleic acid, linoleic acid and palmitic acid were reported as 0.9655, 0.9814 and 0.9728, respectively. The consistency of the results is illustrated with the r-squared values where all the values are greater than 0.99. Accordingly, the concentration of each component (i^{th} component) in the biodiesel sample (j^{th} sample) could be calculated according to Equation 4.10. The composition of derivatised WCO sample is summarised in Table 4.8. It is clearly shown in Table 4.8 that oleic acid and palmitic acid represent the majority of the oil composition (89.8%) while linoleic acid represents 9.3%. Based on these calculations, composition of myristic acid was predicted as 0.9%.

$$C_{ij} = \frac{\text{Area ratio of } i^{\text{th}} \text{ component in the } j^{\text{th}} \text{ sample, } AR_{ij} \times C_{IS}}{\text{Response factor of } i^{\text{th}} \text{ component, } RF_i} \quad (4.10)$$

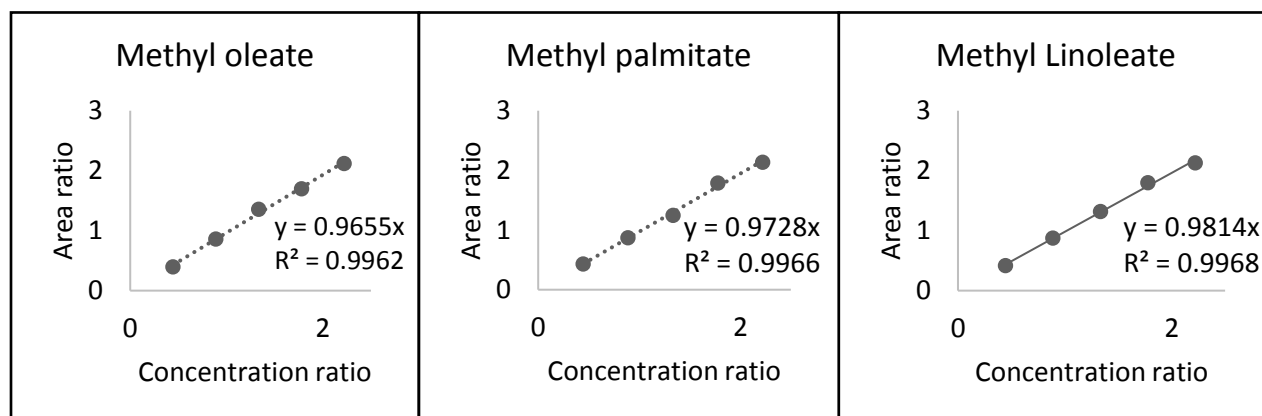


Figure 4.12. Calibration curves of FAME standard

Table 4.8. Composition of the fatty acids in WCO

Fatty Acid	wt (%)
Palmitic acid	41.6
Oleic acid	48.2
Linoleic acid	9.3
Myristic acid	~ 0.8

4.3.2.3. FAME yield calculations

FAME yield calculation for biodiesel production from WCO as a result from transesterification of triglycerides and esterification of free fatty acids was performed using chromatographic analysis. The FAME yield was calculated as a ratio between actual and theoretical yield (Conover, 2009) as shown in Equation 4.11. The theoretical yield was considered as the yield calculated from the derivatised sample as mostly all the fatty acids were converted to FAMEs. However, the actual yield was varied according to each experimental condition. Yield calculations were performed from the chromatographic obtained concentration of each FAME as reported previously (Liu et al., 2008). The FAME yields of methyl-oleate, methyl-palmitate and methyl- linoleate are given in Table 4.9.

$$FAME\ yield = \frac{FAME\ content\ in\ the\ sample}{Maximum\ theoretical\ FAME} \times 100\ (\%) \quad (4.11)$$

4.3.2.4. Models development and adequacy checking

RSM using CCD has been used to fit the experimental results to a quadratic model using regression analysis to represent each reaction response function in reaction variables. Three quadratic models have been developed as shown in Equations 4.12 to 4.14. The predicted models have been subjected for both statistical and experimental validation.

Table 4.9 illustrates the actual experimental results and the predicted results of each response.

$$Y_1 = 99.37 - 0.032 A + 0.089 B - 0.0084 C + 0.036 D + 0.061 AB + 0.024 AC - 0.05 AD + 0.052 BC - 0.066 BD + 0.077 CD - 0.069 A^2 - 0.12 B^2 - 0.056 C^2 - 0.16 D^2 \quad (4.12)$$

$$Y_2 = 99.19 - 0.022 A + 0.023 B - 0.0045 C + 0.01 D + 0.044 AB + 0.017 AC - 0.029 AD + 0.061 BC - 0.047 BD + 0.065 CD - 0.053 A^2 - 0.086 B^2 - 0.026 C^2 - 0.092 D^2 \quad (4.13)$$

$$Y_3 = 99.10 - 0.038 A + 0.038 B - 0.010 C + 0.042 D + 0.054 AB + 0.027 AC - 0.031 AD + 0.036 BC - 0.049 BD + 0.036 CD - 0.016 A^2 - 0.045 B^2 - 0.019 C^2 - 0.099 D^2 \quad (4.14)$$

Where Y_1 , Y_2 and Y_3 represent FAME yield of methyl-oleate, methyl-palmitate and methyl-linoleate, respectively. While, A, B, C and D represent the process variables including M:O molar ratio, temperature, pressure and time, respectively.

The adequacies of the predicted models have been checked through different methods in the present study. Plots for actual *versus* predicted values for each response are presented in Figure 4.13. This plot analyses the accuracy of the model in fitting the experimental data. If the predicted value is exactly the same as the actual value, the point will exactly fit on the 45° line. The very low deviation of the points from the 45° line indicates the adequacy of the predicted models.

Table 4.9. Experimental design matrix with the actual and predicted yields

Run	M:O molar ratio (A)	Temperature (°C) (B)	Pressure (bar) (C)	Time (min) (D)	Actual M-Oleate %	Predicted M-Oleate %	Actual M-Palmitate %	Predicted M-Palmitate %	Actual M-Linoleate %	Predicted M-Linoleate %
1	30	260	135	17	99.2	99.3	99.1	99.1	99.0	99.1
2	35	250	160	22	98.9	98.8	98.9	98.9	98.9	98.8
3	35	250	110	22	98.7	98.8	98.8	98.8	98.8	98.8
4	35	270	160	22	99.0	99.1	99.0	99.0	98.9	99.0
5	35	270	110	12	99.1	99.1	99.0	99.0	98.9	98.9
6	35	250	160	12	98.5	98.6	98.6	98.7	98.6	98.6
7	25	270	160	22	99.1	99.1	99.0	99.0	99.0	98.9
8	30	260	135	17	99.3	99.4	99.2	99.1	99.1	99.0
9	25	250	110	22	99.0	99.1	99.0	99.0	99.1	99.1
10	25	250	160	22	99.2	99.1	99.0	99.0	99.0	99.0
11	30	260	85	17	99.2	99.2	99.1	99.0	99.0	99.0
12	25	270	110	12	99.0	99.1	98.9	98.9	98.9	98.9
13	25	250	160	12	98.6	98.7	98.7	98.7	98.7	98.7
14	30	260	135	17	99.4	99.4	99.2	99.1	99.1	99.0
15	35	250	110	12	98.8	98.8	98.9	98.9	98.7	98.7
16	30	240	135	17	98.6	98.7	98.8	98.7	98.8	98.8
17	30	260	185	17	99.1	99.1	99.0	99.1	98.9	98.9
18	35	270	160	12	99.2	99.1	99.0	99.0	99.0	99.0
19	30	260	135	17	99.4	99.4	99.2	99.1	99.1	99.0
20	30	260	135	27	98.8	98.7	98.8	98.8	98.7	98.7
21	30	260	135	7	98.7	98.6	98.8	98.8	98.6	98.6
22	25	270	160	12	98.9	98.9	98.9	98.9	98.8	98.8
23	20	260	135	17	99.1	99.1	99.0	99.0	99.1	99.1
24	25	250	110	12	99.1	98.9	99.0	99.0	98.9	98.9
25	30	280	135	17	99.1	99.0	98.9	98.8	99.0	98.9
26	30	260	135	17	99.4	99.3	99.2	99.1	99.1	99.1
27	40	260	135	17	99.1	99.0	98.9	98.9	98.9	98.9
28	25	270	110	22	99.0	98.9	98.8	98.8	98.9	98.9
29	30	260	135	17	99.4	99.3	99.2	99.1	99.1	99.1
30	35	270	110	22	98.8	98.8	98.7	98.7	98.8	98.8

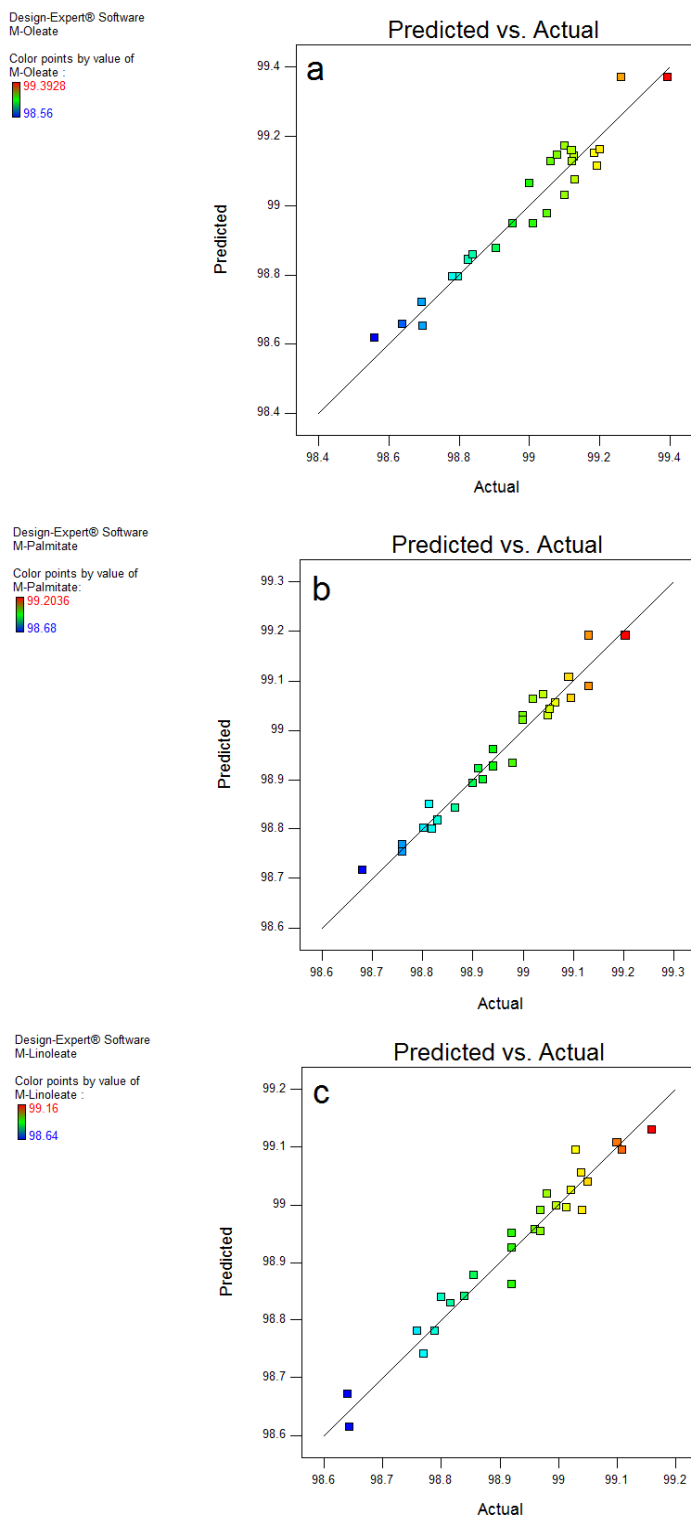


Figure 4.13. Predicted *versus* actual values for methyl-oleate model (a), methyl-palmitate model (b) and methyl-oleate model (c)

The adequacies of predicted models have also been checked using R^2 which assess the accuracy of the predicted values. The closer the R^2 value to one, indicates high accuracy of the predicted model. These values have been reported as 0.992, 0.987, and 0.989 for the models representing the FAME yield of methyl-oleate, methyl-palmitate and methyl-linoleate, respectively. Furthermore, ANOVA has been applied to check the significance of the developed model in predicting similar data to the experimental values. Table 4.10 to Table 4.12 represent the ANOVA results of the predicted models. It has been concluded for the ANOVA tables that the high significance of the developed models with very low p-values (<0.0001). This validates the adequacy of the developed model in predicting the experimental results. In addition, the lack of fit analysis has been applied to measure the fitting efficiencies of the predicted models. The lack of fit analysis resulted in non-significant results of p-values reported as 0.265, 0.311 and 0.319 (more than 0.05) for the FAME yield of methyl-oleate, methyl-palmitate and methyl-linoleate, respectively.

Table 4.10. Analysis of variance for yield of methyl-oleate model

Source	Sum of Squares	df	Mean Square	F- Value	p-value
Model	1.50	14	0.11	24.8	<0.0001
A-MeOH:Oil	0.02	1	0.0	5.5	0.03
B-Temperature	0.18	1	0.18	41.6	<0.0001
C-Pressure	0.001	1	0.001	0.3	0.51
D-Time	0.03	1	0.03	6.9	0.01
AB	0.05	1	0.05	12.9	0.002
AC	0.01	1	0.01	1.9	0.25
AD	0.03	1	0.04	8.6	0.01
BC	0.04	1	0.04	9.4	0.007
BD	0.07	1	0.07	15.4	0.001
CD	0.09	1	0.09	21.0	0.0003
A ²	0.13	1	0.13	28.7	<0.0001
B ²	0.38	1	0.38	84.7	<0.0001
C ²	0.08	1	0.08	19.1	0.0005
D ²	0.71	1	0.71	158.4	<0.0001
Residual	0.06	15	0.01		
Lack of Fit	0.05	10	0.01	1.8	0.26
Pure Error	0.01	5	0.002		

Table 4.11. Analysis of variance for yield of methyl-palmitate model

Source	Sum of Squares	df	Mean Square	F- Value	p-value
Model	0.61	14	0.04	36.39	<0.0001
A-MeOH:Oil	0.01	1	0.01	8.75	0.009
B-Temperature	0.01	1	0.01	10.37	0.005
C-Pressure	0.001	1	0.001	0.39	0.53
D-Time	0.002	1	0.002	2.01	0.17
AB	0.03	1	0.03	24.07	0.0001
AC	0.004	1	0.004	3.65	0.07
AD	0.01	1	0.01	10.79	0.005
BC	0.05	1	0.05	46.09	<0.0001
BD	0.03	1	0.03	27.55	<0.0001
CD	0.06	1	0.06	53.01	<0.0001
A ²	0.07	1	0.07	61.42	<0.0001
B ²	0.20	1	0.20	159.81	<0.0001
C ²	0.01	1	0.01	11.67	0.003
D ²	0.23	1	0.23	184.19	<0.0001
Residual	0.02	15	0.001		
Lack of Fit	0.01	10	0.001	1.61	0.31
Pure Error	0.005	5	0.001		

Table 4.12. Analysis of variance for yield of methyl-linoleate model

Source	Sum of Squares	df	Mean Square	F-Value	p-value
Model	0.56	14	0.04	28.1	<0.0001
A-MeOH:Oil	0.03	1	0.03	24.6	0.0001
B-Temperature	0.03	1	0.03	23.8	0.0002
C-Pressure	0.002	1	0.002	1.69	0.21
D-Time	0.04	1	0.04	28.8	<0.0001
AB	0.04	1	0.04	32.7	<0.0001
AC	0.01	1	0.01	8.01	0.01
AD	0.01	1	0.015	10.6	0.005
BC	0.02	1	0.02	14.4	0.001
BD	0.03	1	0.04	27.2	0.0001
CD	0.02	1	0.02	14.2	0.001
A ²	0.007	1	0.007	5.03	0.04
B ²	0.05	1	0.05	38.7	<0.0001
C ²	0.01	1	0.01	7.01	0.01
D ²	0.27	1	0.27	189.6	<0.0001
Residual	0.02	15	0.001		
Lack of Fit	0.01	10	0.001	1.58	0.31
Pure Error	0.005	5	0.001		

4.3.2.5. Effect of process variables and their interactions

It has been observed from the experimental runs that using supercritical methanol successfully converts most of triglycerides and FFAs to FAMEs through the transesterification/esterification reactions. Within the studied ranges of parameters, the experimental yields have been reported between 98% and 99.5%. These results show high significance of supercritical methanolysis in conversion of triglycerides and FFAs with very similar yield obtained through the standard derivatisation method. Accordingly, the interactive effects of variables on each response have been studied and reported.

4.3.2.5.1. Interactive effect of methanol:oil molar ratio and reaction time

Supercritical methanolysis requires the usage of huge excess of methanol in the reaction within M:O molar ratio from 20:1 up to 126:1 (Zhou et al., 2017). Through this study the increasing effect of methanol ratio has marginally increasing influence on the FAME yields of methyl-oleate, methyl-palmitate and methyl-linoleate at lower reaction time. However, it has negative effect at higher reaction time as shown in Figure 4.14. This highly interactive effect illustrates the significance of studying the variables interaction in addition to OFAT. According to Le Chatelier principle, increasing methanol ratio should enhance the conversion of reactants by shifting the reaction equilibrium towards the products (Torrentes-Espinoza et al., 2017). However, using large excess of methanol would dilute the reactant too much when exceeds a specific limit (Zhou et al., 2017). The optimum limit that should be implemented varies according to the feedstock composition, FFA concentration and water content.

One of the main advantages of using supercritical methanolysis is the significant reduction in reaction time. Through the present study, the reaction time has shown a significant influence on yields of methyl-oleate, methyl-palmitate and methyl-linoleate as shown in Table 4.10 Table 4.12. Increasing reaction time has shown positive effect on all FAMEs yields up to 20 min at lower M:O molar ratio as shown in Figure 4.14. However, at higher M:O molar ratio the reaction time has increasing effect up to 17 min. Interactive effect between M:O molar ratio and reaction time has recorded significant effect on

FAMES' yields as illustrated in Table 4.10. This result is clearly shown in Figure 4.14, where the effect of reaction time on FAMES' yields at lower M:O molar ratio is not similar to its effect at higher M:O molar ratio. Hence, the variation of the reaction time effect should be considered within optimisation process. These results are in agreement with previously reported studies where a significant interaction between reaction time, M:O molar ratio and temperature has been reported previously (Lee et al., 2015). In addition, a study on biodiesel production from high acidity tobacco seed oil has reported the significant interaction between reaction time and M:O molar ratio (García-Martínez et al., 2017). They have observed a decreasing effect on biodiesel yield at longer reaction time. They have addressed thermal degradation of methyl esters as an acceptable cause for the yield drop.

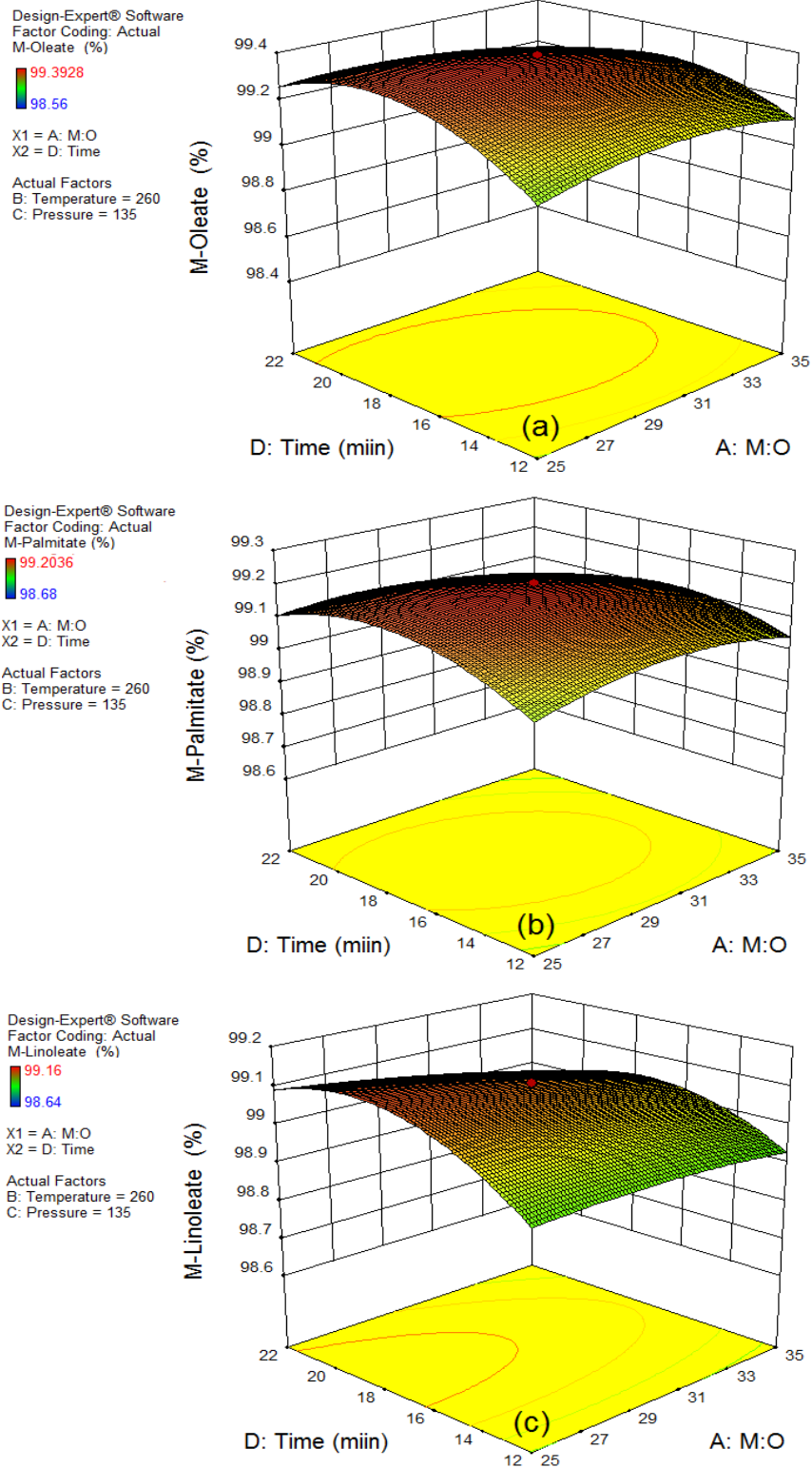


Figure 4.14. Response surface of the effect of reaction time and M:O molar on the FAME yield of methyl-oleate (a), methyl-palmitate (b) and methyl-oleate (c)

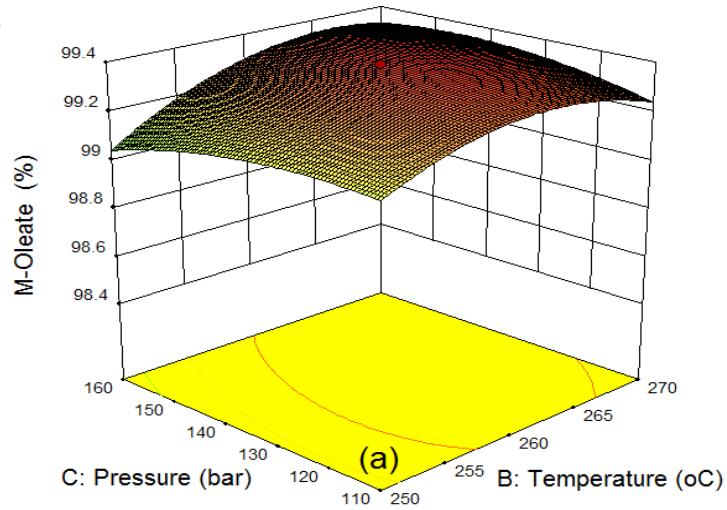
4.3.2.5.2. Interactive effect of reaction temperature and pressure

Using supercritical methanolysis, reaction temperature should be set to the critical temperature of methanol as a minimum condition. Accordingly, the temperature studied range has been started from 240 °C as shown in Table 4.2. The increasing effect of reaction temperature has enhanced the FAME yield of FAMEs as shown in Figure 4.15. However, at higher reaction temperature the yield starts to decrease. Thermal degradation of FAMEs is considered the main reason for decreasing the yield of FAME at temperature higher than 265 °C (Imahara et al., 2008). In addition, reaction pressure has shown positive effect on FAMEs' yields as shown in Figure 4.15.

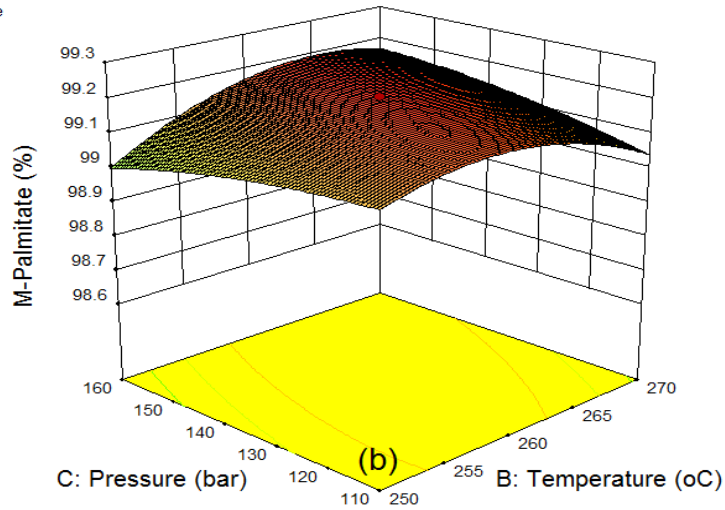
Reaction pressure has negative effect on biodiesel yield at 250°C, however, it has slightly increasingly effect at higher temperature i.e. 270 °C. This attribute to the possible degradation of FAMEs at high pressures, in addition the presence of CO₂ contributes in lowering the system's critical point where higher degradation rate is expected at higher temperature and pressure (Han et al., 2005). Similar results have been reported for the effect of high pressure on biodiesel yield (Qiao et al., 2017). They have reported that the solubility of methanol in oil decreases by increasing the pressure beyond the critical pressure. Similarly, the increasing pressure has negative effect on biodiesel produced from soybean flakes lipids (Xu et al., 2016). However, the total change in yield at extreme conditions has about only 1 % difference in yield, which indicates constant high yield of biodiesel using high FFA feedstock *via* supercritical methanolysis.

Interaction between reaction temperature and pressure has been reported to have highly significant effect on the three responses as shown in Table 4.10, Table 4.11, Table 4.12 with p-values of 0.0013, <0.0001 and 0.0001 for yields of methyl-oleate, methyl-palmitate and methyl-linoleate, respectively. This means that the effect of reaction pressure on the yield is not constant at different levels of temperature, and *vice-versa*. Similarly, the significant interaction between reaction temperature and pressure for biodiesel production from WCO has been reported previously (Ghoreishi and Moein, 2013).

Design-Expert® Software
 Factor Coding: Actual
 M-Oleate (%)
 99.3928
 98.56
 X1 = B: Temperature
 X2 = C: Pressure
 Actual Factors
 A: M:O = 30
 D: Time = 17



Design-Expert® Software
 Factor Coding: Actual
 M-Palmitate (%)
 99.2036
 98.68
 X1 = B: Temperature
 X2 = C: Pressure
 Actual Factors
 A: M:O = 30
 D: Time = 17



Design-Expert® Software
 Factor Coding: Actual
 M-Linoleate (%)
 99.16
 98.64
 X1 = B: Temperature
 X2 = C: Pressure
 Actual Factors
 A: M:O = 30
 D: Time = 17

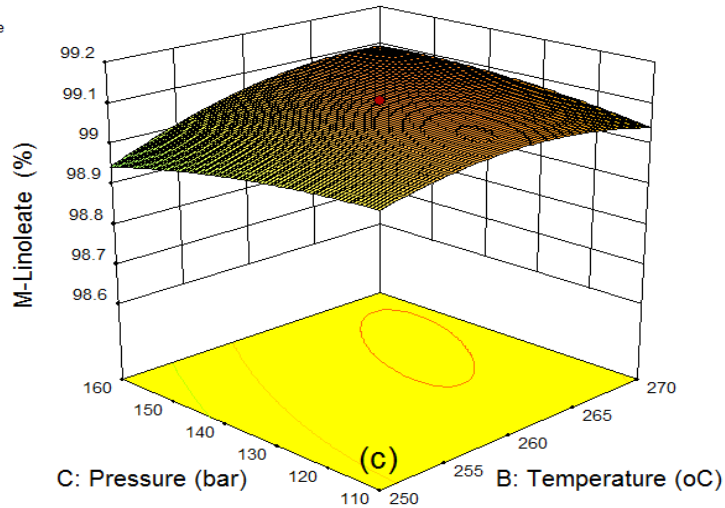


Figure 4.15. Response surface of the effect of reaction temperature and pressure on the FAME yield of methyl-oleate (a), methyl-palmitate (b) and methyl-oleate (c)

4.3.2.6. Process optimisation

Multi-targeting numerical optimisation using RSM has been applied as a result of having multiple reaction variables. The goals have been set to maximise all FAMEs yields while minimising reaction variables. Specific importance has been set for each goal where maximising FAMEs yields have been set to highest importance. Minimising reaction temperature and time have been set with high importance followed by M:O molar ratio and reaction pressure as shown in Table 4.13. RSM has been implemented to evaluate the best combination of reaction parameters that could achieve the required goals with high desirability (García-Martínez et al., 2017; Muthukumaran et al., 2017a). Accordingly, twenty-six solutions have been developed using numerical optimisation where the solution with highest desirability has been considered. It has been concluded that the optimal conditions for 99.2%, 99.3% and 99.13% of methyl-oleate, methyl-palmitate and methyl-linoleate yields, respectively, are M:O molar ratio of 25.6:1, 255°C, 110 bar within 16.7 min. The predicted optimal conditions have been validated experimentally with relative errors between 0.5-0.85%.

Table 4.13. Optimisation constraints used to predict optimum conditions for biodiesel production

Factor	Code	Goal	Importance	Limits	
			Scale 1-5	Lower	Upper
M:O (molar ratio)	A	Minimise	3	25	35
Temperature (°C)	B	Minimise	4	250	270
Pressure (bar)	C	Minimise	3	110	160
Time (min)	D	Minimise	4	12	22
Methyl-oleate yield	Y ₁	Maximise	5	98.3	100
Methyl-palmitate yield	Y ₂	Maximise	5	98.1	100
Methyl-linoleate yield	Y ₃	Maximise	5	98.2	100

4.4. Conclusions

Valorisation of high acid value WCO into biodiesel with very high yield has been achieved using supercritical methanolysis. The effect of process variables on biodiesel yield have shown different behaviours. For instance, the increasing effect of M:O molar ratio has decreased the yield of biodiesel. In addition, the effect of reaction temperature has a negative effect on biodiesel yield. Highly significant interactive effect of M:O molar ratio and temperature has been observed on overall biodiesel yield.

Further, it has been observed that the yield of supercritical methanolysis is very similar to the yield of the standard methylation process where the FAME yields have varied between 98 % and 99.5 %. The optimum overall biodiesel yield has been predicted with 98% at M:O molar ratio of 25:1, reaction temperature of 265 °C and reaction pressure of 110 bar in 20 min. The optimal conditions have been validated experimentally resulting in biodiesel yield of 98.82%, which shows the adequacy of the predicted optimum conditions within 0.83% relative error from the experimental results. However, the optimum yield FAMES of methyl-oleate, methyl-palmitate and methyl-linoleate have been reported as 99.2 %, 99.3 % and 99.13 %, respectively. The optimum yields have been achieved at 25.6:1 M:O molar ratio, 255 °C, 110 bar within 16.7 min. Finally, the properties of the produced biodiesel has been compared with the European biodiesel standard (EN14214), which showed excellent agreement with the standard biodiesel properties.

CHAPTER 5

KINETICS AND OPTIMISATION OF FREE FATTY ACIDS CONVERSION INTO BIODIESEL

Outline of the chapter

This chapter focuses on the esterification of FFAs in the high acidity WCO. Experimental design, modelling and optimisation are considered. The effect of linear and interactive process variables on responses is extensively explained. Two different analysis have been applied for the responses including overall conversion of FFAs and individual conversion of different FFAs. The chapter is organised as follows:

5.1. Introduction

5.2. Materials and methods

5.3. Results and discussion

5.3.1. Overall conversion of FFAs

5.3.2. Chromatographic analysis of individual FFAs

5.4. Conclusions

5. Kinetics, optimisation and simulation of free fatty acids conversion into biodiesel

5.1. Introduction

As esterification reaction converts the existing FFAs to biodiesel, it has been used widely as a pre-treatment step prior triglycerides conversion to FAMEs. This process is called “two-steps biodiesel production”, as it includes conversion of both FFAs and triglycerides to FAMEs (Kostić et al., 2016). The conversion of FFAs to FAMEs through esterification is usually performed using acidic catalysts. However, some limitations have been reported for acidic catalysed processes including costly separation, non-reusability and corrosion. Hence, heterogeneous solid catalysts have been extensively reported in recent years for esterification reaction (Avramidou et al., 2017; Kurniawan et al., 2015; Nur Syazwani et al., 2017; Yunus et al., 2016).

It has been reported that the esterification reaction rate of FFAs using supercritical methanol is very high and hence the FFAs content would not be considered as a limitation for biodiesel production from WCO. Several researches have considered esterification of FFAs using supercritical methanolysis and ethanolysis (de Jesus et al., 2018; dos Santos et al., 2017; Jin et al., 2015; Narayan and Madras, 2017). The focus on esterification reaction of FFAs using supercritical methanolysis would exemplify the ability of this technique to convert the existing FFAs into FAMEs. Several studies on esterification of FFAs have been reported using various techniques including ultrasonic-assisted (Boffito et al., 2014), microwave-assisted (Kim et al., 2011) and catalysed processes (Vengalil et al., 2016). However, very few researchers have considered studying the conversion of FFAs using supercritical technology. Jin et al. (2015) have studied the esterification of FFAs (specifically oleic acid) using supercritical methanol. Mostly, the conversion of FFAs into FAMEs is determined using titration method. The chromatographic analysis for FFAs concentration is frequently reported through derivatisation of FFAs into FAMEs or using

HPLC. Zhang et al. (2015a) have developed and validated a robust method for derivatisation-free analysis of FFAs using GC *via* FID.

In this chapter, esterification of FFAs of a high acidity WCO into biodiesel has been critically studied. A derivatisation-free method for specific FFAs characterisation has been developed to evaluate the concentration of each FFA in the feedstock and the products. The overall conversion of FFAs in addition to the conversion of four main FFAs have been considered as process responses including myristic, palmitic, oleic and linoleic acids. The influence of four independent reaction variables and their interaction, i.e. M:O molar ratio, temperature, pressure, time have been critically discussed. Graphical and numerical optimisation have been applied to optimise the reaction variables for maximum conversion of FFAs. Further, the esterification reaction kinetics have been studied. Finally, a reactor representing the esterification reaction has been designed and simulated.

5.2. Material and methods

5.2.1. Materials

This work has been conducted on the same high acidity WCO that has been collected from Egypt as mentioned in Section 4.2. Methanol 99% was purchased from Fisher Scientific UK Ltd. Toluene 99.8%, 2-propanol 99.7%, 0.1 M volumetric standard hydrochloric acid, 0.1 M standardised solution of potassium hydroxide in 2-propanol, *p*-naphtholbenzein and methyl orange were purchased from Merck, UK. In addition, the standard pure methyl esters used for preparing calibration curves including FAME certified mixture solution (C14-C20), methyl-oleate, methyl-linoleate, methyl-palmitate, methyl-myristate and methyl-heptadecanoate (internal standard) were purchased from Merck, UK. In addition, the standard fatty acids that represents the feedstock. i.e. myristic acid (C14:0), palmitic acid (C16:0), oleic acid (C18:1), linoleic acid (C18:2), and heptadecanoic acid (C17:0) as an internal standard, were purchased from Merck, UK.

Methanol 99% and *iso*-propanol 99% were purchased from Fisher Scientific UK. The liquid CO₂ cylinder (99.9%) equipped with dip tube was purchased from BOC Ltd., UK.

5.2.2. Experimental procedures

The esterification reaction has been carried out using supercritical methanolysis as mentioned previously in Section 4.2. However, this chapter is focusing on the esterification reaction where different responses have been considered including overall conversion of FFAs, that has been calibrated using the standard titration method, in addition to the specific conversion of each FFA using chromatographic analysis.

The fatty acids components of the feedstock were previously calibrated through derivatisation of triglycerides and FFAs into FAMES using the standard methylation process (BS EN ISO 12966-2:2017). The detailed analysis and composition of the feedstock were reported in Section 4.2.

5.2.2.1. Analysis of overall FFAs conversion

In order to analyse overall conversion of FFAs through esterification reaction, the TAN of both feedstock and produced biodiesel was calibrated. The standard method for acid and base number using colour indicator titration (ASTM D974) was implemented to calibrate the TAN of the samples. In summary, the analysis was performed by dissolving a mixture of 2-propanol, toluene and small amount of water to obtain a single-phase solution. Then, the titration technique was employed using 0.1 M KOH in 2-propanol solution using *p*-naphtholbenzein as an indicator. The conversion of FFA in each sample was calculated as shown in Equation 5.1 (Abidin et al., 2012).

$$FFA\ Conversion = (1 - TAN_1 / TAN_0) \times 100\% \quad (5.1)$$

Where TAN₀ and TAN₁ represent total acid number of feed and product, respectively.

5.2.2.2. Chromatographic analysis of FFAs conversion

5.2.2.2.1. Preparation of standard solutions

The pure standards, i.e. myristic acid, palmitic acid, oleic acid and linoleic acid, were dissolved in *iso*-propanol that has been used as a solvent. For calibration curves analysis, five different concentrations of each standard were prepared at 2, 4, 6, 8 and 10 g/L. Each

standard sample was accompanied with a constant concentration of heptadecanoic acid as an internal standard (4.5 g/L). A 2 mL sample of each standard was prepared for chromatographic injections.

5.2.2.2. Calibration curves for standards

The internal standard analytical method has been used to identify the concentration of each fatty acids in samples. Heptadecanoic acid has been used as an internal standard and has been added with a constant concentration for each analysed sample. For each component, the RF as previously explained in Section 4.3.2 at Equation 4.7 to 4.10.

A plot between AR and CR for each sample (at different concentrations) has been used to calculate the response factor. The calibration curves of fatty acids standards have been illustrated in Figure 5.1. It is clearly shown that the RF of myristic, palmitic, oleic and linoleic acids are 0.9757, 0.9788, 0.9697 and 0.9743, respectively. The uniformity of the results has been illustrated with high coefficient of determination (R^2), where all the values are greater than 0.99.

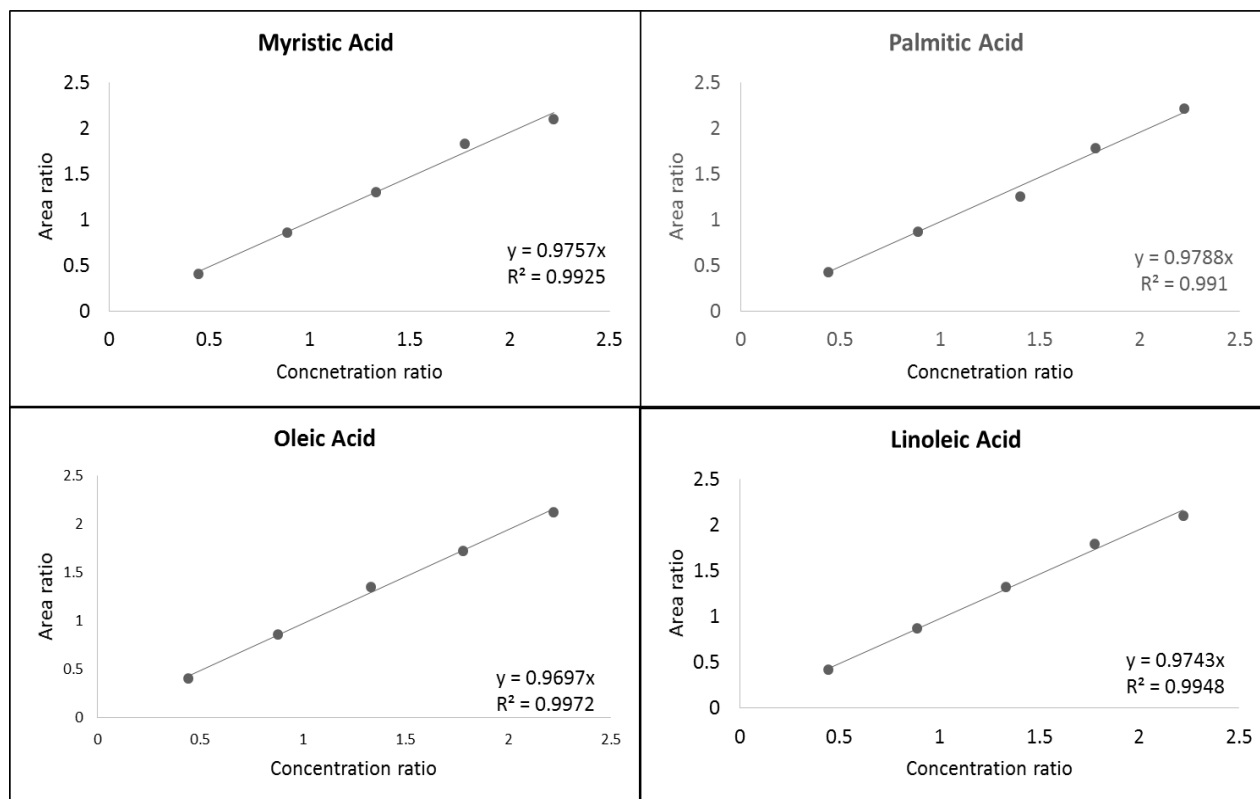


Figure 5.1. Calibration curves of fatty acids standards

5.2.2.2.3. FFAs conversion calculations

The conversion of each FFA has been calculated based on the change in concentration between the feedstock and the produced biodiesel as shown in Equation 5.2. The concentration of each FFA at both reactants and products has been calculated as previously discussed in Section 4.2.

$$\text{Conversion} = (C_{iWCO} - C_{iS} / C_{iWCO}) \times 100\% \quad (5.2)$$

Where C_{iWCO} and C_{iS} represents the concentration of i^{th} fatty acid in WCO and each biodiesel sample, respectively.

5.2.3. Experimental design and analysis

Experimental design and statistical analysis have been performed in a similar fashion to the experiments as described in Section 4.2. However, the responses have been changed in this Chapter to 5 responses including the conversions of overall FFAs, oleic acid,

palmitic acid, linoleic acid and myristic acid. The same four independent variables with the same levels have been studied as described in Section 4.2.

5.2.4. Reaction kinetics

In the present study, the esterification reaction of FFAs has been considered as the main interest. Hence, the esterification reaction kinetics were studied based on the change of the FFAs concentration before and after the reaction. The esterification reaction requires the reaction of 1 mole of FFAs with 1 mole of methanol to produce 1 mole of FAMEs and 1 mole of water as shown in Equation 5.3. The following assumptions have been made to simplify the reaction rate calculations:

- The reaction is single phase.
- The change in methanol concentration is ignored as it is used in large excess.
- The reaction is assumed to be kinetically controlled.



Where FFA, R-OH, FAME and H₂O represent the free fatty acids, methanol, fatty acid methyl ester (biodiesel) and water, respectively.

5.2.5. Reactor Simulation

A biodiesel synthesis reactor for esterification of FFA to FAME was simulated using Aspen HYSYS® commercial simulation software v8.8 (Aspen Technology Inc., USA). The FFAs were represented by both oleic acid (C₁₈H₃₄O₂) and palmitic acid (C₁₆H₃₂O₂) as they represent the majority of the oil composition as shown in Table 5.1. Consequently, methyl-oleate (C₁₉H₃₆O₂) and methyl-palmitate (C₁₇H₃₄O₂) were selected to represent the biodiesel product stream. All the selected chemical components exist in the HYSYS components' library. The reactor type was selected as continuous CSTR. Owing to the presence of polar components i.e. methanol, NRTL thermodynamic activity model was used as the fluid package of the simulation. The reactor was simulated kinetically based on the experimentally obtained kinetic data.

5.3. Results and discussion

This section is divided into two parts including the analysis of overall FFAs conversion using titration and the chromatographic analysis of each FFA conversion.

5.3.1. Overall conversion of FFAs

5.3.1.1. Development of regression model equation

The experimental runs that have been designed *via* CCD, as shown in Table 5.1, have been used to develop a regression model for FFAs conversion as a function of defined reaction variables. Design Expert software has been used to fit the experimental results with four different models including linear, 2FI, quadratic and cubic polynomial models. Various statistical analyses have been employed to check the accuracy of each model i.e. lack of fit analysis, R²_{adj}, R²_{pred} and associated aliased coefficients. Amongst the fitted models, the quadratic model has been suggested by the software as it has the best prediction of the experimental results. Hence, a quadratic regression model has been

developed representing an empirical relationship between FFA conversion and reaction variables including M:O molar ratio, temperature, pressure and time as shown in Equation 5.4.

$$Y = 96.63 + 0.19 A + 0.35 B - 0.5 C + 0.45 D + 0.21 AB - 0.25 AC - 0.065 AD - 0.15 BC + 0.036 BD + 0.063 CD + 0.014 A^2 - 0.029 B^2 + 0.45 C^2 - 0.46 D^2 \quad (5.4)$$

where Y represent FFAs conversion, while, A, B, C and D represent the process variables including M:O molar ratio, temperature, pressure and time, respectively.

The developed regression model has been used to predict the overall effect of process variables and their interactions. The positive sign of each term indicates synergetic effect while the negative sign indicated antagonistic effect (El-Gendy et al., 2015). From the predicted model, some preliminary observations have been reported including the positive effect of M:O molar ratio, temperature and time of FFA conversion. This is in addition to the positive effect of some process variables interactions i.e. M:O molar ratio/temperature, temperature-time and pressure-time. However, reaction pressure has shown negative effect on the reaction response with a negative coefficient. Furthermore, it has been observed that the reaction time has the highest effect on the reaction response with higher coefficient than the other variables.

Table 5.1. Experimental design matrix with the actual and predicted yields

Run	M:O ratio (A)	Temperature (°C) (B)	Pressure (bar) (C)	Time (min) (D)	Actual FFA Conv. (%)	Predicted FFA Conv. (%)
1	30	260	135	17	97.0	96.6
2	35	250	160	22	96.1	96.0
3	35	250	110	22	97.1	97.1
4	35	270	160	22	96.8	96.9
5	35	270	110	12	97.8	97.9
6	35	250	160	12	95.0	95.2
7	25	270	160	22	96.6	96.7
8	30	260	135	17	96.5	96.6
9	25	250	110	22	96.6	96.7
10	25	250	160	22	96.8	96.7
11	30	260	85	17	99.2	99.4
12	25	270	110	12	96.5	96.4
13	25	250	160	12	95.7	95.6
14	30	260	135	17	97.0	96.6
15	35	250	110	12	96.7	96.5
16	30	240	135	17	95.7	95.8
17	30	260	185	17	97.5	97.4
18	35	270	160	12	96.2	95.9
19	30	260	135	17	96.5	96.6
20	30	260	135	27	95.6	95.6
21	30	260	135	7	93.7	93.8
22	25	270	160	12	95.5	95.5
23	20	260	135	17	96.2	96.3
24	25	250	110	12	96.0	95.9
25	30	280	135	17	97.1	97.2
26	30	260	135	17	96.3	96.6
27	40	260	135	17	97.0	97.0
28	25	270	110	22	97.6	97.4
29	30	260	135	17	96.5	96.6
30	35	270	110	22	98.6	98.6

5.3.1.2. Model adequacy checking

The adequacy of the predicted model has been checked using different methods. The accuracy of the model in predicting the actual data has been assessed using R^2 , where the closer the value to the unity exemplify the higher accuracy of the model. Hence, the values of R^2 , R^2_{adj} , R^2_{pred} have been evaluated for the predicted model resulting in 0.991, 0.972 and 0.942, respectively. These results indicated that only 0.9% of the total variation has not been identified precisely by the predicted model. The statistical significance of the predicted model has been investigated using ANOVA as shown in Table 5.2.

Table 5.2. Analysis of variance for FFA conversion of the developed model

Source	Sum of Squares	df	Mean Square	F-value	P-value	Significance
Model	30.3	14	2.17	38.09	< 0.0001	HS
A-MeOH:Oil	0.88	1	0.88	15.45	0.001	HS
B-Temperature	2.93	1	2.93	51.61	< 0.0001	HS
C-Pressure	5.91	1	5.91	104.04	< 0.0001	HS
D-Time	4.85	1	4.85	85.23	< 0.0001	HS
AB	0.73	1	0.73	12.89	0.002	HS
AC	1.00	1	1.00	17.65	0.0008	HS
AD	0.06	1	0.06	1.18	0.2	NS
BC	0.38	1	0.38	6.61	0.02	S
BD	0.02	1	0.02	0.36	0.5	NS
CD	0.06	1	0.06	1.10	0.3	NS
A ²	0.05	1	50.0	0.097	0.7	NS
B ²	0.02	1	0.02	0.40	0.5	NS
C ²	5.66	1	5.66	99.54	< 0.0001	HS
D ²	5.87	1	5.87	103.24	< 0.0001	HS
Residual	0.85	15	0.05			
Lack of Fit	0.42	10	0.04	0.49	0.8451	NS
Pure Error	0.43	5	0.08			
Cor Total	31.1	29				

The significance of the predicted model has assessed from the values of p -value and F-test at 95% confidence level. The model is highly significant with a very low p -value of <0.0001 . This illustrates accuracy of the predicted model in estimating the actual data. In addition, the insignificance of the lack of fit analysis indicated the highly fitting of the predicted model. In the present study, the lack of fit analysis of the predicted model has shown a high p -value of 0.84. This indicates an insignificant result of this analysis and the precision of the predicted model. Finally, a plot between predicted and actual values has been used to examine the accuracy of the predicted model where the closer the points to the 45° line, the more precise the model prediction. The similarity between the actual and the predicted values has been shown in Figure 5.2.

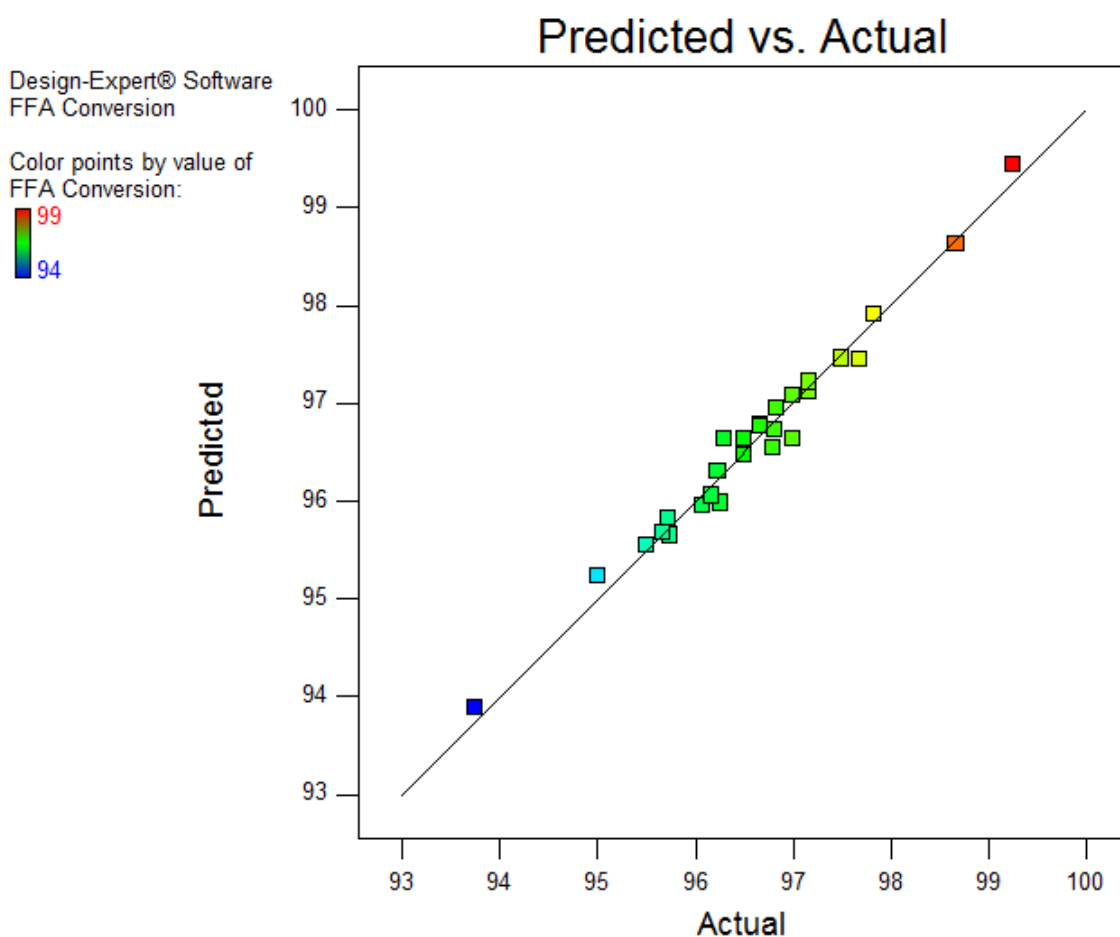


Figure 5.2. Predicted *versus* actual values for FFAs conversion model

Based on the ANOVA results shown in Table 5.2, it has been observed that all the reaction variables have significant effect on the FFA conversion. Specifically, it has been determined that the reaction pressure is the most significant parameter affecting the FFA conversion with F-value of 104.04. In addition, the excess values of both M:O molar ratio and temperature are not significant on the response. However, the excess values of both pressure and time are highly significant. Further, many interaction parameters have been reported to have insignificant effect on the response.

The developed model simplification process starts with excluding the insignificant parameters. In the present study, the insignificant variables including the interaction between M:O molar ratio and time (AD), interaction between temperature and time (BD), interaction between pressure and time (CD), excess of M:O molar ratio (A^2) and high values of temperature (B^2). By excluding the insignificant variables the model has been shortened as shown in Equation 5.5.

$$Y = 96.62 + 0.19 A + 0.35 B - 0.5 C + 0.45 D + 0.21 AB - 0.25 AC - 0.15 BC + 0.46 C^2 - 0.46 D^2 \quad (5.5)$$

The hypotheses associated by the ANOVA have been assessed in order to trust the results obtained by this analysis. Firstly, the normality hypothesis has been examined using the normality plot of the residuals as shown in Figure 5.3. It has been observed that the residuals are approximately fitted to a straight line, which indicates failure to reject the normality hypothesis.

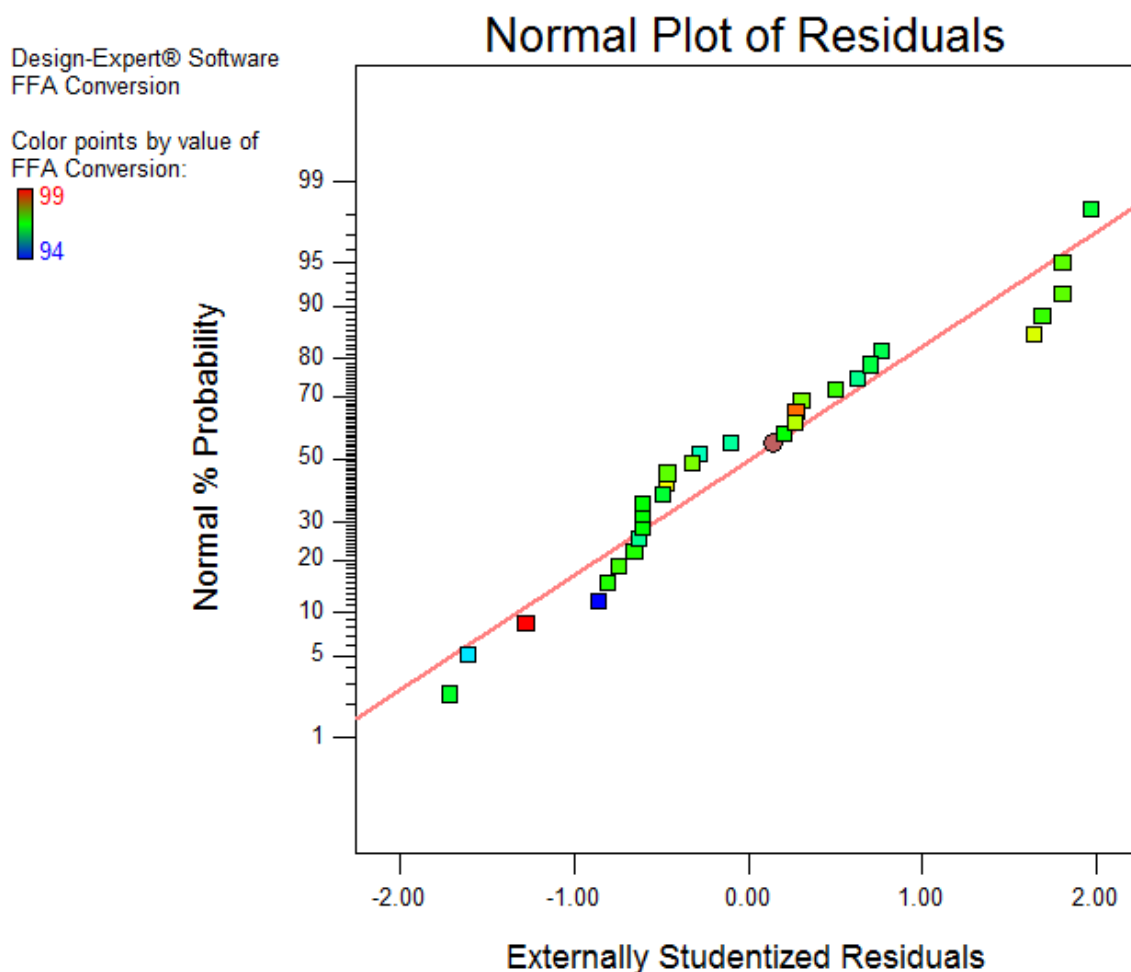


Figure 5.3. Normal plot of residuals for FFA conversion model

The second hypothesis associated with ANOVA is the equal variance of residuals at each level of the parameters. This has been checked using the plot of residuals *versus* predicted values where the temperature variable has been chosen to represent the other variables. As shown in Figure 5.4, the variances are approximately equal at each level where it is difficult to reject the claim of equal variance.

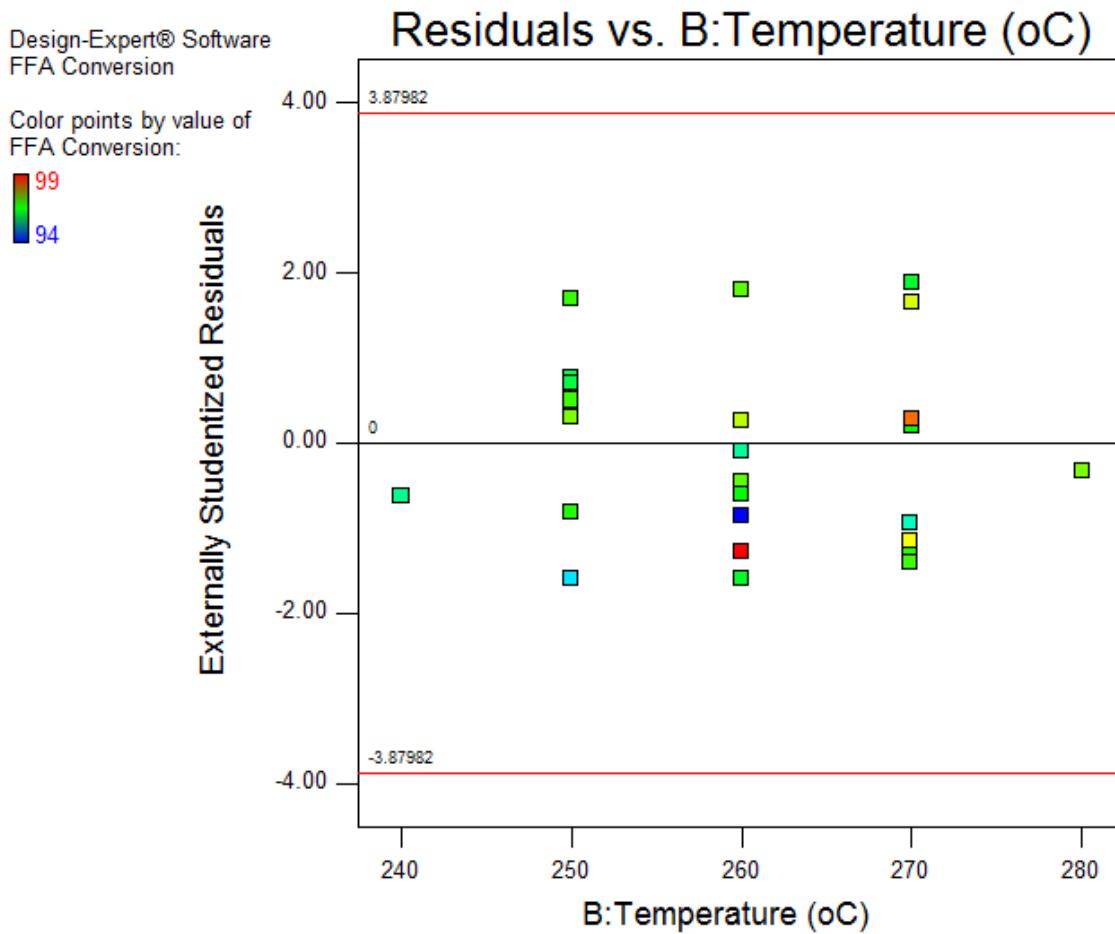


Figure 5.4. Plot of residuals versus predicted values of temperature variable for FFA conversion model

Finally, the third hypothesis of ANOVA is the randomisation of errors. This has been investigated using the plot of residuals *versus* predicted responses values. It has been agreed that the residuals are randomised when they do not follow a specific trend of increasing and/or decreasing. As illustrated in Figure 5.5, the residuals are in random order without following any specific trend where the randomisation hypothesis could be rejected. As per failing to reject the three hypotheses of ANOVA, the developed results based on ANOVA method are considered acceptable and adequate.

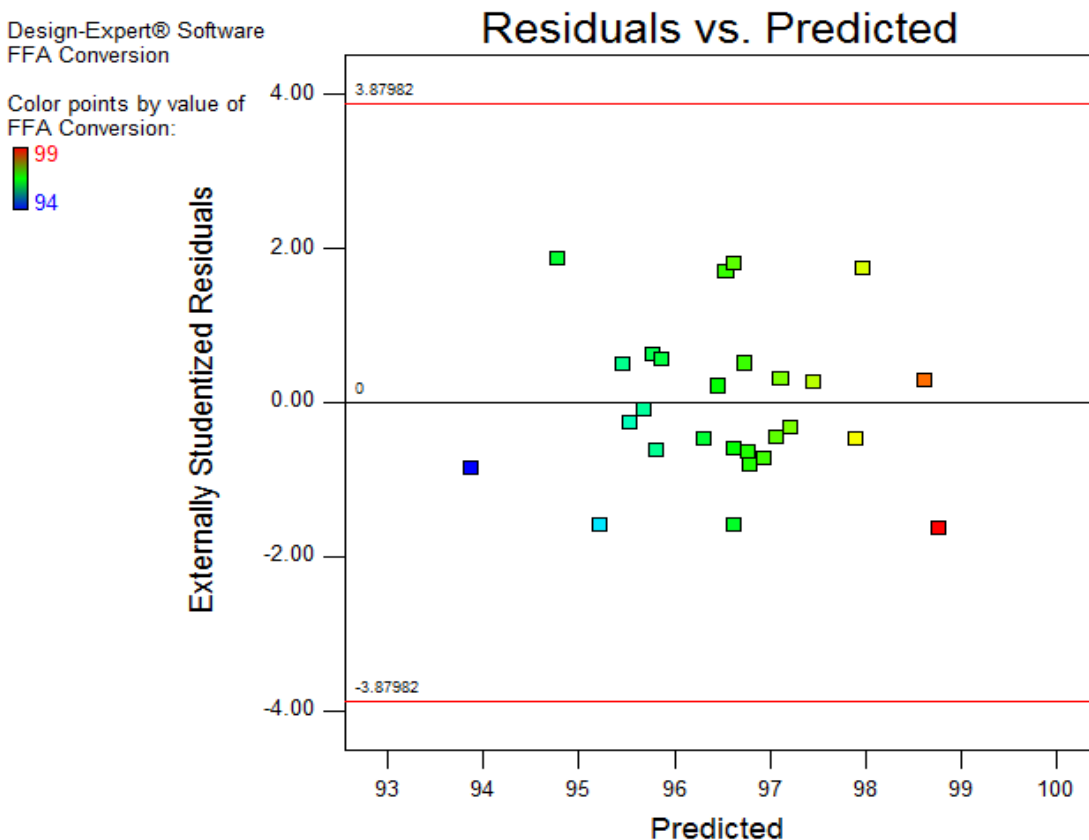


Figure 5.5. The plot of residuals versus predicted response for FFA conversion

5.3.1.3. Effect of process variables and their interactions

Based on the present study, non-catalytic esterification of FFAs using supercritical methanol has reported successful conversion of FFAs into FAMES within conversion range between 94% and 99%. The effects of the four controllable factor have been illustrated using different methods including the coefficient of each variable in the developed model, p-value and F-value of each variable, response surface plot and contour plot. Additionally, the interactive effects of process variables have been exemplified using response surface plots, contour plots and variables interaction plots.

5.3.1.3.1. Effect of M:O molar ratio

It is widely accepted that a huge excess of methanol is an essential requirement for supercritical methanolysis up to 126:1 M:O molar ratio. Chemically, the increasing effect of methanol (reactant) is favourable as it shifts the reaction equilibrium towards the products. Hence, it enhances the production of biodiesel (product). Additionally, using excess of methanol lower the critical point of the solution and hence enhance the supercritical reaction. The effect of methanol ratio varies according to different aspects including the type of feedstock, the variation levels of M:O ratio and the levels of other variables. Hence, the interactive effect of methanol with other variables is important to determine the accurate effect of methanol on FFA conversion (Farobie and Matsumura, 2017a).

In this study, M:O molar ratio has been reported as highly significant variable affecting the FFAs conversion as shown in Table 5.2. Additionally, the overall effect of increasing M:O molar ratio has synergetic effect on FFAs conversion as shown in Equation 5.5. The response surface and contour plots have illustrated the effect of M:O molar ratio where its increasing effect have positive influence on FFAs conversion. The contour plot has also confirmed the same results where it is clearly showed the variation of the colour (response) at different levels of M:O molar ratio as shown in Figure 5.6.

Jin et al. (2015) have studied the esterification of FFAs for biodiesel synthesis using supercritical methanolysis. They have studied the range of M:O molar ratio between 1:1 to 40:1. They have also reported positive effect of M:O molar ratio on esters yield. Similarly, de Jesus et al. (2018) have studied the supercritical esterification of oleic acid for biodiesel production using a tubular reactor at temperature range between 150 °C and 300 °C. They have studied the range of M:O molar ratio between 1:1 and 6:1. They have reported an increasing effect of oiled acid conversion while increasing M:O molar ratio. Narayan and Madras, (2017) have studied the esterification of sebacic acid using supercritical methanol. They have also reported that increasing M:O molar ratio has increasing effect on esters yield. Jin et al. (2015) have studied the esterification of FFAs for biodiesel synthesis using supercritical methanolysis. Nur Syazwani et al. (2017) have studied the esterification of high acidity feedstock (Palm fatty acid distillate) using

supercritical methanol. They have reported that the yield of FAMES increase while increasing M:O molar ratio up to 6:1 ratio. However, at higher ratios, the FAMES yield decrease.

Design-Expert® Software

Factor Coding: Actual

FFA Conversion (%)

● Design points above predicted value

○ Design points below predicted value

99.25

93.75

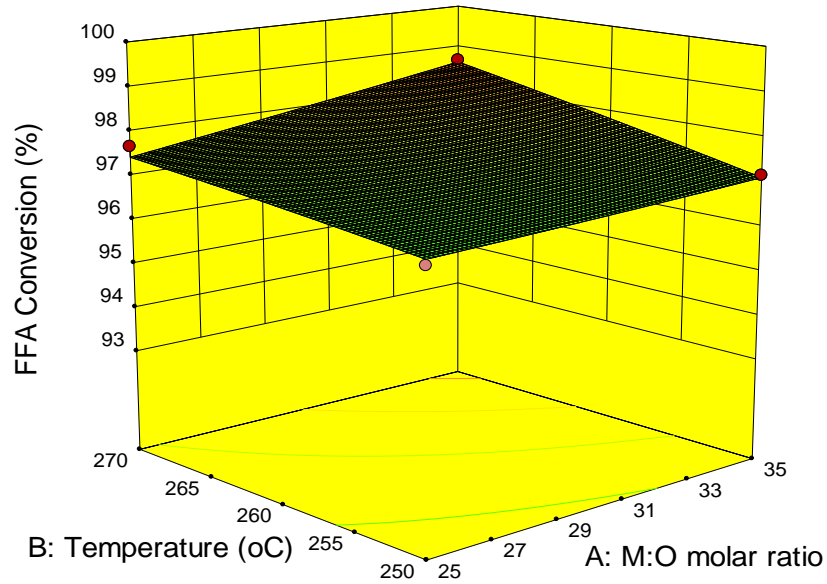
X1 = A: M:O molar ratio

X2 = B: Temperature

Actual Factors

C: Pressure = 110

D: Time = 22



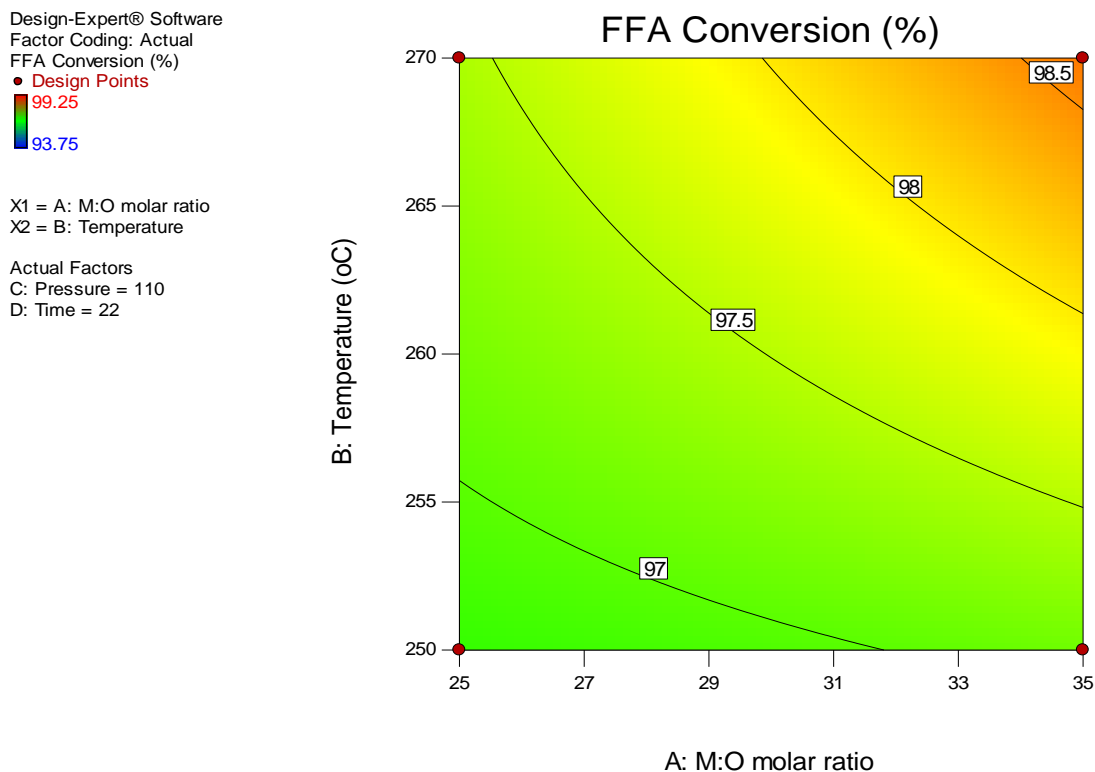


Figure 5.6. Response surface and contour plot for M:O molar ratio and reaction temperature versus FFA conversion

5.3.1.3.2. Effect of reaction temperature

As per using supercritical methanolysis for the esterification reaction of FFAs, the minimum reaction temperature that has been studied is the critical point of methanol i.e. 240 °C. Considering the previously published recommendations (Martinovic et al., 2018) to avoid thermal degradation, the studied temperature did not reach 300°C. Having an endothermic esterification reaction, higher temperatures are expected to achieve high conversions of FFAs (Quitain et al., 2018).

In this study, the reaction temperature has shown a significant effect on FFAs conversion as shown in Table 5.2, with very low p-value. Additionally, it is illustrated in Figure 5.6 that increasing the reaction temperature has an increasing influence on FFA conversion. Similarly, dos Santos et al. (2017) have studied the supercritical esterification of FFAs using a tubular reactor. They have studied the effect of temperature between 220 °C and 280 °C. Their results have reported an increasing effect of temperature on the conversion

of FFAs. The same findings have been reported by different researchers (Lokman et al., 2016; Nur Syazwani et al., 2017; Tavlarides et al., 2018).

5.3.1.3.3. Interactive effect of M:O molar ratio and reaction temperature

The interactive effect between M:O molar ratio and reaction temperature has shown significant effect on FFAs conversion as reported in Table 5.2. This interaction is demonstrated in Figure 5.6 where the increasing effect of temperature at M:O molar ratio 25:1 is approximately negligible as shown in the contour plot where no change in the colour. However, at higher M:O molar ratios up to 35:1, the positive effect of temperature on FFAs conversion is clear. The interaction effect between variables is very important for optimisation. The interaction plot between M:O molar ratio and reaction temperature is illustrated in Figure 5.7. It is clearly shown that the effects lines of both variables are not parallel and are about to intersect.

Design-Expert® Software
Factor Coding: Actual
FFA Conversion (%)
● Design Points
--- 95% CI Bands

X1 = A: M:O molar ratio
X2 = B: Temperature

Actual Factors
C: Pressure = 110
D: Time = 22

B- 250
B+ 270

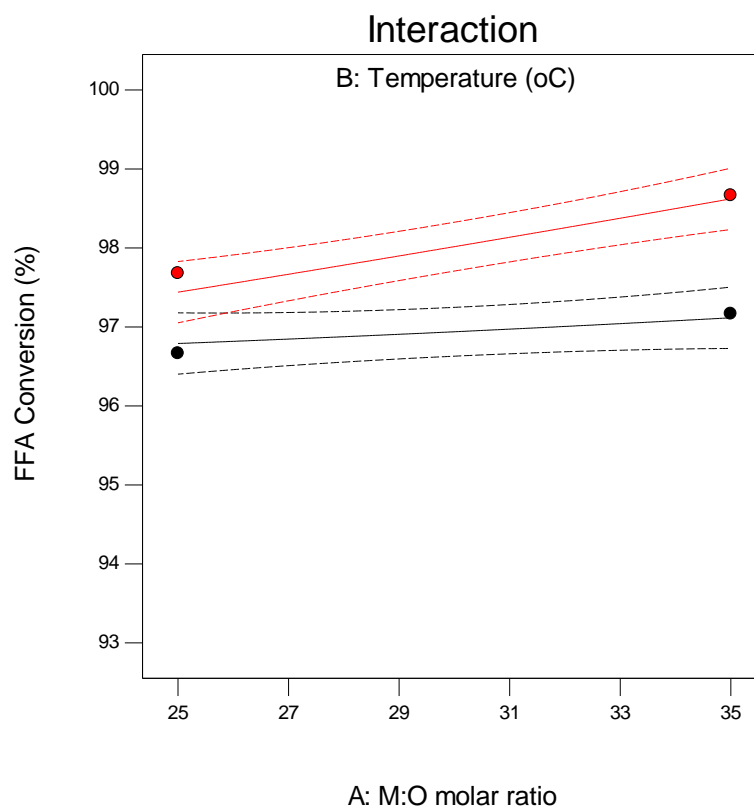


Figure 5.7. Interaction plot showing interactive effect of methanol ratio and temperature on FFA conversion

5.3.1.3.4. Effect of reaction pressure

Reaction pressure variation has a considerable effect on the solution properties including density, viscosity and chemical properties (He et al., 2007). Similar to the reaction temperature range, the minimum pressure used for this study is the critical point of methanol (80 bar). In this paper, CO₂ gas has been used to pressurise the reaction. In addition, it has been used as a cosolvent as it increases the solubility of methanol in the oil (Han et al., 2005). It has been reported that reaction pressure has highly negative effect on FFA conversion as concluded from Equation 5 and Table 5.2. In addition, Figure 5.8 showed that the increasing effect of reaction pressure has decreasing effect on FFAs conversion.

Quitain et al. (2018) have reported similar results for the negative effect of increasing the reaction pressure. They have explained this phenomenon due to the formation of two phases where during depressurising, products' recovery difficulties are highly expected. Jiuxu Liu et al. (2018) have reported that the reaction pressure increase is not significant unless the pressure is employed to avoid phase behaviour interruption.

5.3.1.3.5. Effect of reaction time

Using supercritical methanolysis for esterification of FFAs reduced the reaction time intensely. In comparison with the conventional acidic catalysed methods, supercritical esterification reaction is much shorter in time. Some previous studies have reported esterification reactions up to 8 h (Haigh et al., 2013). In this study the reaction time has been studied between 7 and 27 min. Reaction time has significant effect on FFAs conversion as shown in Table 5.2. Figure 5.8 shows the increasing effect of reaction time up to about 20 min.

5.3.1.3.6. Interactive effect of reaction pressure and time

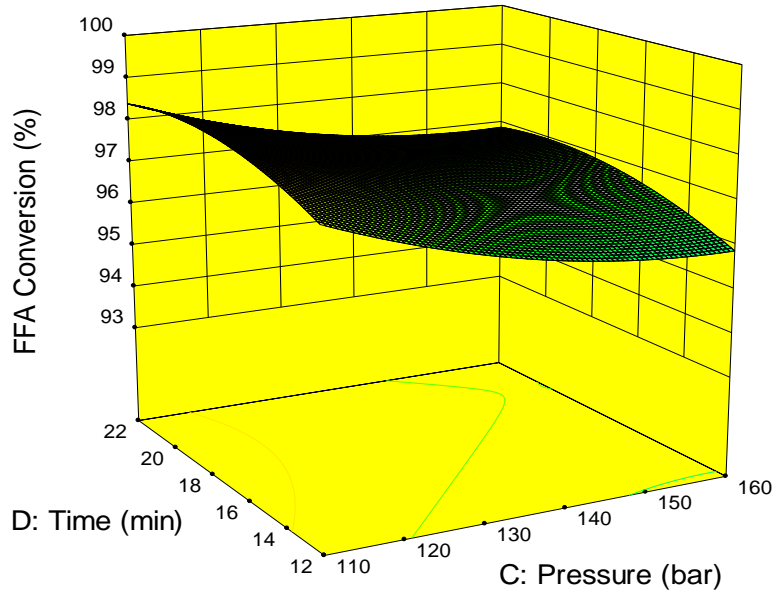
The effect of interactions between reaction pressure and time has insignificant effect on FFAs conversion as shown in Table 5.2. This means that the effect of either pressure on FFAs conversion does not depend on the level of reaction time. In other words, the trend

of the effect of pressure on FFAs conversion is constant at different time and *vice-versa*. The insignificance of the interaction is also illustrated in Figure 5.9, where parallel behaviour is reported and no estimated intersection is observed.

Design-Expert® Software
Factor Coding: Actual
FFA Conversion (%)
99.25
93.75

X1 = C: Pressure
X2 = D: Time

Actual Factors
A: M:O molar ratio = 33.2432
B: Temperature = 270



Design-Expert® Software
Factor Coding: Actual
FFA Conversion (%)
99.25
93.75

X1 = C: Pressure
X2 = D: Time

Actual Factors
A: M:O molar ratio = 33.2432
B: Temperature = 270

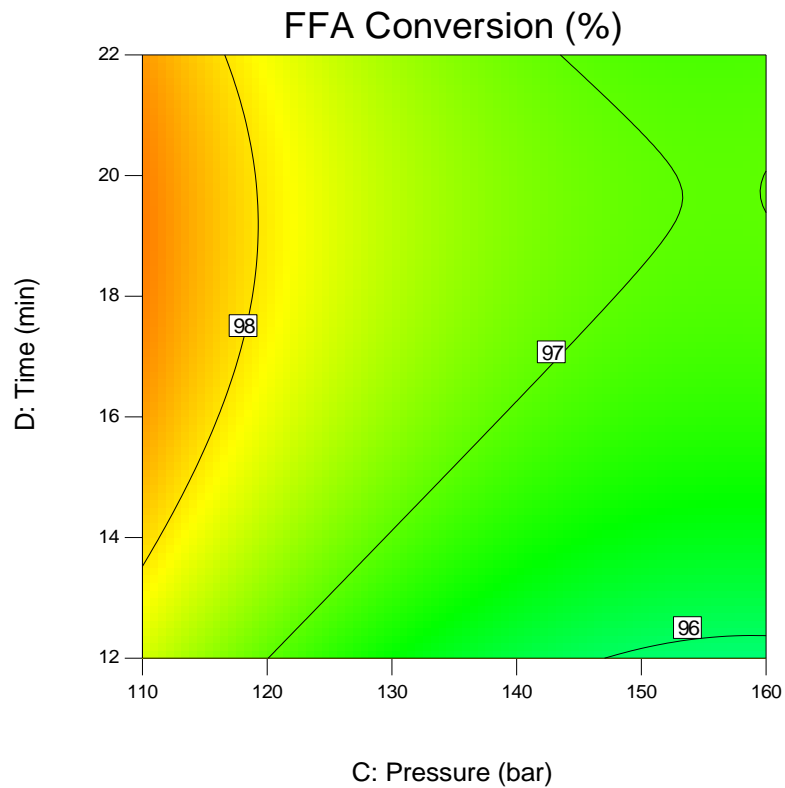


Figure 5.8. Response surface and contour plot for reaction pressure and time versus FFA conversion

Design-Expert® Software
Factor Coding: Actual
FFA Conversion (%)
--- 95% CI Bands

X1 = C: Pressure
X2 = D: Time

Actual Factors
A: M:O molar ratio = 33.2432
B: Temperature = 270

D- 12
D+ 22

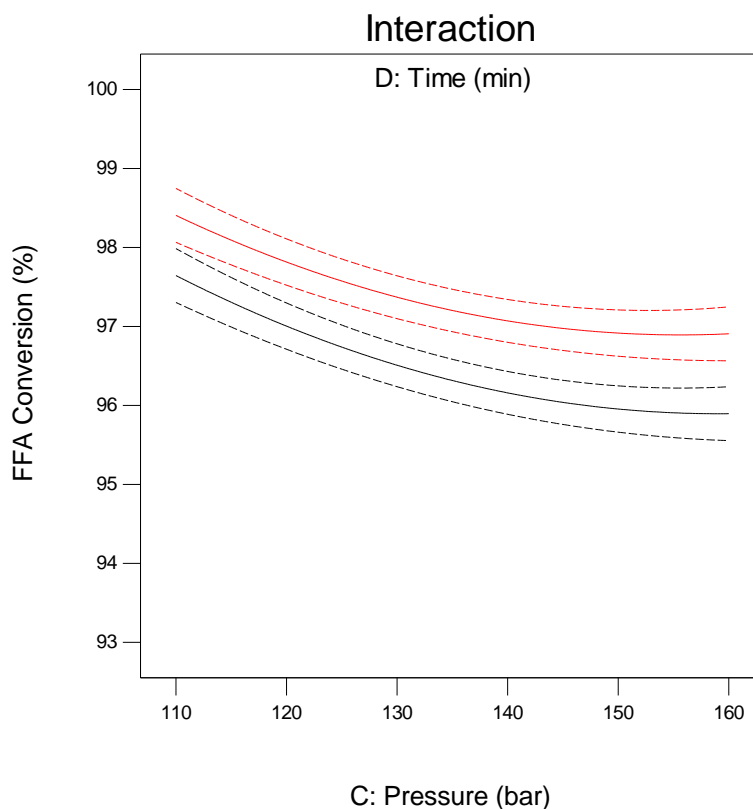


Figure 5.9. Interaction plot showing interactive effect of reaction pressure and time on FFA conversion

5.3.1.4. Process optimisation

Recently, many studies have implemented RSM approach for optimising biodiesel production process variables (Kostić et al., 2016; Muthukumaran et al., 2017b; Sepahvand et al., 2014; Silitonga et al., 2016). Numerical optimisation using Design Expert software has been employed to predict the optimum variables combinations that would fit the desired goals for each process variable. FFA conversion has been set to be maximised while minimising the other controllable reaction variables. The importance of the desired goal for each variable (scale 1-5) has been defined based on economical and environmental considerations. Table 5.3 illustrate the desired goal of each variable for optimisation.

Table 5.3. Optimisation constraints used to predict optimum conditions for biodiesel production

Factor	Code	Goal	Importance	Limits	
			Scale 1-5	Lower	Upper
M:O (molar ratio)	A	Minimise	3	25	35
Temperature (°C)	B	Minimise	4	250	270
Pressure (bar)	C	Minimise	3	110	160
Time (min)	D	Minimise	4	12	22
FFA conversion	Y	Maximise	5	97	100

The software has performed the optimisation based on the desired goals where 61 solutions have been generated. The solution with the highest desirability has been considered for optimum conditions. The optimum conditions have achieved 98% of FFAs conversion at 30.5:1, 261.7 °C, 110 bar and 16.8 min for M:O molar ratio, temperature, pressure and time, respectively.

Experiments have been performed at the predicted optimum conditions for assessing the accuracy of the optimisation process. Three experiments have been performed at the predicted optimum conditions where the average FFAs conversion was found to be 98.3%. Hence, the predicted optimum condition has been validated experimentally with only 0.3% relative error.

5.3.1.5. Reaction kinetics

The reaction rate has been expressed as shown in Equation 5.6. The developed regression model has been used to predict the experimental results required for reaction kinetics studies.

$$r_{FFA} = - \frac{dC_{FFA}}{dt} = k_1 C_{FFA} C_{CH_3OH} - k_2 C_{FAME} C_{H_2O} \quad (5.6)$$

Based on the simplification assumptions, the change of the methanol concentration has been neglected. In addition, according to Le Chatelier principle, the backward reaction has been ignored as using large excess of methanol shifts the equilibrium towards the forward reaction. Accordingly, the reaction rate is expressed as shown in Equations 5.6 to 5.8.

$$r_{FFA} = - \frac{dC_{FFA}}{dt} = k_1 C_{FFA} \quad (5.7)$$

$$C_{FFA} = C_{FFA_0}(1 - X) \quad (5.8)$$

The kinetic and thermodynamic data have been calculated at range of temperature between 250 and 270 °C and reaction time between 12 and 22 min. The hypothesis of the reaction rate has been assumed to be pseudo-first order where a plot between $|\ln(1-Y)|$ versus time within time range from 720 to 1320 s have produced a straight line with $R^2 = 0.9646$. Consequently, the hypothesis has been confirmed that the reaction is pseudo-first order with reaction rate constant value of 0.001 s^{-1} .

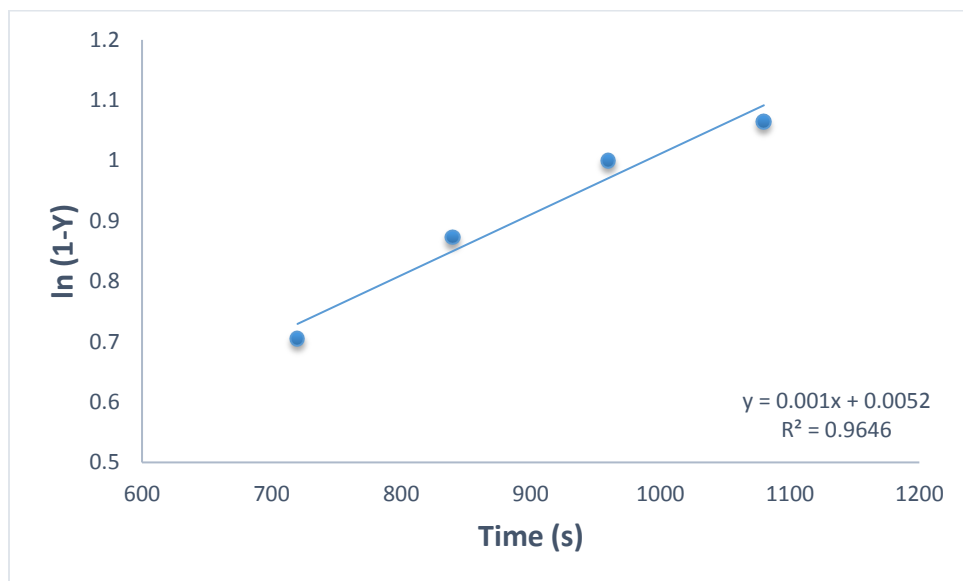


Figure 5.10. Rate constant of esterification

On the other hand, the reaction thermodynamic parameters have been studied. activation energy of the reaction has been calculated using Arrhenius equation. In order to evaluate the activation energy and Arrhenius constant of the reaction, a plot between $|\ln k|$ versus temperature within range from 250 to 270 °C has been performed, where a straight line has been developed with $R^2 = 0.995$. Thus, activation energy and Arrhenius constant have been calculated to be 34.5 kJ/mol and 2.73 s^{-1} , respectively.

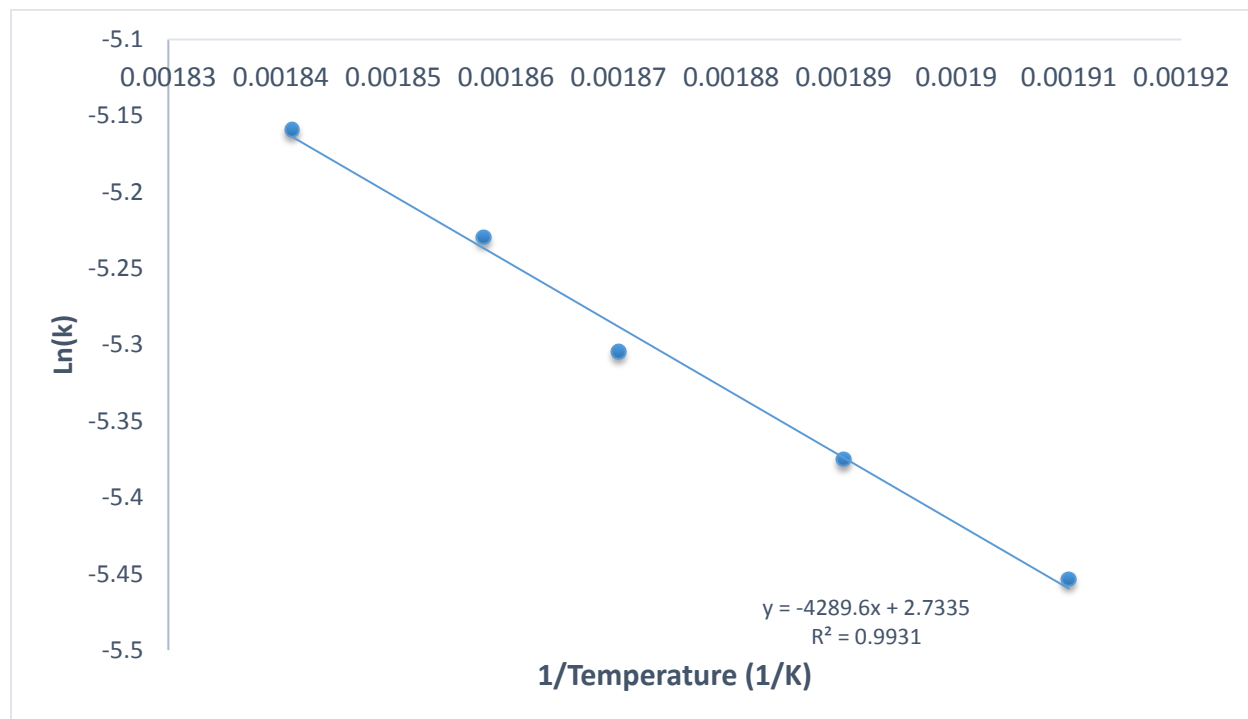


Figure 5.11. Arrhenius plot for esterification of FFA

5.3.1.6. Reactor simulation

The validated optimum conditions for biodiesel synthesis have been used to operate the biodiesel reactor. The feed stream has been identified as a mixture of oleic acid, palmitic acid and methanol. In order to achieve the molar ratio between methanol and oil, the flowrate of the methanol has been identified by 300 kmol/h and both oleic and palmitic acid by 10 kmol/h. The reactor has been simulated using the kinetic model where the kinetic and thermodynamic data of the reaction has to be defined. The stoichiometric coefficient of the esterification reaction set has been defined as the reaction set in the

reactor. Activation energy and Arrhenius constant which have been determined experimentally (34.5 kJ/mol and 2.48 s^{-1}) through this study have been used to define the required kinetic data for the reactor. Consequently, the reactor has successfully simulated 98.77% conversion of both oleic and palmitic acids to methyl oleate and palmitate, respectively. A schematic of the reactor process diagram is presented in Figure 5.12. The conditions and the composition of the reactor streams have been illustrated in Table 5.4

The conversion results of the simulated reactor have shown high similarity with the experimental conversion at the same condition. Experimentally, the conversion has reported 98.3% where accordingly the simulated conversion (98.77%) is very close to the actual conversion with a relative error of 0.478%. These results confirm the accuracy of the kinetic calculation and the adequacy of the predicted model for predicted the required kinetic experimental runs.

Table 5.4. Streams data of the simulated CSTR reactor

Name	101	102	103
Temperature (°C)	261	260.4	260.4
Pressure [bar]	110	110	110
Molar Flow [kgmole/h]	310	0	310
Mole fractions			
Oleic acid	0.01	0.0002	0.0002
Palmitic acid	0.01	0.0002	0.0002
Methanol	0.96	0.93	0.93
M-Oleate	0	0.01	0.01
M-Palmitate	0	0.01	0.01
Water	0	0.03	0.03

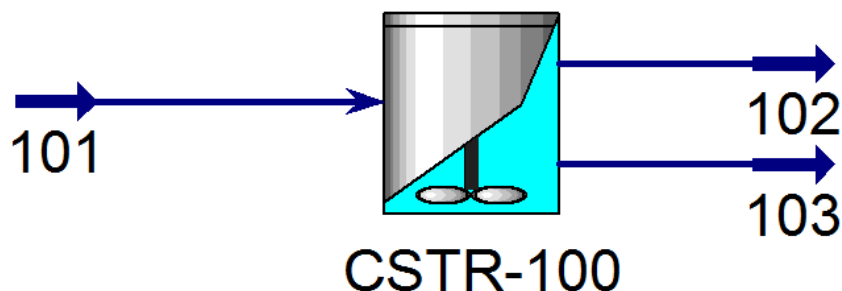


Figure 5.12. Simulated CSTR using optimum parameters obtained from the experimental study

5.3.2. Chromatographic analysis of individual FFAs

5.3.2.1. Chromatographic method development

This work has been developed as a modification for the previously reported derivatisation-free method for FFAs characterisation by Zhang et al. (2015b). The conventional analysis of FFAs has been performed through esterifying the FFAs in FAMES through derivatisation followed by analysis of FAMES. In the present study, the GC column that has been used for analysis is TR-FFAP (30 m × 0.32 mm id, 0.25 μm film thickness, Thermo-Scientific, Cheshire, UK) with a stationary phase consists of a modified PEG bonded terephthalic acid (TPA).

The starting column temperature programming for the GC method has been implemented as reported previously (Zhang et al., 2015a) where the initial oven temperature is 120 °C and ramped directly to 245 °C with rate of 30 °C/min with a flow rate of the carrier gas of 2.8 mL/min and injection temperature of 230 °C. However, an overlap between oleic and linoleic acid has been detected as shown in Figure 5.13. In addition to a combined peak of myristic acid and palmitic acid. Hence, systematic modifications have been applied for the method in order to produce separate and easily defined peaks.

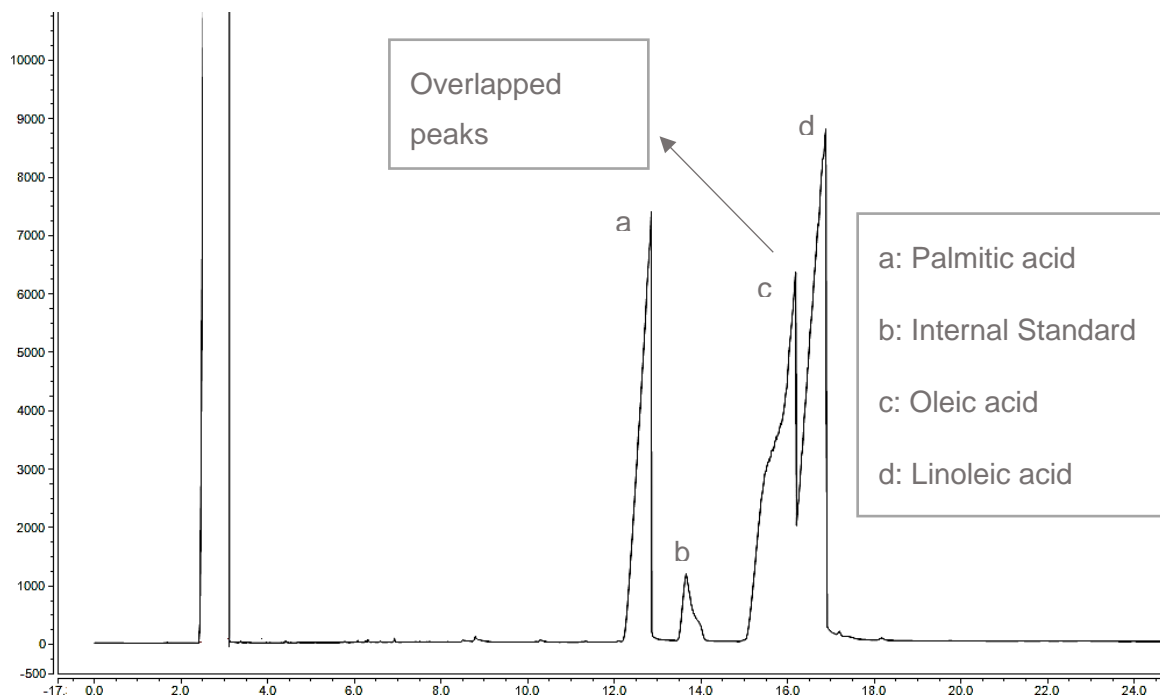


Figure 5.13. Chromatographic results of the standard fatty acids before method modification

The modification process included three main aspects i.e., the optimal carrier gas flow, the optimal temperature ramp in the column programming and the optimal injection temperature. A multivariate optimisation technique using RSM has been established to determine the optimal combination of variables to achieve the best GC method in terms of sensitivity, specificity and precision. Three levels of each variable have been investigated as shown in Table 5.5. BBD has been used to design randomised 17 runs at different variables. At each run the peaks of the standard fatty acids were calibrated and checked for sensitivity and specificity. Using Design Expert 11 software (Stat-Ease Inc., Minneapolis, MN, USA), the optimal conditions have been identified at 40 °C/min, 4.5 mL/min and 245 °C for temperature ramp, carrier gas flow and injection temperature, respectively. Additionally, it has been observed that the peaks have been accurately separated when the column remains at constant temperature of 240 °C for several minutes at constant flow rate of 4.5 mL/min. Hence, high ramp is preferred prior to 240 °C to minimise the overall method time.

Table 5.5. Experimental design variables and their coded levels

Factor	Code	Levels		
		-1	0	+1
Ramp (°C/min)	A	30	40	50
Carrier gas flow (mL/min)	B	2.5	4.5	6.5
Injection temperature (°C)	C	205	230	245

In summary, the GC method has been identified based on the developed optimal conditions. The temperature programme has started from 40 °C and ramped with 40 °C/min to 240 °C and remained for 7 min. Finally, the temperature was ramped to 245 °C with 40 °C/min and remained for 5 min. Both injector and detector temperatures were adjusted at 245 °C. The flow rate of the helium carrier gas has been adjusted at 4.5 mL/min. While modifying the method, the previously overlapped peaks have been separated and viewed in an accurate position as shown in Figure 5.14.

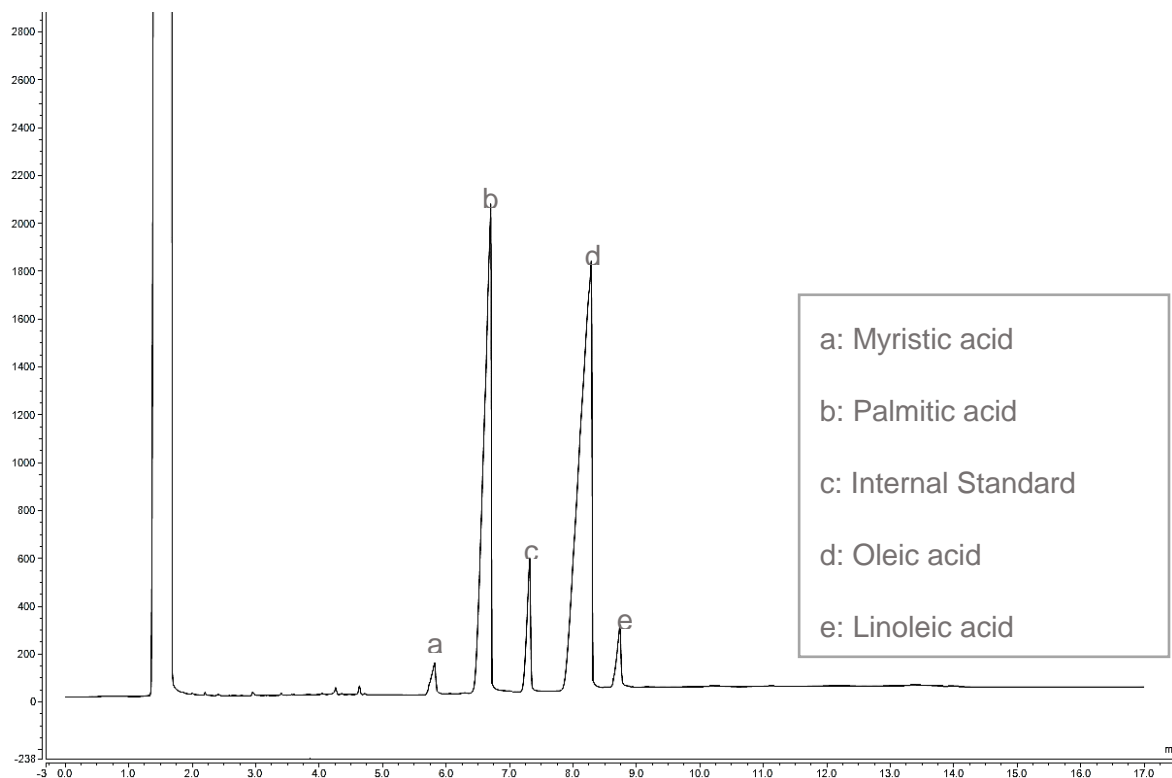


Figure 5.14. Chromatographic results of the standard fatty acids after method modification

Upon injecting the WCO and/or biodiesel samples, the free fatty acids are easily detected and identified. Using the standard samples, the retention time of each fatty acid has been defined as shown in Table 5.6. The concentration of each fatty acid has been calculated based on the response factor of each component as discussed in section 3.2.

Table 5.6. A chromatographic data of the retention time for each fatty acid

Fatty Acid	Retention time
Myristic	5.8
Palmitic	6.6
Heptadecanoic (IS)	7.1
Oleic	8.1
Linoleic	8.6

5.3.2.2. Development of regression model equation

Using the 30 experimental results for myristic, palmitic, oleic and linoleic acids conversion, as shown in Table 5.7, four polynomial regression models have been developed to represent each response function in the experimental variables. The experimental results of each response have been fitted for four different mathematical models including linear, two factors interactions (2FI), quadratic and cubic polynomial models. The most fitted model has been identified using different statistical analysis including R^2_{adj} , R^2_{pred} and associated aliased coefficients. For the four regression models, the quadratic polynomial equation has been suggested by the software as the most fitted model in predicting the experimental results. Consequently, four quadratic models have been developed for the experimental responses function in the process variables as shown in Equations 5.9 to 5.12.

$$Y_1 = 99.23 - 0.025 A + 0.097 B - 0.009 C + 0.031 D + 0.068 AB + 0.050 AC - 0.071 AD + 0.012 BC + 0.095 BD + 0.076 CD - 0.055 A^2 - 0.118 B^2 - 0.045 C^2 - 0.161 D^2 \quad (5.9)$$

$$Y_2 = 99.09 - 0.026 A + 0.029 B + 0.018 C + 0.005 D + 0.046 AB + 0.020 AC + 0.036 AD + 0.064 BC - 0.043 BD + 0.062 CD - 0.051 A^2 - 0.089 B^2 - 0.021 C^2 - 0.101 D^2 \quad (5.10)$$

$$Y_3 = 98.35 - 0.037 A + 0.1 B - 0.012 C + 0.048 D + 0.062 AB + 0.052 AC - 0.057 AD + 0.029 BC + 0.059 BD + 0.072 CD - 0.060 A^2 - 0.124 B^2 - 0.051 C^2 - 0.166 D^2 \quad (5.11)$$

$$Y_4 = 99.59 - 0.043 A + 0.038 B - 0.006 C + 0.045 D + 0.056 AB + 0.031 AC - 0.024 AD + 0.034 BC - 0.053 BD + 0.033 CD - 0.016 A^2 - 0.048 B^2 - 0.017 C^2 - 0.121 D^2 \quad (5.12)$$

Where Y_1 , Y_2 , Y_3 and Y_4 represent conversion of myristic acid, palmitic acid, oleic acid and linoleic acid, respectively. While, A, B, C and D represent the process variables including M:O molar ratio, temperature, pressure and time, respectively.

Table 5.7. Experimental design matrix with the actual and predicted yields

Run	M:O ratio (A)	Temperature (°C) (B)	Pressure (bar) (C)	Time (min) (D)	Actual M-Acid Conv. (%)	Predicted M-Acid Conv. (%)	Actual P-Acid Conv. (%)	Predicted P-Acid Conv. (%)	Actual O-Acid Conv. (%)	Predicted O-Acid Conv. (%)	Actual L-Acid Conv. (%)	Predicted L-Acid Conv. (%)
1	30	260	135	17	99.0	99.2	99.0	99.1	98.2	98.3	99.5	99.5
2	35	250	160	22	98.1	98.7	98.8	98.7	97.9	97.8	99.4	99.3
3	35	250	110	22	98.6	98.5	98.7	98.7	97.8	97.7	99.3	99.3
4	35	270	160	22	98.9	99.0	98.9	98.9	98.1	98.1	99.4	99.5
5	35	270	110	12	99.1	99.1	98.9	98.9	98.1	98.1	99.4	99.4
6	35	250	160	12	98.6	98.6	98.6	98.6	97.5	97.6	99.1	99.1
7	25	270	160	22	99.0	98.9	99.0	98.9	98.1	98.1	99.5	99.4
8	30	260	135	17	99.2	99.2	99.1	99.0	98.4	98.3	99.6	99.5
9	25	250	110	22	98.9	99.0	98.9	98.9	98.0	98.1	99.6	99.6
10	25	250	160	22	99.0	99.0	98.9	98.9	98.2	98.1	99.5	99.5
11	30	260	85	17	99.0	99.0	99.0	98.9	98.2	98.1	99.5	99.5
12	25	270	110	12	98.9	98.9	98.8	98.8	98.0	98.0	99.4	99.4
13	25	250	160	12	98.5	98.5	98.6	98.6	97.6	97.6	99.2	99.2
14	30	260	135	17	99.2	99.2	99.1	99.0	98.3	98.3	99.6	99.5
15	35	250	110	12	98.5	98.6	98.7	98.8	97.7	97.7	99.2	99.2
16	30	240	135	17	98.4	98.5	98.6	98.6	97.6	97.6	99.3	99.3
17	30	260	185	17	99.0	99.0	99.0	99.0	98.1	98.1	99.5	99.5
18	35	270	160	12	99.0	99.0	99.0	98.9	98.1	98.1	99.5	99.5
19	30	260	135	17	99.2	99.2	99.1	99.0	98.3	98.3	99.6	99.5
20	30	260	135	27	98.5	98.6	98.6	98.7	97.7	97.7	99.2	99.2
21	30	260	135	7	98.5	98.5	98.7	98.6	97.7	97.6	99.1	99.0
22	25	270	160	12	98.6	98.7	98.8	98.8	97.8	97.8	99.3	99.3
23	20	260	135	17	99.0	99.0	98.9	98.9	98.1	98.1	99.6	99.6
24	25	250	110	12	98.9	98.8	98.9	98.9	98.0	97.9	99.4	99.4
25	30	280	135	17	99.0	98.9	98.8	98.7	98.1	98.0	99.5	99.4
26	30	260	135	17	99.2	99.2	99.1	99.0	98.4	98.3	99.6	99.5
27	40	260	135	17	99.0	98.9	98.8	98.8	98.1	98.0	99.4	99.4
28	25	270	110	22	99.0	98.9	98.7	98.7	98.1	98.0	99.4	99.4
29	30	260	135	17	99.2	99.2	99.1	99.0	98.4	98.3	99.6	99.5
30	35	270	110	22	98.6	98.7	98.6	98.6	97.8	97.8	99.3	99.3

(M-Acid: myristic; P-Acid: palmitic; O-Acid: oleic; L-Acid: linoleic)

5.3.2.3. Model adequacy checking

For simplicity and length restrictions of the paper, the discussion has only included the adequacy checking of oleic acid conversion regression model. The adequacy of the predicted model has been processed through different checking methods including R^2 , lack of fit and ANOVA. The coefficients of correlation analysis include three parameter named as R^2 , R^2_{adj} , R^2_{pred} , where adjusted and predicted parameters have been included. The higher value of the correlation coefficient up to unity, represent the high accuracy of the model in predicting the actual data. It has been reported that the values of R^2 , R^2_{adj} and R^2_{pred} for the predicted model are 0.989, 0.969 and 0.932, respectively. The significance of the predicted model has been assessed using ANOVA as shown in Table 5.8.

The predicted model is highly significant with p-value less than 0.0001 and F-value of 12.88 as shown in Table 5.8. Further, lack of fit analysis have been implemented to determine the accuracy of the model in fitting the experimental data. The insignificant lack of fit means that the model is successfully representing the actual data. As shown in Table 5.8, the p-value of lack of fit analysis is 0.257 which is higher than 0.05 and hence, not significant. Finally, the predicted values have been plotted *versus* the experimental value on a 45° line, where the closer the points to the line indicates the similarity between both values (experimental and predicted values) as shown in Figure 5.15. The observed points are very close to the 45° line, which indicates the high similarity between the predicted and the actual (experimental) results.

Table 5.8. Analysis of variance for oleic acid conversion of the developed model

Source	Sum of Squares	df	Mean Square	F-value	P-value	Significance
Model	1.70	14	0.12	12.8	< 0.0001	HS
A-MeOH:Oil	0.03	1	0.03	3.49	0.08	NS
B-Temperature	0.23	1	0.23	25.2	0.0002	HS
C-Pressure	0.002	1	0.002	0.23	0.63	NS
D-Time	0.04	1	0.04	4.68	0.04	S
AB	0.07	1	0.07	7.86	0.01	S
AC	0.04	1	0.04	4.56	0.04	S
AD	0.05	1	0.05	5.48	0.03	S
BC	0.01	1	0.01	1.46	0.2	NS
BD	0.05	1	0.05	5.97	0.02	S
CD	0.1	1	0.10	10.6	0.005	HS
A ²	0.09	1	0.10	10.5	0.005	HS
B ²	0.41	1	0.41	43.8	< 0.0001	HS
C ²	0.06	1	0.07	7.35	0.01	S
D ²	0.74	1	0.74	79.3	< 0.0001	HS
Residual	0.14	15	0.01			
Lack of Fit	0.11	10	0.01	1.85	0.25	NS
Pure Error	0.03	5	0.006			
Cor Total	1.84	29				

Design-Expert® Software

Oleic Acid Conversion

Color points by value of
Oleic Acid Conversion:

97.57 98.4

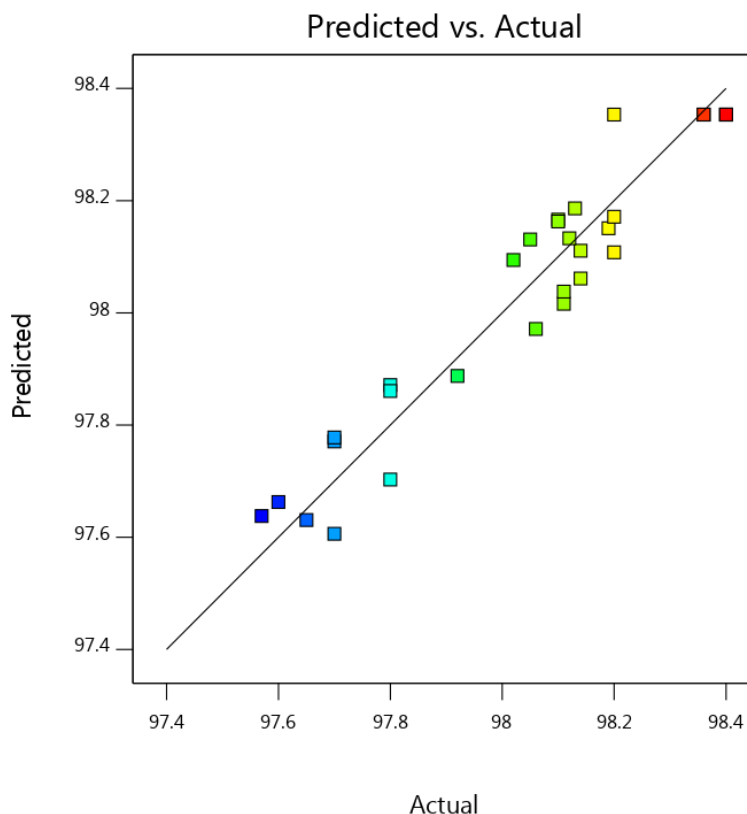


Figure 5.15. Predicted versus actual values for oleic acid conversion model

5.3.2.4. Effect of process variables and their interactions

The present study has investigated the conversion of four different FFAs including myristic, palmitic, oleic and linoleic acid. As the oleic acid represent the majority of the FFAs in the feedstock, its model has been checked for adequacy. This section is a continued study for the effect of reaction parameters on the conversion of oleic acid into FAMES. The present study has included four process variables i.e. M:O molar ratio, temperature, pressure and time. The effect of process variables and their interactions on the conversion of oleic acid has been extensively discussed in this section. It is clearly shown in Table 5.7 that the conversion of FFAs are in the range between 96.5 and 98.8%. This indicates that using supercritical methanol, most of the oleic free acids have been converted into FAMES.

5.3.2.4.1. Effect of M:O molar ratio

The stoichiometry of the esterification reaction of oleic acid into methyl oleate included the reaction of 1 mol of oleic acid with 1 mol of methanol to produce 1 mol of methyl oleate and water as shown in Equation 5.11. However, using supercritical methanolysis for biodiesel production usually requires large excess of methanol. Using excess of methanol has several advantages as it shifts the reaction equilibrium towards the products (biodiesel) and decrease the critical conditions of the mixture.



In the present study, a non-significant influence of increasing methanol ratio on oleic acid conversion has been reported as shown in Table 5.8. In addition, an antagonistic effect has been observed for the linear effect of increasing M:O molar ratio as shown in Equation 10 with a negative sign coefficient. However, the excess usage of methanol has a significant antagonistic effect as shown in Equation 10 with a negative sign for (A²) coefficient. This indicates that with an increase in M:O molar ratio decreases the conversion of oleic acid. Additionally, Figure 5.16 illustrates the effect of M:O molar ratio on the conversion of oleic acid conversion where non-significant impact has been observed at low reaction time. In addition, a negative influence has been observed for increasing M:O molar ratio on oleic acid conversion at longer reaction time.

Lokman et al. (2016) has reported similar results where for the esterification of FFAs using methanol range between 1:1 and 15:1. They have observed that increasing the ratio of methanol decreases the FAME yield beyond 9:1 M:O molar ratio. In addition, they have reported insignificant change in FAME yield between 6:1 and 9:1 and hence, they have considered 6:1 as the optimum M:O molar ratio. Similarly, Alenezi et al. (2010) have reported decreasing effect of M:O molar ratio using supercritical methanol at ratios higher than 1.6:1. They have referred to the complete solubility of supercritical methanol where large excess of methanol ratios would act to inhibit the esterification reaction. However, other researchers have reported increasing effect of M:O molar ratio on biodiesel yield (de Jesus et al., 2018; Jin et al., 2015; Narayan and Madras, 2017).

In conclusion, M:O molar ratio is a significant parameter that affects the esterification reaction. This ratio should exceed the stoichiometric 1:1 ratio. Mostly, increasing the M:O molar ratio would increase the overall biodiesel yield, which includes esterification and transesterification reactions. However, increasing M:O molar ratio beyond a ratio of 30:1 decreases the conversion of FFAs as shown in Figure 5.16.

5.3.2.4.2. Effect of reaction time

Reaction time reduction is considered as one of the major advantages of supercritical methanolysis over conventional catalysed methods. In the present study, the reaction time has showed a significant influence on oleic acid conversion as shown in Table 5.8. Furthermore, an increasing effect of high level reaction time has shown a highly significant effect on oleic acid conversion. It has been exemplified in Figure 5.16 that increasing reaction time (at high and low levels of temperature) has positive impact on oleic acid conversion up to 18 min. However, longer reaction time has negative impact on the conversion.

5.3.2.4.3. Interactive effect of M:O molar ratio and reaction time

According to the ANOVA results, the interaction effect between M:O molar ratio and reaction time has shown a significant effect on oleic acid conversion as shown in Table 5.8. The interaction effect is clearly shown in Figure 5.17, where a visible intersection between both reaction time and M:O molar ratio. The interaction is also clearly viewed in Figure 5.16, where at 12 min reaction time, the effect of increasing effect of M:O molar ratio on oleic acid conversion is different than at longer reaction time i.e. at 22 min.

Design-Expert® Software

Factor Coding: Actual

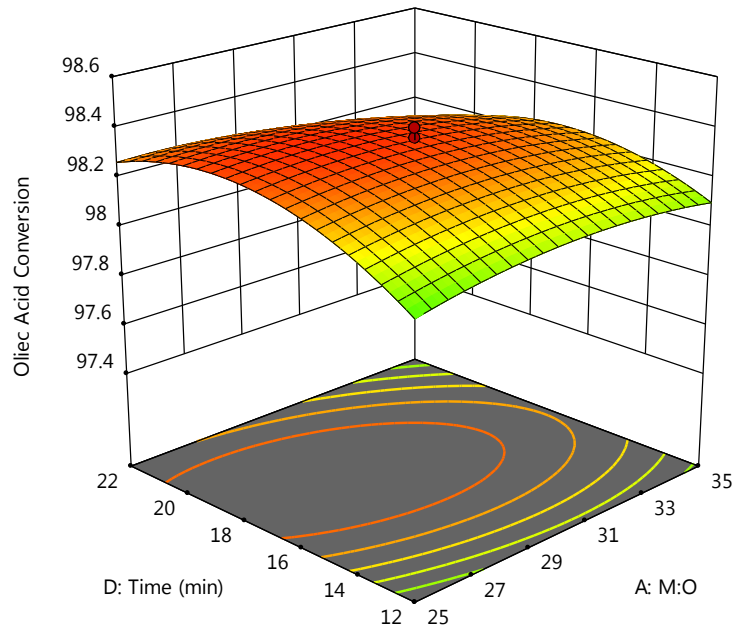
Oleic Acid Conversion

- Design points above predicted value
 - Design points below predicted value
- 97.57  98.4

X1 = A: M:O
X2 = D: Time

Actual Factors

B: Temperature = 260
C: Pressure = 135



Design-Expert® Software

Factor Coding: Actual

Oleic Acid Conversion

- Design Points
- 97.57  98.4

X1 = A: M:O
X2 = D: Time

Actual Factors

B: Temperature = 260
C: Pressure = 135

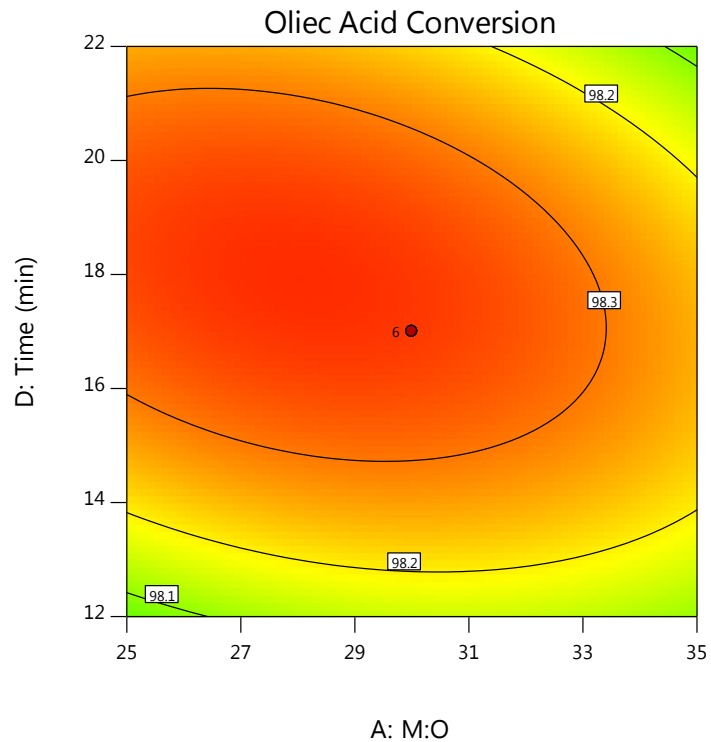


Figure 5.16. Response surface and contour plot for M:O molar ratio and reaction time versus oleic acid conversion

Design-Expert® Software

Factor Coding: Actual

Oleic Acid Conversion

● Design Points

----- 95% CI Bands

X1 = A: M:O

X2 = D: Time

Actual Factors

B: Temperature = 260

C: Pressure = 135

D- 12

D+ 22

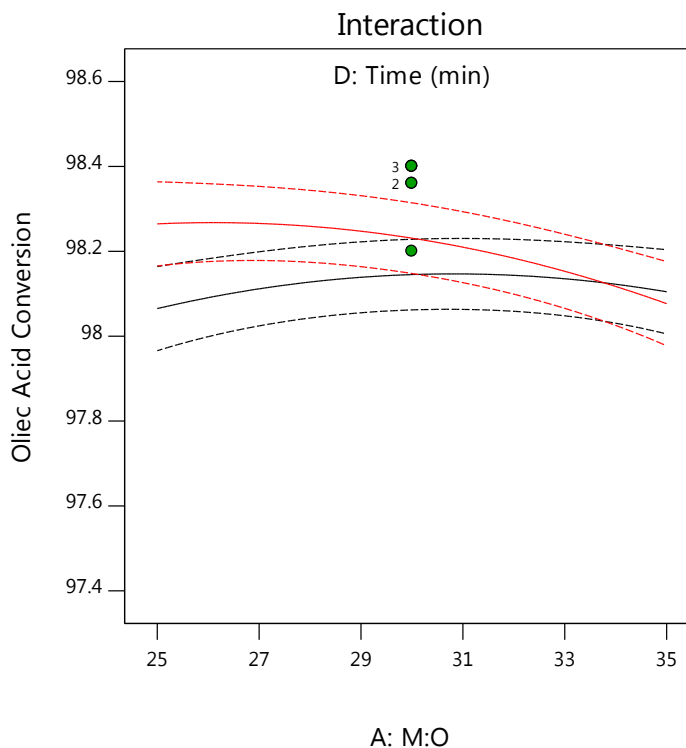


Figure 5.17. Interaction plot showing interactive effect of methanol ratio and temperature on FFA conversion

5.3.2.4.4. Effect of reaction pressure

By implementing supercritical methanolysis technique, the minimum reaction pressure is 80 bar, which reflects to the critical pressure of methanol. In this paper, the effect of reaction pressure on oleic acid conversion has been investigated between 85 and 185 bar. Increasing the reaction pressure has been performed using CO₂ gas, which also acts as a co-solvent for the reaction by enhancing the solubility of methanol in oil (Han et al., 2005).

In the present study, increasing the reaction pressure has negative effect on oleic acid conversion as shown in Equation 5.11 with a negative sign for the pressure coefficient. However, the only high level of pressure has significant effect on oleic acid conversion while the linear effect of pressure is not significant as shown in Table 5.8. Similar results have been reported by Jiuxu Liu et al. (2018), where they have reported insignificant effect of increasing the reaction pressure.

5.3.2.4.5. Effect of reaction temperature

Elevated temperatures have been used for non-catalytic production of biodiesel using supercritical methanol. It is widely accepted that increasing temperature enhance the reaction rate of supercritical methanolysis and increase the conversion of the reactants (Quitain et al., 2018). However, at elevated temperatures, thermal degradability should be considered as an important constraint that would breakdown the bonds of FAMEs and hence the biodiesel yield is reduced. The reaction temperature should be kept below 280°C to avoid any possibilities for thermal degradation (Román-Figueroa et al., 2016). In addition, the critical temperature of methanol is 240 °C which is considered as the minimum temperature for supercritical methanolysis. Consequently, the present study has investigated the effect of reaction temperature between 240 °C and 280 °C as shown in the previous chapter in Table 4.2.

In the present study, reaction temperature has been reported as a highly significant parameter affecting the conversion as shown in Table 5.8. As demonstrated in Figure 5.18, the increasing effect of temperature increase the conversion up to 265°C, where the conversion starts to decrease beyond this temperature. Similar researchers have reported the increasing effect of FFAs conversion while increasing the reaction temperature (dos Santos et al., 2017; Lokman et al., 2016; Nur Syazwani et al., 2017; Tavlarides et al., 2018).

5.3.2.4.6. Interactive effect of reaction pressure and temperature

As shown in Table 5.8, the interaction effect between reaction temperature and pressure has a non-significant effect on the conversion. It has been illustrated in Figure 5.18, parallel effects of both temperature and pressure on the response. This means that effect of each variable is not affected by varying the other parameter. This conclusion is clearly demonstrated in Figure 5.19, where the effect of increasing the temperature on the conversion is similar at both 110 and 160 bar. Hence, the pressure level does not affect the increasing effect of temperature on the conversion.

Design-Expert® Software

Factor Coding: Actual

Oleic Acid Conversion

● Design points above predicted value

○ Design points below predicted value

97.57 98.4

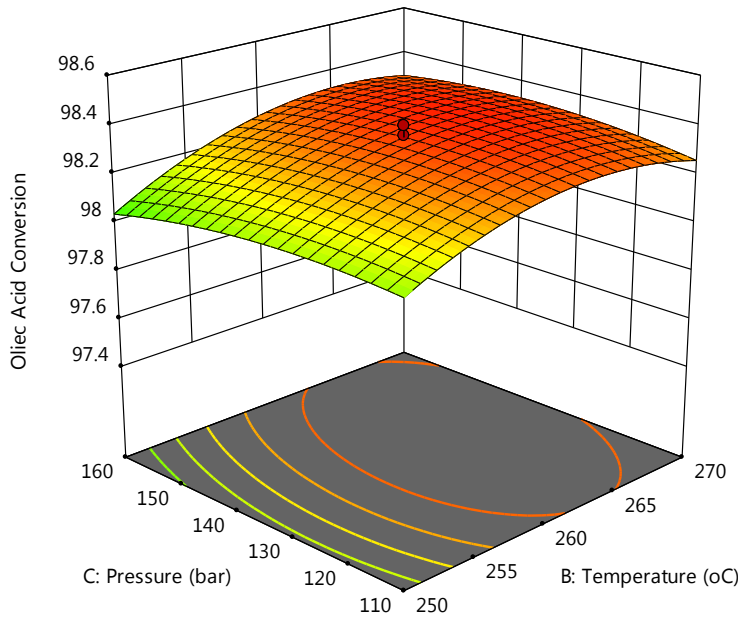
X1 = B: Temperature

X2 = C: Pressure

Actual Factors

A: M:O = 30

D: Time = 17



Design-Expert® Software

Factor Coding: Actual

Oleic Acid Conversion

● Design Points

97.57 98.4

X1 = B: Temperature

X2 = C: Pressure

Actual Factors

A: M:O = 30

D: Time = 17

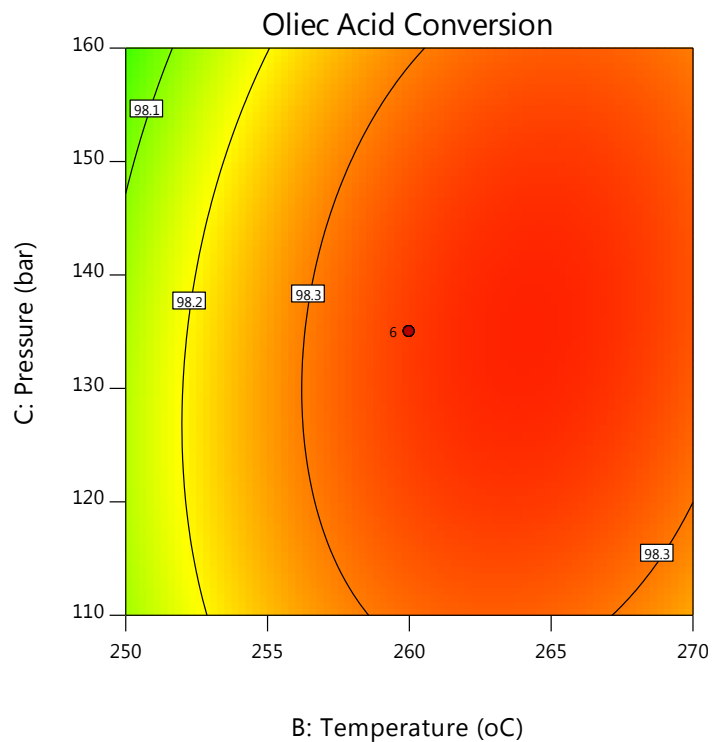


Figure 5.18. Response surface and contour plot for reaction pressure and time versus FFA conversion

Design-Expert® Software

Factor Coding: Actual

Oleic Acid Conversion

● Design Points

--- 95% CI Bands

X1 = B: Temperature

X2 = C: Pressure

Actual Factors

A: M:O = 35

D: Time = 22

C- 110

C+ 160

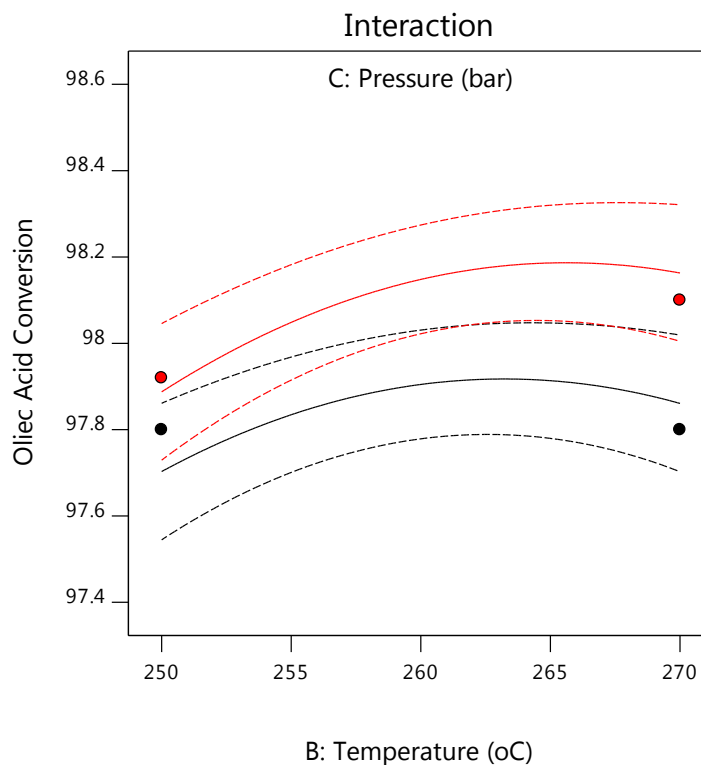


Figure 5.19. Interaction plot showing interactive effect of reaction pressure and time on FFA conversion

5.4. Process optimisation

Numerical and graphical optimisation using RSM method has been reported extensively during the last years for either biodiesel production (Knothe and Razon, 2017; Kostić et al., 2016; Muthukumaran et al., 2017b; Nikhom et al., 2018) or different applications (Saada et al., 2018). In the present study, both numerical and graphical optimisation have been employed to minimise the process variables and to maximise the process responses using Design Expert software. The optimisation targets for process variables and responses have been demonstrated in Table 5.9. A rank for each variable has been defined based on a scale from 1 to 5 for the importance of each target. The highest rank has been given to the reaction responses to achieve the maximum conversion. However, the 4th rank of importance has been provided to minimise reaction temperature and pressure as being the most energy consuming parameters in the reaction. This was followed by the 3rd rank of importance to minimise reaction pressure and M:O molar ratio.

Table 5.9. Optimisation constraints used to predict optimum conditions for biodiesel production

Factor	Code	Goal	Importance		
			Scale 1-5	Lower	Upper
M:O (molar ratio)	A	Minimise	3	25	35
Temperature (°C)	B	Minimise	4	250	270
Pressure (bar)	C	Minimise	3	110	160
Time (min)	D	Minimise	4	12	22
Myristic acid conversion	Y ₁	Maximise	5	98.5	100
Palmitic acid conversion	Y ₂	Maximise	5	98	100
Oleic acid conversion	Y ₃	Maximise	5	97.5	100
Linoleic acid conversion	Y ₄	Maximise	5	99	100

The software has used the combination of the targets and developed 68 solutions with different desirability. Hence, the solution with the highest desirability has been chosen as the optimal process variables for this study. The predicted optimum conditions with highest desirability of 92.3% have achieved conversion FAMEs of 99.2%, 99.1%, 98.35% and 99.65% for myristic, palmitic, oleic and linoleic acids, respectively. The optimal conditions have been reported at 25:1, 256.5 °C, 110 bar and 17 min for M:O molar ratio, temperature, pressure and time, respectively.

It is worth mentioning that using graphical optimisation has effectively exemplified the wide range of desirability at different variables levels. This demonstrate the difference between OFAT and multivariable optimisation. For instance, the optimal point could have different possibilities, where it could be observed at a low or high levels of variables as shown in Figure 5.20. The optimal conditions could also be developed at the axial level of a variable and in-between range of other variables as shown in Figure 5.21. Finally, the last option that the predicted optimal point could be located in-between range of both variables where it would be impossible to be predicted using OFAT as shown in Figure 5.22.

Design-Expert® Software
Factor Coding: Actual

Desirability
0 1

X1 = A: M:O
X2 = C: Pressure

Actual Factors
B: Temperature = 256.698
D: Time = 17.0221

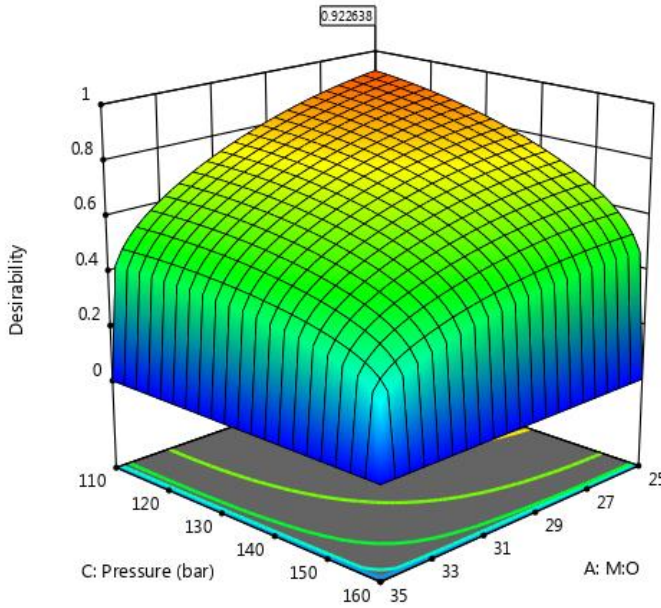


Figure 5.20. Surface plot showing the interactive effect of M:O molar ratio and reaction pressure on optimisation desirability

Design-Expert® Software
Factor Coding: Actual

Desirability
0 1

X1 = A: M:O
X2 = D: Time

Actual Factors
B: Temperature = 256.698
C: Pressure = 110

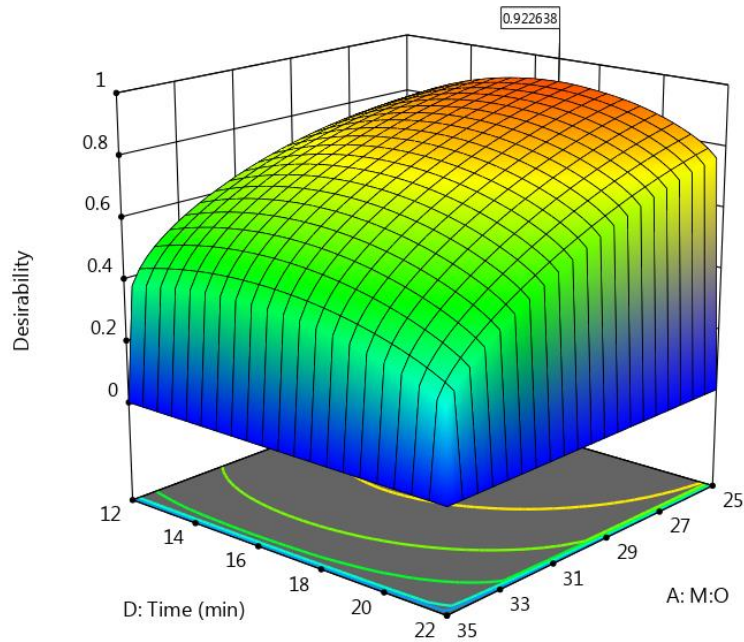


Figure 5.21. Surface plot showing the interactive effect of M:O molar ratio and reaction time on optimisation desirability

Design-Expert® Software

Factor Coding: Actual

Desirability

● Design points above predicted value

0  1

X1 = B: Temperature

X2 = D: Time

Actual Factors

A: M:O = 25

C: Pressure = 110

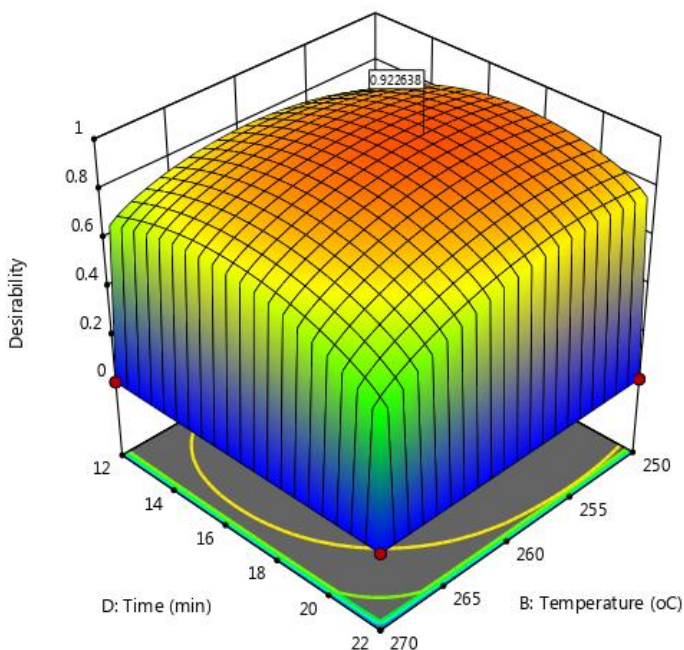


Figure 5.22. Surface plot showing the interactive effect of reaction temperature and time on optimisation desirability

The predicted optimal conditions have been validated experimentally by performing 3 experimental runs at the same predicted conditions. The experimental average results have reported 99.15%, 99.12%, 98.4% and 99.7% conversion for myristic, palmitic, oleic and linoleic acids, respectively. Consequently, the predicted optimal conditions have been confirmed experimentally with a relative error range between 0.05 and 0.2% for all responses.

5.5. Conclusions

FFA esterification reaction using supercritical methanol has been studied extensively. The conversion of FFAs has been analysed using two different ways including conventional titration and chromatographic analysis using a modified derivatisation-free characterisation of specific FFAs. Four independent variables have been investigated for the reaction including M:O molar ratio, temperature, pressure and time. Reaction temperature has been observed as the most significant variable affecting the conversion of most of FFAs followed by reaction time. Additionally, highly significant interactive effect has been reaction pressure and time, temperature and time and M:O molar ratio and temperature. Further, numerical and graphical optimisation have been employed to optimise the reaction variables for maximum conversion of fatty acids. The optimal conditions have been developed at 30.5:1, 261.7 °C, 110 bar and 16.8 min for M:O molar ratio, temperature, pressure and time, respectively for 98% conversion of FFA%. A kinetic study has been developed and confirmed a pseudo-first order reaction with the values of activation energy and Arrhenius constant of 34.5 kJ/mol and 2.48 s⁻¹, respectively. Reactor simulation at the validated optimum conditions using the experimentally determined kinetics has been performed. Simulation results showed reaction conversion of 98.77% with 0.478% relative error from the experimental data.

CHAPTER 6

CONCEPTUAL DESIGN OF AN ENERGY INTEGRATED SCHEME FOR SUPERCRITICAL BIODIESEL PRODUCTION

Outline of the chapter

This chapter describes the process design and simulation procedures. It includes both design and integration work. The chapter is organised as follows:

6.1. Introduction

6.2. Materials and methods

6.3. Process design

6.4. Process integration

6.5. Conclusions

6. Conceptual design of an energy integrated scheme for supercritical biodiesel production

6.1. Introduction

Non-catalytic transesterification has been considered as an ideal technique for biodiesel production from WCO as it prevents all the above-mentioned problems. It tolerates both esterification of FFA and transesterification of triglycerides in a single step reaction. However, it requires high reaction temperature and pressure, where the alcohol should be at the supercritical state (Lee et al., 2011). Several supercritical technologies have been used for non-catalytic production of biodiesel using methanol, ethanol, 1-propanol, DMC, MTBE and methyl acetate (Farobie et al., 2017).

West et al. (2008) designed and simulated four biodiesel production processes using different techniques including homogenous alkaline catalysed, homogenous acidic catalysed, heterogeneous alkaline catalysed and non-catalytic supercritical processes. They also performed an economic comparative analysis between the designed processes for the cost of production 8,000 tonne/y of biodiesel from WCO. They concluded that supercritical processing was the second most profitable process next to heterogeneous catalysed process. Lee et al. (2011) simulated production process for biodiesel using both fresh and used cooking oils. They have reported that the cost of the feedstock attributes with about 64-84% of the produced biodiesel cost. They have also reported that using supercritical methanol is the most economically favourable process over alkaline catalysed processes. Manuale et al. (2015) simulated an energy-integrated biodiesel production process using supercritical methanol. They have proposed that using the enthalpy content of the reactor product stream to separate most of the unreacted methanol in a flash drum decreased the process required heating energy.

Pinch technology is recognised as one of the most effective methods used to assess the efficiency of energy utilisation for production processes. The idea was proposed in 1978 by Umeda et al. (1978) which has been developed for further aspects by

Linnhoff and Hindmarsh (1983). The principle has been subsequently extended into several areas including mass Pinch, hydrogen Pinch and water Pinch. Smith, (2005) has discussed the principles for Pinch Analysis which have been implemented in mass and energy integration applications and extensively applied in heat recovery. The applications of such principles are very critical for providing energy and mass targets that should ideally be achieved in a process (Gadalla, 2015a). Srinivas and El-Halwagi (1994) introduced systematic and graphical procedures based on Pinch Analysis to design both mass and heat exchanger networks in complicated process industries.

Process integration for energy or materials savings can be achieved through two approaches, one which is based on insights derived from Pinch Analysis and the other is based on mathematical programming methodologies. The first approach normally comprises of two stages, first determining the energy (or mass) targets known as targeting, and then designing the heat and/or mass exchanger network to achieve these targets (Klemeš and Kravanja, 2013). The mathematical programming-based approach relies on building superstructure for all alternatives and then using simultaneous optimisation and integration to explore all interconnection within the proposed superstructure. This is followed by screening of all the alternative to find the optimal combination (El-Halwagi, 2011; Grossmann et al., 2018). The recent handbook of Klemeš (2013) is a good source for such literature.

Gadalla, (2015b) has reported a novel graphical technique for HEN designs based on Pinch technology. The graphical method has been defined by plotting process hot streams *versus* process cold streams. Each process heat exchanger has been represented by a straight line where its gradient is function of the ratio between heat flows and capacities. In addition, each line is proportional to the flow of the heat transferred across the exchanger. This method could easily analyse any proposed HEN to identify inappropriate exchangers whether across the Pinch, network Pinch and improper placements. In addition, he reported that the developed method could be implemented in designing optimum HENs using numerical process streams matching technique. Gadalla, (2015c) has also extended the same conceptual novel graphical method for mass integration applications and mass exchanger networks (MEN) designs.

In this chapter, a comprehensive integrated design for biodiesel production process using supercritical methanol has been simulated. The reactor has been designed based on previous experimentally reported kinetic parameters. Energy and mass integration principles have been applied to reduce the process required external energy and fresh resources, respectively. Graphical Pinch method has been applied to design and develop a new optimum HEN responsible for reduction of heating and cooling required energies. In addition, it has been used to evaluate previously reported designs.

6.2. Materials and methods

The transesterification/esterification reactions for WCO were carried out using supercritical methanol. Aspen HYSYS simulation programme version 8.8 was used for simulating the biodiesel process (Aspen Technology Inc., USA). The procedures for process simulation based on HYSYS simulator consist of several steps including selection of chemical components for the process, appropriate thermodynamic models, required process units and operating conditions. The actual existing pressure drop in different equipment was neglected in the present study.

The assumptions associated with the present simulation are as follows:

- The transesterification reaction steps were represented by only overall step where TG are converted to FAME.
- Glycerol methanol side reaction was ignored.
- Heat exchangers were selected as counter flow type and were simulated by a means of a shortcut module.

6.2.1. Chemical components

Most of the required information for chemical components used in the process design were included in HYSYS data bank library. Triolein ($C_{57}H_{104}O_6$) and Trilinolein ($C_{57}H_{98}O_6$) were used to represent the triglycerides in the WCO as they were reported as the major compositions (~86%) based on the chromatographic analysis reported previously in Section 3.2. Oleic and linoleic acids have been used to represent the FFAs exist in the WCO. Methyl oleate ($C_{19}H_{36}O_2$) and methyl linoleate ($C_{19}H_{34}O_2$) were considered as the

desirable product of the reaction. Referring to the WCO's TAN of 0.8 mg KOH/ g oil, the FFAs weight FAME were equivalent to 1.6%. Trilinolein component was not available in the HYSYS data bank library where it has been introduced as a hypo-component using hypo-manager tool by identifying its physicochemical properties (Plazas-González et al., 2018).

6.2.2. Thermodynamic model

Owing to the presence of polar components in the process, i.e.; methanol and glycerol, NRTL activity model was selected as the fluid thermodynamic package for the activity coefficient calculations. Some binary interaction coefficients were not available in the HYSYS data bank library. Accordingly, the missing coefficients were estimated using UNIFAC liquid-liquid equilibrium and UNIFAC vapour-liquid equilibrium methods. Since the activity coefficient based model such as NRTL is not recommended to be used at pressure greater than 1000 kPa, In addition, NRTL fails to provide appropriate prediction for the physical separation of components including FAMES and glycerol in decanter unit. Accordingly, Peng-Robinson EOS was used in the process streams at high pressure and at separating units (Lee et al., 2011).

6.2.3. Plant capacity, unit operations and operating conditions

The biodiesel plant capacity was specified by 9.2 kgmol/h of fresh WCO feed. Conversion reactor unit exists in the simulation environment, which requires only the final reaction conversion, used in most of the process designs in the literature was replaced by kinetic CSTR reactor. Kinetic and thermodynamic data required for the reactor including reaction rate constant (k), activation energy and frequency factor, were identified based on previous reported experimental data as of 0.0006 s^{-1} , 50.5 kJ/mol and 4.05 s^{-1} , respectively (as developed in Section 3.3). Reactor operating conditions were identified based on the experimentally concluded optimum conditions reported previously, i.e. methanol to oil (M:O) molar ratio of 37:1, reaction temperature of 253°C , reaction pressure of 198.5 bar in 14.8 min reaction time (as developed in Section 3.3). The process units include reactor, distillation columns, flash drum, heat exchangers and pumps.

6.3. Process design

Biodiesel production process consists of several process stages including reactants preparation, transesterification/esterification reactions, methanol recovery and finally biodiesel purification. The process has been designed as a modified version for a previous process design reported by Lee et al. (2011). Methanol and WCO have been pressurised and then heated to the specified conditions; then both reactants have been mixed and fed to the reactor. The reactor has been identified based on the developed kinetic experimental data described in Chapter 3. The reactor product stream has been depressurised and proceeded for further biodiesel purification units. Reactor product stream (Stream 106) has been processed to a simulation tool called “Cutter” which has changed the thermodynamic model from NRTL to Peng-Robinson. The product stream has been fed to a flash separator to separate the vaporised unreacted methanol. Further methanol separation has been performed using a distillation column. Then, the glycerol has been separated physically using a decanter unit. Finally, the unreacted triglycerides have been separated using a vacuum distillation. Fresh reactants streams for both WCO and methanol have been labelled as 100 and 101. Products’ streams including glycerol and biodiesel have been labelled as 112 and 114A, respectively. Process flowsheet is presented in Figure 6.1 and the properties of main streams are given in Table 6.1 and Table 6.2. A summary of the units’ operating conditions is presented in Table 6.3.

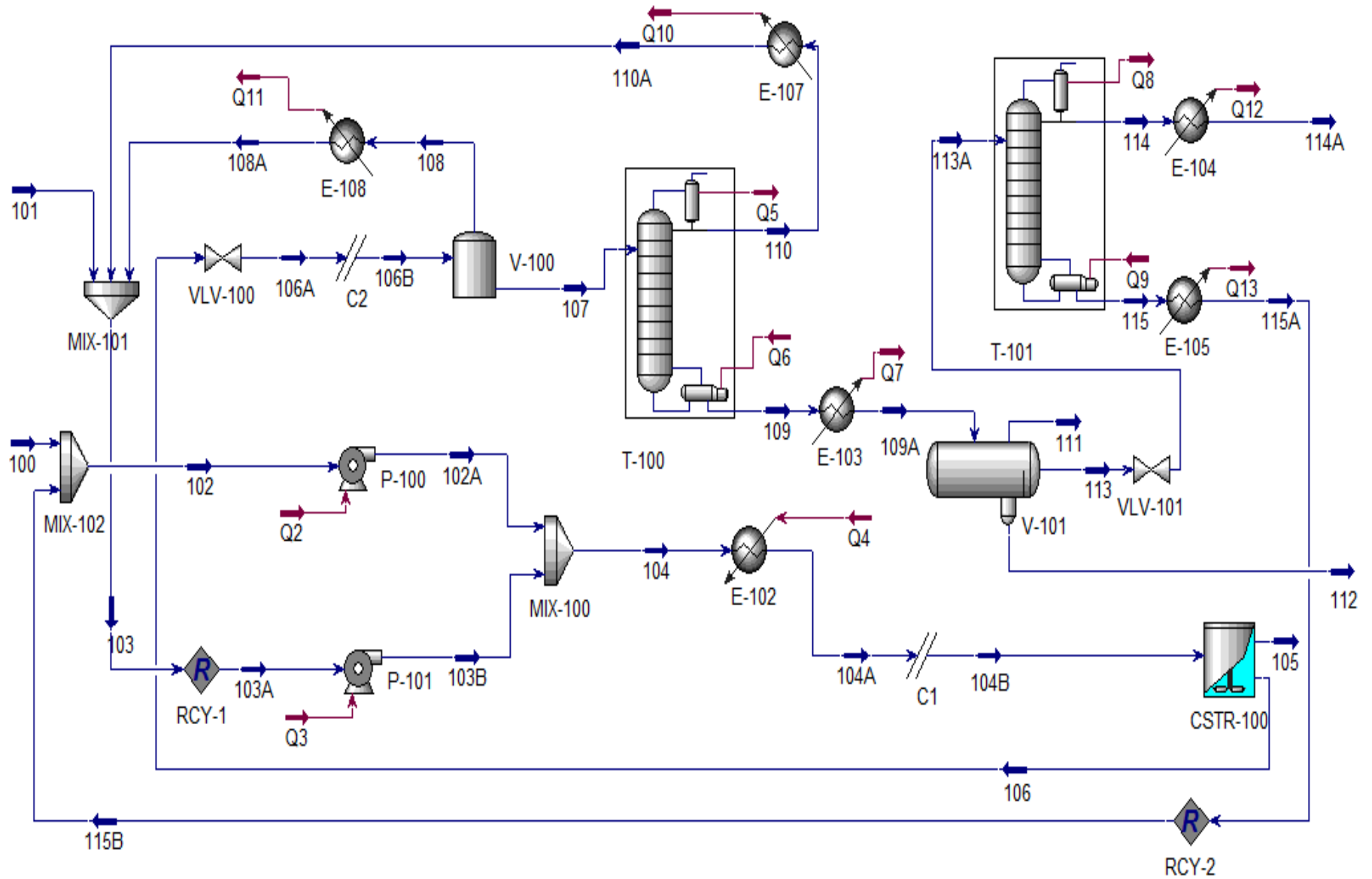


Figure 6.1. Process flowchart for biodiesel production (numbers below streams refer to stream names)

Table 6.1. Stream table for the designed process (Part 1)

Name	100	101	102	103	104A	105	106	107
Temperature (°C)	25	25	25	62	253.5	230	230	87.9
Pressure [kPa]	101	101	101	101	19850	19840	19840	105
Molar Flow [kmol/h]	9.2	27	11.3	386	397.3	0	397.3	53.6
Mole fractions								
Triolein	0.69	0	0.61	0	0.017	0	0.001	0.01
Trilinolein	0.25	0	0.23	0	0.0066	0	0.0006	0.004
Methanol	0	1	0	0.92	0.848	0	0.78	0.22
Methyl oleate	0	0	0.11	0	0.003	0	0.05	0.38
Methyl linoleate	0	0	0.001	0.002	0.0003	0	0.01	0.13
Linoleic acid	0.01	0	0.01	0	0.0003	0	0	0.0002
Oleic acid	0.03	0	0.03	0	0.0009	0	0.0001	0.0004
Glycerol	0	0	0	0	0	0	0.02	0.16
Water	0	0	0	0.07	0.12	0	0.12	0.07

Table 6.2. Stream table for the designed process (Part 2)

Name	108A	109	110	111	112	113	114A	115A
Temperature (°C)	65	254	72.3	25	25	25	25	25
Pressure [kPa]	101	112	101	101	101	101	101	101
Molar Flow [kmol/h]	343.7	37.9	15.6	0	8.8	29.1	27	1.17
Mole fractions								
Triolein	0	0.01	0	0	0	0.06	0	0.72
Trilinolein	0	0.006	0	0	0	0.02	0	0.22
Methanol	0.8	0.008	0.76	0	0.006	0.0009	0.008	0
Methyl oleate	0	0.54	0	0	0	0.67	0.72	0.04
Methyl linoleate	0	0.19	0	0	0	0.23	0.27	0
Linoleic acid	0	0.0002	0	0	0	0.0003	0	0
Oleic acid	0	0.0006	0	0	0	0.0007	0	0.02
Glycerol	0	0.23	0	0	0.9	0	0.0001	0
Water	0.13	0.0001	0.24	0	0	0	0	0

Table 6.3. Summary of units operating conditions of each process

Operating parameter	Value
Reactor (CSTR-100)	
Temperature (°C)	253.5
Pressure (bar)	198.5
Methanol:Oil molar ratio	37:1
Residence time (min)	14.8
Conversion (%)	91.7
Methanol Separating Column (T-100)	
Reflux ratio	1
Number of stages	10
Condenser pressure (kPa)	101
Reboiler pressure (kPa)	112
Methanol recovery	97.8%
Distillate flowrate (kgmol/h)	16.57
Distillate purity (wt%)	84.5
FAME Separating Column (T-101)	
Reflux ratio	1
Number of stages	10
Condenser pressure (kPa)	2
Reboiler pressure (kPa)	5
Distillate flowrate (kgmol/h)	27
Distillate purity (wt %)	99.9

6.3.1. Non-catalytic reactor

The reactor feed stream (Stream 104A) has been pre-processed to the reaction conditions i.e. temperature of 253.5 °C and pressure of 198.5 bar. The volume of the reactor has been identified based on the experimental optimum time of reaction and the flow rate of the reactants where the residence time of the reaction has been adjusted at 14.8 min.

Consequently, the reactor has resulted in 91.7% conversion of both triolein and trilinolein to methyl oleate and methyl linoleate as similarly reported experimentally in Section 3.3. Esterification reactions of FFAs i.e. oleic and linoleic acids to methyl oleate and methyl linoleate, respectively, have been included to the reaction set. Reaction product stream (Stream 106) has been processed for further separation unit to separate methyl oleate from unreacted components and side products.

In addition, a sensitivity analysis has been performed to investigate the effect of the variation of k on the simulated conversion in the kinetic reactor. A variation of ± 0.0001 of the value k has been applied, where new values of activation energy and Arrhenius constant have been determined. Using the new values of k , activation energy and Arrhenius constant have been varied within ranges of 44.26-58.97 kJ/mol and 3.01-6.08 s⁻¹, respectively resulting in a significant variation of the simulated conversion results between ranges of 70.1-97.2 %. The results of this analysis could highlight the high sensitivity of the simulated conversion based on the kinetic data. Hence, it is highly recommended to perform accurate experimental kinetic calculations.

6.3.2. Separation of unreacted methanol

The actual M:O molar ratio (37:1) used in the reactor is much higher than the stoichiometric requirements for both transesterification of triglycerides (3:1) and esterification of FFAs (1:1). Accordingly, the product stream includes a significant excess of unreacted methanol. Reactor product stream (Stream 106) has been depressurised to the atmospheric pressure using an expansion valve (VLV-100), where the enthalpy difference of the mixture has converted some of the liquid

methanol to the vapour state. The de-pressurised product stream (Stream 106D) has been fed to a flash drum (V-100) which has separated different liquid and gas phases. The top product stream (Stream 108) composed mainly from methanol in addition to water. However, the bottom liquid stream (Stream 107) contains a mixture of reactions products and unreacted reactants as shown in Table 6.1. The adiabatic flash drum has separated 96% of the unreacted methanol from the reactor product stream (Stream 106).

Further methanol separation has been carried out using a distillation column (T-100) with 10 stages to provide sufficient separation (Lee et al., 2011). Using distillation column, 97.8% of the unreacted methanol in the feed stream (Stream 107) has been separated in the top product stream (Stream 110). The bottom product (Stream 109), which mainly consists of unreacted triglycerides, produced methyl esters, fatty acids and glycerol, as shown in Table 6.1, has left the column at 253.9 °C and cooled to 25 °C for further separation processes. The unreacted methanol could be completely separated at temperatures higher than 278°C. However, the column's reboiler temperature has not exceeded 253.9 °C for several reasons including avoiding thermal degradation of FAMES that shows only stability up to 270 °C (Imahara et al., 2008) and avoiding having traces of vaporised glycerol at the top stream where its boiling temperature is 280°C. In addition, increasing the temperature from 253.9 °C to 270 °C has no significant increase in methanol recovery.

6.3.3. Glycerol separation

Separation of glycerol from biodiesel is considered as an essential purification step as the high content of glycerol could lead to storage problems due to phase separation, higher emission of aldehyde in combustion process and clogging of the fuel injector (Wolf Maciel et al., 2009). The separation processes that have been reported in previous studies involved several techniques including gravity settling and washing with water (West et al., 2008). In this work, gravity settling using phase separator has been applied. The cooled bottom product stream from distillation column (Stream 109A) has been fed to the settling unit (phase

separator). Glycerol has been separated in the bottom product stream (Stream 112), where biodiesel associated with the unreacted triglycerides has been separated in the middle product stream (Stream 113). About 99.9% of glycerol in the feed stream (Stream 109A) has been separated in bottom stream (Stream 112) associated with traces of unreacted methanol. Finally, as the influent stream to the separator does not include any gases, nothing has been reported at the top product stream (Stream 111).

6.3.4. Biodiesel purification

According to the European standard for biodiesel specifications, EN14214, maximum concentration of triglycerides in the pure biodiesel is 0.2% by weight (Lee et al., 2011). In this study, the glycerol free biodiesel mixture stream (Stream 113) contains 8.38% by weight of triglycerides, where it exceeds the specification of EN14214. Accordingly, further purification process has been applied for biodiesel mixture stream in order to separate the residuals of triolein. VDU has been used to avoid any thermal cracking or degradation of FAMES. Imahara et al. (2008) have reported that at high temperature, FAMES show stability up to 270°C, while beyond this temperature FAME starts to decompose due to isomerisation from *cis*-form to *trans*-form.

The feed stream has been de-pressurised using vacuum pump, which has been represented in the simulation environment as an expansion valve tool (VLV-101). Ten stages column has been used for the separation process (Lee et al., 2011). The purified biodiesel stream (Stream 114) exits the column with less than 0.02% by weight of triolein, which is in agreement with the European standard biodiesel specifications, EN14214

6.4. Process integration

Conservation of mass and energy in the developed industries has been considered as the most effective approach for sustainable design. Hence, implementation of HEN and MEN has gained a great interest in process engineering research through the last decades. The highlights of these researches are to minimise the

external usage of energy, minimise waste discharge, minimise purchasing of fresh resources and to maximise the production of the desired product. All of these aspects are implemented through both energy and mass integration for the designed processes (Klemeš, 2013).

6.4.1. Mass integration

In the present study, the designed process has been subjected to different mass integration aspects. Firstly, optimising the reaction conditions has been applied experimentally as reported previously (as developed in Section 3.2) by maximising the desired product and minimising reaction conditions. In addition, mass integration principles have been applied for the developed process. As the designed process did not include any mass exchanging units, mass integration would be only highlighted through minimising waste and fresh resources. The fresh resources used for this process are WCO and methanol. Methanol is considered as a major reactant, which is used in large excess in the non-catalytic transesterification reaction. Hence, minimising fresh and waste methanol is considered as an essential requirement for biodiesel integrated process.

In the existing process, two available sources streams for methanol have been observed including streams separated from both adiabatic flash drum unit and distillation column unit, i.e.; streams 108 and 110. On the other hand, there is only one sink that require fresh methanol, which is the reactor (CSTR-100). The required flowrate of fresh methanol for the process sink is 386 kgmol/h which is a massive amount to be purchased. Moreover, the reactor requires huge excess of methanol where waste methanol is considerably high. Consequently, using simple source-sink mapping shown in Figure 6.2, a proposed scheme for methanol recycling has been developed. The reactor required methanol with maximum composition of impurities of 5% where the available sources are having much lower impurities (<1%). Accordingly, simple recovery for both available sources has been implemented as shown in the process flow chart shown in Figure 6.1, where both sources streams have been mixed directly with the minimum required fresh methanol stream to be fed to the reactor. After applying this mass integration

recycling, the actual fresh methanol used is only 27 kgmol/h (Stream 101) instead of 386 kgmol/h in case of having no recycling approach which represents 93% savings for the fresh methanol requirements.

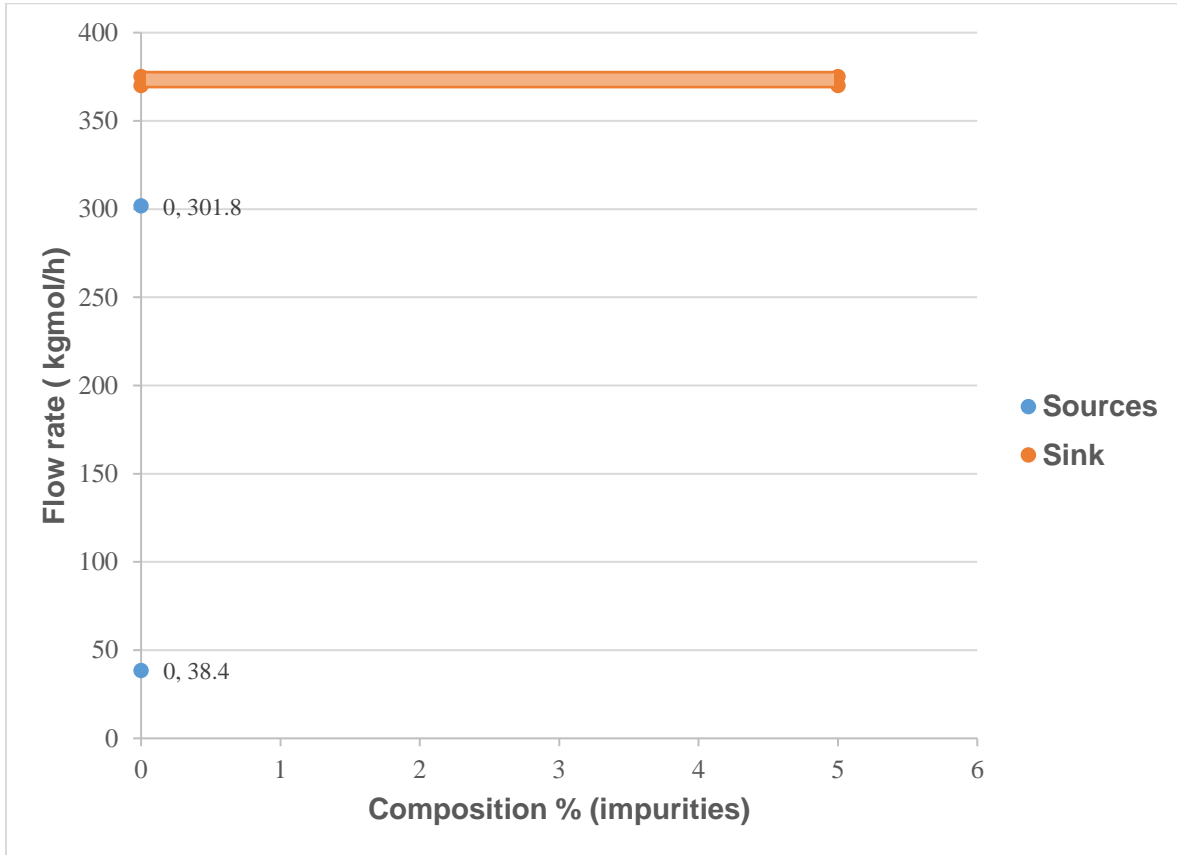


Figure 6.2. Source-sink mapping

6.4.2. Heat integration

Pinch technology has been used to integrate the energy required for both heating and cooling for all process streams. The list of the process hot and cold streams has been presented in Table 6.4. An assumption of ΔT_{\min} of 10 °C has been proposed as generally accepted by Pinch method (Klemeš, 2013). Identifying Pinch temperatures would be proceeded using either problem table algorithm and/or heat composite curve. In the present study, the Pinch temperatures have been identified using the second method. Aspen Energy Analyzer[®] V8.8 simulation

software has been used in identify the Pinch temperatures, minimum heating and cooling energy requirements and plotting composite curve for the process streams.

Table 6.4. Process hot and cold streams

Stream	Hot/Cold	Inlet T (°C)	Outlet T (°C)	C_p (kJ/kg.°C)	Heat duty ($\times 10^6$ kJ/h)
104		72.6	253.5	6.07	10.5
REB1		124.1	256.4	3.05	4.95
REB2		224.5	226	176.6	10.9
108		89	65	1,633.1	12.8
109		253.9	25	2.41	5.8
110		66.5	65	3.68	0.002
114		80.4	25	2.01	0.62
115		241.3	25	1.51	0.44
COND1		66.5	66.4	9,012.8	0.96
COND2		214.1	63.7	4.1	10.1

A composite curve for the process streams has been developed as shown in Figure 6.3. The overlap between hot and cold composite curves represents the prospective integration between hot and cold streams according to Pinch rules (Farrag et al., 2016). The minimum energies required for both heating (Q_h) and cooling (Q_c) have been observed from Figure 6.3 Figure 6.4, 108 kW and 5,400 kW, respectively.

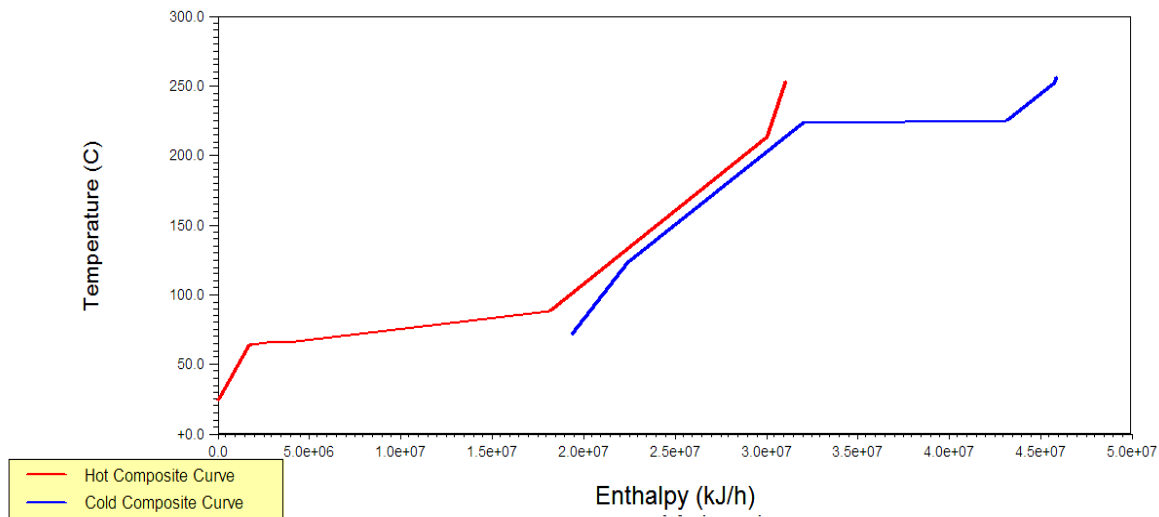


Figure 6.3. Composite curve of the process streams

In an attempt to minimise the process energy consumption and increase energy integration between process streams, design of a new HEN design has been developed using graphical Pinch Analysis method using only 5 heat exchangers as shown in Figure 6.4. Using numerical matching in graphical method eases the process of exchanger streams' selection and streams splitting. In addition, it investigates the validity of the exchangers according to Pinch rules. The designed exchangers have been analysed graphically where the exchangers fulfil the method guidelines as shown in Figure 6.5. The graphical method shortened the trial procedures that would be applied to achieve the optimum network using conventional Pinch methods. Consequently, the developed HEN has resulted in achieving 100% of both minimum heating and cooling energies requirements.

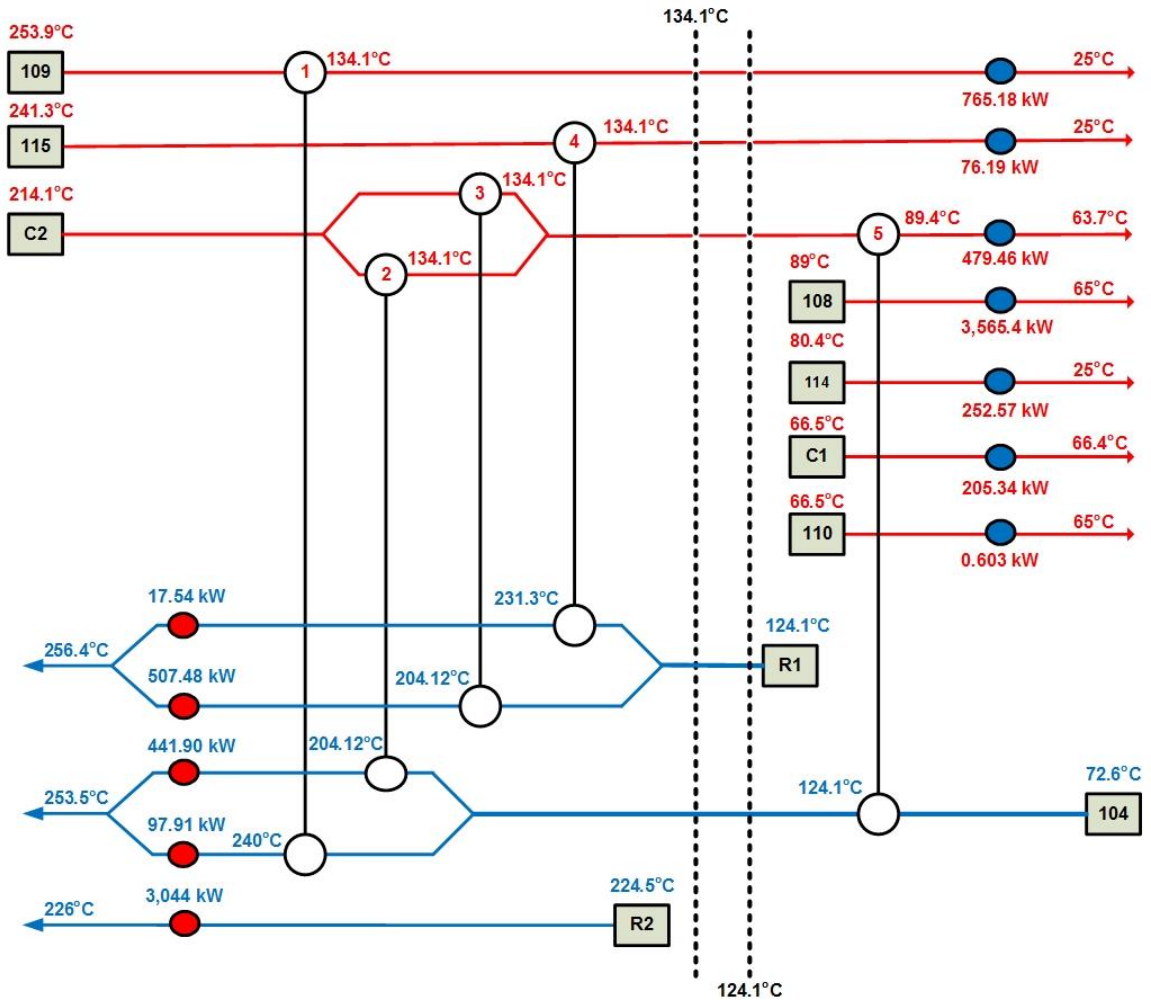


Figure 6.4. Heat exchanger network designed for the integrated process

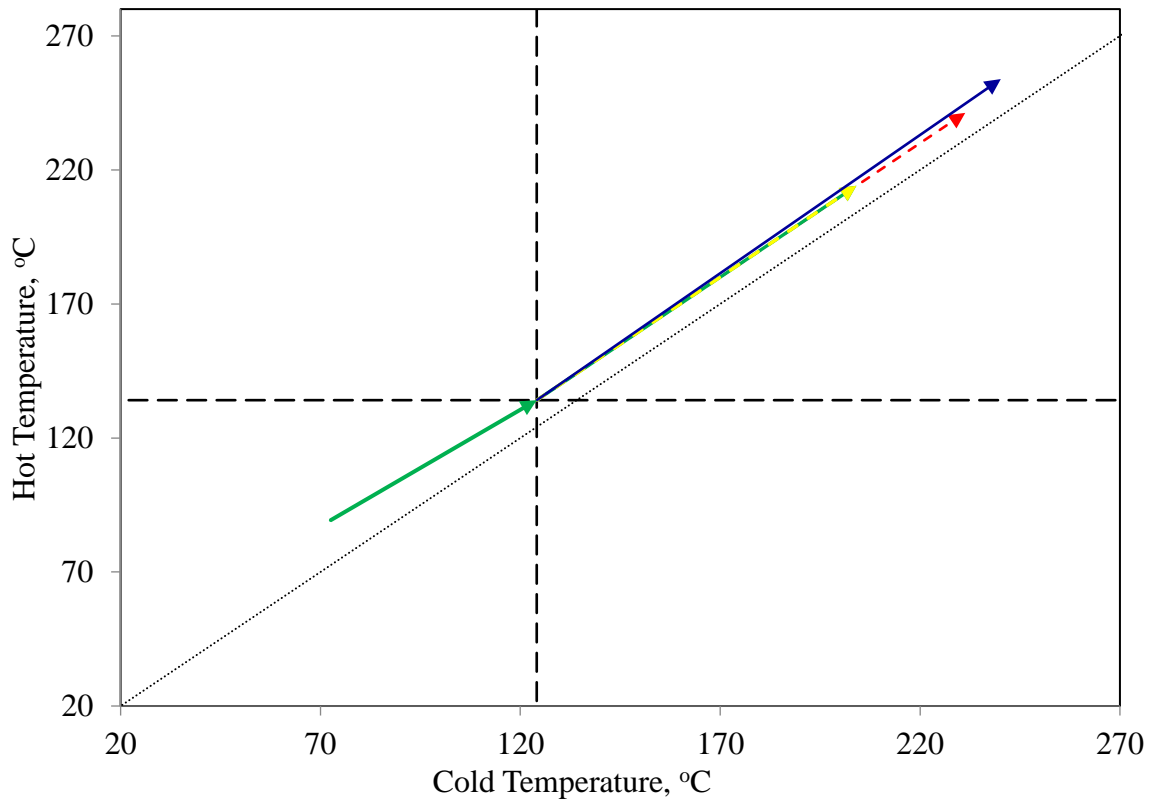


Figure 6.5. Graphical representation of the designed HEN on T-T diagram

These results have been compared with the automated designs developed by Aspen Energy Analyzer software. It has been observed that the optimum automated design has used 6 heat exchangers and achieved 118% and 113.9% of the minimum heating and cooling energies requirements, respectively. A schematic of the auto-generated HEN is shown in Figure 6.6. This implies that the automated design consumes more energy than the targets. Graphical Pinch method has been used to investigate the proposed automated design and to highlight the problems associated with the design using simple and quick observations. Figure 6.7 illustrates a graphical representation of the proposed design using graphical Pinch method on T-T plot. It could be easily observed that 3 of the proposed automated exchangers are existing within the non-optimum integration area where a revamping design is required to relocate the exchangers within the optimum integrating areas.

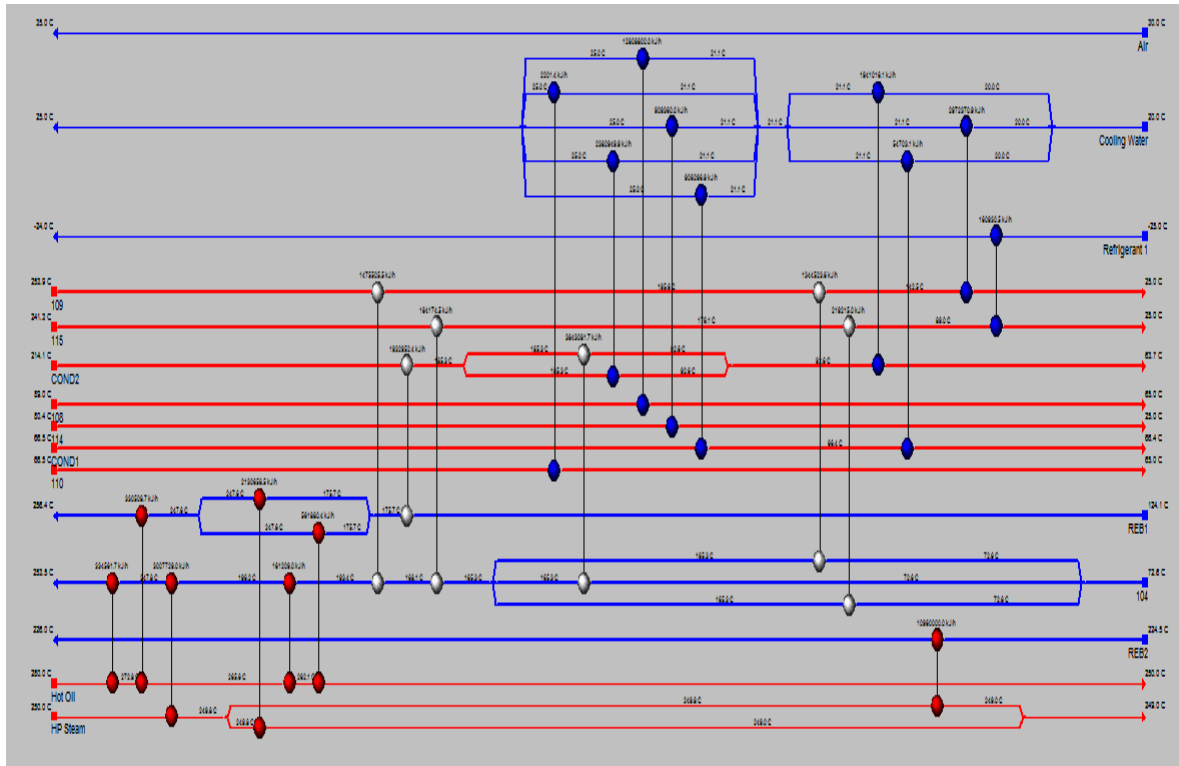


Figure 6.6. Auto-generated HEN for biodiesel process

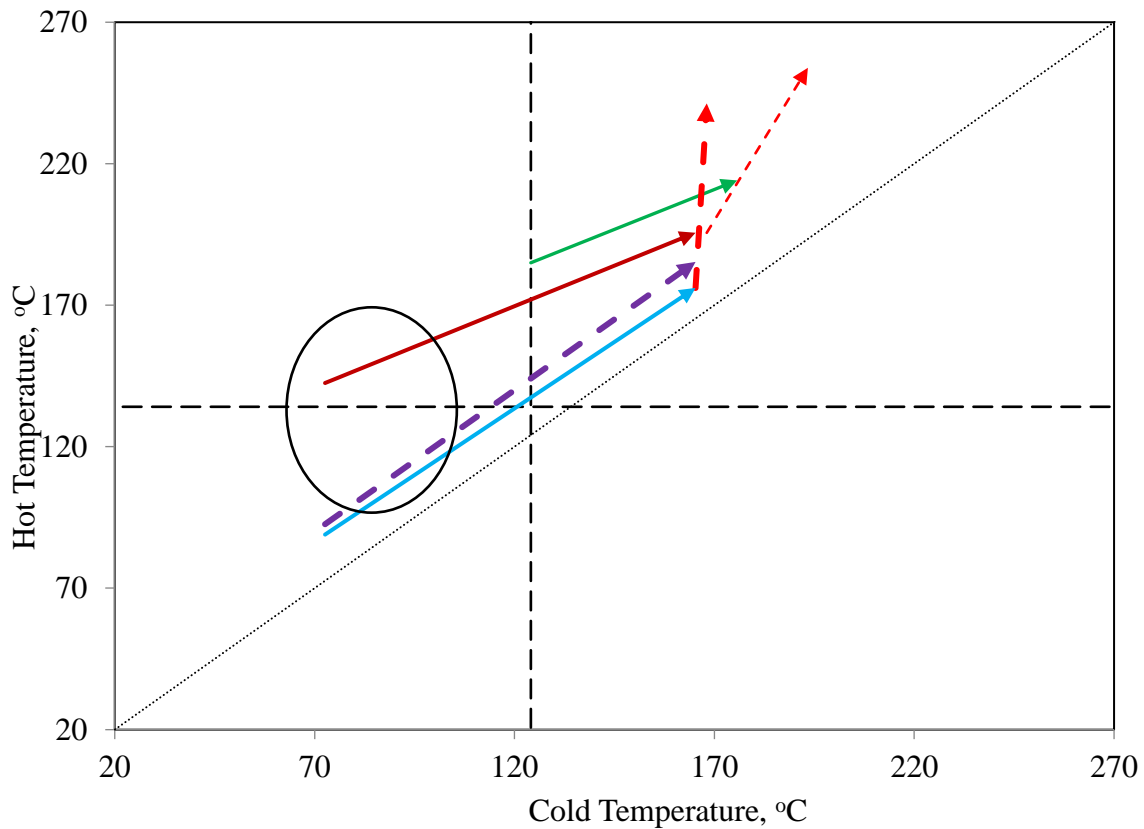


Figure 6.7. Graphical representation of the automated proposed HEN on T-T diagram

Lee et al. (2011) have designed an energy integrated process for biodiesel using supercritical methanol. They have included only 2 heat exchangers to the process HEN. Their developed HEN has been also analysed using graphical Pinch method as shown in Figure 6.8. The simple designed HEN includes two exchangers with major problems. The first exchanger is a network Pinch exchanger where the developed straight line representing the exchanger touches the Pinch line as shown in Figure 6.8. This disseminates that the exchanger is not fulfilling Pinch rules with insufficient minimum heat transfer temperature difference. When an exchanger touches the Pinch line, it indicates that the process streams temperature difference is equal to zero and accordingly, an inefficient exchanger. On the other hand, the second exchanger has been included within the non-optimum integration area and the temperatures are crossing the Pinch line.

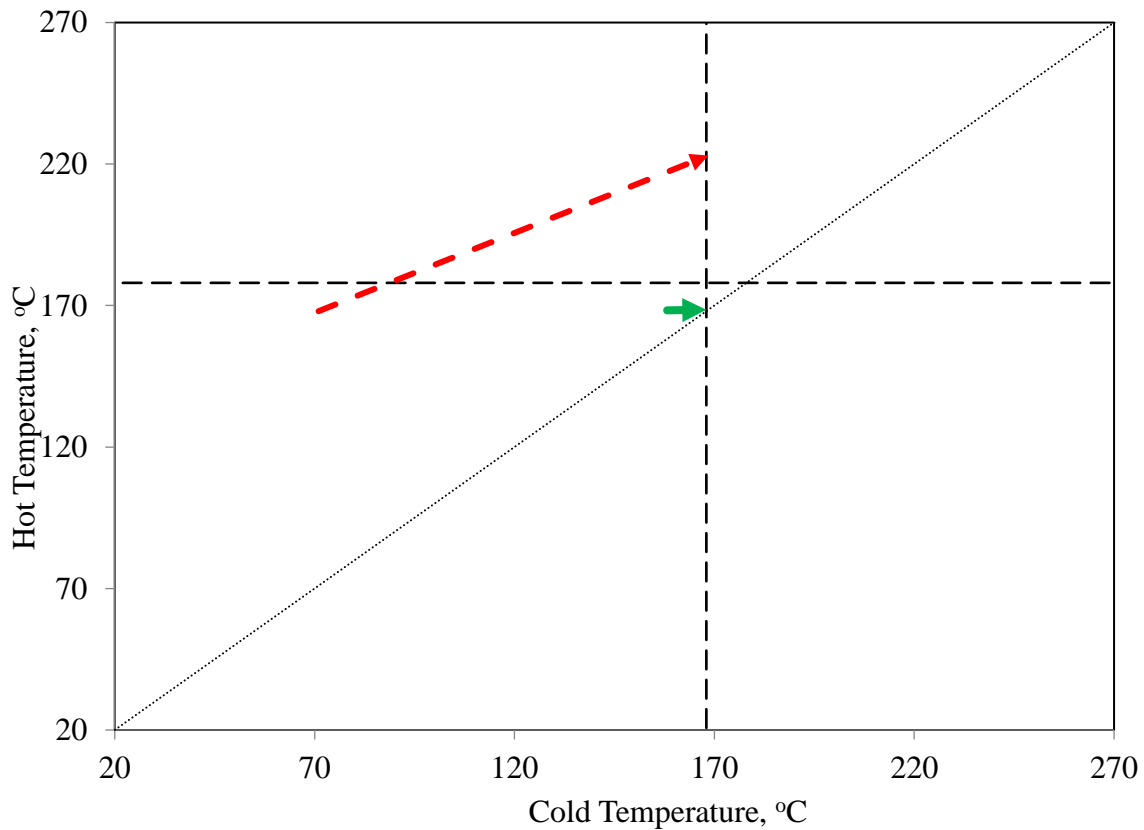


Figure 6.8. Graphical representation of the literature proposed HEN on T-T diagram

These results exemplify the significance of using graphical Pinch method in analysing existing HENs where the inefficient exchangers would be easily observed. In addition, using graphical matching technique for process streams simplify the integration procedures where it could be implemented to match many streams in relatively short time compared with the conventional methods.

A comparative study for the energy savings between the mentioned HEN designs. i.e., the developed HEN in this study, the auto-generated HEN by Aspen Energy Analyzer and the integrated process reported in the literature has been analysed. The results have showed that the developed HEN has saved 42% of the consumed heating energy required for the non-integrated process (i.e. Figure 6.1). However, the auto-generated HEN design has resulted in saving only 33% of the required

heating energy. Finally, the HEN design reported in the literature has resulted in saving 21% of the required heating energy. The comparative study results are presented in Table 6.5.

Table 6.5. Comparative study for the HEN designs

HEN design	Heating energy (kW)	% Savings
Basic (No HEN)	7263	0
Literature design (Lee et al., 2011)	5763	21
Auto-generated HEN	4859	33
Graphical design (developed in this study)	4109	43

6.5. Conclusions

In this chapter, an integrated process for non-catalytic biodiesel production from WCO using supercritical methanol has been simulated. The process has been designed where the produced biodiesel relies in agreement with the European Standard for biodiesel specifications, EN14214. The developed process has been subjected to both mass and energy integration to minimise the fresh methanol requirements and to minimise the external required energies for heating and cooling, respectively. Methanol recycling strategies have contributed to minimise fresh required methanol. Graphical Pinch method has been implemented to design a HEN using numerical matching strategy. The designed HEN has achieved 100% of the targeted optimum required energies by Pinch technology with heating and cooling energy requirements 4,108 kW and 5,400 kW, respectively. A comparative analysis between the developed HEN with an integrated process in the literature and an auto-generated HEN by Aspen Energy Analyser has been studied. The results have showed that the developed HEN has saved 42% of the energy consumption in comparison 33% and 21% for the auto-generated HEN and the integrated process in the literature, respectively.

CHAPTER 7

CONCLUSIONS AND RECOMMENDATIONS FOR FUTURE WORK

Outline of the chapter

This chapter provides the overall conclusions of thesis where the achievement of each research objective has been discussed. Furthermore, research recommendations for future work have been addressed. The chapter is organised as follows:

7.1. Conclusions

7.2. Challenges and recommendations for future work

7. Conclusions and recommendations for future work

7.1. Conclusions

This work has investigated biodiesel production *via* supercritical technology. Two WCOs with different acidity have been used for biodiesel synthesis. Using low acidity WCO, the developed optimum conditions for biodiesel production were at M:O molar ratio of 37:1, reaction temperature of 253.5 °C, reaction pressure of 198.5 bar in 14.8 min yielding 91% biodiesel. However, the developed optimal conditions for biodiesel from the high acidity WCO at M:O molar ratio of 25:1, reaction temperature of 265 °C and reaction pressure of 110 bar in 20 min yielding 98% biodiesel. It has been observed higher yield of biodiesel from higher acid value feedstock at milder conditions. This attributes to the rate of esterification reaction is much higher than transesterification reaction. Hence, it is not preferable to implement supercritical methanolysis for low acidity feedstock.

A kinetic and thermodynamic study have been performed for both transesterification and esterification reactions. For low acidity WCO, the kinetic calculations of overall transesterification reaction have been reported with reaction rate constant of 0.0006 s^{-1} at the optimum conditions. Activation energy and Arrhenius constant have been calculated as 4.05 s^{-1} and 50.5 kJ/mol , respectively. However, for high acid value WCO, the esterification reaction kinetics have developed a pseudo-first order reaction with reaction rate constant value of 0.00103 s^{-1} . Activation energy and Arrhenius constant have been calculated to be 34.5 kJ/mol and 2.48 s^{-1} , respectively.

The experimental results developed in this work have been used to design and simulate a biodiesel production process. The process reactor has been defined based on the optimal experimental conditions and the conversion has been evaluated based on the developed experimental kinetic data. Process energy and mass integration have been applied to optimise the process energy requirements.

The minimal required energies for the process have been achieved by designing an efficient HEN using graphical Pinch method.

7.2. Challenges and recommendations

The advantages and potentials of using supercritical technology for biodiesel production is enormous in comparison with the conventional catalysed processes in terms of higher biodiesel yield, simple separation and higher reaction rate. However, many limitations and challenges need to be solved before implementing the method in commercial scale. This section covers some recommendations for improving the process and enhancing its applicability and profitability.

7.2.1. Oxidation stability study

The implementation of harsh operational conditions in biodiesel production process *via* supercritical technology would have a direct effect on the oxidation stability of the produced biodiesel as it would enhance the polymerisation of the alkyl esters. It is highly recommended to perform an extensive study to compare the stability of biodiesel produced *via* supercritical methanolysis *versus* the conventional catalytic methods.

7.2.2. Extensive integrated processes

Biodiesel production using supercritical technologies require huge amount of energy for elevating both temperature and pressure to the critical point and maintaining these conditions throughout the reaction. The reaction product stream has massive energy that should be ideally utilised through process integration. Additionally, the energy of other process streams i.e. methanol recovered stream would be integrated.

On the other hand, most of the researches are only considering the mass and heat integration without considering work integration. In fact, the high-pressure reaction product stream could be integrated for work generation in addition to energy integration. Hence, simultaneous work-heat exchanger network (WHEN) synthesis is highly recommended for such application. This technology has been implemented in other applications between high and low pressure streams (Huang and Karimi, 2016). However, it has not yet been implemented in supercritical biodiesel production.

7.2.3. Two-steps reactions

Most of the studies have reported that the rate of supercritical hydrolysis and esterification is much higher than transesterification in addition they require milder conditions. Accordingly, two pathways for two-steps reactions should be implemented including esterification of FFAs followed by transesterification or hydrolysis of triglycerides to FFAs followed by esterification of FFAs. The second pathway has reported higher yield of biodiesel in shorter time and most importantly at lower conditions. This would perfectly suit low quality feedstocks with high FFAs contents. Additionally, most of the process simulations are focusing on the single-step transesterification/esterification. Hence, the focus should be shifted towards the two-steps where more process designs and techno-economic studies are highly recommended.

7.2.4. Glycerol-free biodiesel

Recently, many studies have reported glycerol-free biodiesel where the reaction includes oil with other chemicals than alcohols. Accordingly, other value-added by-products than glycerol are produced. These methods are very promising where studies should be focused toward this direction. Additionally, optimising these processes would ensure a sustainable route for biodiesel production.

7.2.5. Techno-economic analysis

There is a lack of economic analysis for the profitability of the process. The main factor that would enhance the investors for up-scaling the process is the profitability of the proposed method. Hence, extensive techno-economic studies should investigate the applicability of these processes for large scale implementation. The studies should focus on the recent energy integrated processes.

7.2.6. Thermal and storage stability study

There is a gap in the literature regarding the stability of either FAPes or FABEs. The optimal conditions for maximum production of both FAPes and FABEs have been reported at temperatures higher than 300 °C. This should be considered for further research including thermal stability. In addition, storage stability for most of the produced FAAs need to be considered as an important factor that could affect the efficiency of the product.

REFERENCES

References

- Abidin, S.Z., Haigh, K.F., Saha, B., 2012. Esterification of free fatty acids in used cooking oil using ion-exchange resins as catalysts: An efficient pretreatment method for biodiesel feedstock. *Ind. Eng. Chem. Res.* 51, 14653–14664. <https://doi.org/10.1021/ie3007566>
- Abidin, S.Z., Patel, D., Saha, B., 2013. Quantitative analysis of fatty acids composition in the used cooking oil (UCO) by gas chromatography-mass spectrometry (GC-MS). *Can. J. Chem. Eng.* 91, 1896–1903. <https://doi.org/10.1002/cjce.21848>
- Aboelazayem, O., El-Gendy, N.S., Abdel-Rehim, A.A., Ashour, F., Sadek, M.A., 2018. Biodiesel production from castor oil in Egypt: Process optimisation, kinetic study, diesel engine performance and exhaust emissions analysis. *Energy* 157, 843–852. <https://doi.org/10.1016/j.energy.2018.05.202>
- Aghbashlo, M., Hosseinpour, S., Tabatabaei, M., Dadak, A., 2017. Fuzzy modeling and optimization of the synthesis of biodiesel from waste cooking oil (WCO) by a low power, high frequency piezo-ultrasonic reactor. *Energy* 132, 65–78. <https://doi.org/10.1016/j.energy.2017.05.041>
- Alenezi, R., Leeke, G.A., Winterbottom, J.M., Santos, R.C.D., Khan, A.R., 2010. Esterification kinetics of free fatty acids with supercritical methanol for biodiesel production. *Energy Convers. Manag.* 51, 1055–1059. <https://doi.org/10.1016/j.enconman.2009.12.009>
- Ang, G.T., Tan, K.T., Lee, K.T., 2014. Recent development and economic analysis of glycerol-free processes via supercritical fluid transesterification for biodiesel production. *Renew. Sustain. Energy Rev.* 31, 61–70. <https://doi.org/10.1016/j.rser.2013.11.004>

- Avramidou, K. V., Zaccheria, F., Karakoulia, S.A., Triantafyllidis, K.S., Ravasio, N., 2017. Esterification of free fatty acids using acidic metal oxides and supported polyoxometalate (POM) catalysts. *Mol. Catal.* 439, 60–71. <https://doi.org/10.1016/j.mcat.2017.06.009>
- Awad, O.I., Mamat, R., Ibrahim, T.K., Hammid, A.T., Yusri, I.M., Hamidi, M.A., Humada, A.M., Yusop, A.F., 2018. Overview of the oxygenated fuels in spark ignition engine: Environmental and performance. *Renew. Sustain. Energy Rev.* 91, 394–408. <https://doi.org/10.1016/j.rser.2018.03.107>
- Azcan, N., Danisman, A., 2007. Alkali catalyzed transesterification of cottonseed oil by microwave irradiation. *Fuel* 86, 2639–2644. <https://doi.org/10.1016/j.fuel.2007.05.021>
- Banković-Ilić, I.B., Stamenković, O.S., Veljković, V.B., 2012. Biodiesel production from non-edible plant oils. *Renew. Sustain. Energy Rev.* 16, 3621–3647. <https://doi.org/10.1016/j.rser.2012.03.002>
- Bender, N., Staudt, P.B., Soares, R.P., Cardozo, N.S.M., 2013. Performance of predictive models in phase equilibria of complex associating systems: PC-SAFT and CEoS/GE. *Brazilian J. Chem. Eng.* 30, 75–82. <https://doi.org/10.1590/S0104-66322013000100009>
- Bi, Y., Zhou, H., Jia, H., Wei, P., 2017. A flow-through enzymatic microreactor immobilizing lipase based on layer-by-layer method for biosynthetic process: Catalyzing the transesterification of soybean oil for fatty acid methyl ester production. *Process Biochem.* 54, 73–80. <https://doi.org/10.1016/j.procbio.2016.12.008>
- Boffito, D.C., Galli, F., Pirola, C., Bianchi, C.L., Patience, G.S., 2014. Ultrasonic free fatty acids esterification in tobacco and canola oil. *Ultrason. Sonochem.* 21, 1969–1975. <https://doi.org/10.1016/j.ultsonch.2014.01.026>

- Boon-anuwat, N. nan, Kiatkittipong, W., Aiouache, F., Assabumrungrat, S., 2015. Process design of continuous biodiesel production by reactive distillation: Comparison between homogeneous and heterogeneous catalysts. *Chem. Eng. Process. Process Intensif.* 92, 33–44. <https://doi.org/10.1016/j.cep.2015.03.025>
- Budiman Abdurakhman, Y., Adi Putra, Z., Bilad, M.R., Md Nordin, N.A.H., Wirzal, M.D.H., 2018. Techno-economic analysis of biodiesel production process from waste cooking oil using catalytic membrane reactor and realistic feed composition. *Chem. Eng. Res. Des.* 134, 564–574. <https://doi.org/10.1016/j.cherd.2018.04.044>
- Budžaki, S., Miljić, G., Tišma, M., Sundaram, S., Hessel, V., 2017. Is there a future for enzymatic biodiesel industrial production in microreactors? *Appl. Energy* 201, 124–134. <https://doi.org/10.1016/j.apenergy.2017.05.062>
- Chen, Y.H., Huang, Y.H., Lin, R.H., Shang, N.C., 2010. A continuous-flow biodiesel production process using a rotating packed bed. *Bioresour. Technol.* 101, 668–673. <https://doi.org/10.1016/j.biortech.2009.08.081>
- Choedkiatsakul, I., Ngaosuwan, K., Assabumrungrat, S., Mantegna, S., Cravotto, G., 2015a. Biodiesel production in a novel continuous flow microwave reactor. *Renew. Energy* 83, 25–29. <https://doi.org/10.1016/j.renene.2015.04.012>
- Choedkiatsakul, I., Ngaosuwan, K., Assabumrungrat, S., Tabasso, S., Cravotto, G., 2015b. Integrated flow reactor that combines high-shear mixing and microwave irradiation for biodiesel production. *Biomass and Bioenergy* 77, 186–191. <https://doi.org/10.1016/j.biombioe.2015.03.013>
- Ciftci, O.N., Temelli, F., 2013. Enzymatic conversion of corn oil into biodiesel in a batch supercritical carbon dioxide reactor and kinetic modeling. *J. Supercrit. Fluids* 75, 172–180. <https://doi.org/10.1016/j.supflu.2012.12.029>

- Conover, W., 2009. Chemistry, 8th Edition (by Stephen S. Zumdahl and Susan A. Zumdahl), Journal of Chemical Education.
<https://doi.org/10.1021/ed086p1273>
- Cotabarren, N., Hegel, P., Pereda, S., 2014. Thermodynamic model for process design, simulation and optimization in the production of biodiesel. Fluid Phase Equilib. 362, 108–112. <https://doi.org/10.1016/j.fluid.2013.09.019>
- Coutinho, J.A.P., Pillot, D., Tschamber, V., Clavier, J.-Y., Mokbel, I., Sergent, M., Coniglio, L., Jolibert, F., Pons, M.-N., Jose, J., 2014. Biodiesel via supercritical ethanolysis within a global analysis “feedstocks-conversion-engine” for a sustainable fuel alternative. Prog. Energy Combust. Sci. 43, 1–35. <https://doi.org/10.1016/j.peecs.2014.03.001>
- Cui, Y., Liang, Y., 2014. Direct transesterification of wet *Cryptococcus curvatus* cells to biodiesel through use of microwave irradiation. Appl. Energy 119, 438–444. <https://doi.org/10.1016/j.apenergy.2014.01.016>
- de Jesus, A.A., de Santana Souza, D.F., de Oliveira, J.A., de Deus, M.S., da Silva, M.G., Franceschi, E., da Silva Egues, S.M., Dariva, C., 2018. Mathematical modeling and experimental esterification at supercritical conditions for biodiesel production in a tubular reactor. Energy Convers. Manag. 171, 1697–1703. <https://doi.org/10.1016/j.enconman.2018.06.108>
- De Meyer, F.J.M., Venturoli, M., Smit, B., 2008. Molecular simulations of lipid-mediated protein-protein interactions, Biophysical Journal.
<https://doi.org/10.1529/biophysj.107.124164>
- de Paula Amaral do Valle, P.W., Fortes, I.C.P., Pasa, V.M.D., 2016. A systematic multivariate analysis of the supercritical synthesis of soy biodiesel using 92.8% w/w hydrated ethanol. Biomass and Bioenergy 91, 17–25.
<https://doi.org/10.1016/j.biombioe.2016.03.036>

- Dehghani Kiadehi, A., Ebadi, A., Aghaeinejad-Meybodi, A., 2017. Removal of methyl tert-butyl ether (MTBE) from aqueous medium in the presence of nano-perfluorooctyl alumina (PFOAL): Experimental study of adsorption and catalytic ozonation processes. *Sep. Purif. Technol.* 182, 238–246.
<https://doi.org/10.1016/j.seppur.2017.03.039>
- Demirbas, A., 2009. Biodiesel from waste cooking oil via base-catalytic and supercritical methanol transesterification. *Energy Convers. Manag.* 50, 923–927. <https://doi.org/10.1016/j.enconman.2008.12.023>
- dos Santos, P.R.S., Voll, F.A.P., Ramos, L.P., Corazza, M.L., 2017. Esterification of fatty acids with supercritical ethanol in a continuous tubular reactor. *J. Supercrit. Fluids* 126, 25–36. <https://doi.org/10.1016/j.supflu.2017.03.002>
- El-Gendy, N.S., Deriase, S.F., Hamdy, A., 2014. The optimization of biodiesel production from waste frying corn oil using snails shells as a catalyst. *Energy Sources, Part A Recover. Util. Environ. Eff.* 36, 623–637.
<https://doi.org/10.1080/15567036.2013.822440>
- El-Gendy, N.S., El-Gharabawy, A.A.S.A., Abu Amr, S.S., Ashour, F.H., 2015. Response surface optimization of an alkaline transesterification of waste cooking oil. *Int. J. ChemTech Res.* 8, 385–398.
- El-Halwagi, M.M., 2011. Mathematical Techniques for the Synthesis of Heat-Exchange Networks. *Sustain. Des. Through Process Integr.* 345–356.
<https://doi.org/10.1016/b978-1-85617-744-3.00019-9>
- Esteban, J., Vorholt, A.J., 2018. Obtaining glycerol carbonate and glycols using thermomorphic systems based on glycerol and cyclic organic carbonates: Kinetic studies. *J. Ind. Eng. Chem.* 63, 124–132.
<https://doi.org/10.1016/j.jiec.2018.02.008>

- Farobie, O., Leow, Z.Y.M., Samanmulya, T., Matsumura, Y., 2017. In-depth study of continuous production of biodiesel using supercritical 1-butanol. *Energy Convers. Manag.* 132, 410–417. <https://doi.org/10.1016/j.enconman.2016.09.042>
- Farobie, O., Leow, Z.Y.M., Samanmulya, T., Matsumura, Y., 2016. New insights in biodiesel production using supercritical 1-propanol. *Energy Convers. Manag.* 124, 212–218. <https://doi.org/10.1016/j.enconman.2016.07.021>
- Farobie, O., Matsumura, Y., 2017a. State of the art of biodiesel production under supercritical conditions. *Prog. Energy Combust. Sci.* 63, 173–203. <https://doi.org/10.1016/j.pecs.2017.08.001>
- Farobie, O., Matsumura, Y., 2017b. Continuous production of biodiesel under supercritical methyl acetate conditions: Experimental investigation and kinetic model. *Bioresour. Technol.* 241, 720–725. <https://doi.org/10.1016/j.biortech.2017.05.210>
- Farobie, O., Matsumura, Y., 2015. A comparative study of biodiesel production using methanol, ethanol, and tert-butyl methyl ether (MTBE) under supercritical conditions. *Bioresour. Technol.* 191, 306–311. <https://doi.org/10.1016/j.biortech.2015.04.102>
- Farobie, O., Sasanami, K., Matsumura, Y., 2015. A novel spiral reactor for biodiesel production in supercritical ethanol. *Appl. Energy* 147, 20–29. <https://doi.org/10.1016/j.apenergy.2015.02.033>
- Farobie, O., Yanagida, T., Matsumura, Y., 2014. New approach of catalyst-free biodiesel production from canola oil in supercritical tert-butyl methyl ether (MTBE). *Fuel* 135, 172–181. <https://doi.org/10.1016/j.fuel.2014.06.049>
- Farrag, N.M., Gadalla, M.A., Fouad, M.K., 2016. Reaction parameters and energy optimisation for biodiesel production using a supercritical process. *Chem. Eng. Trans.* 52, 1207–1212. <https://doi.org/10.3303/CET1652202>

- Filho, R.M., Da Silva, N.D.L., Maciel, M.R.W., Garnica, J.A.G., Batistella, C.B., 2010. Use of experimental design to investigate biodiesel production by multiple-stage Ultra-Shear reactor. *Bioresour. Technol.* 102, 2672–2677. <https://doi.org/10.1016/j.biortech.2010.10.136>
- Fu, Q., Song, C., Kansha, Y., Liu, Y., Ishizuka, M., Tsutsumi, A., 2015. Energy saving in a biodiesel production process based on self-heat recuperation technology. *Chem. Eng. J.* 278, 556–562. <https://doi.org/10.1016/j.cej.2014.11.027>
- Gadalla, M.A., 2015a. A novel graphical technique for Pinch Analysis applications: Energy Targets and grassroots design. *Energy Convers. Manag.* 96, 499–510. <https://doi.org/10.1016/j.enconman.2015.02.079>
- Gadalla, M.A., 2015b. A new graphical method for Pinch Analysis applications: Heat exchanger network retrofit and energy integration. *Energy* 81, 159–174. <https://doi.org/10.1016/j.energy.2014.12.011>
- Gadalla, M.A., 2015c. A new graphical-based approach for mass integration and exchange network design. *Chem. Eng. Sci.* 127, 239–252. <https://doi.org/10.1016/j.ces.2015.01.036>
- García-Martínez, N., Andreo-Martínez, P., Quesada-Medina, J., de los Ríos, A.P., Chica, A., Beneito-Ruiz, R., Carratalá-Abril, J., 2017. Optimization of non-catalytic transesterification of tobacco (*Nicotiana tabacum*) seed oil using supercritical methanol to biodiesel production. *Energy Convers. Manag.* 131, 99–108. <https://doi.org/10.1016/j.enconman.2016.10.078>
- Garlapati, V.K., Shankar, U., Budhiraja, A., 2016. Bioconversion technologies of crude glycerol to value added industrial products. *Biotechnol. Reports* 9, 9–14. <https://doi.org/10.1016/j.btre.2015.11.002>
- Gerpen, J. Van, 2005. Biodiesel processing and production. *Fuel Process. Technol.* 86, 1097–1107. <https://doi.org/10.1016/j.fuproc.2004.11.005>

- Ghoreishi, S.M., Mooin, P., 2013. Biodiesel synthesis from waste vegetable oil via transesterification reaction in supercritical methanol. *J. Supercrit. Fluids* 76, 24–31. <https://doi.org/10.1016/j.supflu.2013.01.011>
- Goembira, F., Saka, S., 2015. Advanced supercritical Methyl acetate method for biodiesel production from *Pongamia pinnata* oil. *Renew. Energy* 83, 1245–1249. <https://doi.org/10.1016/j.renene.2015.06.022>
- Goembira, F., Saka, S., 2014. Effect of additives to supercritical methyl acetate on biodiesel production. *Fuel Process. Technol.* 125, 114–118. <https://doi.org/10.1016/j.fuproc.2014.03.035>
- Goembira, F., Saka, S., 2013. Optimization of biodiesel production by supercritical methyl acetate. *Bioresour. Technol.* 131, 47–52. <https://doi.org/10.1016/j.biortech.2012.12.130>
- Granjo, J.F.O., Duarte, B.P.M., Oliveira, N.M.C., 2017. Integrated production of biodiesel in a soybean biorefinery: Modeling, simulation and economical assessment. *Energy* 129, 273–291. <https://doi.org/10.1016/j.energy.2017.03.167>
- Grossmann, I.E., Čuček, L., Maréchal, F., Ibrić, N., Kravanja, Z., Ahmetović, E., Kermani, M., 2018. Simultaneous optimisation and heat integration of evaporation systems including mechanical vapour recompression and background process. *Energy* 158, 1160–1191. <https://doi.org/10.1016/j.energy.2018.06.046>
- Gui, M.M., Lee, K.T., Bhatia, S., 2009. Supercritical ethanol technology for the production of biodiesel: Process optimization studies. *J. Supercrit. Fluids* 49, 286–292. <https://doi.org/10.1016/j.supflu.2008.12.014>
- Gui, M.M., Lee, K.T., Bhatia, S., 2008. Feasibility of edible oil vs. non-edible oil vs. waste edible oil as biodiesel feedstock. *Energy* 33, 1646–1653. <https://doi.org/10.1016/j.energy.2008.06.002>

- Gutiérrez, L.F., Sánchez, Ó.J., Cardona, C.A., 2009. Process integration possibilities for biodiesel production from palm oil using ethanol obtained from lignocellulosic residues of oil palm industry. *Bioresour. Technol.* 100, 1227–1237. <https://doi.org/10.1016/j.biortech.2008.09.001>
- Gutiérrez Ortiz, F.J., de Santa-Ana, P., 2017. Techno-economic assessment of an energy self-sufficient process to produce biodiesel under supercritical conditions. *J. Supercrit. Fluids* 128, 349–358. <https://doi.org/10.1016/j.supflu.2017.03.010>
- Haigh, K.F., Abidin, S.Z., Vladisavljević, G.T., Saha, B., 2013. Comparison of Novozyme 435 and Purolite D5081 as heterogeneous catalysts for the pretreatment of used cooking oil for biodiesel production. *Fuel* 111, 186–193. <https://doi.org/10.1016/j.fuel.2013.04.056>
- Hajjari, M., Tabatabaei, M., Aghbashlo, M., Ghanavati, H., 2017. A review on the prospects of sustainable biodiesel production: A global scenario with an emphasis on waste-oil biodiesel utilization. *Renew. Sustain. Energy Rev.* 72, 445–464. <https://doi.org/10.1016/j.rser.2017.01.034>
- Han, H., Cao, W., Zhang, J., 2005. Preparation of biodiesel from soybean oil using supercritical methanol and CO₂ as co-solvent. *Process Biochem.* 40, 3148–3151. <https://doi.org/10.1016/j.procbio.2005.03.014>
- Hasan, M.M., Rahman, M.M., 2017. Performance and emission characteristics of biodiesel–diesel blend and environmental and economic impacts of biodiesel production: A review. *Renew. Sustain. Energy Rev.* 74, 938–948. <https://doi.org/10.1016/j.rser.2017.03.045>
- He, H., Wang, T., Zhu, S., 2007. Continuous production of biodiesel fuel from vegetable oil using supercritical methanol process. *Fuel* 86, 442–447. <https://doi.org/10.1016/j.fuel.2006.07.035>

- Hegel, P., Andreatta, A., Pereda, S., Bottini, S., Brignole, E.A., 2008. High pressure phase equilibria of supercritical alcohols with triglycerides, fatty esters and cosolvents. *Fluid Phase Equilib.* 266, 31–37.
<https://doi.org/10.1016/j.fluid.2008.01.016>
- Hernando, J., Leton, P., Matia, M.P., Novella, J.L., Alvarez-Builla, J., 2007. Biodiesel and FAME synthesis assisted by microwaves: Homogeneous batch and flow processes. *Fuel* 86, 1641–1644.
<https://doi.org/10.1016/j.fuel.2006.11.003>
- Hinkelmann, K., 2012. *Design and Analysis of Experiments, Design and Analysis of Experiments*, Wiley Series in Probability and Statistics. John Wiley & Sons, Inc., Hoboken, NJ, USA. <https://doi.org/10.1002/9781118147634>
- Hong, I.K., Jeon, H., Kim, H., Lee, S.B., 2016. Preparation of waste cooking oil based biodiesel using microwave irradiation energy. *J. Ind. Eng. Chem.* 42, 107–112. <https://doi.org/10.1016/j.jiec.2016.07.035>
- Hoseini, S.S., Najafi, G., Ghobadian, B., Mamat, R., Ebadi, M.T., Yusaf, T., 2018. *Ailanthus altissima* (tree of heaven) seed oil: Characterisation and optimisation of ultrasonication-assisted biodiesel production. *Fuel* 220, 621–630. <https://doi.org/10.1016/j.fuel.2018.01.094>
- Huang, K., Karimi, I.A., 2016. Work-heat exchanger network synthesis (WHENS). *Energy* 113, 1006–1017. <https://doi.org/10.1016/j.energy.2016.07.124>
- Ilham, Z., Saka, S., 2012. Optimization of supercritical dimethyl carbonate method for biodiesel production. *Fuel* 97, 670–677.
<https://doi.org/10.1016/j.fuel.2012.02.066>
- Ilham, Z., Saka, S., 2010. Two-step supercritical dimethyl carbonate method for biodiesel production from *Jatropha curcas* oil. *Bioresour. Technol.* 101, 2735–2740. <https://doi.org/10.1016/j.biortech.2009.10.053>

- Ilham, Z., Saka, S., 2009. Dimethyl carbonate as potential reactant in non-catalytic biodiesel production by supercritical method. *Bioresour. Technol.* 100, 1793–1796. <https://doi.org/10.1016/j.biortech.2008.09.050>
- Imahara, H., Minami, E., Hari, S., Saka, S., 2008. Thermal stability of biodiesel in supercritical methanol. *Fuel* 87, 1–6. <https://doi.org/10.1016/j.fuel.2007.04.003>
- Jaliliannosrati, H., Amin, N.A.S., Talebian-Kiakalaieh, A., Noshadi, I., 2013. Microwave assisted biodiesel production from *Jatropha curcas* L. seed by two-step in situ process: Optimization using response surface methodology. *Bioresour. Technol.* 136, 565–573. <https://doi.org/10.1016/j.biortech.2013.02.078>
- Jazzar, S., Olivares-Carrillo, P., Pérez de los Ríos, A., Marzouki, M.N., Ación-Fernández, F.G., Fernández-Sevilla, J.M., Molina-Grima, E., Smaali, I., Quesada-Medina, J., 2015. Direct supercritical methanolysis of wet and dry unwashed marine microalgae (*Nannochloropsis gaditana*) to biodiesel. *Appl. Energy* 148, 210–219. <https://doi.org/10.1016/j.apenergy.2015.03.069>
- Jin, T., Wang, B., Zeng, J., Yang, C., Wang, Y., Fang, T., 2015. Esterification of free fatty acids with supercritical methanol for biodiesel production and related kinetic study. *RSC Adv.* 5, 52072–52078. <https://doi.org/10.1039/c5ra03709c>
- Jookjantra, K., Wongwuttanasatian, T., 2017. Optimisation of biodiesel production from refined palm oil with heterogeneous CaO catalyst using pulse ultrasonic waves under a vacuum condition. *Energy Convers. Manag.* 154, 1–10. <https://doi.org/10.1016/j.enconman.2017.10.050>
- Khajeh, M., 2009. Optimization of microwave-assisted extraction procedure for zinc and copper determination in food samples by Box-Behnken design. *J. Food Compos. Anal.* 22, 343–346. <https://doi.org/10.1016/j.jfca.2008.11.017>

- Kim, D., Choi, J., Kim, G.J., Seol, S.K., Jung, S., 2011. Accelerated esterification of free fatty acid using pulsed microwaves. *Bioresour. Technol.* 102, 7229–7231. <https://doi.org/10.1016/j.biortech.2011.04.074>
- Klemeš, J.J., 2013. Handbook of Process Integration (PI), Handbook of Process Integration (PI). Woodhead Publishing Limited. <https://doi.org/10.1533/9780857097255>
- Klemeš, J.J., Kravanja, Z., 2013. Forty years of Heat Integration: Pinch Analysis (PA) and Mathematical Programming (MP). *Curr. Opin. Chem. Eng.* 2, 461–474. <https://doi.org/10.1016/j.coche.2013.10.003>
- Knothe, G., Razon, L.F., 2017. Biodiesel fuels. *Prog. Energy Combust. Sci.* 58, 36–59. <https://doi.org/10.1016/j.pecs.2016.08.001>
- Kostić, M.D., Veličković, A. V., Joković, N.M., Stamenković, O.S., Veljković, V.B., 2016. Optimization and kinetic modeling of esterification of the oil obtained from waste plum stones as a pretreatment step in biodiesel production. *Waste Manag.* 48, 619–629. <https://doi.org/10.1016/j.wasman.2015.11.052>
- Kumar, G., 2017. Ultrasonic-assisted reactive-extraction is a fast and easy method for biodiesel production from *Jatropha curcas* oilseeds. *Ultrason. Sonochem.* 37, 634–639. <https://doi.org/10.1016/j.ultsonch.2017.02.018>
- Kumar, G., Singh, V., Kumar, D., 2017. Ultrasonic-assisted continuous methanolysis of *Jatropha curcas* oil in the appearance of biodiesel used as an intermediate solvent. *Ultrason. Sonochem.* 39, 384–391. <https://doi.org/10.1016/j.ultsonch.2017.05.002>
- Kumar, M., Sharma, M.P., 2016. Selection of potential oils for biodiesel production. *Renew. Sustain. Energy Rev.* <https://doi.org/10.1016/j.rser.2015.12.032>

- Kurniawan, A., Ong, L., Lin, C., Zhao, X., Ismadji, S., 2012. Catalyst-free biodiesel production: Transesterification of jatropha oil using supercritical methanol. *Chemeca 2012 Qual. life through Chem. Eng.* 23-26 Sept. 2012, Wellington, New Zeal. 832.
- Kurniawan, W., Hidayat, A., Hinode, H., Rochmadi, Budiman, A., Yoshikawa, K., Wijaya, K., Nurdiawati, A., 2015. Esterification of Palm Fatty Acid Distillate with High Amount of Free Fatty Acids Using Coconut Shell Char Based Catalyst. *Energy Procedia* 75, 969–974.
<https://doi.org/10.1016/j.egypro.2015.07.301>
- Kusdiana, D., Saka, S., 2004. Effects of water on biodiesel fuel production by supercritical methanol treatment. *Bioresour. Technol.* 91, 289–295.
[https://doi.org/10.1016/S0960-8524\(03\)00201-3](https://doi.org/10.1016/S0960-8524(03)00201-3)
- Kusdiana, D., Saka, S., 2001. Kinetics of transesterification in rapeseed oil to biodiesel fuel as treated in supercritical methanol. *Fuel* 80, 693–698.
[https://doi.org/10.1016/S0016-2361\(00\)00140-X](https://doi.org/10.1016/S0016-2361(00)00140-X)
- Lamba, N., Modak, J.M., Madras, G., 2017. Fatty acid methyl esters synthesis from non-edible vegetable oils using supercritical methanol and methyl tert-butyl ether. *Energy Convers. Manag.* 138, 77–83.
<https://doi.org/10.1016/j.enconman.2017.02.001>
- Lee, K.T., Lim, S., Pang, Y.L., Ong, H.C., Chong, W.T., 2014. Integration of reactive extraction with supercritical fluids for process intensification of biodiesel production: Prospects and recent advances. *Prog. Energy Combust. Sci.* 45, 54–78. <https://doi.org/10.1016/j.pecs.2014.07.001>
- Lee, K.T., Tan, K.T., Ooi, S.N., Mohamed, A.R., Ang, G.T., 2015. Optimization and kinetic studies of sea mango (*Cerbera odollam*) oil for biodiesel production via supercritical reaction. *Energy Convers. Manag.* 99, 242–251.
<https://doi.org/10.1016/j.enconman.2015.04.037>

- Lee, S., Posarac, D., Ellis, N., 2011. Process simulation and economic analysis of biodiesel production processes using fresh and waste vegetable oil and supercritical methanol. *Chem. Eng. Res. Des.* 89, 2626–2642. <https://doi.org/10.1016/j.cherd.2011.05.011>
- Lertsathapornsuk, V., Pairintra, R., Aryasuk, K., Krisnangkura, K., 2008. Microwave assisted in continuous biodiesel production from waste frying palm oil and its performance in a 100 kW diesel generator. *Fuel Process. Technol.* 89, 1330–1336. <https://doi.org/10.1016/j.fuproc.2008.05.024>
- Leung, D.Y.C., Wu, X., Leung, M.K.H., 2010. A review on biodiesel production using catalyzed transesterification. *Appl. Energy* 87, 1083–1095. <https://doi.org/10.1016/j.apenergy.2009.10.006>
- Levchuk, I., Bhatnagar, A., Sillanpää, M., 2014. Overview of technologies for removal of methyl tert-butyl ether (MTBE) from water. *Sci. Total Environ.* 476–477, 415–433. <https://doi.org/10.1016/j.scitotenv.2014.01.037>
- Li, L., Wang, X., Song, C., Ding, H., Liu, D., Ye, W., Gui, J., Wang, Y., Ji, N., 2017. Process intensification of transesterification for biodiesel production from palm oil: Microwave irradiation on transesterification reaction catalyzed by acidic imidazolium ionic liquids. *Energy* 144, 957–967. <https://doi.org/10.1016/j.energy.2017.12.072>
- Lin, J.J., Chen, Y.W., 2017. Production of biodiesel by transesterification of *Jatropha* oil with microwave heating. *J. Taiwan Inst. Chem. Eng.* 75, 43–50. <https://doi.org/10.1016/j.jtice.2017.03.034>
- Linnhoff, B., Hindmarsh, E., 1983. The pinch design method for heat exchanger networks. *Chem. Eng. Sci.* 38, 745–763. [https://doi.org/10.1016/0009-2509\(83\)80185-7](https://doi.org/10.1016/0009-2509(83)80185-7)
- Liu, J., Cao, X., Chu, Y., Zhao, Y., Wu, P., Xue, S., 2018. Novel approach for the direct transesterification of fresh microalgal cells via micro-reactor. *Algal Res.* 32, 38–43. <https://doi.org/10.1016/j.algal.2018.03.008>

- Liu, J., He, D., 2018. Transformation of CO₂ with glycerol to glycerol carbonate by a novel ZnWO₄-ZnO catalyst. *J. CO₂ Util.* 26, 370–379.
<https://doi.org/10.1016/j.jcou.2018.05.025>
- Liu, X., He, H., Wang, Y., Zhu, S., Piao, X., 2008. Transesterification of soybean oil to biodiesel using CaO as a solid base catalyst. *Fuel* 87, 216–221.
<https://doi.org/10.1016/j.fuel.2007.04.013>
- Lokman, I.M., Goto, M., Rashid, U., Taufiq-Yap, Y.H., 2016. Sub- and supercritical esterification of palm fatty acid distillate with carbohydrate-derived solid acid catalyst. *Chem. Eng. J.* 284, 872–878.
<https://doi.org/10.1016/j.cej.2015.08.102>
- Luo, X., Ge, X., Cui, S., Li, Y., 2016. Value-added processing of crude glycerol into chemicals and polymers. *Bioresour. Technol.* 215, 144–154.
<https://doi.org/10.1016/j.biortech.2016.03.042>
- Ma, F., Clements, L.D., Hanna, M.A., 1999. The effect of mixing on transesterification of beef tallow. *Bioresour. Technol.* 69, 289–293.
[https://doi.org/10.1016/S0960-8524\(98\)00184-9](https://doi.org/10.1016/S0960-8524(98)00184-9)
- Ma, J., Xiong, D., Li, H., Ding, Y., Xia, X., Yang, Y., 2017. Vapor intrusion risk of fuel ether oxygenates methyl tert-butyl ether (MTBE), tert-amyl methyl ether (TAME) and ethyl tert-butyl ether (ETBE): A modeling study. *J. Hazard. Mater.* 332, 10–18. <https://doi.org/10.1016/j.jhazmat.2017.02.057>
- Magdouli, S., Guedri, T., Tarek, R., Brar, S.K., Blais, J.F., 2017. Valorization of raw glycerol and crustacean waste into value added products by *Yarrowia lipolytica*. *Bioresour. Technol.* 243, 57–68.
<https://doi.org/10.1016/j.biortech.2017.06.074>
- Man, X., Tang, C., Zhang, J., Zhang, Y., Pan, L., Huang, Z., Law, C.K., 2014. An experimental and kinetic modeling study of n-propanol and i-propanol ignition at high temperatures. *Combust. Flame* 161, 644–656.
<https://doi.org/10.1016/j.combustflame.2013.08.003>

- Manco, I., Giordani, L., Vaccari, V., Oddone, M., 2012. Microwave technology for the biodiesel production: Analytical assessments. *Fuel* 95, 108–112.
<https://doi.org/10.1016/j.fuel.2011.09.047>
- Manuale, D.L., Torres, G.C., Vera, C.R., Yori, J.C., 2015. Study of an energy-integrated biodiesel production process using supercritical methanol and a low-cost feedstock. *Fuel Process. Technol.* 140, 252–261.
<https://doi.org/10.1016/j.fuproc.2015.08.026>
- Mardhiah, H.H., Ong, H.C., Masjuki, H.H., Lim, S., Lee, H.V., 2017. A review on latest developments and future prospects of heterogeneous catalyst in biodiesel production from non-edible oils. *Renew. Sustain. Energy Rev.* 67, 1225–1236. <https://doi.org/10.1016/j.rser.2016.09.036>
- Martin, S., Albrecht, F.G., Van Der Veer, P., Lieftink, D., Dietrich, R.U., 2016. Evaluation of on-site hydrogen generation via steam reforming of biodiesel: Process optimization and heat integration. *Int. J. Hydrogen Energy* 41, 6640–6652. <https://doi.org/10.1016/j.ijhydene.2016.02.138>
- Martinovic, F.L., Kiss, F.E., Micic, R.D., Simikić, M., Tomić, M.D., 2018. Comparative techno-economic analysis of single-step and two-step biodiesel production with supercritical methanol based on process simulation. *Chem. Eng. Res. Des.* 132, 751–765. <https://doi.org/10.1016/j.cherd.2018.02.024>
- Marulanda, V.F., 2012. Biodiesel production by supercritical methanol transesterification: Process simulation and potential environmental impact assessment. *J. Clean. Prod.* 33, 109–116.
<https://doi.org/10.1016/j.jclepro.2012.04.022>
- Mazzocchia, C., Modica, G., Kaddouri, A., Nannicini, R., 2004. Fatty acid methyl esters synthesis from triglycerides over heterogeneous catalysts in the presence of microwaves. *Comptes Rendus Chim.* 7, 601–605.
<https://doi.org/10.1016/j.crci.2003.12.004>

- Micic, R.D., Tomić, M.D., Kiss, F.E., Martinovic, F.L., Simikić, M., Molnar, T.T., 2016. Comparative analysis of single-step and two-step biodiesel production using supercritical methanol on laboratory-scale. *Energy Convers. Manag.* 124, 377–388. <https://doi.org/10.1016/j.enconman.2016.07.043>
- Mostafaei, M., Ghobadian, B., Barzegar, M., Banakar, A., 2015. Optimization of ultrasonic assisted continuous production of biodiesel using response surface methodology. *Ultrason. Sonochem.* 27, 54–61. <https://doi.org/10.1016/j.ultsonch.2015.04.036>
- Motasemi, F., Ani, F.N., 2012. A review on microwave-assisted production of biodiesel. *Renew. Sustain. Energy Rev.* 16, 4719–4733. <https://doi.org/10.1016/j.rser.2012.03.069>
- Muthukumar, C., Praniash, R., Navamani, P., Swathi, R., Sharmila, G., Manoj Kumar, N., 2017a. Process optimization and kinetic modeling of biodiesel production using non-edible *Madhuca indica* oil. *Fuel* 195, 217–225. <https://doi.org/10.1016/j.fuel.2017.01.060>
- Muthukumar, C., Praniash, R., Navamani, P., Swathi, R., Sharmila, G., Manoj Kumar, N., 2017b. Process optimization and kinetic modeling of biodiesel production using non-edible *Madhuca indica* oil. *Fuel* 195, 217–225. <https://doi.org/10.1016/j.fuel.2017.01.060>
- Narayan, R.C., Madras, G., 2017. Esterification of Sebacic Acid in Near-Critical and Supercritical Methanol. *Ind. Eng. Chem. Res.* 56, 2641–2649. <https://doi.org/10.1021/acs.iecr.6b04769>
- Nikhom, R., Petchkaew, A., Iewkittayakorn, J., Prasertsit, K., Mueanmas, C., 2018. Extraction and esterification of waste coffee grounds oil as non-edible feedstock for biodiesel production. *Renew. Energy* 133, 1414–1425. <https://doi.org/10.1016/j.renene.2018.08.102>

- Niza, N.M., Tan, K.T., Lee, K.T., Ahmad, Z., 2013. Biodiesel production by non-catalytic supercritical methyl acetate: Thermal stability study. *Appl. Energy* 101, 198–202. <https://doi.org/10.1016/j.apenergy.2012.03.033>
- Noureddini, H., Harkey, D., Medikonduru, V., 1998. A continuous process for the conversion of vegetable oils into methyl esters of fatty acids. *JAOCs, J. Am. Oil Chem. Soc.* 75, 1775–1783. <https://doi.org/10.1007/s11746-998-0331-1>
- Nur Syazwani, O., Lokman Ibrahim, M., Wahyudiono, Kanda, H., Goto, M., Taufiq-Yap, Y.H., 2017. Esterification of high free fatty acids in supercritical methanol using sulfated angel wing shells as catalyst. *J. Supercrit. Fluids* 124, 1–9. <https://doi.org/10.1016/j.supflu.2017.01.002>
- Ong, L.K., Kurniawan, A., Suwandi, A.C., Lin, C.X., Zhao, X.S., Ismadji, S., 2013. Transesterification of leather tanning waste to biodiesel at supercritical condition: Kinetics and thermodynamics studies. *J. Supercrit. Fluids* 75, 11–20. <https://doi.org/10.1016/j.supflu.2012.12.018>
- Patil, P., Deng, S., Isaac Rhodes, J., Lammers, P.J., 2010. Conversion of waste cooking oil to biodiesel using ferric sulfate and supercritical methanol processes. *Fuel* 89, 360–364. <https://doi.org/10.1016/j.fuel.2009.05.024>
- Petchsoongsakul, N., Ngaosuwan, K., Kiatkittipong, W., Aiouache, F., Assabumrungrat, S., 2017. Process design of biodiesel production: Hybridization of ester-and transesterification in a single reactive distillation. *Energy Convers. Manag.* 153, 493–503. <https://doi.org/10.1016/j.enconman.2017.10.013>
- Plazas-González, M., Guerrero-Fajardo, C.A., Sodr e, J.R., 2018. Modelling and simulation of hydrotreating of palm oil components to obtain green diesel. *J. Clean. Prod.* 184, 301–308. <https://doi.org/10.1016/j.jclepro.2018.02.275>

- Ponnusamy, S., Dailey, P., Muppaneni, T., Deng, S., Reddy, H.K., Patil, P.D., Sun, Y., 2012. Optimization of biodiesel production from palm oil under supercritical ethanol conditions using hexane as co-solvent: A response surface methodology approach. *Fuel* 107, 633–640.
<https://doi.org/10.1016/j.fuel.2012.11.046>
- Ponnusamy, S., Li, C., Patil, P.D., Sun, Y., Deng, S., Jiang, L., Muppaneni, T., Reddy, H.K., 2014. Optimization of high-energy density biodiesel production from camelina sativa oil under supercritical 1-butanol conditions. *Fuel* 135, 522–529. <https://doi.org/10.1016/j.fuel.2014.06.072>
- Priyadarshi, D., Paul, K.K., 2018. Single phase blend: An advanced microwave process for improved quality low-cost biodiesel production from kitchen food waste. *Biochem. Eng. J.* 137, 273–283.
<https://doi.org/10.1016/j.bej.2018.06.006>
- Qiao, B.-Q., Zhou, D., Li, G., Yin, J.-Z., Xue, S., Liu, J., 2017. Process enhancement of supercritical methanol biodiesel production by packing beds. *Bioresour. Technol.* 228, 298–304.
<https://doi.org/10.1016/j.biortech.2016.12.085>
- Qin, M., Yuan, J., Xie, G., Tong, J., Wu, G., Huang, J., Duan, J., 2015. Multiple responses optimization of ultrasonic-assisted extraction by response surface methodology (RSM) for rapid analysis of bioactive compounds in the flower head of *Chrysanthemum morifolium* Ramat. *Ind. Crops Prod.* 74, 192–199.
<https://doi.org/10.1016/j.indcrop.2015.04.057>
- Quitain, A.T., Mission, E.G., Sumigawa, Y., Sasaki, M., 2018. Supercritical carbon dioxide-mediated esterification in a microfluidic reactor. *Chem. Eng. Process. - Process Intensif.* 123, 168–173.
<https://doi.org/10.1016/j.cep.2017.11.002>

- Rade, L.L., Arvelos, S., De Souza Barrozo, M.A., Romanielo, L.L., Watanabe, E.O., Hori, C.E., 2015a. Evaluation of the use of degummed soybean oil and supercritical ethanol for non-catalytic biodiesel production. *J. Supercrit. Fluids* 105, 21–28. <https://doi.org/10.1016/j.supflu.2015.05.017>
- Rade, L.L., Arvelos, S., De Souza Barrozo, M.A., Romanielo, L.L., Watanabe, E.O., Hori, C.E., 2015b. Evaluation of the use of degummed soybean oil and supercritical ethanol for non-catalytic biodiesel production. *J. Supercrit. Fluids* 105, 21–28. <https://doi.org/10.1016/j.supflu.2015.05.017>
- Ramachandran, K., Suganya, T., Nagendra Gandhi, N., Renganathan, S., 2013. Recent developments for biodiesel production by ultrasonic assist transesterification using different heterogeneous catalyst: A review. *Renew. Sustain. Energy Rev.* 22, 410–418. <https://doi.org/10.1016/j.rser.2013.01.057>
- Ren, S., Ye, X.P., 2015. Catalytic conversion of glycerol to value-added chemicals in alcohol. *Fuel Process. Technol.* 140, 148–155. <https://doi.org/10.1016/j.fuproc.2015.09.008>
- Rodríguez-Guerrero, J.K., Rubens, M.F., Rosa, P.T.V., 2013. Production of biodiesel from castor oil using sub and supercritical ethanol: Effect of sodium hydroxide on the ethyl ester production. *J. Supercrit. Fluids* 83, 124–132. <https://doi.org/10.1016/j.supflu.2013.08.016>
- Román-Figueroa, C., Olivares-Carrillo, P., Paneque, M., Palacios-Nereo, F.J., Quesada-Medina, J., 2016. High-yield production of biodiesel by non-catalytic supercritical methanol transesterification of crude castor oil (*Ricinus communis*). *Energy* 107, 165–171. <https://doi.org/10.1016/j.energy.2016.03.136>
- Saada, R., AboElazayem, O., Kellici, S., Heil, T., Morgan, D., Lampronti, G.I., Saha, B., 2018. Greener synthesis of dimethyl carbonate using a novel tin-zirconia/graphene nanocomposite catalyst. *Appl. Catal. B Environ.* 226, 451–462. <https://doi.org/10.1016/j.apcatb.2017.12.081>

- Saada, R., Heil, T., Kellici, S., Morgan, D., Saha, B., 2014. Greener synthesis of dimethyl carbonate using a novel ceria–zirconia oxide/graphene nanocomposite catalyst. *Appl. Catal. B Environ.* 168–169, 353–362. <https://doi.org/10.1016/j.apcatb.2014.12.013>
- Saha, B., Haigh, K.F., Vladisavljević, G.T., Reynolds, J.C., Nagy, Z., 2014. Kinetics of the pre-treatment of used cooking oil using Novozyme 435 for biodiesel production. *Chem. Eng. Res. Des.* 92, 713–719. <https://doi.org/10.1016/j.cherd.2014.01.006>
- Sajid, Z., Khan, F., Zhang, Y., 2016. Process simulation and life cycle analysis of biodiesel production. *Renew. Energy* 85, 945–952. <https://doi.org/10.1016/j.renene.2015.07.046>
- Sajjadi, B., Raman, A.A.A., Arandiyan, H., 2016. A comprehensive review on properties of edible and non-edible vegetable oil-based biodiesel: Composition, specifications and prediction models. *Renew. Sustain. Energy Rev.* 63, 62–92. <https://doi.org/10.1016/j.rser.2016.05.035>
- Saka, S., Isayama, Y., 2009. A new process for catalyst-free production of biodiesel using supercritical methyl acetate. *Fuel* 88, 1307–1313. <https://doi.org/10.1016/j.fuel.2008.12.028>
- Saka, S., Kusdiana, D., 2001. Biodiesel fuel from rapeseed oil as prepared in supercritical methanol. *Fuel* 80, 225–231. [https://doi.org/10.1016/S0016-2361\(00\)00083-1](https://doi.org/10.1016/S0016-2361(00)00083-1)
- Salar-García, M.J., Ortiz-Martínez, V.M., Olivares-Carrillo, P., Quesada-Medina, J., De Los Ríos, A.P., Hernández-Fernández, F.J., 2016. Analysis of optimal conditions for biodiesel production from *Jatropha* oil in supercritical methanol: Quantification of thermal decomposition degree and analysis of FAMES. *J. Supercrit. Fluids* 112, 1–6. <https://doi.org/10.1016/j.supflu.2016.02.004>

- Saluja, R.K., Kumar, V., Sham, R., 2016. Stability of biodiesel – A review. *Renew. Sustain. Energy Rev.* 62, 866–881. <https://doi.org/10.1016/j.rser.2016.05.001>
- Samniang, A., Tipachan, C., Kajorncheappun-ngam, S., 2014. Comparison of biodiesel production from crude *Jatropha* oil and Krating oil by supercritical methanol transesterification. *Renew. Energy* 68, 351–355. <https://doi.org/10.1016/j.renene.2014.01.039>
- Sánchez-Cantú, M., Morales Téllez, M., Pérez-Díaz, L.M., Zeferino-Díaz, R., Hilario-Martínez, J.C., Sandoval-Ramírez, J., 2019. Biodiesel production under mild reaction conditions assisted by high shear mixing. *Renew. Energy* 130, 174–181. <https://doi.org/10.1016/j.renene.2018.06.035>
- Sánchez-Cantú, M., Pérez-Díaz, L.M., Morales-Téllez, M., Martínez-Santamaría, I., Hilario-Martínez, J.C., Sandoval-Ramírez, J., 2017. A sustainable method to produce biodiesel through an emulsion formation induced by a high shear mixer. *Fuel* 189, 436–439. <https://doi.org/10.1016/j.fuel.2016.10.107>
- Santana, A., MaçAira, J., Larrayoz, M.A., 2012. Continuous production of biodiesel from vegetable oil using supercritical ethanol/carbon dioxide mixtures. *Fuel Process. Technol.* 96, 214–219. <https://doi.org/10.1016/j.fuproc.2011.12.021>
- Santana, H.S., Tortola, D.S., Reis, É.M., Silva, J.L., Taranto, O.P., 2016. Transesterification reaction of sunflower oil and ethanol for biodiesel synthesis in microchannel reactor: Experimental and simulation studies. *Chem. Eng. J.* 302, 752–762. <https://doi.org/10.1016/j.cej.2016.05.122>
- Sawangkeaw, R., Bunyakiat, K., Ngamprasertsith, S., 2010. A review of laboratory-scale research on lipid conversion to biodiesel with supercritical methanol (2001-2009). *J. Supercrit. Fluids* 55, 1–13. <https://doi.org/10.1016/j.supflu.2010.06.008>

- Semwal, S., Arora, A.K., Badoni, R.P., Tuli, D.K., 2011. Biodiesel production using heterogeneous catalysts. *Bioresour. Technol.* 102, 2151–2161. <https://doi.org/10.1016/j.biortech.2010.10.080>
- Sepahvand, A., Rahimi, M., Aghel, B., Ghasempour, H.R., Alitabar, M., 2014. Optimization of biodiesel production from soybean oil in a microreactor. *Energy Convers. Manag.* 79, 599–605. <https://doi.org/10.1016/j.enconman.2013.12.065>
- Shin, H.Y., Lee, S.H., Ryu, J.H., Bae, S.Y., 2012. Biodiesel production from waste lard using supercritical methanol. *J. Supercrit. Fluids* 61, 134–138. <https://doi.org/10.1016/j.supflu.2011.09.009>
- Silitonga, A.S., Masjuki, H.H., Ong, H.C., Yusaf, T., Kusumo, F., Mahlia, T.M.I., 2016. Synthesis and optimization of *Hevea brasiliensis* and *Ricinus communis* as feedstock for biodiesel production: A comparative study. *Ind. Crops Prod.* 85, 274–286. <https://doi.org/10.1016/j.indcrop.2016.03.017>
- Song, C., Chen, G., Ji, N., Liu, Q., Kansha, Y., Tsutsumi, A., 2015. Biodiesel production process from microalgae oil by waste heat recovery and process integration. *Bioresour. Technol.* 193, 192–199. <https://doi.org/10.1016/j.biortech.2015.06.116>
- Sotoft, L.F., Rong, B.G., Christensen, K. V., Norddahl, B., 2010. Process simulation and economical evaluation of enzymatic biodiesel production plant. *Bioresour. Technol.* 101, 5266–5274. <https://doi.org/10.1016/j.biortech.2010.01.130>
- Srinivas, B.K., El-Halwagi, M.M., 1994. Synthesis of combined heat and reactive mass-exchange networks. *Chem. Eng. Sci.* 49, 2059–2074. [https://doi.org/10.1016/0009-2509\(94\)E0016-J](https://doi.org/10.1016/0009-2509(94)E0016-J)
- Stavarache, C., Vinatoru, M., Nishimura, R., Maeda, Y., 2005. Fatty acids methyl esters from vegetable oil by means of ultrasonic energy. *Ultrason. Sonochem.* 12, 367–372. <https://doi.org/10.1016/j.ultsonch.2004.04.001>

- Sun, P., Sun, J., Yao, J., Zhang, L., Xu, N., 2010. Continuous production of biodiesel from high acid value oils in microstructured reactor by acid-catalyzed reactions. *Chem. Eng. J.* 162, 364–370.
<https://doi.org/10.1016/j.cej.2010.04.064>
- Suresh, M., Jawahar, C.P., Richard, A., 2018. A review on biodiesel production, combustion, performance, and emission characteristics of non-edible oils in variable compression ratio diesel engine using biodiesel and its blends. *Renew. Sustain. Energy Rev.* 92, 38–49.
<https://doi.org/10.1016/j.rser.2018.04.048>
- Talebian-Kiakalaieh, A., Amin, N.A.S., Mazaheri, H., 2013. A review on novel processes of biodiesel production from waste cooking oil. *Appl. Energy* 104, 683–710. <https://doi.org/10.1016/j.apenergy.2012.11.061>
- Tan, K.T., Gui, M.M., Lee, K.T., Mohamed, A.R., 2010. An optimized study of methanol and ethanol in supercritical alcohol technology for biodiesel production. *J. Supercrit. Fluids* 53, 82–87.
<https://doi.org/10.1016/j.supflu.2009.12.017>
- Tanawannapong, Y., Kaewchada, A., Jaree, A., 2013. Biodiesel production from waste cooking oil in a microtube reactor. *J. Ind. Eng. Chem.* 19, 37–41.
<https://doi.org/10.1016/j.jiec.2012.07.007>
- Tavlarides, L.L., Huang, X., Bond, J.Q., Nan, Y., Liu, J., 2018. Continuous esterification of oleic acid to ethyl oleate under sub/supercritical conditions over $\gamma\text{-Al}_2\text{O}_3$. *Appl. Catal. B Environ.* 232, 155–163.
<https://doi.org/10.1016/j.apcatb.2018.03.050>
- Teo, S.H., Goto, M., Taufiq-Yap, Y.H., 2015. Biodiesel production from *Jatropha curcas* L. oil with Ca and La mixed oxide catalyst in near supercritical methanol conditions. *J. Supercrit. Fluids* 104, 243–250.
<https://doi.org/10.1016/j.supflu.2015.06.023>

- Tiwari, A., Rajesh, V.M., Yadav, S., 2018. Biodiesel production in micro-reactors: A review. *Energy Sustain. Dev.* 43, 143–161.
<https://doi.org/10.1016/j.esd.2018.01.002>
- Torrentes-Espinoza, G., Miranda, B.C., Vega-Baudrit, J., Mata-Segreda, J.F., 2017. Castor oil (*Ricinus communis*) supercritical methanolysis. *Energy* 140, 426–435. <https://doi.org/10.1016/j.energy.2017.08.122>
- Trinh, H., Yusup, S., Uemura, Y., 2018. Optimization and kinetic study of ultrasonic assisted esterification process from rubber seed oil. *Bioresour. Technol.* 247, 51–57. <https://doi.org/10.1016/j.biortech.2017.09.075>
- Tsai, Y.T., Lin, H. mu, Lee, M.J., 2013. Biodiesel production with continuous supercritical process: Non-catalytic transesterification and esterification with or without carbon dioxide. *Bioresour. Technol.* 145, 362–369.
<https://doi.org/10.1016/j.biortech.2012.12.157>
- Umeda, T., Itoh, J., Shiroko, K., 1978. Heat Exchange Systems Synthesis (Umeda, 1978).Pdf. *Chem. Eng. Prog.*
- Varma, M.N., Deshpande, P.A., Madras, G., 2010. Synthesis of biodiesel in supercritical alcohols and supercritical carbon dioxide. *Fuel* 89, 1641–1646.
<https://doi.org/10.1016/j.fuel.2009.08.012>
- Vengalil, R., Suresh, R., Kochimoolayil, G.E., Joseph, R., Antony, J.V., 2016. Esterification of free fatty acids in non- edible oils using partially sulfonated polystyrene for biodiesel feedstock. *Ind. Crops Prod.* 95, 66–74.
<https://doi.org/10.1016/j.indcrop.2016.09.060>
- Vinet, L., Zhedanov, A., 2011. A “missing” family of classical orthogonal polynomials. *J. Phys. A Math. Theor.* 44, 1–52. <https://doi.org/10.1088/1751-8113/44/8/085201>

- Vlysidis, A., Binns, M., Webb, C., Theodoropoulos, C., 2011. Glycerol utilisation for the production of chemicals: Conversion to succinic acid, a combined experimental and computational study. *Biochem. Eng. J.* 58–59, 1–11. <https://doi.org/10.1016/j.bej.2011.07.004>
- Vyas, A.P., Verma, J.L., Subrahmanyam, N., 2010. A review on FAME production processes. *Fuel* 89, 1–9. <https://doi.org/10.1016/j.fuel.2009.08.014>
- Wan, Y., Lei, Y., Lan, G., Liu, D., Li, G., Bai, R., 2018. Synthesis of glycerol carbonate from glycerol and dimethyl carbonate over DABCO embedded porous organic polymer as a bifunctional and robust catalyst. *Appl. Catal. A Gen.* 562, 267–275. <https://doi.org/10.1016/j.apcata.2018.06.022>
- Warabi, Y., Kusdiana, D., Saka, S., 2004. Reactivity of triglycerides and fatty acids of rapeseed oil in supercritical alcohols. *Bioresour. Technol.* 91, 283–287. [https://doi.org/10.1016/S0960-8524\(03\)00202-5](https://doi.org/10.1016/S0960-8524(03)00202-5)
- Wen, D., Jiang, H., Zhang, K., 2009. Supercritical fluids technology for clean biofuel production. *Prog. Nat. Sci.* 19, 273–284. <https://doi.org/10.1016/j.pnsc.2008.09.001>
- Wen, Z., Yu, X., Tu, S.T., Yan, J., Dahlquist, E., 2009. Intensification of biodiesel synthesis using zigzag micro-channel reactors. *Bioresour. Technol.* 100, 3054–3060. <https://doi.org/10.1016/j.biortech.2009.01.022>
- West, A.H., Posarac, D., Ellis, N., 2008. Assessment of four biodiesel production processes using HYSYS.Plant. *Bioresour. Technol.* 99, 6587–6601. <https://doi.org/10.1016/j.biortech.2007.11.046>
- Wolf Maciel, M.R., Santana, G.C.S., Maciel Filho, R., Martins, P.F., Batistella, C.B., de Lima da Silva, N., 2009. Simulation and cost estimate for biodiesel production using castor oil. *Chem. Eng. Res. Des.* 88, 626–632. <https://doi.org/10.1016/j.cherd.2009.09.015>

- Wu, T.N., 2011. Electrochemical removal of MTBE from water using the iridium dioxide coated electrode. *Sep. Purif. Technol.* 79, 216–220.
<https://doi.org/10.1016/j.seppur.2011.02.008>
- Xie, F., Lu, Q., de Toledo, R.A., Shim, H., 2016. Enhanced simultaneous removal of MTBE and TCE mixture by *Paracoccus* sp. immobilized on waste silica gel. *Int. Biodeterior. Biodegrad.* 114, 222–227.
<https://doi.org/10.1016/j.ibiod.2016.07.003>
- Xin, J., Imahara, H., Saka, S., 2008. Oxidation stability of biodiesel fuel as prepared by supercritical methanol. *Fuel* 87, 1807–1813.
<https://doi.org/10.1016/j.fuel.2007.12.014>
- Xu, Q.-Q., Li, Q., Yin, J.-Z., Guo, D., Qiao, B.-Q., 2016. Continuous production of biodiesel from soybean flakes by extraction coupling with transesterification under supercritical conditions. *Fuel Process. Technol.* 144, 37–41.
<https://doi.org/10.1016/j.fuproc.2015.12.018>
- Xu, Y., Du, W., Liu, D., 2005. Study on the kinetics of enzymatic interesterification of triglycerides for biodiesel production with methyl acetate as the acyl acceptor. *J. Mol. Catal. B Enzym.* 32, 241–245.
<https://doi.org/10.1016/j.molcatb.2004.12.013>
- Yao, X., Zhang, Y., Du, L., Liu, J., Yao, J., 2015. Review of the applications of microreactors. *Renew. Sustain. Energy Rev.* 47, 519–539.
<https://doi.org/10.1016/j.rser.2015.03.078>
- Yin, J.Z., Xiao, M., Song, J. Bin, 2008. Biodiesel from soybean oil in supercritical methanol with co-solvent. *Energy Convers. Manag.* 49, 908–912.
<https://doi.org/10.1016/j.enconman.2007.10.018>
- Yunus, N.B.M., Roslan, N.A.B., Yee, C.S., Abidin, S.Z., 2016. Esterification of Free Fatty Acid in Used Cooking Oil Using Gelular Exchange Resin as Catalysts. *Procedia Eng.* 148, 1274–1281.
<https://doi.org/10.1016/j.proeng.2016.06.450>

- Zadaka-Amir, D., Nasser, A., Nir, S., Mishael, Y.G., 2012. Removal of methyl tertiary-butyl ether (MTBE) from water by polymer-zeolite composites. *Microporous Mesoporous Mater.* 151, 216–222.
<https://doi.org/10.1016/j.micromeso.2011.10.033>
- Zhang, H., Wang, Z., Liu, O., 2015a. Development and validation of a GC-FID method for quantitative analysis of oleic acid and related fatty acids. *J. Pharm. Anal.* 5, 223–230. <https://doi.org/10.1016/j.jpha.2015.01.005>
- Zhang, H., Wang, Z., Liu, O., 2015b. Development and validation of a GC-FID method for quantitative analysis of oleic acid and related fatty acids. *J. Pharm. Anal.* 5, 223–230. <https://doi.org/10.1016/j.jpha.2015.01.005>
- Zhang, X., Yan, S., Tyagi, R.D., Surampalli, R.Y., Valéro, J.R., 2014. Ultrasonication aided in-situ transesterification of microbial lipids to biodiesel. *Bioresour. Technol.* 169, 175–180.
<https://doi.org/10.1016/j.biortech.2014.06.108>
- Zhang, Y., Dubé, M.A., McLean, D.D., Kates, M., 2003. Biodiesel production from waste cooking oil: 1. Process design and technological assessment. *Bioresour. Technol.* [https://doi.org/10.1016/S0960-8524\(03\)00040-3](https://doi.org/10.1016/S0960-8524(03)00040-3)
- Zhou, D., Qiao, B., Li, G., Xue, S., Yin, J., 2017. Continuous production of biodiesel from microalgae by extraction coupling with transesterification under supercritical conditions. *Bioresour. Technol.* 238, 609–615.
<https://doi.org/10.1016/j.biortech.2017.04.097>
- Zhu, L., Hiltunen, E., Shu, Q., Zhou, W., Li, Z., Wang, Z., 2014. Biodiesel production from algae cultivated in winter with artificial wastewater through pH regulation by acetic acid. *Appl. Energy* 128, 103–110.
<https://doi.org/10.1016/j.apenergy.2014.04.039>